WAVE TRANSFORMATION AND VELOCITY FIELDS IN THE BREAKER ZONE

A thesis submitted to the University of London

for the degree of Doctor of Philosophy

by

M.D. Adeyemo

University College London

August 1967

Page Numbering as Bound

SYNOPSIS

This thesis is concerned with the quantitative study of the geometrical asymmetry and velocity asymmetry associated with shallow water oscillatory waves. The region of interest in the work is the shallow water zone defined by the depth to wave length ratio $\frac{d}{L} < 0.15$, including the breaker-zone. Three descriptions of wave asymmetry are defined and examined:-

1) wave vertical asymmetry,

2) wave slope asymmetry,

and 3) wave horizontal asymmetry.

Two methods of defining horizontal velocity asymmetry are investigated, namely:

1) horizontal velocity (magnitude) asymmetry,

and 2) horizontal velocity (time) asymmetry.

The effects of shoaling, produced by beaches of different slope, on the wave asymmetry and the velocity fields are examined.

Six beach slopes in the range 1 : 4 to 1 : 18 were employed, and a quantitative correlation was found to exist between the wave slope asymmetry, wave horizontal asymmetry and the wave vertical asymmetry, as well as between the wave asymmetry and the velocity asymmetry. General expressions are given on the basis

of existing wave theories for the wave horizontal asymmetry and the horizontal velocity (magnitude) asymmetry.

A detailed study was made of the effect of the backwash of the wave on the wave asymmetry and the velocity fields seaward of the breakers.

The mechanics of sediment movement under the action of waves is discussed in the light of the time-history of the velocity curves.

Finally a preliminary investigation of the effect of the phase-difference of uprush and backwash on the wave motion at the breaker position was made. This involved systematic variation of the incident wave characteristics in order to obtain different breaker types.

ACKNOWLEDGEMENTS

The author wishes to express his gratitude to Dr. P.H. Kemp who supervised this work, for his continual interest and encouragement.

Lots of thanks and appreciation are also due to Mr. D.W. Vale who gave much help concerning the experimental aspects of the work, and also during the preparation of the thesis.

The generous help of the technical staff particularly T.G. Gurman and Mick Gregory is also gratefully acknowledged.

Much gratitude is also due Miss M. Lancaster who helped to type the thesis.

The author is greatly indebted to the Commonwealth Scholarship Commission and the Nigerian Government for the financial support of this project.

CONTENTS

INTRODUCTION

As the wave leaves the generating area in fairly deep water ($\frac{d}{L} \geq \frac{1}{2}$) the water particle velocities associated with the wave are negligibly small at a depth from the surface equal to about half the wave length. As the wave progresses into shallower water, the effect of the wave soon starts to be felt at the sea bed. The geometry of the wave is then affected as well as the orbital velocity of the fluid particles. In the very shallow water zone of about $\frac{d}{L} < 0.15$ and including the breaker zone, the asymmetry of the wave becomes marked and there is an associated asymmetry of the orbital velocities. There must be both qualitative and quantitative correlation between the asymmetry of the wave and the asymmetry of the resulting velocity field.

Up to the present time, few studies have been made of wave asymmetry and of the asymmetry of the orbital velocity field. Some of these studies have been expressed in general descriptive terms whilst others are limited to experimental observations.

The study described in this thesis involved the use of an hydraulic model with an impermeable beach, and may thus be regarded as the first phase of a research programme into the quantitative correlation

between the wave asymmetry and the velocity fields under natural conditions. The impermeable beach was chosen to permit beach slope variation, and to enable a detailed study of the effect of the backwash to be made.

In order to overcome the scale limitations imposed by the model size, the measurements were based on parameters used in certain aspects of wave theory, so that the behaviour of the model could be assessed. The expression in the Cnoidal theory corresponding to the wave vertical asymmetry was used in the investigation. This theory is presented in the thesis with some notes on the elliptic integrals given in the appendix. The experimental results of the wave slope asymmetry are compared with the theory of Biesel[5].

The correlation of wave geometry with velocity asymmetry, leads to the correlation of wave characteristics with sediment movement. This is the ultimate objective, of the research programme. It is common knowledge that beach material is in almost continuous movement under the action of waves and currents. The action of the waves is complicated by tidal variations which move the active zone periodically landward and seaward, and in addition expand and contract the width of the active zone. Considerable quantities of sediment may be in movement and accretion or depletion in any locality

depends on the net result of the inflow of material to the area and outflow both along and normal to the shoreline. The better understanding of the shallow water wave processes is of extreme importance in the design of coastal engineering projects.

In the presentation of this thesis, brief summaries and comments on previous work of relevance to the study have been included in the appropriate chapters.

CHAPTER 1

WAVES

1.1 Waves in Shoaling Water

The transformation of ocean waves in shoaling water is a complex process which is not yet fully understood, but certainly this is the region of the greatest concern to the coastal engineer.

As an oscillatory wave advances into shoaling water, a depth is eventually reached at which the unsteady fluid particle motion caused by the wave reaches the bottom. From that stage forward the height, length and asymmetry of the wave become markedly affected. The quasi-circular orbits of the water particles associated with the motion of the waves when in deeper water gradually change, as the waves approach the breaker zone, into quasi-elliptical paths. Finally, the wave reaches so shallow a depth that the waves become unstable and break. It is generally considered that the combination of the beach slope and the deep water wave steepness determines the ultimate form of the breaker.

Wiegel[54], Iversen[16] and Eagleson[8] performed some experiments on shoaling waves and compared their respective results with those computed from the small amplitude wave theory of Airy. They concluded that

the predicted wave heights (on the basis of the small amplitude theory) were usually smaller than the measured wave heights. This is as one would anticipate, since the requirements of the small amplitude wave theory are not in agreement with the wave characteristics near the breaker zone.

The concensus of opinion at the present time [Morison and Crooke[39]; Miller and Zeigler[38], Masch[33] and others] seems to be that in the shoaling region Stokes finite amplitude theory holds reasonably well, but only up to a limit of $\frac{d}{L} \simeq 0.10$. The cnoidal wave theory applies in the region $0.10 \geqslant \frac{d}{L} \geqslant 0.02$, and the solitary wave theory in the region $\frac{d}{L} < 0.02$. A review of both Stokes and the Cnoidal wave theories are given below in so far as they are relevant to the present study. An expression, corresponding to the wave vertical asymmetry, given by the Cnoidal theory is used in the investigation. Since this theory is less well known, it is presented rather more fully.

1.2 Surface Wave Theories

1.2.1 Stokes' Finite Amplitude Wave Theory

In order to study waves of small but finite wave steepness, Stokes[47] expanded the velocity potential about the still water level, and obtained a non-linear surface condition for the potential on the plane of the still water level. This consists of an infinite series containing partial derivatives of the potential. The solution required successive approximations. Levi-Civita[29] proved the series convergent for deep water, and Struik[48] for water of finite depth. Stokes himself pointed out that the restriction on wave steepness is more severe for water of finite depth as the approximation then becomes much slower. However, unlike the linear theory, Stokes waves showed the existence of mass transport. Longuet Higgins later extended the study of mass transport into the boundary layer. In addition, Stokes theory predicts asymmetrical orbital motion. The horizontal component of water particle velocity at a point (x,y) in water of depth d is given to the second order of Stokes theory by the expression :

$$u = \frac{\pi H}{T} \frac{\cosh 2\pi\left(\frac{y+d}{L}\right)}{\sinh \frac{2\pi d}{L}} \cos 2\pi\left(\frac{x}{L} - \frac{t}{T}\right) +$$

$$\frac{3}{4}\left(\frac{\pi H}{T}\right)\left(\frac{\pi H}{L}\right) \frac{\cosh 4\pi\left(\frac{y+d}{L}\right)}{\sinh^4 \frac{2\pi d}{L}} \cos 4\pi\left(\frac{x}{L} - \frac{t}{T}\right)$$

or in simplified form

$$u = A\cos 2\pi X + B\cos 4\pi X \qquad \cdots (1.1)$$

An inspection of equation 1.1 shows that the velocity components due to the first term on the right hand side are positive under the wave crest and negative under the trough, while the second term is positive under both crest and trough, and gives maximum negative components at $\frac{L}{4}$ and $\frac{3L}{4}$ from the crest. The net effect as noted by Inman and Nasu[14] is to increase the value of the magnitude under the crest, and decrease it under the trough, thus producing asymmetry in the magnitudes of the orbital velocity. On the other hand the duration of the forward motion under the crest is reduced, and the duration of the reverse motion under the trough is increased.

Stokes extended his work to the third order and several other investigators have in fact extended it to higher order. Aside from the fact that the Stokes' theory is not as accurate as the Cnoidal wave theory for $\frac{d}{L} < 0.10$, the coefficients in the series for the higher orders are rather complicated. Thus in order to render the theory more useful, Skjelbreia[46]

simplified the problem by tabulating the various coefficients involved in the series solution as a function of the wave height, period and water depth. The tabulated values are based on Stokes' third order approximation.

Equation 1.1 was compared with the experimental results of the velocity studies in Chapter 5, where discussion of the validity of the expression in the present context is given.

1.2.2 Cnoidal Wave Theory

Note:- As the Cnoidal wave theory makes use of the elliptic functions, some introductory statements, definitions and important summaries on the elliptic integrals are given in appendix III. The summary of the theory given below is not intended to be complete, but rather to illustrate the way in which cnoidal theory provides a link between sinusoidal waves and solitary waves. The expression for wave height asymmetry is also developed.

Introduction

Korteweg and de Vries[24] developed the Cnoidal wave theory which is generally considered very useful for describing the propagation of periodic waves in shallow water where the depth is less than one-tenth of the wave length.

The properties of the waves are given in terms of the complete elliptic integrals of the first and second kind, and the Jacobian elliptic functions hence the term 'Cnoidal', analogous to sinusoidal.

As indicated by Keulegan[22] the theory of cnoidal waves is based on the assumption that the square of the inclination of the water surface is small in relation to unity.

More studies on the Cnoidal wave theory were made by Laitone[26,27], Keulegan and Patterson[23], Littman[30] Iwasa[17], and Benjamin and Lighthill[4]. Keller[19] treated the problem using non-linear shallow water theory and obtained formulae which were similar to those of Korteweg and De Vries. Despite these quite extensive studies, little use has been made of the theory in experimental studies. Wiegel[55,56] summarised much of the existing work on cnoidal waves and presented the leading results of Korteweg and De Vries[24] and Keulegan and Patterson[23] in a more useable form. However, solutions of Wiegel's equations for the wave characteristics involve either trial and improvement computations, or extensive use of graphs of many of the functions. In order to further facilitate the use of the theory, Masch and Wiegel[34] computed several of the cnoidal wave characteristics from the equations obtained by Wiegel[55]

based on the work of Korteweg and De Vries, and they presented the results together with the elliptic integrals and the Jacobian elliptic functions in tabular form.

Masch(33), with the useful graphs and necessary tables of functions for the cnoidal wave made available, investigated the application of cnoidal wave theory to the transformation of long waves in shoaling water by calculating the power transmission of cnoidal waves in terms of the geometric wave characteristics and the complete elliptic integrals of the first and second kind, assuming no reflections or loss of energy as the waves move into shallow water. The results were compatible with expectations. It was found that both the wave height and steepness increase as the depth becomes shallower, whereas the wave length decreases with decreasing water depth.

Summary of Cnoidal Wave Equations

The notations used in the equations below are defined as follows:

L	wave length
d	still water depth
C	wave velocity
$K(k)$	complete elliptic integral of the first kind.
$E(k)$	complete elliptic integral of the second kind.

k modulus of elliptic integral

H wave height (trough to crest)

T wave period

u horizontal component of water particle velocity

$\bar{u}$ incomplete elliptic integral of the first kind

v vertical component of water particle velocity

x horizontal coordinate

y vertical coordinate measured from the ocean bottom

y_s vertical distance from ocean bottom to wave surface

y_t vertical distance from bottom to wave trough

y_c vertical distance from bottom to wave crest

Korteweg and De Vries[24], Keulegan and Patterson[23], and Keller[19] used different symbols, but the formulae obtained by them are essentially the same. The equations below are obtained by Wiegel[55] based mainly on the theory of Korteweg and De Vriess, and for completion some of the equations from the work of Keulegan and Patterson[23] and Littman[30] are also indicated.

The wave length is given by

$$\frac{L}{d} = \frac{4}{\sqrt{3}} K(k) \left(2\bar{L} + 1 - \frac{y_t}{d}\right)^{-1/2} \quad \cdots \quad (1.2)$$

where $\bar{L}$ and κ are defined by the following two equations

$$\kappa^2 = \frac{\left(\frac{y_c}{d}\right) - \left(\frac{y_t}{d}\right)}{2\bar{L} + 1 - \left(\frac{y_t}{d}\right)} \quad \cdots \quad (1.3)$$

$$\left(2\bar{L}+1-\frac{y_t}{d}\right)E(k) = \left(2\bar{L}+2-\frac{y_c}{d}-\frac{y_t}{d}\right)K(k) \qquad \ldots \quad (1.4)$$

For k to be real in equation (1.3), the following equations must also hold

$$2\bar{L}+1 > \frac{y_c}{d} > \frac{y_t}{d} \quad \text{and} \quad 0 < k^2 \leq 1 \qquad \ldots \quad (1.5)$$

Equation (1.3) can be re arranged in the form

$$\left(2\bar{L}+1-\frac{y_t}{d}\right) = \frac{\left(\frac{y_c}{d}\right)-\left(\frac{y_t}{d}\right)}{k^2} = \frac{H/d}{k^2} \qquad \ldots \quad (1.6)$$

substituting eq.(1.6) into equation (1.2) and squaring gives

$$\frac{HL^2}{d^3} = \frac{16}{3}\left[k\,K(k)\right]^2 \qquad \ldots \quad (1.7)$$

$$\text{i.e.} \quad L = \sqrt{\frac{16d^3}{3H}}\; k\,K(k) \qquad \ldots \quad (1.8)$$

Equation (1.4) can be re-arranged to give

$$E(k)-K(k) = \frac{\left(1-\left[\frac{y_c}{d}\right]\right)K(k)}{\left[2\bar{L}+1-\left(\frac{y_t}{d}\right)\right]} \qquad \ldots \quad (1.9)$$

Substituting equation (1.2) into equation (1.9) and re-arranging terms we have

$$\frac{y_c}{d} = \frac{16d^2}{3L^2}\left[K(k)\left(K(k)-E(k)\right)\right]+1 \qquad \ldots (1.10)$$

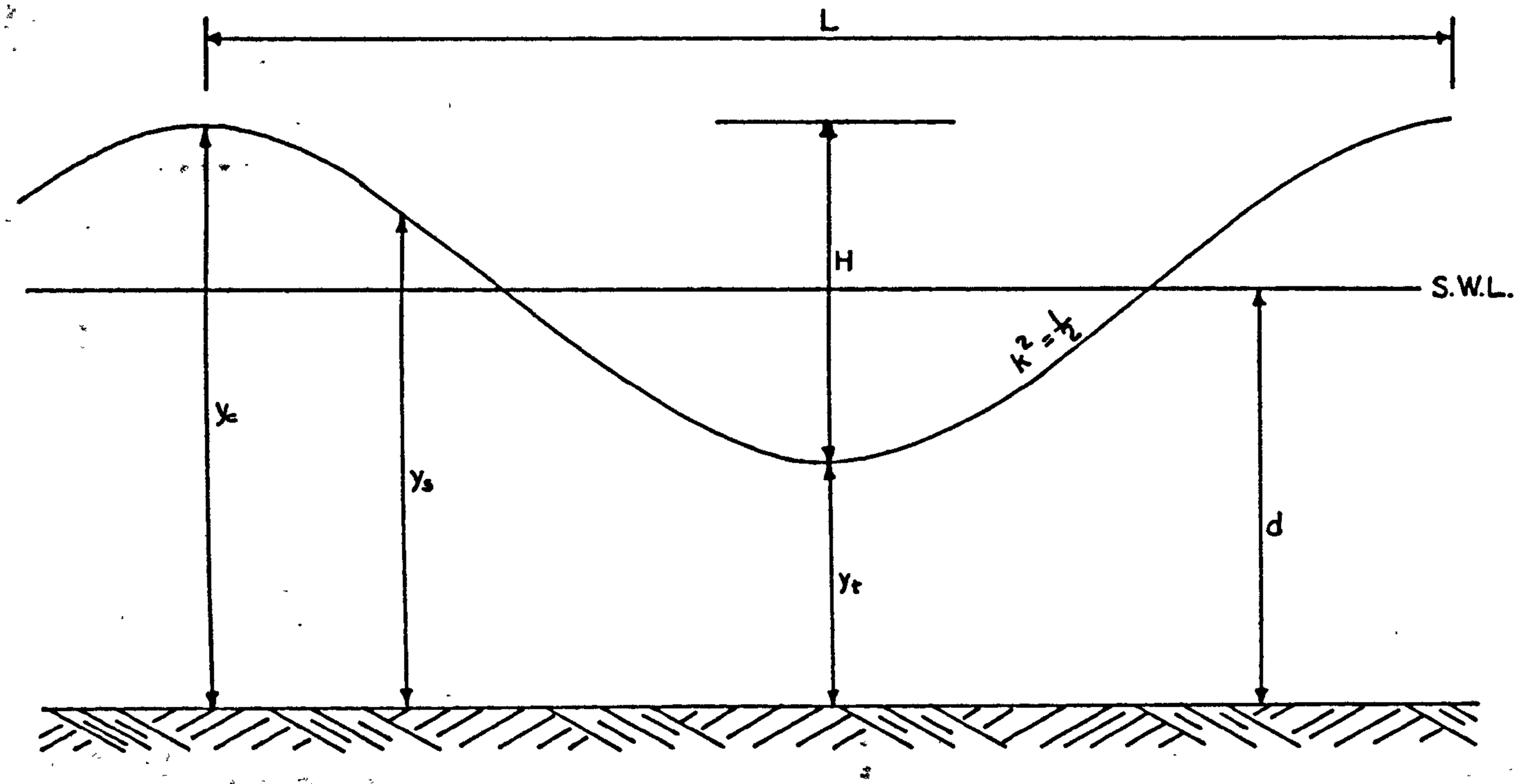

Figure 1.1 Definition Sketch

multiplying equation (1.10) by $\frac{d}{H}$ we get

$$\frac{y_c - d}{H} = \frac{16 d^3}{3L^2 H}\left[K(k)\left(K(k) - E(k)\right)\right] \qquad \ldots (1.11)$$

Equation (1.11) is important as it expresses the WAVE VERTICAL ASYMMETRY.

The wave profile is

$$y_s = y_t + H\,cn^2\left[2K(k)\left(\frac{x}{L} - \frac{t}{T}\right), k\right] \qquad \ldots (1.12)$$

Although as stated in Appendix III cn is in general doubly periodic, it will be singly periodic (period 4K) providing K is a real number and $0 \leq k \leq 1$. It is important to note that when $k = 0$ $sn\bar{u} = \sin\bar{u}$, $cn\,\bar{u} = \cos\bar{u}$ and $K = \pi/2$ ie. the period $4K = 2\pi$. Thus when $k = 0$ the elliptic cosine reduces to the circular cosine and the wave profile is given by the trigonometric functions. On the other hand when $k = 1$, $cn\,\bar{u} = \text{sech}\,\bar{u}$, and we have the hyperbolic function, with $K(k) = \infty$, hence the period becomes infinite and we have the solitary wave expression. Thus the cnoidal wave theory gives the solitary wave and the sinusoidal wave as its two limiting cases. This is demonstrated below.

The wave velocity (using Stokes' second definition of wave velocity, which is the velocity of the propagation of

of the wave form when the horizontal momentum of the liquid has been reduced to zero by the superposition of a uniform motion) is

$$C = \sqrt{gd}\left[1 + \frac{H}{d}\,\frac{1}{k^2}\left(\frac{1}{2} - \frac{E(k)}{K(k)}\right)\right] \qquad \ldots (1.13)$$

From equation (1.7) $\quad \frac{1}{k^2} = \frac{16d^3}{3L^2H}\,K^2_{(k)}$

so we have

$$C = \sqrt{gd}\left[1 + \frac{16d^2}{3L^2}K^2_{(k)}\left(\frac{1}{2} - \frac{E(k)}{K(k)}\right)\right] \qquad \ldots (1.14)$$

For one limiting case k^2 approaches unity (solitary wave), K(k) is infinity and equation (1.13) becomes

$$C = \sqrt{gd}\left(1 + \frac{H}{2d}\right) \qquad \ldots (1.15)$$

this approximates to $\quad C = \sqrt{gd\left(1 + \frac{H}{d}\right)}$

For the other limiting case (the linear theory where $k^2 \to 0$)

$\frac{E(k)}{K(k)} \longrightarrow 1$, $\qquad K(k) \longrightarrow \pi/2$

and equation (1.14) becomes

$$C = \sqrt{gd}\left(1 - \frac{2\pi^2 d^2}{3L^2}\right) \qquad \ldots (1.16)$$

which is an approximation of

$$C = \sqrt{gd\left(1 - \frac{4\pi^2 d^2}{3L^2}\right)} \qquad \ldots (1.17)$$

Considering the linear theory expression for wave velocity

$$C = \sqrt{\frac{gL}{2\pi} \tanh \frac{2\pi d}{L}} \qquad \ldots (1.18)$$

the series expansion for $\tanh \frac{2\pi d}{L}$ is

$$\tanh \frac{2\pi d}{L} = \frac{2\pi d}{L} - \frac{8\pi^3 d^3}{3L^3} + \text{- - - - -}$$

Substituting the first two terms in equation (1.18) gives

$$C = \sqrt{gd\left(1 - \frac{4\pi^2 d^2}{3L^2}\right)}$$

which is in agreement with equation (1.17)

As cnoidal waves are periodic and of permanent type ,

$L = CT$ i.e. $T = L/C$, thus from equations (1.8) and (1.13) the wave period is given by

$$T\sqrt{\frac{g}{d}} = \sqrt{\frac{16d}{3H}}\left\{\frac{k K(k)}{1+\left(\frac{H}{d}\right)\left(\frac{1}{k^2}\right)\left[\frac{1}{2} - \frac{E(k)}{K(k)}\right]}\right\} \qquad \ldots (1.19)$$

The horizontal and vertical components of water particle velocities based on the equations of Keulegan and Patterson[23] are

$$\frac{u}{\sqrt{gd}} = \left[\frac{h}{d} - \frac{h^2}{4d^2} + \left(\frac{d}{3} - \frac{y^2}{2d}\right)\frac{\partial^2 h}{\partial x^2}\right] \quad \cdots (1.20)$$

and

$$\frac{v}{\sqrt{gd}} = y\left[\left(\frac{h}{2d^2} - \frac{1}{d}\right)\frac{\partial h}{\partial x} + \frac{1}{3}\left(\frac{y^2}{2d} - d\right)\frac{\partial^3 h}{\partial x^3}\right] \quad \cdots (1.21)$$

where

$$h = (y_s - d) = -d + y_t + H\,cn^2\left[2K(k)\left(\frac{x}{L} - \frac{t}{T}\right), k\right]$$

Equations (1.20) and (1.21) become

$$\frac{u}{\sqrt{gd}} = \left[-\frac{5}{4} + \frac{3y_t}{2d} - \frac{y_t^2}{4d^2} + \left(\frac{3H}{2d} - \frac{y_t H}{2d^2}\right)cn^2(\,) - \frac{H}{4d^2}\,cn^4(\,)\right.$$

$$\left. - \frac{8HK^2_{(k)}}{L^2}\left(\frac{d}{3} - \frac{y^2}{2d}\right)\left\{-k^2 sn^2(\,)\,cn^2(\,) + cn^2(\,)\,dn^2(\,) - sn\gamma(\,)\,dn\gamma(\,)\right\}\right] \quad \cdots (1.22)$$

and

$$\frac{V}{\sqrt{gd}} = \frac{y2H\ K(k)}{Ld}\left[1 + \frac{y_t}{d} + \frac{H}{d}\,cn^2( ) + \frac{32\,K^2(k)}{3L^2}\left(d^2 - \frac{y^2}{2}\right)\left\{k^2\,sn^2( ) - k^2\,cn^2( ) - dn^2( )\right\}\right] sn( )\ cn( )\ dn( )$$

(1.23)

where $Sn( )$ refers to $Sn\left[2K(k)\left\{\frac{x}{L} - \frac{t}{T}\right\},\ k\right]$.

Similarly for $cn( )$ and $dn( )$ Keulegan and Patterson[23] and Littman[30] gave the equation of wave velocity, which is the velocity of wave crest with respect to fixed co-ordinates as

$$C^2 = gd\left[1 + \frac{H}{d}\left\{-1 + \frac{1}{k^2}\left(2 - \frac{3E(k)}{K(k)}\right)\right\}\right]$$

. . . (1.24)

It is worth noting that since most of the cnoidal wave equations are three variable equations, families of curves are usually necessary to represent the results.

1.3 Wave Slope Asymmetry

In studying the progression of periodic waves in water of variable depth Biesel[5] produced a second-order theory for the wave slope asymmetry at still water level. Since the results of Biesel's Theory were used in the study and since the theory is not well known, it is produced below.

Let OX and OY be rectangular coordinate axes located at mean sea level, with x positive in the direction of wave propagation and OY being directed vertically upward. The other notations are defined as follows:

u,v = OX and OY velocity components

X,Y displacements of particles from their mean positions.

T Wave period

ω Angular frequency

L Wave length

$m = \frac{2\pi}{L}$

a wave amplitude

d water depth

$\gamma = -\left(\frac{\partial d}{\partial x}\right)$ = slope of the bed

Suffix o denotes deep water conditions

ϕ velocity potential

Under conditions of irrotational and incompressible flow, the continuity equation gives

$$\frac{\partial^2\phi}{\partial x^2} + \frac{\partial^2\phi}{\partial y^2} = 0 \qquad \cdots (1.25)$$

The velocity components are given by

$$u = \frac{\partial\phi}{\partial x} \qquad v = \frac{\partial\phi}{\partial y} \qquad (1.26)$$

In order to satisfy the boundary condition at the bed we have

$$\frac{\partial\phi}{\partial y} - \gamma\frac{\partial\phi}{\partial x} = 0 \qquad \text{for} \quad y = -d \qquad \cdots (1.27)$$

Assuming constant surface pressure we have

$$\frac{1}{g}\frac{\partial^2\phi}{\partial t^2} + \frac{\partial\phi}{\partial y} = 0 \qquad \text{for} \quad y = 0 \qquad \cdots (1.28)$$

From Biesel the above four conditions are satisfied by the function

$$\phi(x,y,t) = -\frac{a\omega}{m}\frac{1}{\sinh md}\Big[\cosh m(y+d)\sin(\omega t - \int m\,dx) + \gamma\Big\{\frac{1}{D^2\tanh md}\, m(y+d)\sinh m(y+d) - m(y+d)\cosh m(y+d) + \frac{m^2(y+d)^2}{D\sinh md\cosh md}\cosh m(y+d)\Big\}\cos(\omega t - \int m\,dx)\Big] \qquad \cdots (1.29)$$

where $$\Pi = 1 + \frac{md}{\sinh md \cosh md} \quad \ldots (1.30)$$

m, ω and d are related by

$$gm \tanh md = \omega^2 \quad \ldots (1.31)$$

and

$$a = \frac{a_0}{(\Pi \tanh md)^{1/2}} \quad \ldots (1.32)$$

Also

$$u = \frac{\partial \phi}{\partial x} = \frac{a\omega}{\sinh md}\Bigg[\cosh m(y+d)\cos(\omega t - \int m dx) - \gamma\Bigg\{\frac{1}{\Pi^2 \tanh md}\Big(\cosh m(y+d) + m(y+d)\sinh m(y+d)\Big) + \frac{1}{\Pi \sinh md \cosh md}\Big(m(y+d)\sinh m(y+d) + \frac{m^2(y+d)^2}{2}\cosh m(y+d)\Big) - \Big(\sinh m(y+d) + m(y+d)\cosh m(y+d)\Big)\Bigg\}\sin(\omega t - \int m dx)\Bigg] \quad \ldots (1.33)$$

$$V = \frac{\partial \phi}{\partial y} = \frac{-a\omega}{\sinh md}\left[\sinh m(y+d)\ \sin\left(\omega t - \int m dx\right)\right.$$

$$+ \gamma\left\{\frac{1}{D^2 \tanh md}\left(\sinh m(y+d) + m(y+d)\cosh m(y+d)\right)\right.$$

$$+ \frac{1}{D \sinh md \cosh md}\left(m(y+d)\cosh m(y+d) + \frac{m^2(y+d)^2}{2}\sinh m(y+d)\right)$$

$$\left.\left. - \left(\cosh m(y+d) + m(y+d)\sinh m(y+d)\right)\right\}\cos\left(\omega t - \int m dx\right)\right] \quad \ldots (1.34)$$

Taking into account equation (1.31) and the particular way in which ϕ depends on the time, equation (1.28) may be written

$$\phi m \tanh md = \frac{\partial \phi}{\partial y}, \quad \text{for} \quad y = 0 \quad \ldots (1.35)$$

The expressions of ϕ and $\frac{\partial \phi}{\partial y}$ for $y = 0$ are

$$\phi_{y=0} = \frac{-a\omega}{m \sinh md}\left[\cosh md\ \sin\left(\omega t - \int m dx\right)\right.$$

$$+ \gamma\left\{\frac{1}{D^2 \tanh md}\left(md \sinh md - md \cosh md\right)\right.$$

$$\left.\left. + \frac{m^2 d^2 \cosh md}{2D \sinh md \cosh md}\right\}\cos\left(\omega t - \int m dx\right)\right] \quad \ldots (1.36)$$

$$\left(\frac{\partial\phi}{\partial y}\right)_{y=0} = \frac{-a\omega}{\sinh md}\left[\sinh md\,\sin(\omega t - \int m dx) + \gamma\left\{\frac{md\cosh md + \sinh md}{\Pi^2\tanh md}\right.\right.$$

$$+ \frac{1}{\Pi\sinh md\cosh md}\left(md\cosh md + \frac{m^2d^2}{2}\sinh md\right)$$

$$\left.\left.-(\cosh md + md\sinh md)\right\}\cos(\omega t - \int m dx)\right]$$

$\cdots$ (1.37)

Equations (1.36) and (1.37) are found to satisfy equation (1.35)

Transforming the equations into Lagrange coordinates, with the X and Y components of the displacement of the particle, having the initial coordinates x and y, Biesel gives

$$X = \frac{a\sin(\omega t - \int m dx)}{\tanh md} + \gamma a\left\{\frac{1 + md\tanh md}{\Pi^2(\tanh md)^2}\right.$$

$$\left. + \frac{1}{\Pi\sinh md\cosh md}\left(md + \frac{m^2d^2}{2\tanh md}\right) - \left(1 + \frac{md}{\tanh md}\right)\right\}\cos(\omega t - \int m dx)$$

$\ldots$ (1.38)

$$Y = a\cos(\omega t - \int m dx) - \gamma a\left\{\frac{1}{\Pi^2}\left(\frac{1}{\tanh md} + \frac{md}{(\tanh md)^2}\right)\right.$$

$$\left. + \frac{1}{\Pi\sinh md\cosh md}\left[\frac{md}{\tanh md} + \frac{(md)^2}{2}\right] - \left[\frac{1}{\tanh md} + md\right]\right\}\sin(\omega t - \int m dx)$$

$\ldots$ (1.39)

Equations (1.38) and (1.39) can be more simply written as

$$X = a_0 A \sin(\omega t - \int m\,dx) + a_0 \gamma A_1 \cos(\omega t - \int m\,dx) \quad \ldots (1.40)$$

$$Y = a_0 B \cos(\omega t - \int m\,dx) + a_0 \gamma B_1 \sin(\omega t - \int m\,dx) \quad \ldots (1.41)$$

where A, A_1, B and B_1 are functions of md. The free surface equation can be expressed parametrically by the equations

$$\eta = x + a_0 A \sin(\omega t - \int m\,dx) + a_0 \gamma A_1 \cos(\omega t - \int m\,dx) \quad \ldots (1.42)$$

$$\lambda = a_0 B \cos(\omega t - \int m\,dx) + a_0 \gamma B_1 \sin(\omega t - \int m\,dx) \quad \ldots (1.43)$$

η and λ being the coordinates of a point on the free surface. The free surface slope of the wave is given by

$$S = \frac{\frac{d\lambda}{dx}}{\frac{d\eta}{dx}} = \frac{m a_0 B \sin(\omega t - \int m\,dx) + (-m\gamma a_0 B_1 + a_0 B)\cos(\omega t - \int m\,dx)}{1 - m a_0 A \cos(\omega t - \int m\,dx) + (m\gamma a_0 A_1 + a_0 A)\sin(\omega t - \int m\,dx)} \quad \ldots (1.44)$$

For the wave slope in the neighbourhood of a particle with the initial coordinates (x,o) at the instant when the particle crosses the plane y = 0 we then have

$y = 0$ or

$$B\cos(\omega t - \int m dx) + \gamma B_1 \sin(\omega t - \int m dx) = 0$$

Hence there are two sets of possible values for $\cos(\omega t - \int m dx)$ and $\sin(\omega t - \int m dx)$.

ie.

$$\cos(\omega t - \int m dx) = \frac{\gamma B_1}{B}\ ; \qquad \sin(\omega t - \int m dx) = -1 \qquad \ldots(1.45)$$

or

$$\cos(\omega t - \int m dx) = -\frac{\gamma B_1}{B}\ ; \qquad \sin(\omega t - \int m dx) = +1 \qquad \ldots(1.46)$$

Equation (1.45) corresponds to the passage of the front face of the wave, and equation (1.46) to the passage of the back face of the wave.

Combining equation (1.45) and (1.46) with (1.44) and noting that terms of γ^2 have been neglected we have:- for the front of the wave:

$$S_F = -m a_0 B - m^2 a_0^2 \gamma(AB_1 + A_1 B) - m a_0^2 AB \qquad \ldots(1.47)$$

and for the back of the wave:

$$S_B = m a_0 B - m^2 a_0^2 \gamma(AB_1 + A_1 B) - m a_0^2 AB \qquad \ldots(1.48)$$

The mean slope $S = \frac{1}{2}(S_F + S_B)$ is a measure of asymmetry of the wave.

Thus from equations (1.47) and (1.48)

$$S = -m^2 a_0^2 \gamma (A B_1 + A_1 B) - m a_0^2 A B \qquad \cdots(1.49)$$

Replacing A, B, A_1 and B_1 by their values we have

$$S = m^2 a_0^2 \gamma \left\{ \frac{3 + \frac{md}{\tanh md} - 3md \tanh md}{D^2 (\sinh md)^2 \tanh md} \right\} \qquad \cdots(1.50)$$

where $$D = 1 + \frac{md}{\sinh md \cosh md} \qquad \cdots(1.30)$$

As pointed out by Biesel[5] the analysis above assumes that the slope of the bottom is small.

This theory had not previously been tested experimentally, and its verification formed part of the present work (See Appendix 4). Satisfactory agreement was obtained, and this enabled Biesel's theory to be adapted to the description of the asymmetrical velocities associated with wave slope asymmetry.

1.4 Wave Vertical Asymmetry

The 'wave vertical asymmetry' is defined in this work as

$$\frac{\text{vertical distance from crest to s.w.l}}{\text{total wave height}}$$

The experimental results are compared with the cnoidal wave theory expression corresponding to the wave vertical asymmetry given by

$$\frac{y_c - d}{H} = \frac{16 d^3}{3 L^2 H}\left[K(k)\left(K(k) - E(k)\right)\right] \qquad \ldots (1.11)$$

All the necessary functions and graphs are obtained from 'CNOIDAL WAVE TABLES OF FUNCTIONS' Masch and Wiegel[34].

1.5 Wave Horizontal Asymmetry

In order to completely define the asymmetry of the wave in shoaling water, note has to be taken of the assymmetry of the wave in the horizontal sense too. For this purpose, two types of wave horizontal asymmetry are noted and are given the symbols HA and HA'. They are defined as follows:

$$HA = \frac{\text{Horizontal distance from crest to front face at s.w.l}}{\text{Horizontal distance from crest to back face at s.w.l.}}$$

$$HA' = \frac{\text{Horizontal distance from crest to proceding wave trough}}{\text{Horizontal distance from crest to following wave trough}}$$

The definition sketch is shown in figure 1.2.

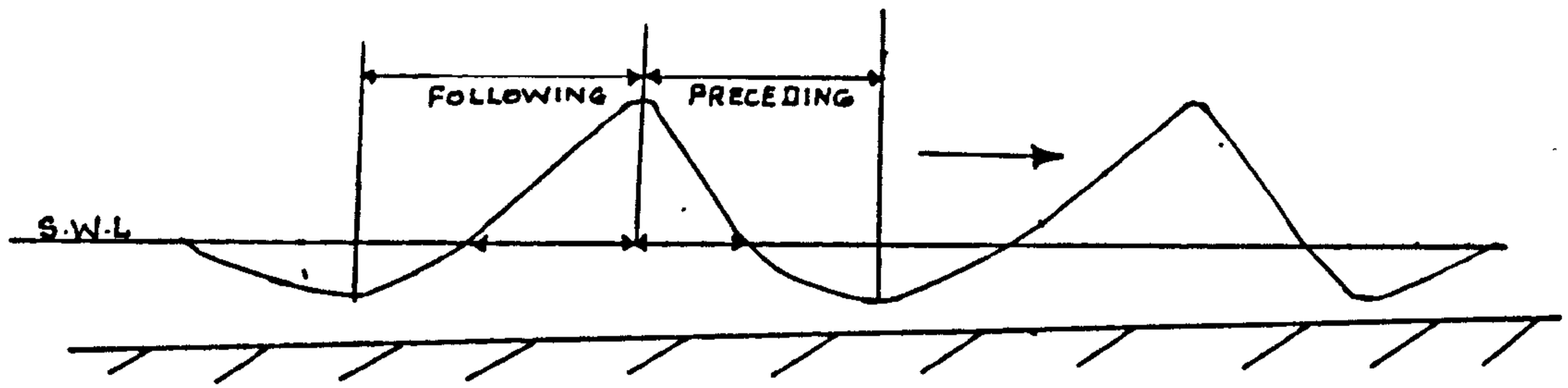

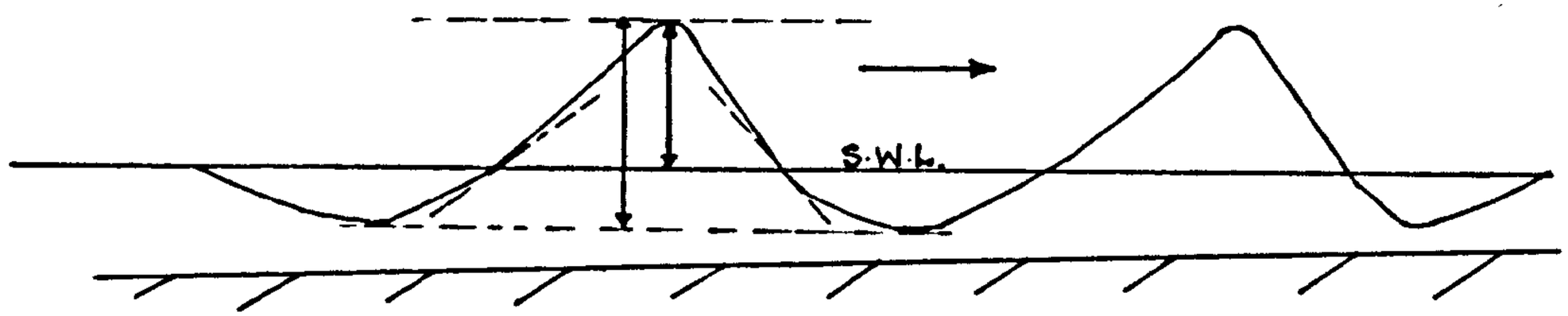

Figure 1.2

As far as the author is aware, there is not theory describing wave horizontal asymmetry for shoaling waves.

As will be shown later in this work it was found that the two types of wave horizontal asymmetry ie. HA and HA' follow the same trend. It was found possible therefore to produce an empirical relationship expressing one in terms of the other. Except in a quantitative sense therefore, one can refer to wave horizontal asymmetry to denote either HA or HA' or both, without much loss of generality. As shallow water waves are akin to long waves, it is evident from the definitions of HA and HA' that measurement of HA would give much better precision than HA'.

Later in this work an expression is given for the wave horizontal asymmetry HA based on the theoretical expression for the wave vertical asymmetry from the Cnoidal wave theory.

1.6 Horizontal Velocity Asymmetry

The horizontal velocity of the fluid particle in the neighbourhood of the breakers has a higher magnitude in the onshore direction than in the offshore direction, but the duration of the forward motion is less than that of the backward motion. This behaviour thus leads to a definition of two types of horizontal velocity asymmetry; one based on magnitude and the other on time. They are defined as follows:

Horizontal velocity (magnitude) asymmetry =

$$\frac{\text{Maximum horizontal shoreward velocity}}{\text{Maximum horizontal seaward velocity.}}$$

Horizontal velocity (time) asymmetry =

$$\frac{\text{Time for the shoreward motion}}{\text{Time for the seaward motion}}$$

The significance of both types of horizontal velocity asymmetry are discussed later in the work, as well as the effect of backwash on the velocity asymmetry and also the use of the time history of the velocity curve as a criterion for predicting sediment motion.

1.7 Mass Transport

The engineer concerned with the movement of sediment must take account of every aspect of fluid motion in the neighbourhood of the particles. The net movement is predominantly affected by any lack of symmetry in this motion. This may exist in the form of a prevailing wind direction, velocity or duration differences in the flood and ebb currents of the tide, or in the oscillatory motion of the waves. The present study is concentrated on wave shape asymmetry. It is, however, appreciated that other influences are present, and the phenomenon of mass transport is one of the more important of these. Even with waves of the low amplitude sinusoidal type, it is clear that the derivation of the expression for particle orbital motion, based on the assumption that the position of the particle can be expressed by fixed coordinates, does not give a true description of the motion. In other words, even with a wave of symmetrical shape, asymmetry of particle motion can occur, even though the fluid is inviscid.

Stokes analysis led to the following expression for the velocity of mass transport in deep water:-

$$\bar{U} = \frac{1}{2}\left(\frac{\pi H}{T}\right)\left(\frac{\pi H}{L}\right)\frac{\cosh 4\pi\left(\frac{y_o+d}{L}\right)}{\sinh^2 \frac{2\pi d}{L}} \qquad \ldots(1.51)$$

The observation that a marked mass transport velocity

occurred at the bed, in a way not predicted by Stokes, led to Longuet-Higgins[31] analysis, based on the assumption of vorticity generation close to the boundary. Longuet-Higgins evaluation of the mass transport or drift velocity is given by:

$$\overline{U} = \frac{1}{4}\left(\frac{\pi H}{T}\right)\left(\frac{\pi H}{L}\right)\frac{1}{\sinh^2 \frac{2\pi d}{L}}\left\{2\cosh\left[\frac{4\pi d}{L}\left\{\frac{y}{d}-1\right\}\right] + 3 + \frac{2\pi d}{L}\left[\frac{3y^2}{d^2}-\frac{4y}{d}+1\right]\sinh\frac{4\pi d}{L}\right.$$

$$\left. + 3\left(\frac{\sinh\frac{4\pi d}{L}}{\frac{4\pi d}{L}} + \frac{3}{2}\right)\left(\frac{y^2}{d^2}-1\right)\right\} \quad \cdots(1.52)$$

Russell and Osorio[42] were able to obtain satisfactory experimental confirmation of the validity of this expression, but only in the regions remote from the influence of the backflow from the beach. Mass transport currents certainly exist almost up to the breakers, but their velocity is not accurately predicted by theory.

As Allen and Gibson[1] have remarked, if the mass transport effect occurs in nature to the scale predicted, bed current velocities of 0.97 ft./sec. would occur for waves of period 10 seconds with a wave height 10 ft., in a water depth of 30 ft., and these would be of considerable significance.

For the present purpose, however, the effect of wave shape asymmetry on mass transport velocity in the zone close to the breakers has had to be left as an implicit factor in the asymmetrical velocities measured from studies of single wave cycles.

CHAPTER 2

APPARATUS, MEASURING TECHNIQUES AND EVALUATION OF RESULTS

2.1 Type of Model and Choice of Variables

The work described in this thesis involved careful control of several parameters, and it was considered that an hydraulic model approach was the only way of studying the different variables in a closely controlled manner. In addition a model study allows visual observation of the phenomena by the use of transparent windows in the side of the flume. It is evident that the regularity associated with monochromatic waves rarely, if ever, occurs in nature. Nevertheless, past experience has shown that it is often possible to accept such a simplification, especially when this is designed to identify and compare processes which would be obscured under irregular or random conditions.

The use in the present study of an hydraulic model with an impermeable beach slope, was regarded as an intermediate step leading eventually to an equivalent study in a loose boundary model. The choice of variables was therefore made in the light of recent experiments by Kemp[20,21] and Plinston[40] of wave action on granular beaches. These examined amongst

other things the variation of beach slope with wave characteristics, and the phase relationship between two successive waves breaking on the beach. These experiments showed clearly that the wave characteristics, beach slope and phase difference were inter-related, the relationship changing with variations in beach material.

It was considered necessary for the present study to be able to accentuate beach slope effects in order to examine variations in the internal particle velocities. In addition, the elimination or reduction of the backwash could most satisfactorily be achieved on a plane rigid slope. It followed therefore that although the results of experiments made on such a beach would be directly related to the loose boundary case, the wave/beach interaction would not be the same. The change of beach slope using a plane beach and constant wave characteristics is equivalent to a change in beach material size, although the effect of permeability is not allowed for. Nevertheless, the reduction in phase difference with increasing beach slope, and higher backwash velocities are both produced, and are important factors in the movement of beach material.

From these considerations, and those relating to the construction of the apparatus and the time available, it was decided to hold the wave characteristics constant for

the main part of the study. It was thus essential to examine these wave characteristics in relation to previous work and existing theory.

The main variables were (a) the beach slope, and (b) the reduction or elimination of the backwash.

2.2 Description of Wave Generating and Measuring Apparatus

2.2.1 Wave Flume

The overall size of the apparatus was limited by the space available. The wave flume was 24ft. long, 9 inches wide, and 15 inches deep. At the wave generator end, the bed of the channel sloped down to a depth of 21 inches. The channel was made of marine plywood, with the exception of long perspex windows which formed the sides of the channel at the beach end. These enabled the hydrogen bubble tracers used for velocity measurements to be illuminated by back-lighting, and photographed through the front window by cine camera.

A satisfactory convex shaped slatted wave absorber was built behind the paddle to damp out reflections from the generator end. The beach was plane, rigid and impermeable made of marine plywood, and stiffened at the back with an I section to prevent vibration of the beach. The toe of the beach was hinged to the beach plate. A

false toe was used for the flat beach slope in order to contain the beach in the tank. The upper end of the artificial beach was supported by a vertical screwed rod by which the beach slope was raised. Plate 1 shows the beach arrangement.

2.2.2 The Wave Generator

The wave generator was of the paddle type, driven by a 1 H.P. 3 phase Induction motor at 930 rpm. A "Kopp" variable speed gear box was used for speed variation. This enabled wave periods in the range 0.3 - 3.0 seconds to be produced. An eccentric permitted variation in the throw of the connecting rod and thus varied the wave amplitude. The paddle itself was a 0.2 inch thick Dural Aluminium plate. It was 21 ins high and hinged at the base to the bed of the channel. The wave generator is shown on Plate 2.

2.2.3 Wave Quality

In nature, waves on reaching the beach or any other coastal structure would be wholly or partially reflected seawards, usually on a journey of no return. Within the limited laboratory flume the position is quite different; the wave reflected from the beach end would be re-reflected at the wave generator, and so return to the beach.

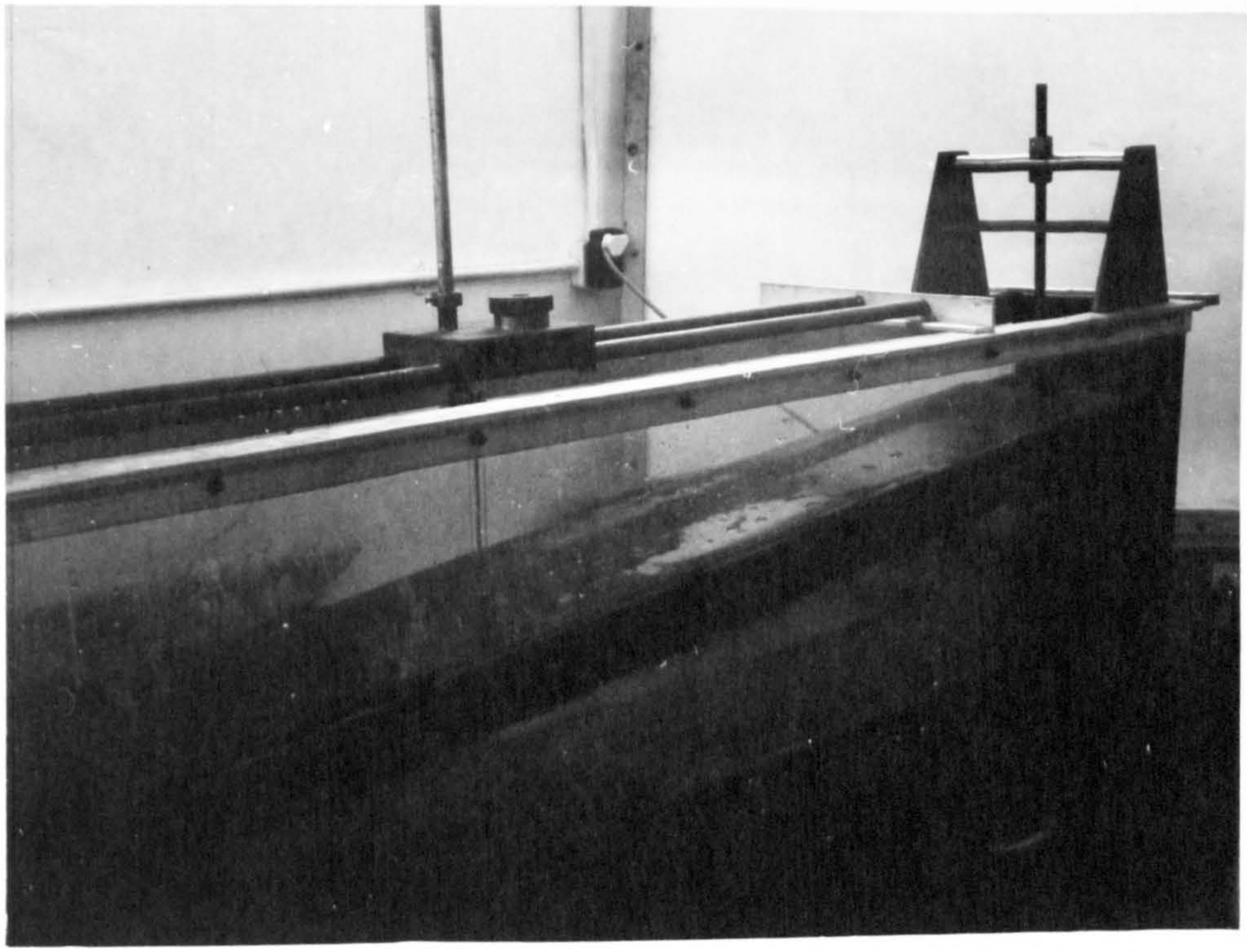

Plate 1

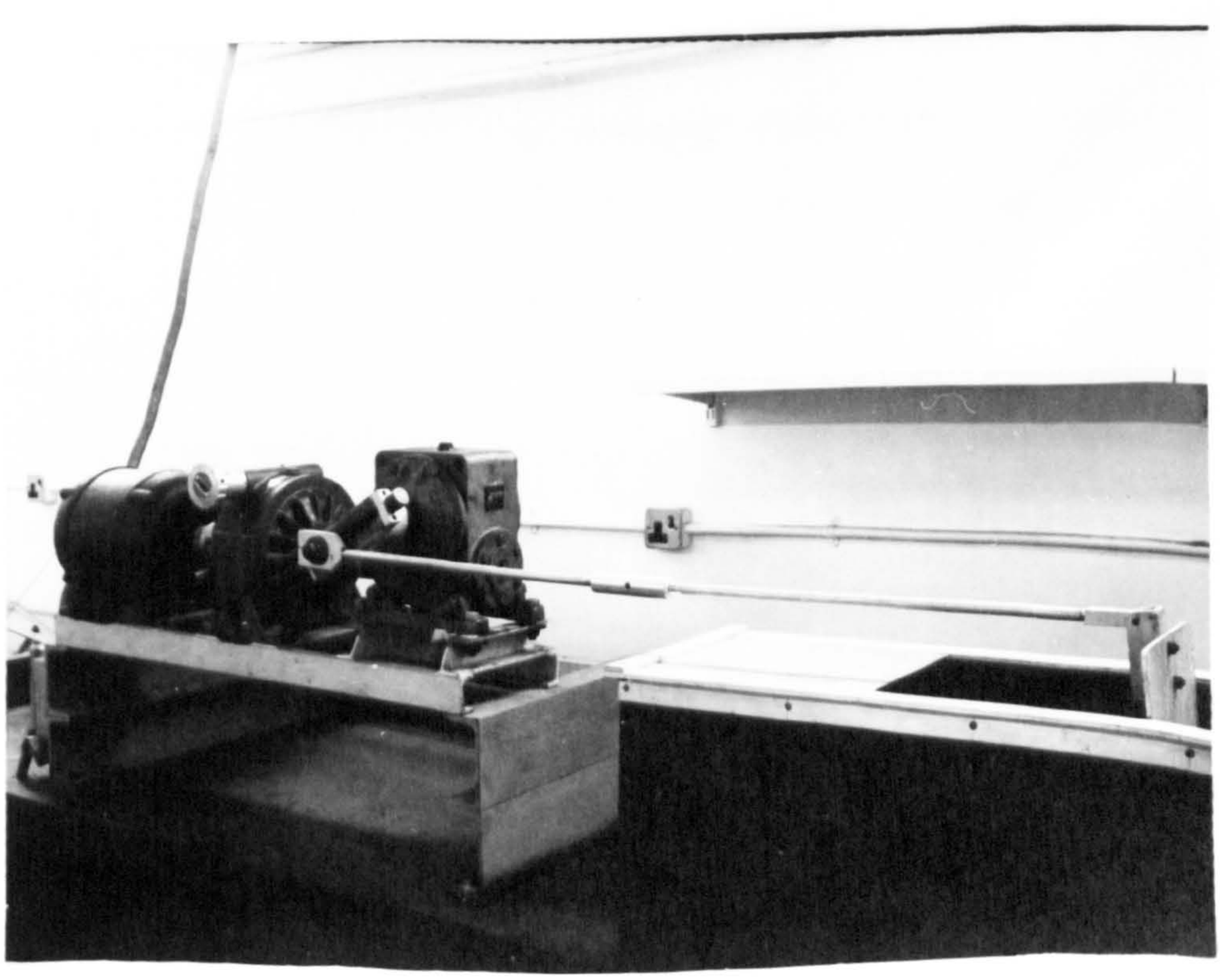

Plate 2

Clearly then, in the absence of a suitable filter this reflection and re-reflection will persist, and the model conditions will be far different from those obtained in nature. Another consequence is that these successive reflections will give to the surface of the water, between the wave machine and the beach, a disorderly agitation which will affect the measurements to a large extent.

The filters used in the present work consisted of $\frac{1}{2}$ ins chicken mesh folded many times so as to suitably occupy the width of the channel for a length of $6\frac{1}{2}$ft. The filters were placed at a suitable distance in front of the paddle. The filters are shown in Plate 3.

A special feature of the design was that the motor and reduction gears were mounted on a very strong support, and were quite separate from the channel. Thus there would not be any vibration of the flume arising from the machinery. The quality of the wave produced in this work was satisfactory, there being negligible variation in height or shape along the constant depth portion of the channel.

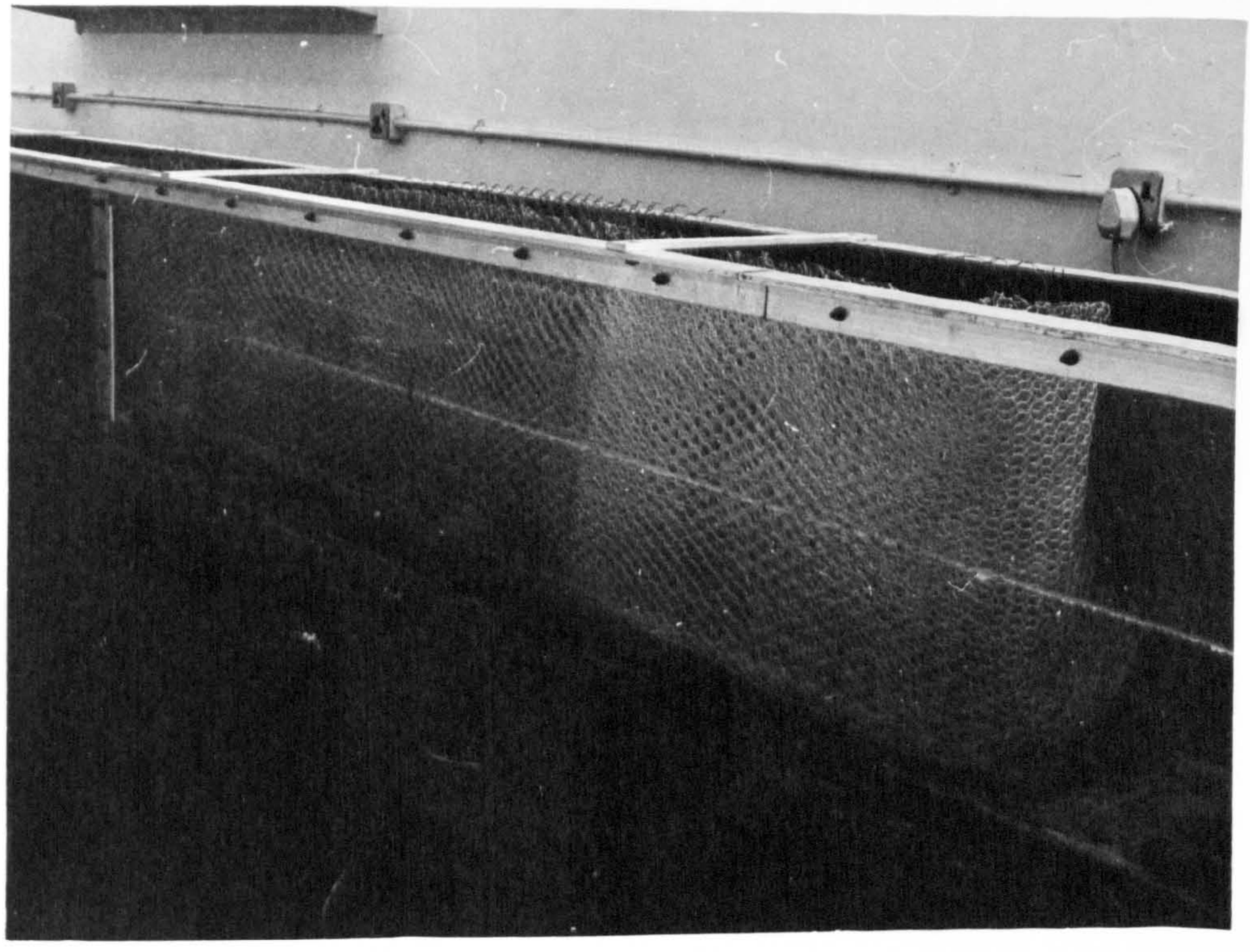

Plate 3

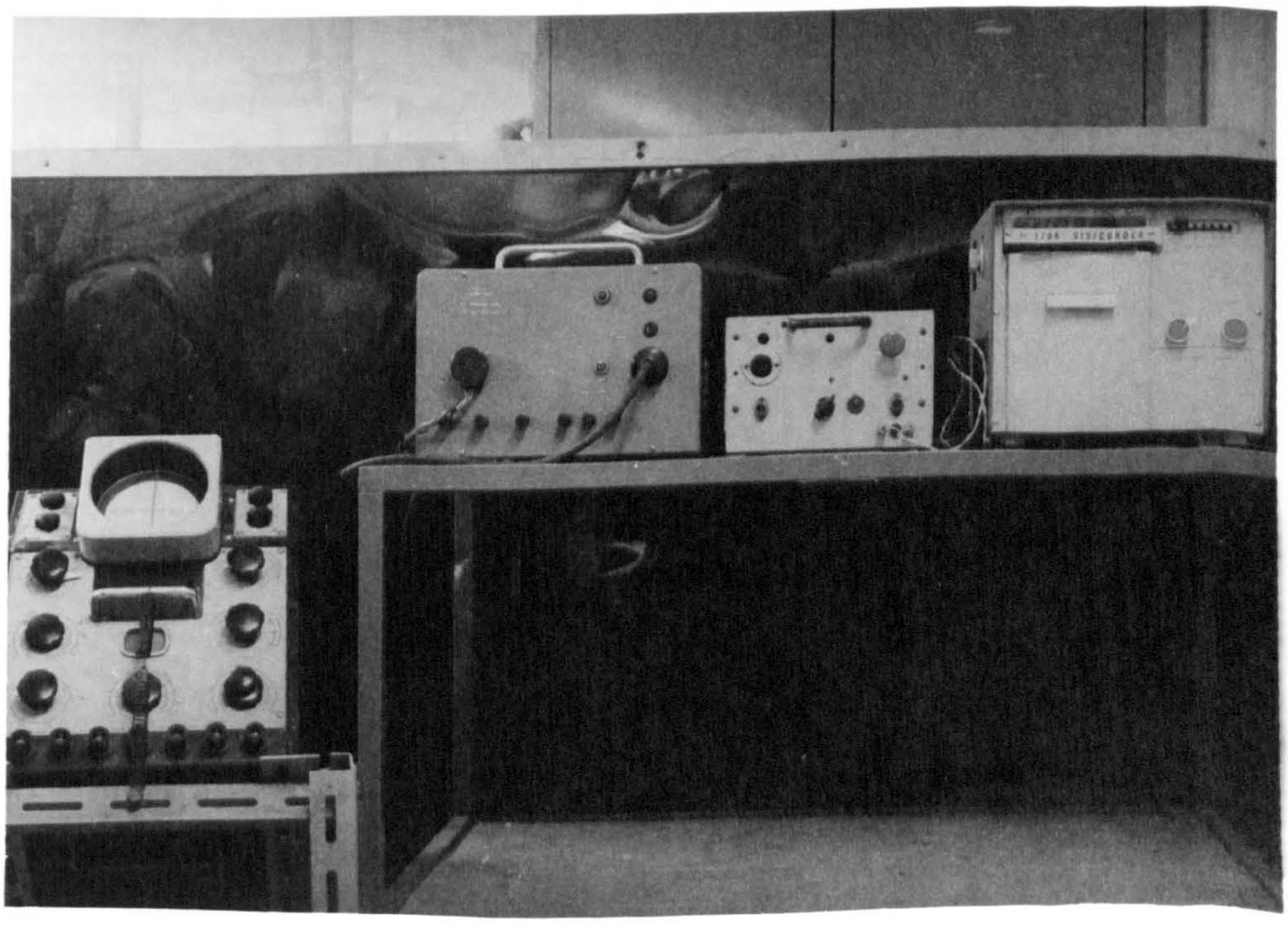

Plate 4

2.2.4 Capacitance-Wire Probe for Wave Measurement

The wave lengths were measured by using two capacitance-wire probes. The output wave form from the wave meter was displayed on a D.C. oscilloscope. The wave meter was a frequency modulated system, employing capacitance-wire probes to detect the changes in water level. This arrangement allowed visual observations to be made on D.C. oscilloscope.

The two probes were suspended separately on a carriage with the ends inserted in water in the tank to the mean operating depth, and the leads connected to a junction box which was fitted to take up to four capacitance probe leads. The two probes were tried at various positions apart one on each side of the section for which the wave length was required, the object being to synchronise the wave forms on the oscilloscope. The method was certainly not without some difficulties but it proved satisfactory on the whole. The capacitance-wire probe together with the oscilloscope was also used for locating the break-point. The method is described later in this chapter.

The design of the capacitance-wire probe was based on the apparatus described by M.J. Tucker and H. Charnock[49]. The wave height and the wave shape at the different positions along the beach were found by using the capacitance-wire probe system in conjunction with a

"visicorder" - ultra violet type instrument, giving a permanent trace on paper. This recorder offers 8 paper speeds (6 to 800 mm/sec) and also 0.1 and 1 second timing intervals. The timing interval of the Visicorder used in this work was 0.1 sec, and the paper speed used depended on the type of measurement involved. The frequency response of the galvanometer used in the visicorder was 0 - 50 cycles per second. Plate 4 shows the assembly of the stabilised power supply, wave meter, 1706 Visicorder and the oscilloscope.

Cine photography and the hydrogen bubble technique were used for the velocity studies. The method is described and discussed in this chapter in section 2.5.

2.2.5 Elimination of Backwash

A pump was used in connection with the study of the effect of elimination of the backwash. This is described later in this chapter in section 2.7.

2.3 Preliminary experiment Concerning tank Performance

2.3.1 Note

In order to assess the quality of the generated wave, the suitability of the wave filter, and the overall suitability of the wave tank including the beach, some preliminary experiments were carried out. These were designed to choose the wave characteristics to be used in the main experiments, to determine the amount of wave reflection in the wave tank for the six beach slopes treated in this work, and finally to compare the measured values of the wave length with those based on the cnoidal wave theory.

Two graduated scales were made on the side of the wave channel for the purpose of reading the still water depth. The scales were graduated in $\frac{1}{10}$ of an inch divisions.

Several sets of waves were generated by varying the wave period and the deep water wave height with the intention of selecting suitable wave characteristics, and also finding the position on the horizontal portion of the channel at which the wave had become steady. This enabled a wave measuring station to be chosen in the horizontal section of the channel. For this aspect of the experiment a single capacitance-wire probe was used and the wave height was read off from the oscilloscope.

The wave characteristics selected were: - Period T = 0.8 sec. Ho = 1.45 ins. and horizontal section still water depth = 9.5 ins. These wave characteristics were held constant. The beach slopes used were $\frac{1}{4}$, $\frac{1}{6}$, $\frac{1}{9}$, $\frac{1}{12}$, $\frac{1}{15}$ and $\frac{1}{18}$.

2.3.2 Determination of the Amount of Wave Reflection in the Wave Tank

An experiment was conducted to determine the amount of wave reflection in the wave tank so that the incident wave height could be deduced.

The experiment was first carried out for the beach slope of $\frac{1}{4}$. With the wave generator on, the capacitance wire probe was positioned in the horizontal portion of the channel. Then the wire probe was very steadily moved a total distance of about three feet along the length of the channel in the zone of constant depth. The resulting profiles of the wave trains were obtained from the ultra violet recorder. The experiment was repeated for each of the beach slopes $\frac{1}{6}$, $\frac{1}{9}$, $\frac{1}{12}$, $\frac{1}{15}$ and $\frac{1}{18}$.

The analysis was based on the assumption that in the presence of the incident wave and the reflected wave trains, the resulting wave trains will be irregular. The highest value of the observed wave height in the

wave train will correspond to the situation where the incident and the reflected waves are in phase and additive, while the minimum value corresponds to the situation where the incident and the reflected waves are in phase but subtractive.

Let HI be the height of the incident wave and H_R the height of the reflected wave. Then the incident wave may be given by

$$y_{sI} = \frac{H_I}{2} \cos 2\pi\left(\frac{x}{L} - \frac{t}{T}\right) \quad \cdots(2.1)$$

and for the reflected wave

$$y_{sR} = \frac{H_R}{2} \cos 2\pi\left(\frac{x}{L} + \frac{t}{T}\right) \quad \cdots(2.2)$$

The resultant water surface for these two waves travelling in opposite directions is

$$y_s = \frac{H_I}{2} \cos 2\pi\left(\frac{x}{L} - \frac{t}{T}\right) + \frac{H_R}{2} \cos 2\pi\left(\frac{x}{L} + \frac{t}{T}\right) \cdots(2.3)$$

i.e. $$y_s = \frac{1}{2}\left(H_I + H_R\right) \cos\frac{2\pi x}{L} \cos\frac{2\pi t}{T} + \frac{1}{2}\left(H_I - H_R\right) \sin\frac{2\pi x}{L} \sin\frac{2\pi t}{T} \quad \cdots(2.4)$$

The envelope of Ys has a maximum H max of HI + H_R at $x = 0, \frac{L}{2}$, L etc. and a minimum H min of HI - H_R at $x = \frac{L}{4}, \frac{3L}{4}$ etc.

so we have

$$H_{max} = H_I + H_R \quad \ldots(2.5)$$

$$H_{min} = H_I - H_R \quad \ldots(2.6)$$

Adding and subtracting

$$2H_I = H_{max} + H_{min} \quad \ldots(2.7)$$

$$2H_R = H_{max} - H_{min} \quad \ldots(2.8)$$

Thus the coefficient of reflection is

$$\frac{H_R}{H_I} = \frac{H_{max} - H_{min}}{H_{max} + H_{min}} \quad \ldots(2.9)$$

The lowest value of the coefficient of reflection was found to be about 3% for the flattest beach slopes used in this work, and the highest value was about 8% for the steepest slopes of $\frac{1}{4}$ and $\frac{1}{6}$. These values correspond with typical values from Miche[37].

2.3.3 Preliminary Experiment on Wave Length Measurement

As a preliminary experiment on wave length measurements, observations of wave length were made at different positions on the beach, for each of the six beach slopes, and the results compared with theoretical values.

Two capacitance-wire probes were used in this experiment as already described in paragraph 2.2.4. Some of the graphs of experimental $\frac{d}{L}$ against theory are shown in figures 2.1, 2.2 and 2.3. Deviations between the experimental results and the theory were found to be of the order of about 9% which was considered quite acceptable bearing in mind that the measurements were made on a sloping beach.

Prior to the study reported in this thesis, the wave tank was also used by the author in a pilot experiment on the effect of degree of beach permeability on wave characteristics and judging from the fact that the results showed good agreement with those of Bretschneider and Reid[6] and Reid and Kajiura[41] the wave tank and the experimental techniques were considered suitable for the projected study.

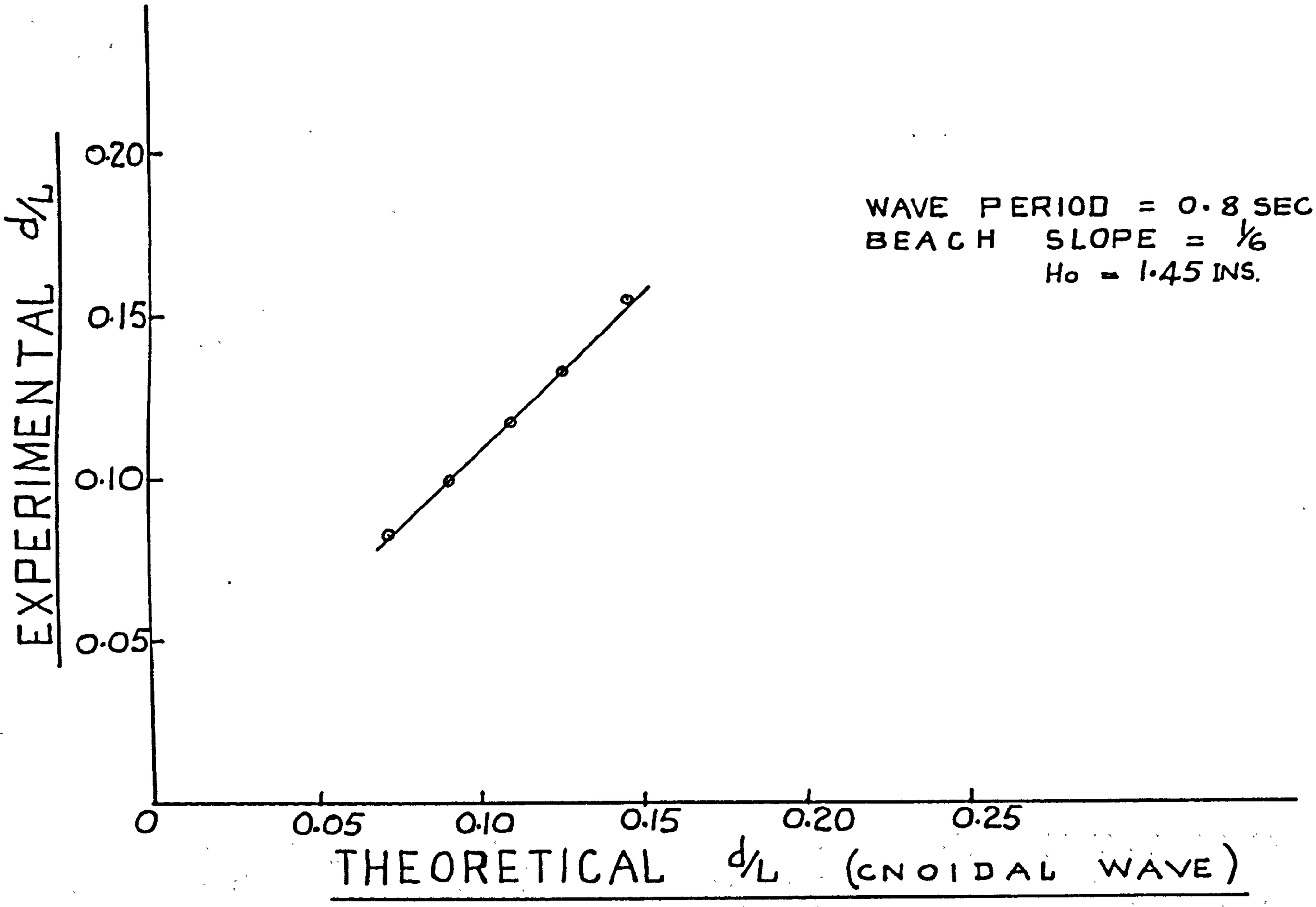

WAVE PERIOD = 0.8 SEC.
BEACH SLOPE = 1/6
Ho = 1.45 INS.

Figure 2.1 Graph of Experimental d/L against Theory.

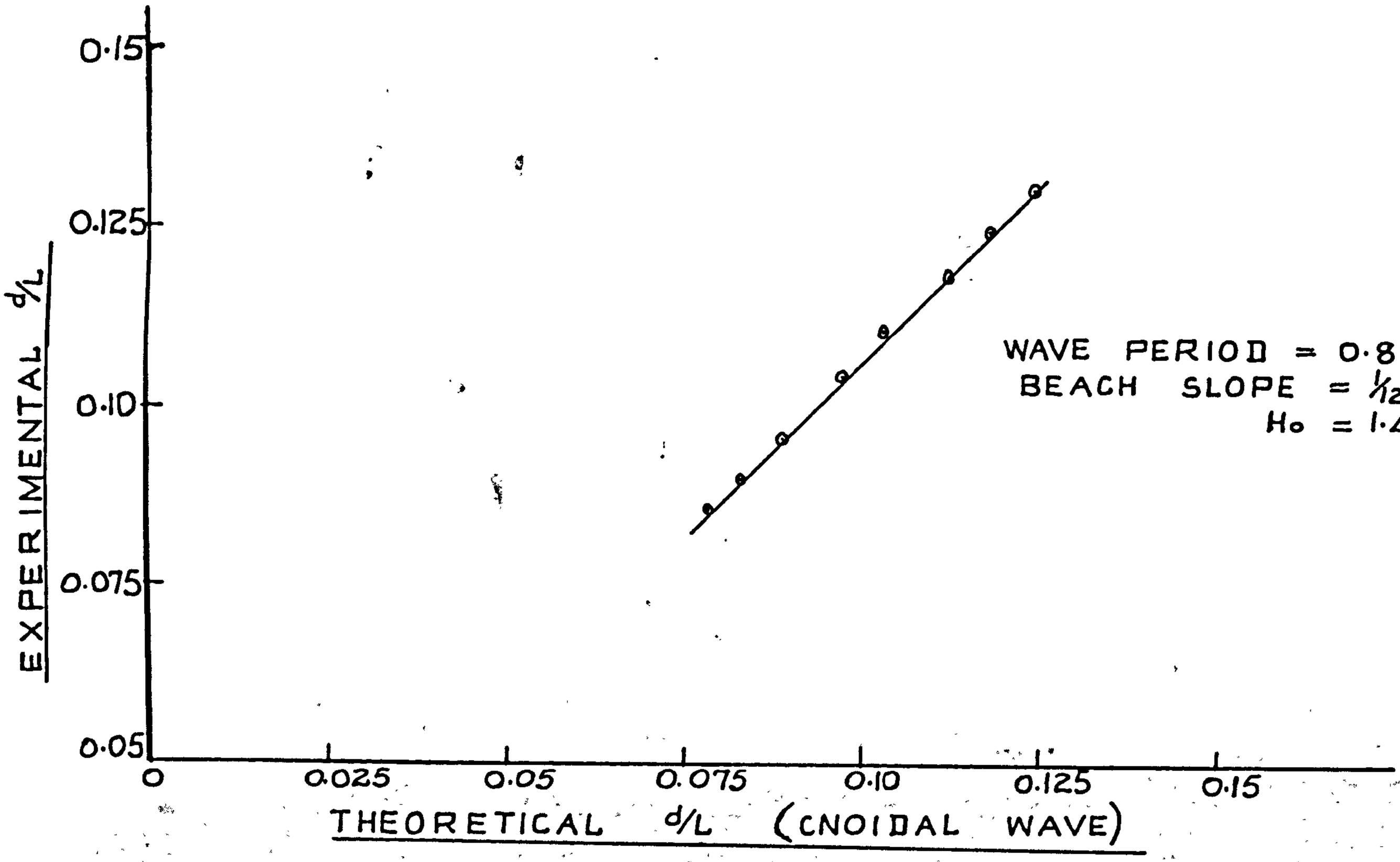

Figure 2.2 Graph of Experimental d/L against Theory

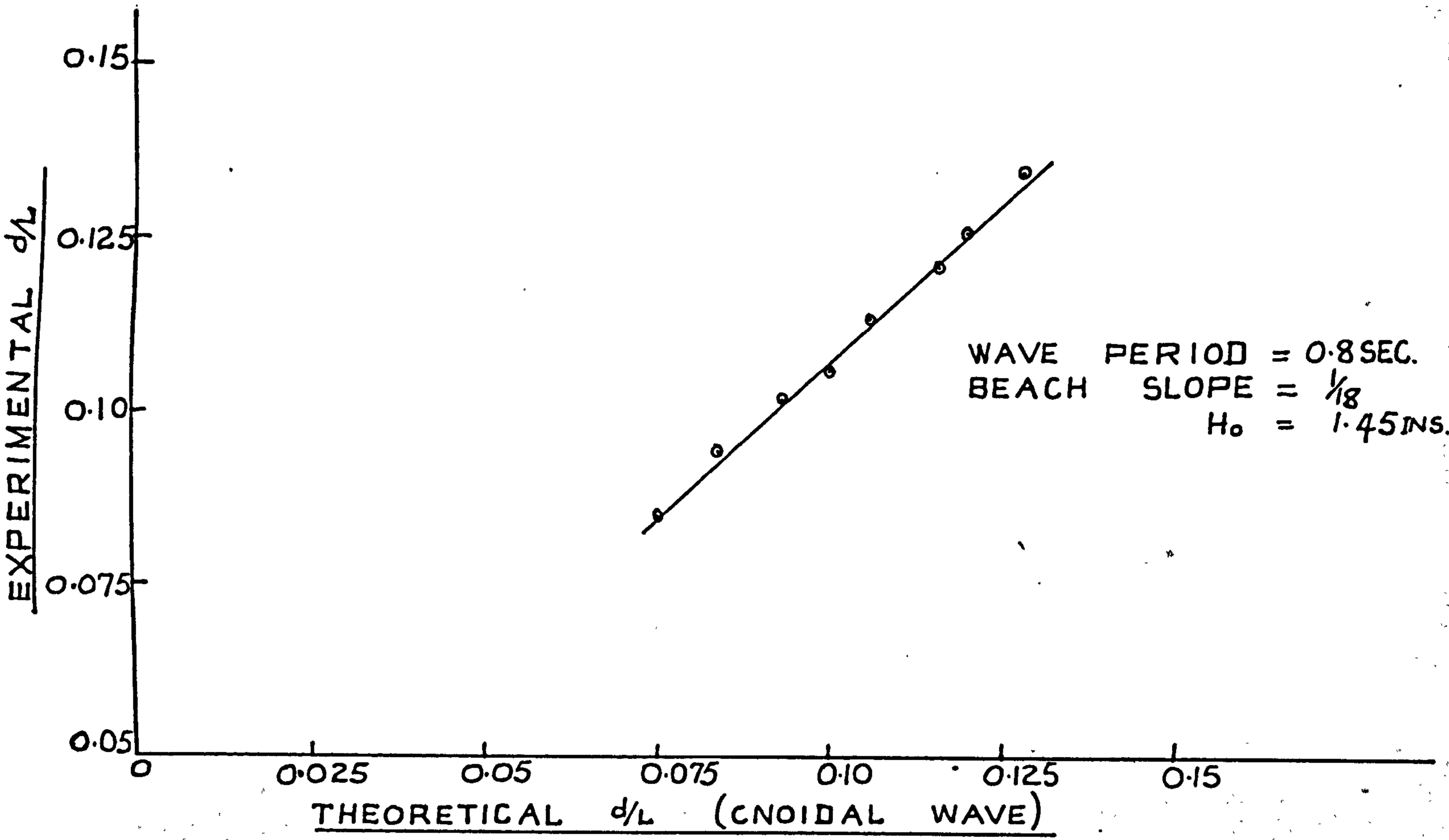

Figure 2.3 Graph of Experimental d/L against Theory

2.4 Measuring Technique and Evaluation of Wave Asymmetry

2.4.1 General Procedure

The set of apparatus used in the experiment consisted of the Ultra Violet Recorder, a wave meter, and the oscilloscope. A capacitance wire probe was used to obtain the wave profile at a particular position and two probes for the wave length measurements. The six beach slopes were studied in this way.

The first step for every beach slope was to locate the wave break-point by using the capacitance-wire probe and noting the deflection registered on the oscilloscope. It is generally known that as the wave moves into shoaling water, the wave height first decreases and then increases and is maximum at the break-point. So the method used to locate the break-point was to place the capacitance wire probe at several marked places very close to each other in the neighbourhood of the position where the wave was visually observed to be breaking. The position at which the wave height was a maximum and shoreward of which the wave lost its wave form was selected as the wave break-point.

The location of the wave break-point was followed by the marking out of the several positions along the beach where the detailed study of the wave asymmetry was to be made. The capacitance wire probe was positioned at each of the places marked out, and while

the wave generator was switched off a line corresponding to the s.w.l. was defined on the recording paper. This was done at the start and end of every reading.

After marking out the s.w.l. line the wave generator was then switched on. With the capacitance wire probe still in position the visicorder was then also switched on, and the wave profile for the particular position of the wire probe were recorded. The wave length measurements were then made using the method already described.

The probe position was then changed and by repeating the processes again for each probe position the wave trace and wave length measurements were obtained for the different positions marked out along the beach, up to the breakpoint. At the end of such a series of experiments a calibration test was carried out for the particular setting of the visicorder. This was done with the wave generator switched off. The initial reading on the visicorder was noted. Then with the wire probe still in position, the water depth was increased by $\frac{1}{4}$ ins. and the corresponding deflection on the visicorder was also noted. The water depth was further increased in step of $\frac{1}{4}$ ins. to obtain about five readings of the deflection on the visicorder. The change in deflection of the visicorder was found to be constant for every $\frac{1}{4}$ ins. change in water depth. This thus gave the

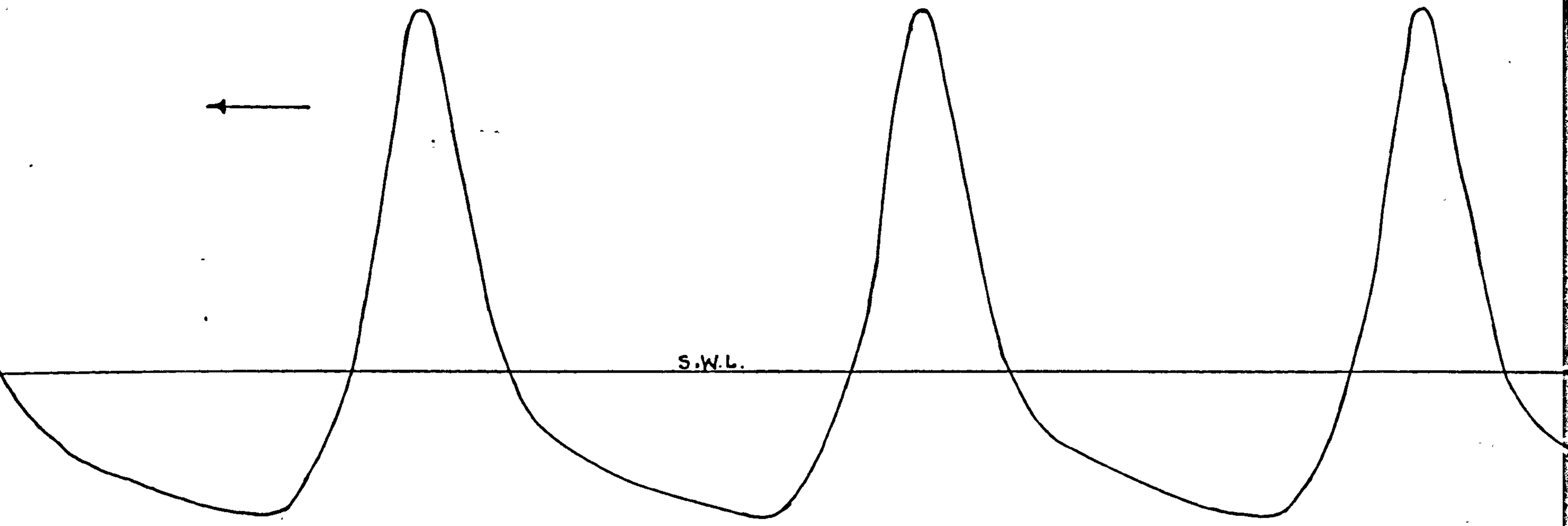

Figure 2.4 Sample Wave Trace.

multiplying factor for obtaining the wave height values from the wave traces. Sample wave traces are shown in figure 2.4.

2.4.2 Evaluation of Wave Vertical Asymmetry

The s.w.l. mark lines on the wave trace paper, one at the start and the other at the end of every reading for every position of the capacitance-wire probe were joined, thus providing the s.w.l line from which measurements were made. The more desirable thing was to have the s.w.l. line corresponding to the datum line of the visicorder as this would always appear on the wave trace. However, having obtained the s.w.l. line on the trace paper, both the measurements of the vertical distance from the wave crest to the s.w.l and the total wave height were scaled off. The wave vertical asymmetry is defined as

$$\frac{\text{Vertical distance from the wave crest to s.w.l}}{\text{total wave height.}}$$

2.4.3 Evaluation of Wave Horizontal Asymmetry

Two alternative definitions of horizontal asymmetry are possible. The evaluation of these two values HA and HA' required the measurements of the horizontal distances from crest to the front and rear faces of the wave at s.w.l., and the horizontal distances from crest to the preceding and the following wave trough.

The two types of wave horizontal asymmetry HA and HA' have already been defined as

$$HA = \frac{\text{Horizontal distance from crest to front face at s.w.l.}}{\text{Horizontal distance from crest to back face at s.w.l}}$$

and

$$HA' = \frac{\text{Horizontal distance from crest to preceding wave trough}}{\text{Horizontal distance from crest to following wave trough}}$$

2.4.4 Evaluation of Wave Slope Asymmetry

In the evaluation of the wave vertical asymmetry and the wave horizontal asymmetry any scale exaggeration of the output wave trace from the visicorder would be of no importance, as the wave vertical asymmetry and the wave horizontal asymmetry are dimensionless ratios, of which the terms involved are either both horizontal measurements or both vertical measurements, in which case any scale exaggeration of the output wave trace would cancell out.

On the other hand, the wave slope asymmetry is measured in radians, and because of the scale exaggeration of the wave trace, the profile had to be reproduced to the natural scale from the wave trace.

To evaluate the wave slope asymmetry, the angles made by the front and rear faces of the wave with the still water level line were measured in degrees and then

converted into radians. The wave slope asymmetry is defined as

$\frac{1}{2}$(front face slope at s.w.l. + back slope at s.w.l) radians

The front face slope was taken as negative and the back face slope as positive. Thus a negative mean slope would indicate that the wave front is steeper than the rear face slope.

2.5 Measuring Techniques and Evaluation of Velocity Asymmetry

The technique used for the velocity measurements is a method usually called the "Hydrogen bubble method". Essentially it consists of a fine wire which forms the negative electrode of a D.C. circuit, while two small metal plates, positioned at each side of the tank with a reasonable depth of the metal inside the water, serve as the second electrode. Hydrogen bubbles are formed on the negative electrode. The arrangement was such that the support for the wire and the metal plates serving as the positive electrode were integral, see plate 5. Two advantages of such an arrangement were that, as measurements were made at different positions along the beach, the apparatus could be moved intact. Secondly it was found that the quality of the bubbles was affected when the positive electrode was not close enough to the wire, as the circuit then became weak.

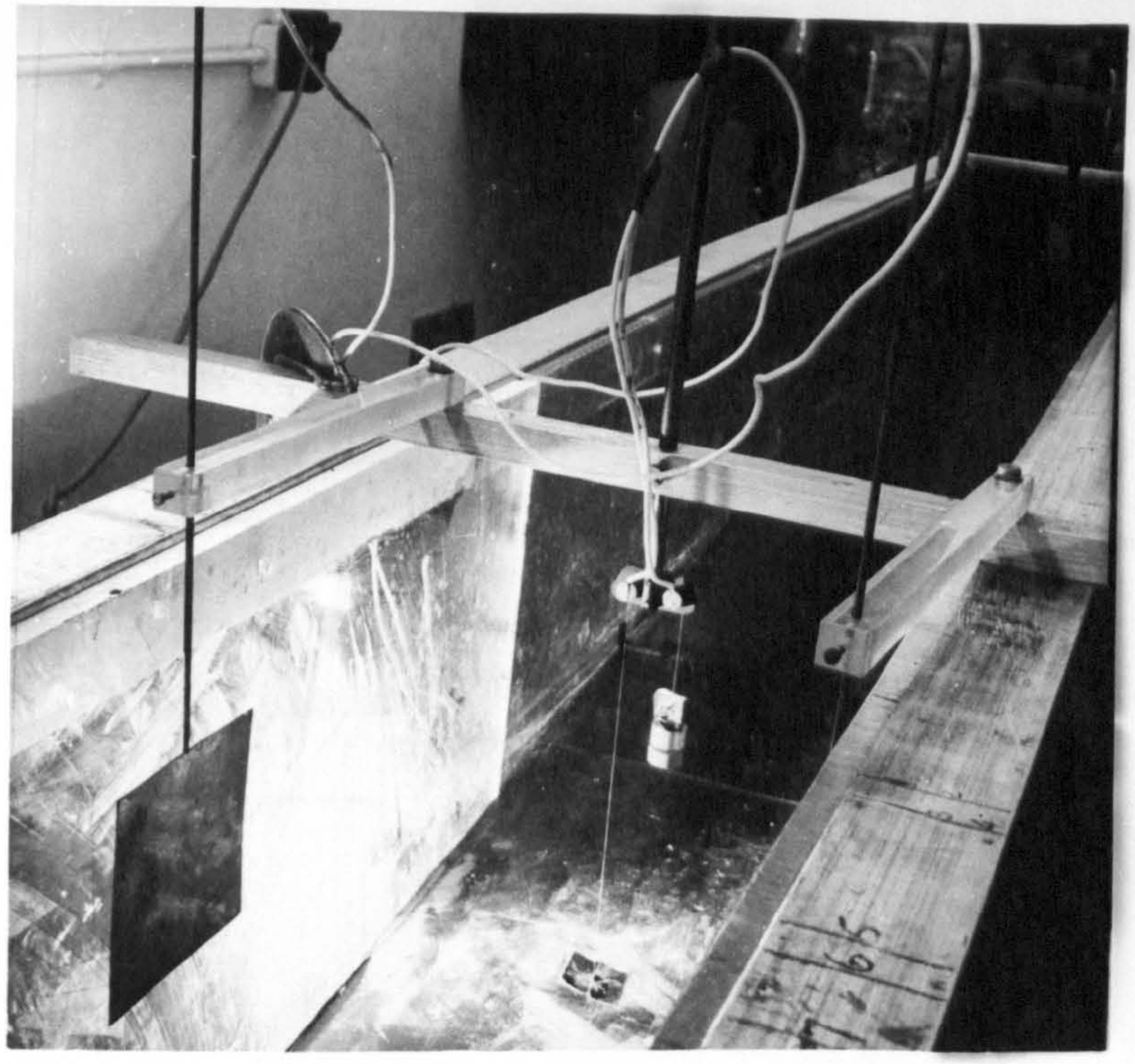

Plate 5

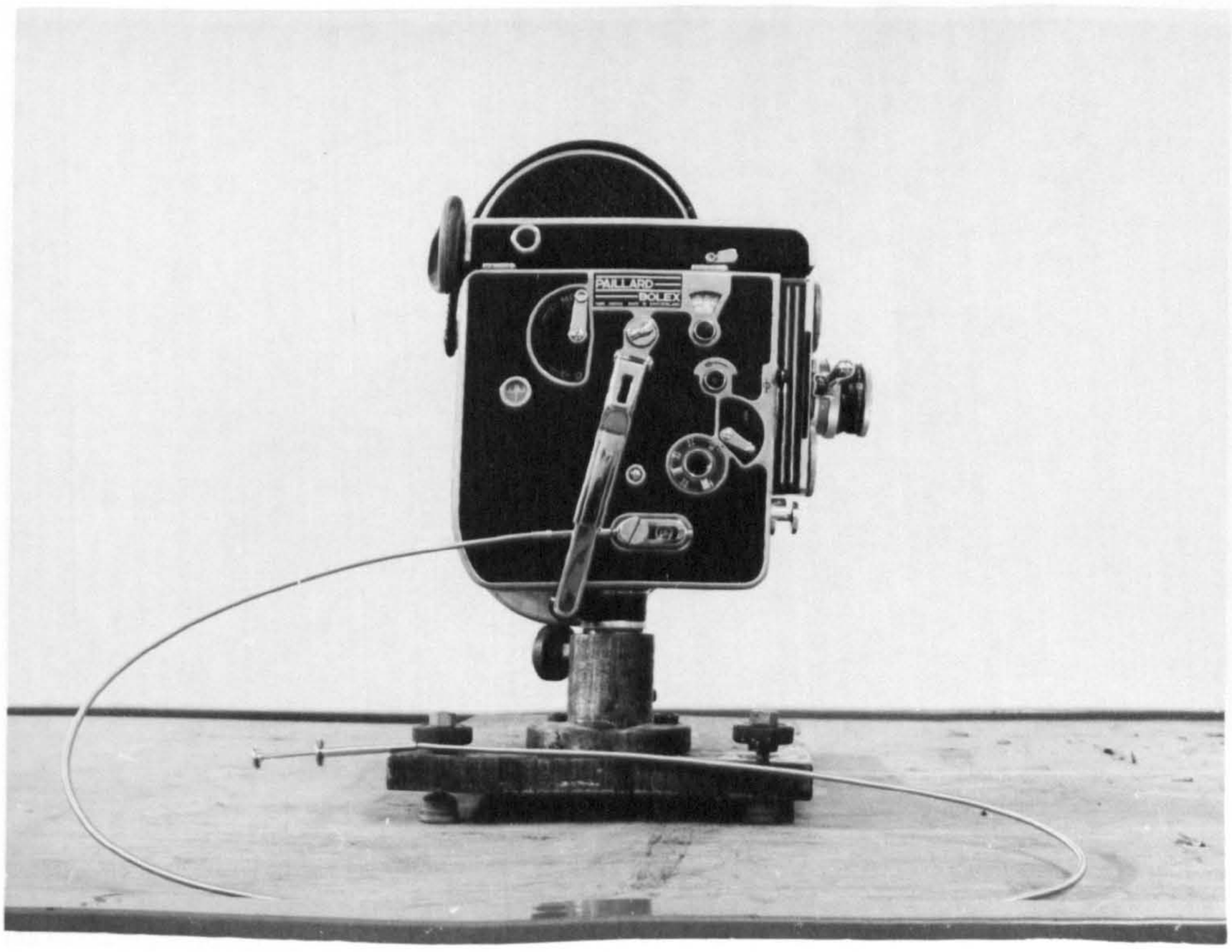

Plate 6

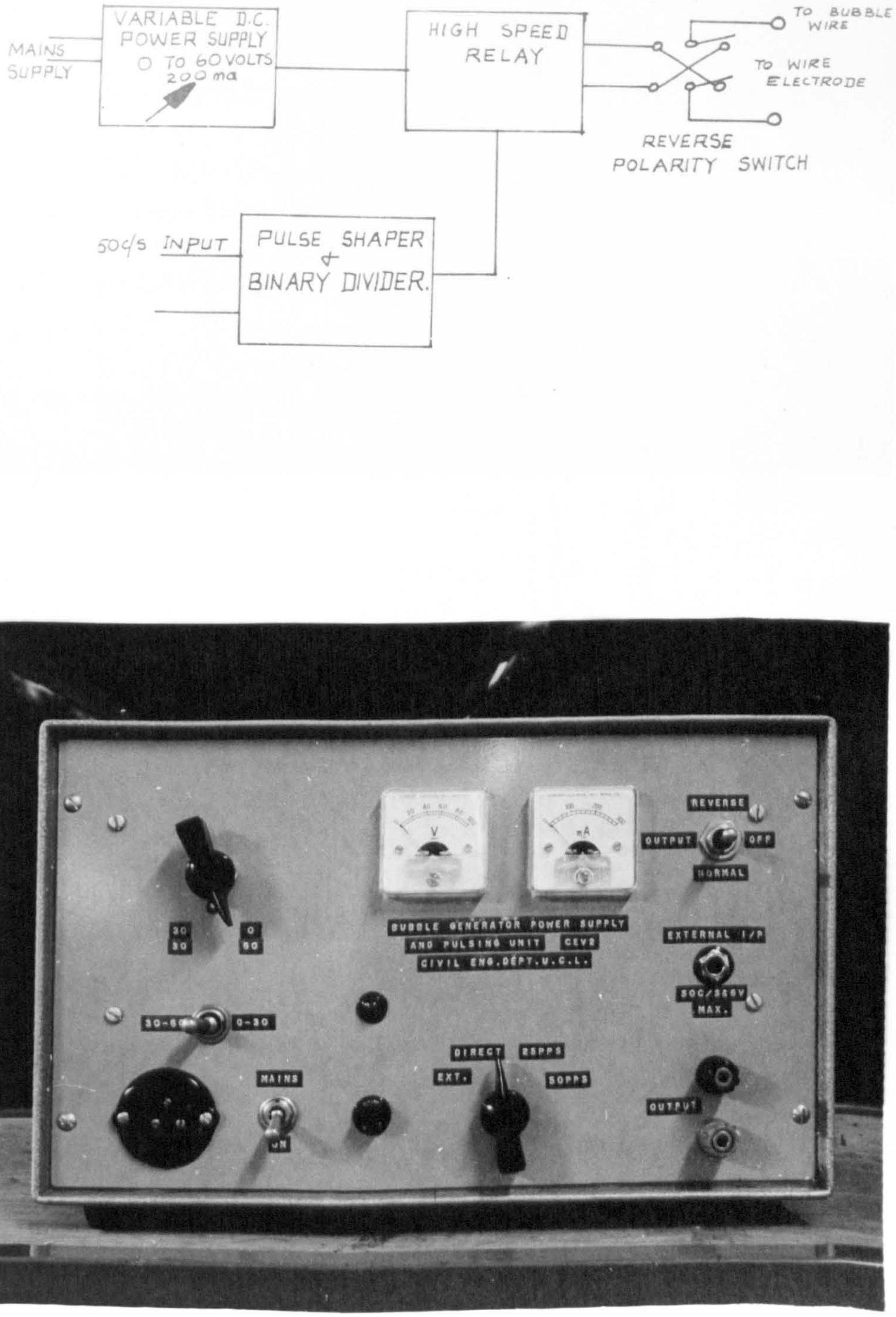

Figure 2.5 a and b

The material used for bubble generating wires is not critical, except with respect to corrosion and frangibility. Platinum,copper and stainless steel wires have all been used successfully, Schraub, F.A. et al(43). However, platinum is usually preferred as it has the important quality that during operation the wire can easily be cleansed by reversing the polarity for a few seconds. This process tends to destroy wires other than platinum.

In water at speeds in the range of 0.1 to 1 ft./s the hydrogen bubbles, formed at the wire, are swept off by the hydrodynamic forces and follow the flow. The bubbles thus provide good tracers for the fluid.

The wire used in this work was 0.002 inch diameter platinum wire, with brass plates as the positive electrodes. The Hydrogen bubble generator is shown in figures 2.5a and b. The output voltage control was obtained by using a variable transformer to feed a double wound isolating transformer. The output from the isolating transformer was full wave rectified using silicon diodes and smoothed by a conventional R.C. filter. For the bubble generation a 50c/s signal was squared and applied to a bi-stable binary dividing stage. An output from either the squaring stage or the binary divider could be selected

to drive a high speed relay to chop the High Tension line. For continuous bubble generation, the relay was switched to a side stable position to connect the High Tension Line directly to the wire electrode. A double pole polarity reversing switch was incorporated in the output circuit to enable the wire electrode to be quickly depolarized and cleaned.

The platinum wire was insulated at regular intervals, so as to produce solid "squares" of bubbles. Black cellulose aerosol spray was used for the insulation. It dried rapidly. However, one of the difficulties encountered in the experiment was that in oscillatory flow such as this, it was not possible in most cases to get the bubbles in nice square forms especially very close to the breakers. In the photography, it was found that a much better result was obtained by attaching a cable to the camera, and pressing the cable release simultaneously as the bubble generator was switched on. Cine photography was employed and a suitable lighting arrangement was therefore devised. The camera used was a 16 mm Reflex Bolex (see Plate 6). A trial run was made to select the number of frames per second, the "f" number and the shutter opening to use. In the end, 64 frames/sec. was selected with f number of 4 and the variable shutter $\frac{1}{4}$ open. For the lighting arrangement, an Aldis Tutor 1000 Watt Slide projector was used. The light source

was located on the opposite side of the channel to the camera, and orientated at an oblique angle to the channel. Slits were used to prevent stray light from scattering in the water. The arrangement was such as to get a sharply collimated light. The beach was covered with black "fablon", plastic sheet to give a dark background for the illuminated bubbles.

In operation, one end of the wire was fixed to the beach with a tape, while the other end was passed over a support and was tensioned by a suitable weight. It was found that on every working day at the first time of using, the wires required "aging" under operating conditions for a few minutes before starting to produce bubbles uniformly.

To assist in the subsequent measurements during the analysis of the films, the linear and time scales were determined during the experiments by first photographing a reference grid and a stop watch. The photographing of the grid was carried out for every position of the wire. A commercial curve analysing table (see Plate 7) was used in analysing the films. The coordinates of the instantaneous positions of the bubbles were automatically punched on to computer tape as an output from the commercial curve analysing table. The velocities close to the wire at the different positions were evaluated from the coordinates thus

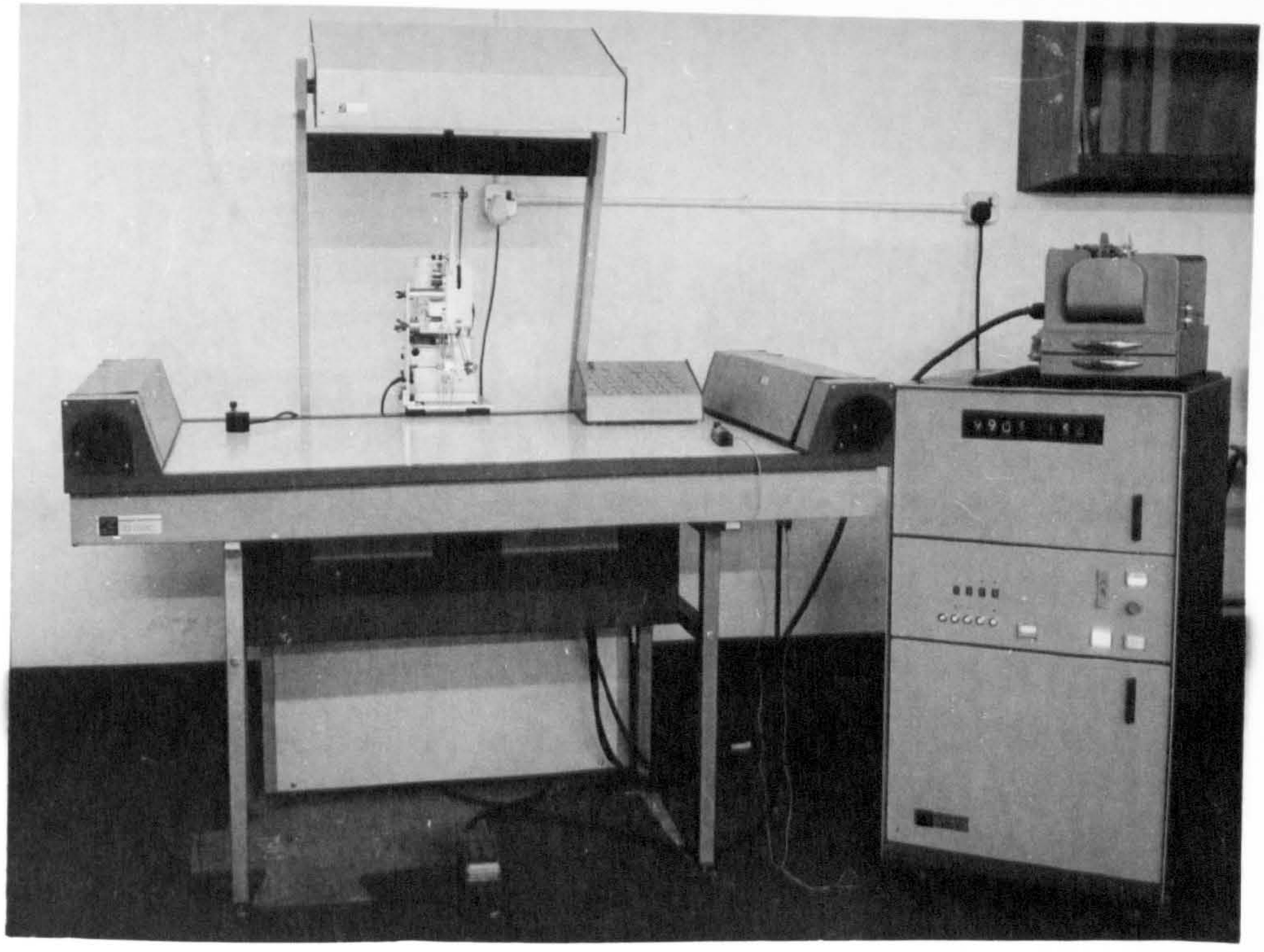

Plate 7

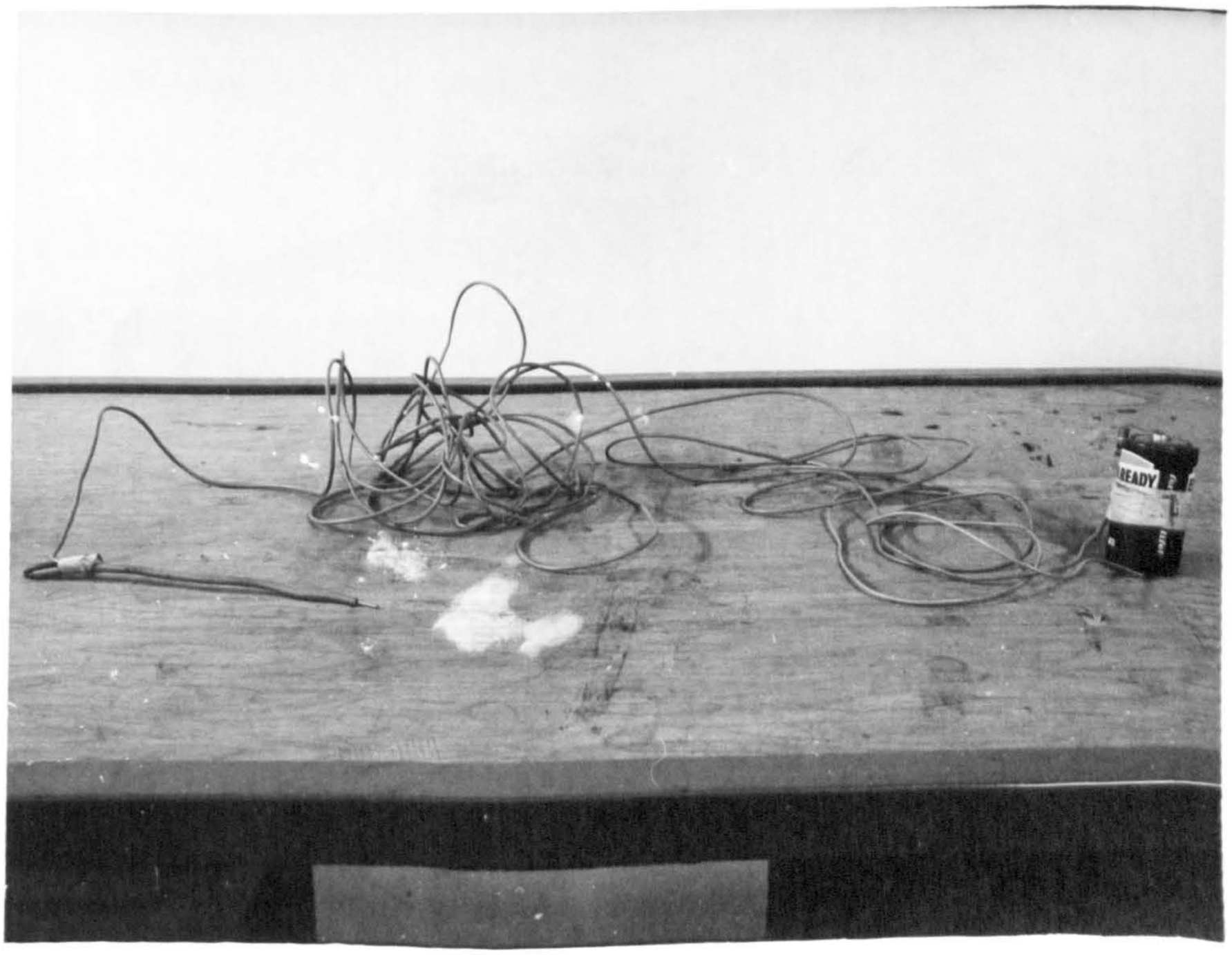

Plate 8

obtained by evaluating the displacement of the bubbles generated at different but known times. With a bubble pulse rate of 50 cycles per second, fluctuations above 50 cps could not be detected, however the method proved satisfactory.

The orbital velocity measurements were made at a height of 0.2 ins from the bed and were outside the boundary layer. The horizontal velocity (magnitude) asymmetry and the horizontal velocity (time) asymmetry are already defined in Chapter 1 section 1.6. A detailed discussion of the work on the velocity studies is given in Chapter 5.

2.6 Measuring Technique and Evaluation of Phase-difference of Uprush and Backwash of the Wave

The measurements of the phase difference of uprush and backwash of the wave is essentially the measurement of the time of travel of the uprush from the wave crest at the break point to the limit of uprush, after which the backwash then begins.

The phase difference of uprush and backwash of the wave is defined by Kemp[20,21] as

$$\frac{\text{Time of travel from wave breakpoint to the limit of uprush}}{\text{wave period}} = \frac{t'}{T}$$

The measurement of the time of travel from wave breakpoint to the limit of uprush was made by connecting a step probe (see plate 8) to the Visicorder. The step probe was a make

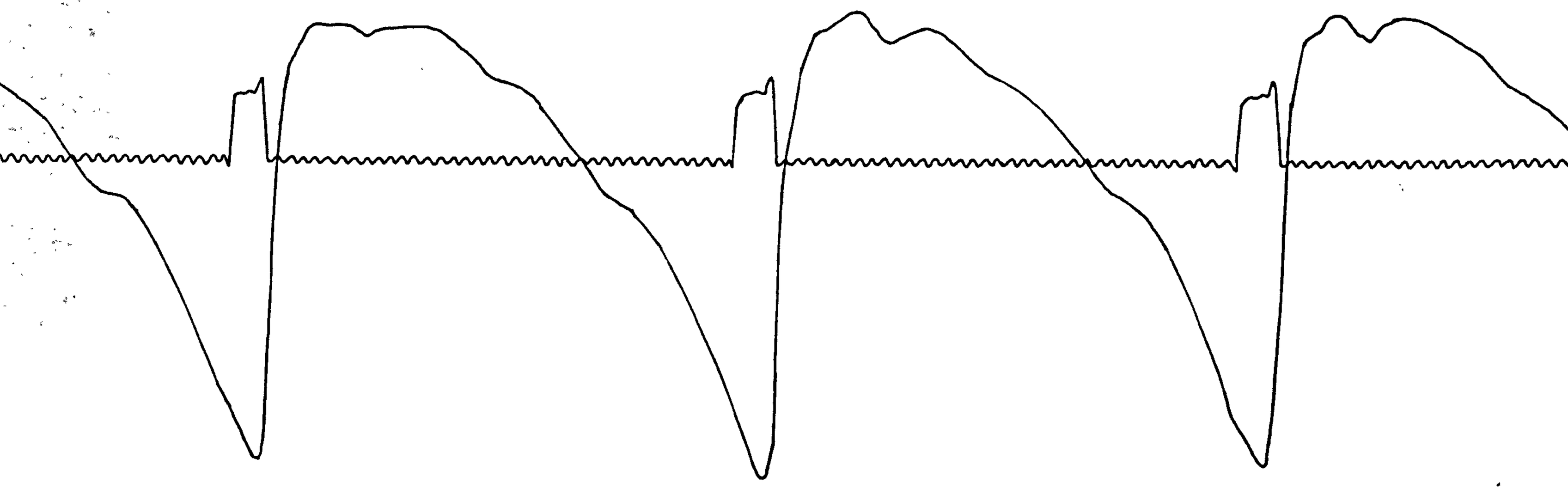

and break device. Well positioned at the limit of uprush, it would make and break contact with the fluid when the uprush reached its limit. The output from the step probe was recorded on the Ultra-violet Recorder. Thus by placing the capacitance wire probe at the breakpoint and the step probe at the limit of uprush, and employing the time marking device of the recorder, the time of travel from wave break-point to the limit of uprush was obtainable from the wave trace.

A check was first carried out to test that the capacitance probe and the step probe were in phase. This was done by mounting both the capacitance wire probe and the step probe side by side at the same water depth. The step probe being positioned for a make and break contact with the passing of the wave. The recorder was then switched on. It was found that the 'make contact' of the step probe corresponded with the wave crest, see figure 2.6. Thus it showed that the capacitance probe and the step probe were in phase. Otherwise, as they were mounted separately, there would have been a relative delay in one of them.

A typical measurement involving the time of travel from wave break-point to the limit of uprush using the step probe and the capacitance wire probe is shown in figure 2.7. The main discussion of the work on the phase

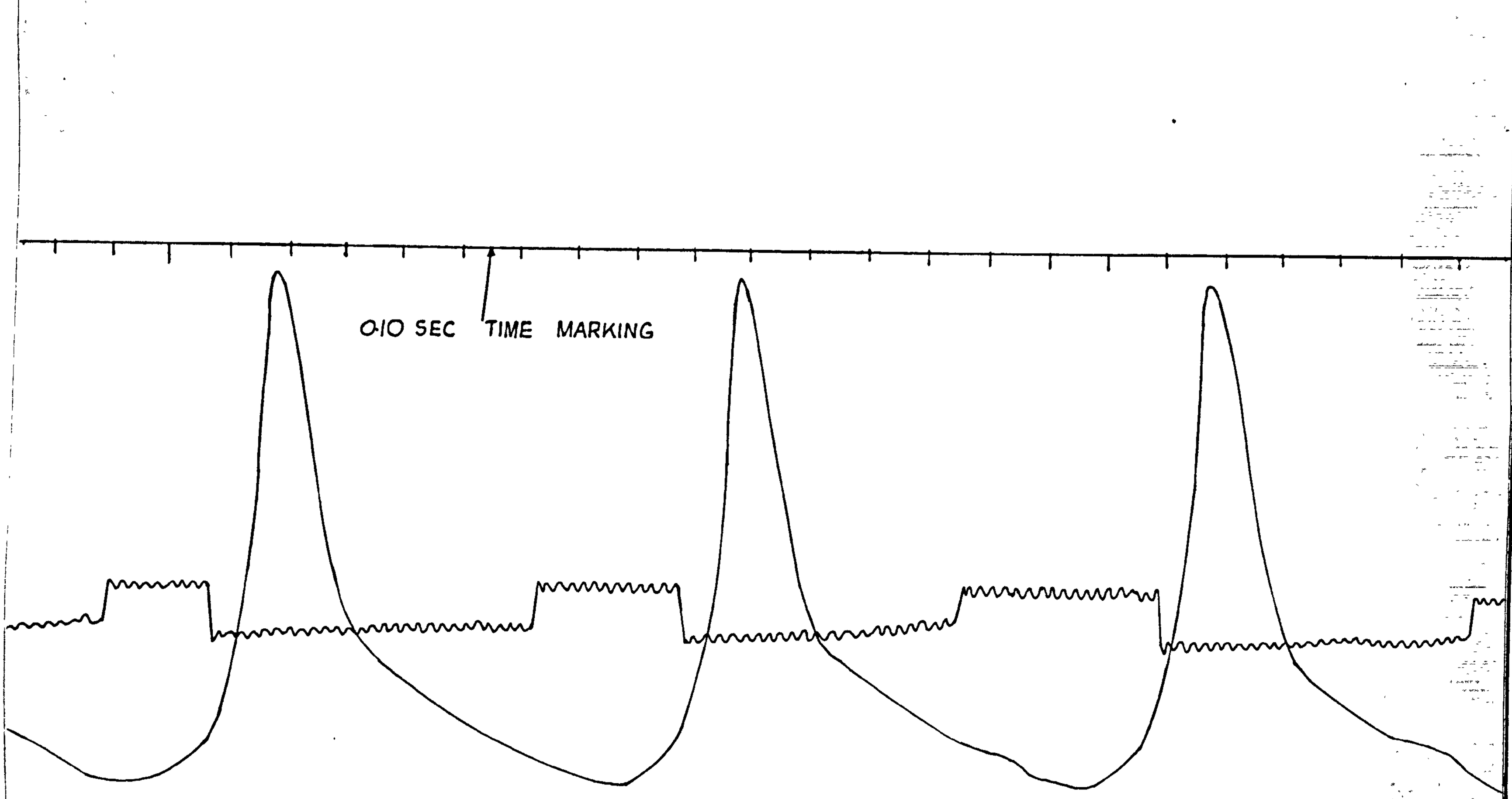

Figure

difference of uprush and backwash of the wave is given in Chapter 7.

2.7 Method of Eliminating the Backwash of the Wave

It was considered that the backwash of the wave played an important part in the overall effect of the wave on the beach. A study was therefore made in this work on the effect of eliminating the backwash of the wave on the wave asymmetry and the resulting velocity fields seaward of the breakers.

In order to carry out the studies, inclusion of additional devices and some modifications had to be made in the apparatus. As the aim was to eliminate the wave just after breaking, the critical beach slope in the modification was the one on which the wave would break farthest away from the shore. The portion of the marine plywood (used for the beach) from this point to the shore end of the beach was therefore cut off except for a small projecting length of about $\frac{1}{2}$" in thickness of the marine plywood on each side. The shoreward end of the beach was then provided with an adjustable plate. The support for the shore end of the beach was effected by using dural aluminium sections at the sides and end of the beach. The main I section centre support running the whole length of the beach was left in position. The full length of the beach was

then covered by three dural aluminium plates, with the plate nearest the beach toe being chamfered so as to be flush with the toe of the beach. Then starting with the plate farthest from the beach toe, the plates were removed as necessary and the rest adjusted such that for the particular beach slope setting, the wave was eliminated by running over the end of the plate after breaking.

For the purpose of returning the flow and so keeping the still water level constant, a 0.5 H.P., 2850 R.P.M Pump was incorporated. A 1¼ inch diameter pipe was run from an outlet at the end wall (shore end) of the tank and connected to the pump, while another 1¼ inch diameter pipe was run from the pump outlet and was introduced into the tank at the back of the wave filter at the wave generator end. A gate valve, fixed into the delivery pipe connected to the pump provided a control to maintain the right balance desired.

The method of investigation of the wave asymmetry and the velocity asymmetry when the backwash of the wave was eliminated followed the same line as explained in sections 2.4 and 2.5 respectively for normal conditions. The experimental arrangement and the various techniques of measurement proved satisfactory.

CHAPTER 3

EFFECT OF BEACH SLOPE AND SHOALING ON WAVE ASYMMETRY

3.1 Introduction

As waves approach shallow water over bed slopes similar to those reproduced in the model, they change from the deep water to the shallow water category and become markedly asymmetric before breaking. The shoreward side of the wave becomes nearly vertical whilst the seaward face is appreciably inclined. The actual configuration is affected by the bed slope.

Owing to the continually varying geometry of waves in shallow water and in order to have a detailed understanding of wave transformation in shoaling water, the three main types of wave asymmetry already defined in the present work were measured. Diagrams showing the definitions of the wave asymmetry are shown in the graphs discussed in this chapter.

Some mention of the wave vertical asymmetry has been made in the literature. For instance, the trochoidal wave theory gives the positions of the wave crest and trough relative to the still water level in the shallow water as

$$\text{Height of the crest} = \frac{H}{2} + \frac{\pi H^2}{4L} \coth \frac{2\pi d}{L} \quad \ldots(3.1)$$

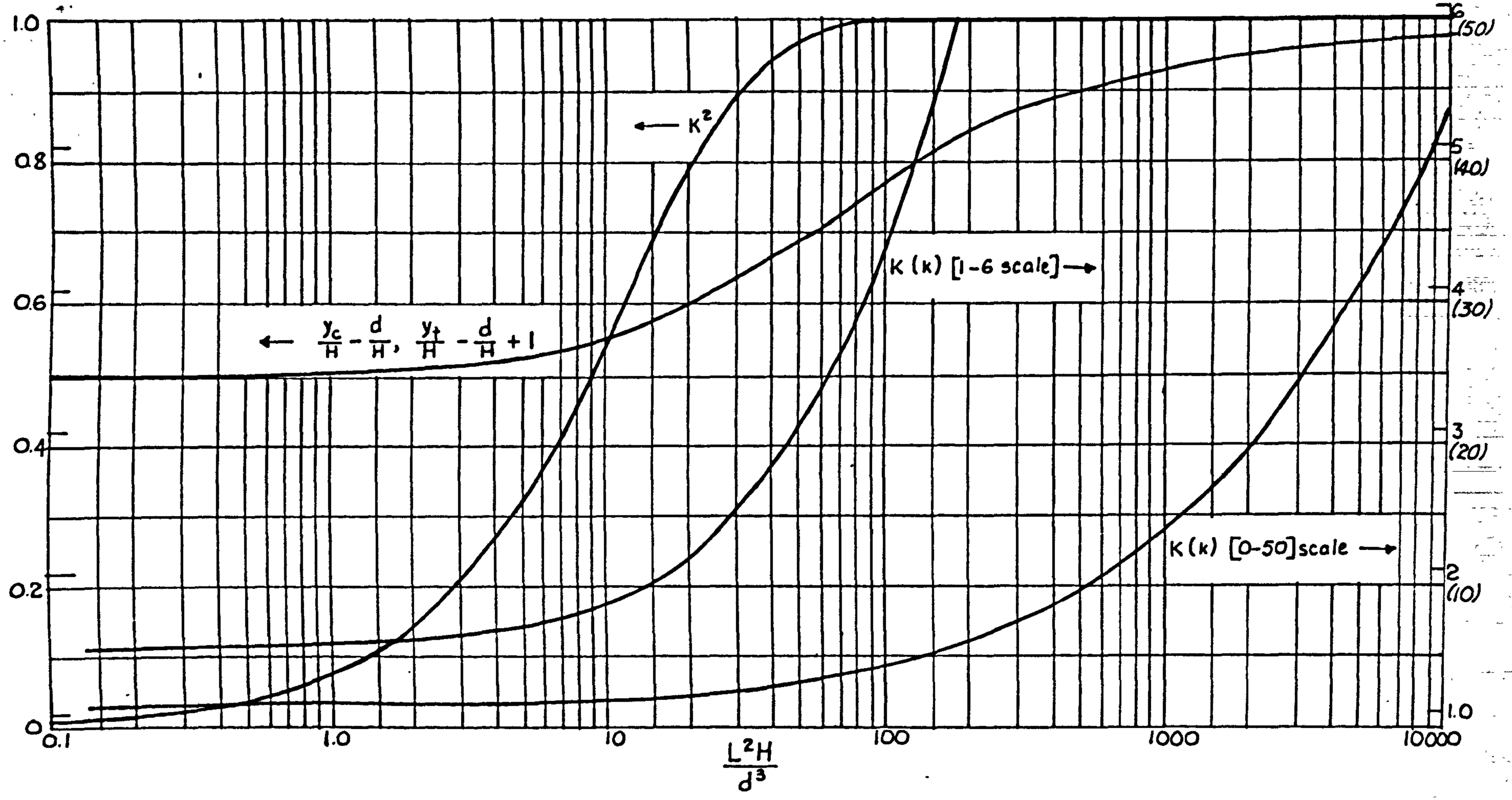

$$\frac{L^2H}{d^3} = \frac{16}{3}K^2 \quad K^2(k) \qquad \frac{y_c}{H} - \frac{d}{H} = \frac{y_t}{H} - \frac{d}{H} + 1 = \frac{16d^3}{3L^2H}\left\{K(k)\left[K(k) - E(k)\right]\right\}$$

Figure 3.1 Relationship among $\frac{L^2H}{d^3}$ and the square of the elliptic modulus (k^2), $\frac{y_c}{H}$, $\frac{y_t}{H}$, and $K(k)$ [After Wiegel[55] (1960)]

and depth of trough $= \frac{H}{2} - \frac{\pi H^2}{4L} \coth \frac{2\pi d}{L}$ (3.2)

Stokes finite amplitude wave theory shows that the wave crest lies above the still water level by the amount

$$\frac{\pi H^2}{4L}\left\{1 + \frac{3}{2\sinh^2 \frac{2\pi d}{L}}\right\} \coth \frac{2\pi d}{L}$$

which is more than the value given by the troichoidal wave theory by the factor $\left(1 + \frac{3}{2\sinh^2 \frac{2\pi d}{L}}\right)$

The experimental results of the wave vertical asymmetry in this work were compared with the expression from the cnoidal wave theory already noted in equation (1.11). The graph of equation (1.11) is shown in figure 3.1.

It is important to note that whereas the cnoidal wave theory predicts wave vertical asymmetry, it does not predict wave horizontal asymmetry and wave slope asymmetry. An expression for the wave horizontal asymmetry is provided later in the work reported in this thesis based on the expression for the wave vertical asymmetry from the cnoidal wave theory.

The theoretical study of wave slope asymmetry made by Biesel[5] and the results of the experimental work on the wave slope asymmetry in the present work are later compared.

3.2 Review of Previous Experimental Work

Wiegel[54] conducted a series of experiments to compare the wave profile with the trochoidal wave theory. He commented that the surface profiles were similar to that given by the trochoidal wave theory for $\frac{d}{L} > 0.15$ on a beach slope of $\frac{1}{20}$. In shallow water, he found that the wave profile differed very much from the trochoidal wave theory. For the percentages of wave height lying above still water level (see Fig.3.2) he remarked that for the beach slope of $\frac{1}{10.8}$ the experimental points were below the curve in fairly deep water, while for the $\frac{1}{20}$ beach slope they were above the theoretical curve predicted by the trochoidal wave theory. For both beach slopes, the experimental results near the breakers were found to be considerably higher than those given by the theory.

Iversen[16], in an experiment on the study of breakers, examined such features as breaker height, backwash depth, forward stagnation position and the breaker face angles (see fig. 3.3). He noted that for a given wave train on a steep beach as compared to a flat beach, the breaker is higher, and breaks with a higher crest elevation, and has a flatter back face and a steeper front face. The type of breakers whether spilling or plunging observed in the present studies

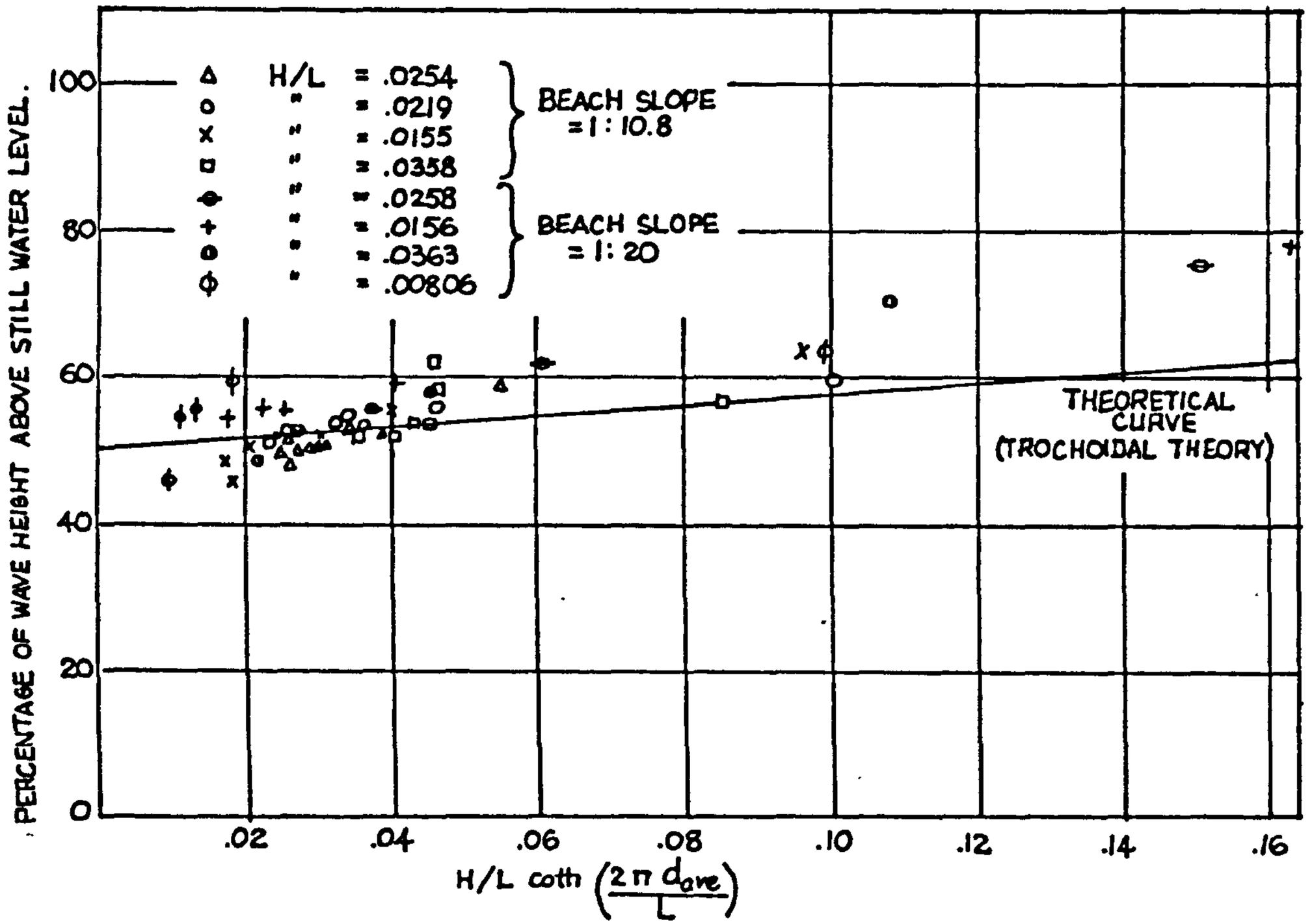

Figure 3.2 Comparison between experimental and theoretical percentages of wave height above still water level (After Wiegel[54] (1950).

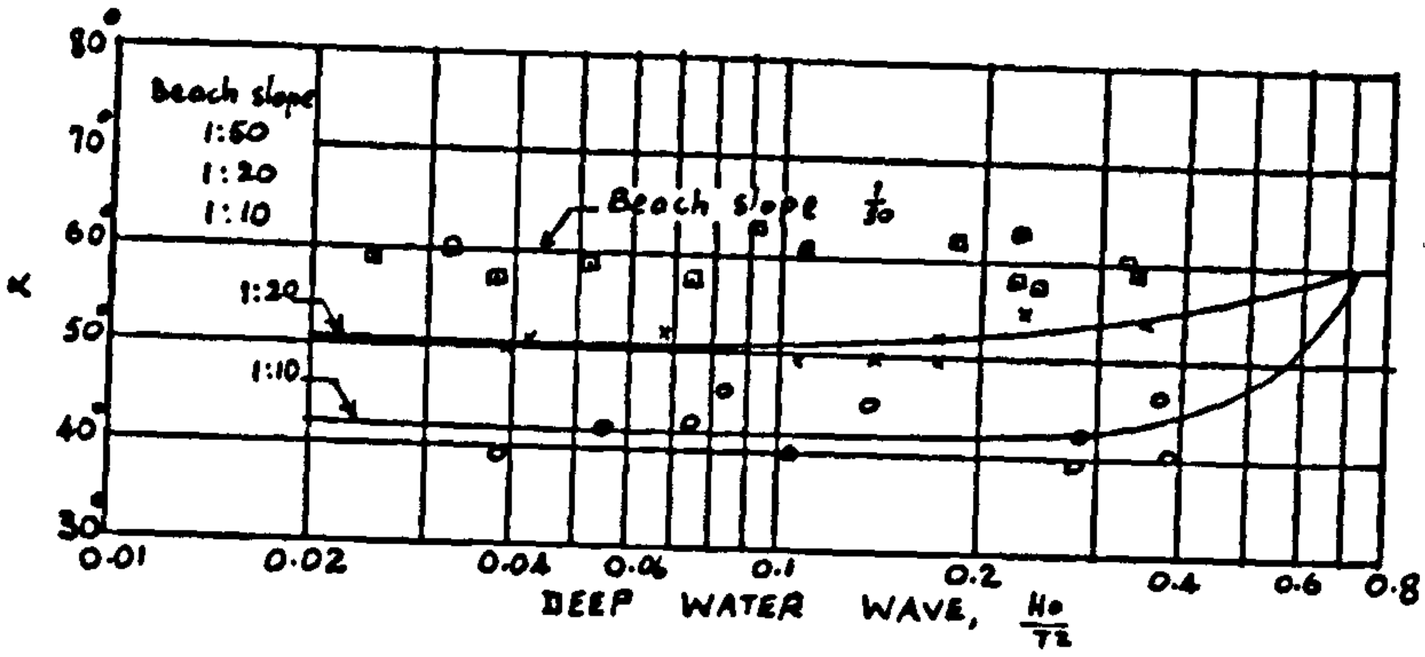

FRONT FACE ANGLE INDEX

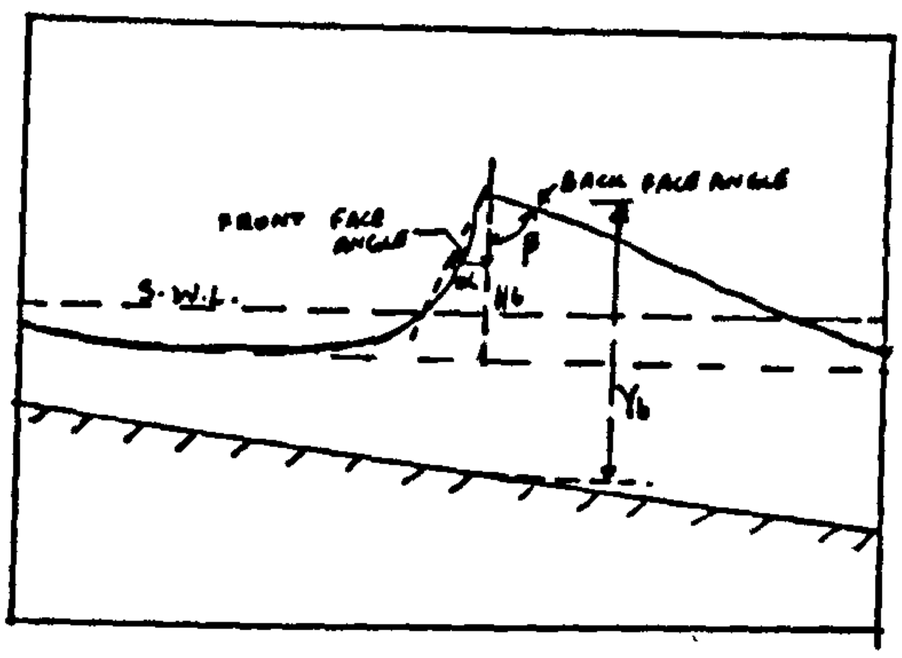

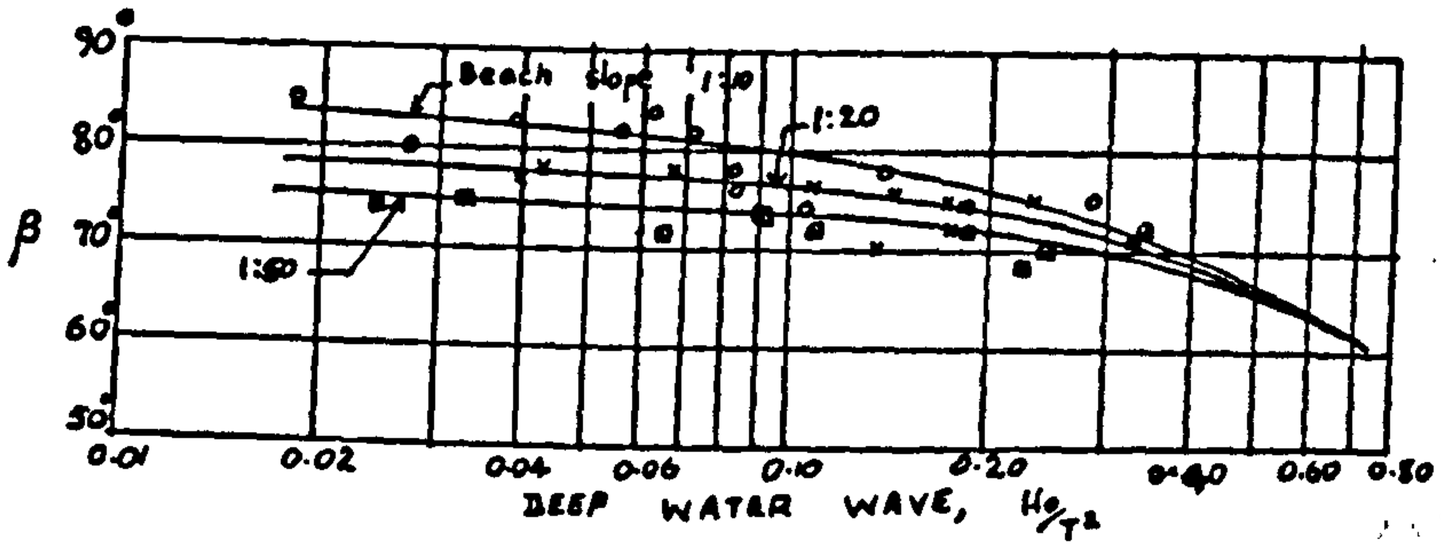

BACK FACE ANGLE INDEX

Figure 3.3 After Iversen[16] (1953)

agreed with Iversen's classification (see fig. 3.4).

In a study of breakers and beach erosion Hamada[12] remarked that at breaking, the displacement of the orbital centre above the still water level was $0.204H_b$ on a $\frac{1}{10}$ slope and $0.228\,H_b$ on a slope of $\frac{1}{15}$. He noted the observation that when a wave is about to break on a shallow sloping beach the trough becomes wide and flat, and the crest narrow and steep. He considered that the forward leaning of the wave crest might be an important factor in wave breaking.

Eagleson[8] compared experimental values of wave height steepness and wave length with Stokes' theory. He commented that Stokes third order theory applied only in the early stages of transformation, the divergencies being too large as the wave begins to deform. Using the Stokes relationships for surface profile, he gave an expression for the crest height a_1 as

$$\frac{2a_1}{H} = 1 + \frac{3}{8}\pi\frac{H}{L}\frac{\sinh\frac{4\pi d}{L}}{\left(\sinh\frac{2\pi d}{L}\right)^4} \qquad \cdots(3.3)$$

Eagleson compared the above expression with his experimental results and remarked that the experimental results gave a wave crest which was steeper than the theory early in the transformation but flatter than the theory in the breaker region.

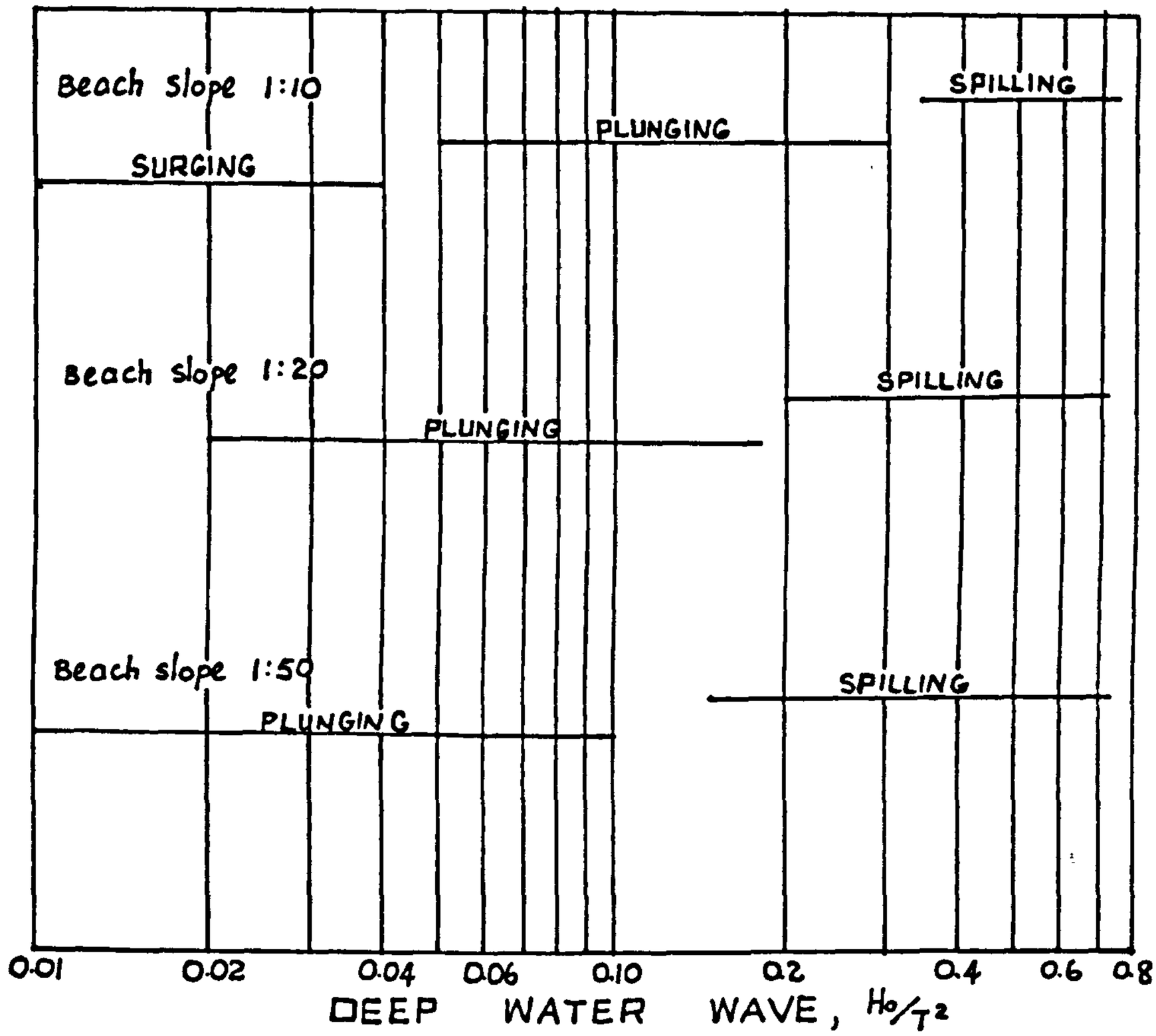

Figure 3.4 Breaker type index (After Iversen[16] (1953)

Ursell[50] theoretically predicted in a qualitative sense the effect of shoaling on wave asymmetry by consideration of the parameter $\frac{HL^2}{d^3}$. He concluded that large values of the parameter $\frac{HL^2}{d^3}$ would predict an increased tendency towards wave asymmetry.

Ippen and Kulin[15] studied the shoaling and breaking of the solitary wave. They observed that on a slope of 0.065 the deformation of the breaker began gradually, with a rapid acceleration of the process occurring just before breaking. They observed that in addition to the violent nature of the breaker, the front face of the wave at breaking was nearly vertical. They remarked that on the other hand, on a slope of 0.023, the wave breaking was a more gentle process with the wave initially deforming as well as breaking in a much more gradual fashion.

Ippen and Kulin[15] classified breakers as "symmetric", "asymmetric" and "intermediate". They described waves which retained much of their original symmetry during shoaling and which deformed by what they termed 'peaking up' of the crest, as symmetric breakers. On the other hand, they classified as asymmetric breakers, waves which showed a marked steepening of the front face. They did not define what they termed as the intermediate breaker, but

presumably they intended something between what they called the symmetric and the asymmetric breakers. When they tried to translate their results into a graph, they found that there was some scatter and they rightly noted that their classification depended very much on personal judgement. From the studies made in the work reported in this thesis, and within the experimental limits, it is evident that nothing like a symmetric breaker was observed.

3.3 Experimental Results on Wave Vertical Asymmetry

On all the beach slopes it was found that as the wave progressed shoreward, the wave vertical asymmetry was continuously increasing and was maximum at the break-point. On the beach slope of $\frac{1}{4}$ (see figure 3.5) it was found that the experimental results gave values very slightly higher than the theory for $\frac{d}{L} > 0.18$. Shoreward of this, the experimental results were lower than the theory. The maximum divergence was about 18% of the theoretical value, and that was the greatest divergence found throughout the work including the other beach slopes.

On the beach slope of $\frac{1}{6}$, the wave vertical asymmetry was 0.505 at a $\frac{d}{L}$ value of 0.26 (see fig.3.6)

WAVE PERIOD = 0·8 SEC.
BEACH SLOPE = 1/4
H_o = 1·45 INS

$$\text{WAVE VERTICAL ASYMMETRY} = \frac{\text{VERTICAL DIST. FROM CREST TO S.W.L.}}{\text{TOTAL WAVE HEIGHT}}$$

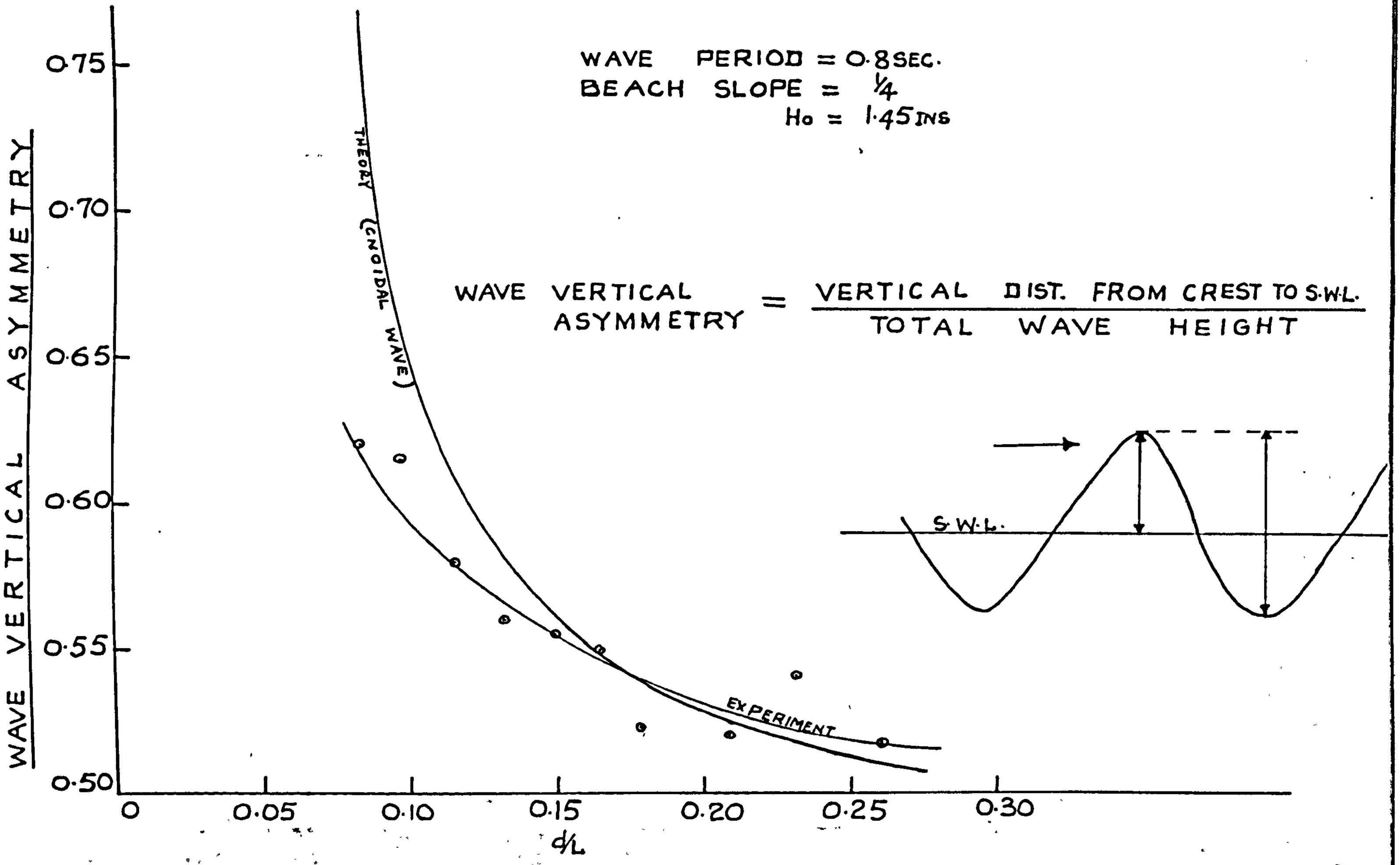

Fig. 3.5 Wave Vertical Asymmetry: Experimental and Theoretical Results

WAVE PERIOD = 0·8 SEC.
BEACH SLOPE = 1/6
H_o = 1·45 INS.

$$\text{WAVE VERTICAL ASYMMETRY} = \frac{\text{VERTICAL DIST. FROM CREST TO S.W.L.}}{\text{TOTAL WAVE HEIGHT.}}$$

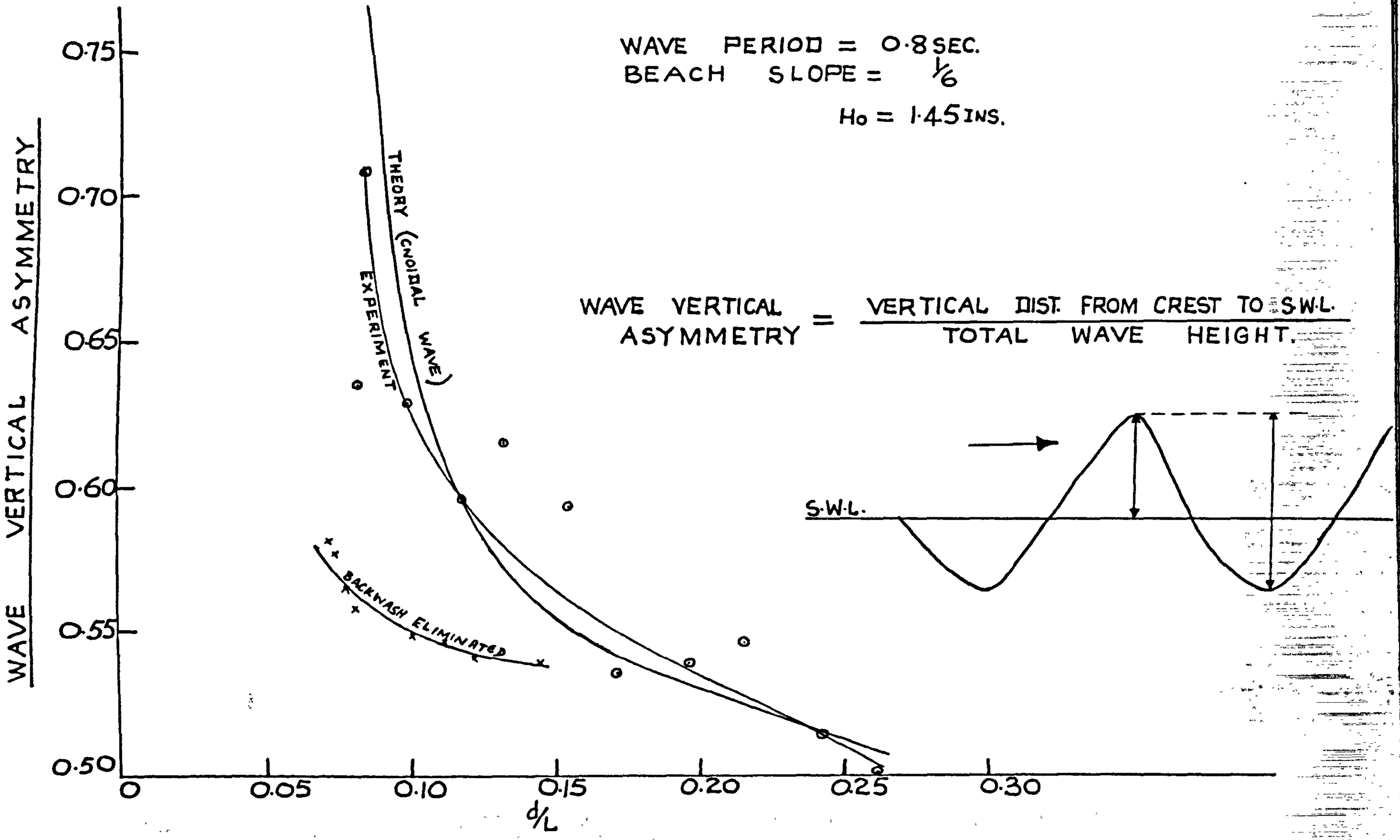

Fig. 3.6 Wave Vertical Asymmetry: Experimental & Theoretical Results.

Within the range of $\frac{d}{L}$ values of 0.24 and 0.12 the theoretical curve was about 2% less than the experimental results. For $\frac{d}{L}$ less than 0.12, the experimental results became lower than the theoretical prediction. The maximum divergence between the experimental results and the theory for the beach slope of $\frac{1}{6}$ was 10% of the theoretical prediction. The experimental value of the wave vertical asymmetry at the wave break-point on the beach slope of $\frac{1}{6}$ was found to be 0.707, which was higher than the corresponding value of 0.62 at the breakpoint on the beach slope of $\frac{1}{4}$.

On the beach slope of $\frac{1}{9}$, it was found that within the range of $\frac{d}{L}$ values of 0.26 and 0.10 the experimental results of the wave vertical asymmetry were higher than the theoretical curve, whilst shoreward of $\frac{d}{L}$ value of 0.10 the experimental results became lower than the theoretical values. The maximum divergence between the theoretical values and the experimental results was 9.8% of the theoretical prediction. The experimental result of the wave vertical asymmetry at the wave break-point was found to be 0.725.

On the beach slope of $\frac{1}{12}$, the curves of the experimental results and the theory showed that the experimental results were rather lower than the theoretical predictions. The maximum divergence was 7% of the theoretical prediction. It was found that at a $\frac{d}{L}$

value of 0.10 the wave vertical asymmetry on the beach slope of $\frac{1}{12}$ was 0.656, which was higher than the corresponding values for the steeper slopes. This tendency for the wave vertical asymmetry to be higher on the flatter slope continued as the wave advanced into shallower water. Whereas on the beach slopes of $\frac{1}{4}$, $\frac{1}{6}$ and $\frac{1}{9}$ the breakers formed were plunging breakers, on the beach slope of $\frac{1}{12}$ and for the flatter slopes of $\frac{1}{15}$ and $\frac{1}{18}$ the breaker in each case was spilling.

It was found that whereas the graphs of wave vertical asymmetry against $\frac{d}{L}$ were non-linear for the steeper beach slopes, they became linear for beach slopes $< \frac{1}{12}$. The experimental results of the wave vertical asymmetry on the beach slope of $\frac{1}{15}$ were quite close to the theoretical predictions. However, the theoretical curve was non-linear. The experimental results were slightly higher than the theoretical curve for $\frac{d}{L} > 0.10$, but shoreward of this the experimental results became lower than the theory. The maximum divergence between the experimental results and the theoretical prediction was 8.7% of the theoretical prediction, and occurred at the break-point where one would not normally expect good agreement. For the portion where the experimental

results were higher than the theory, the divergence was about 3%. The linearity of the curves of the wave vertical asymmetry on the flat slopes will be considered again in the next chapter when considering the effect of the backwash on the wave asymmetry.

The graph of wave vertical asymmetry against $\frac{d}{L}$ on the beach slope of $\frac{1}{18}$ (see figure 3.7) showed the same trend on shoaling as on the beach slope of $\frac{1}{15}$. The maximum divergence between the values of the experimental results and the theory was 5% of the theoretical prediction. The value of the wave vertical asymmetry at the break-point on the beach slope of $\frac{1}{18}$ was 0.74 which was considerably higher than the corresponding value of 0.62 at the breaker position on the beach slope of $\frac{1}{4}$.

The effect of beach slopes on wave vertical asymmetry is shown in Figure 3.8, and it indicated that the wave vertical asymmetry is greater for flat slopes when the wave is in very shallow water of about $\frac{d}{L} < 0.10$

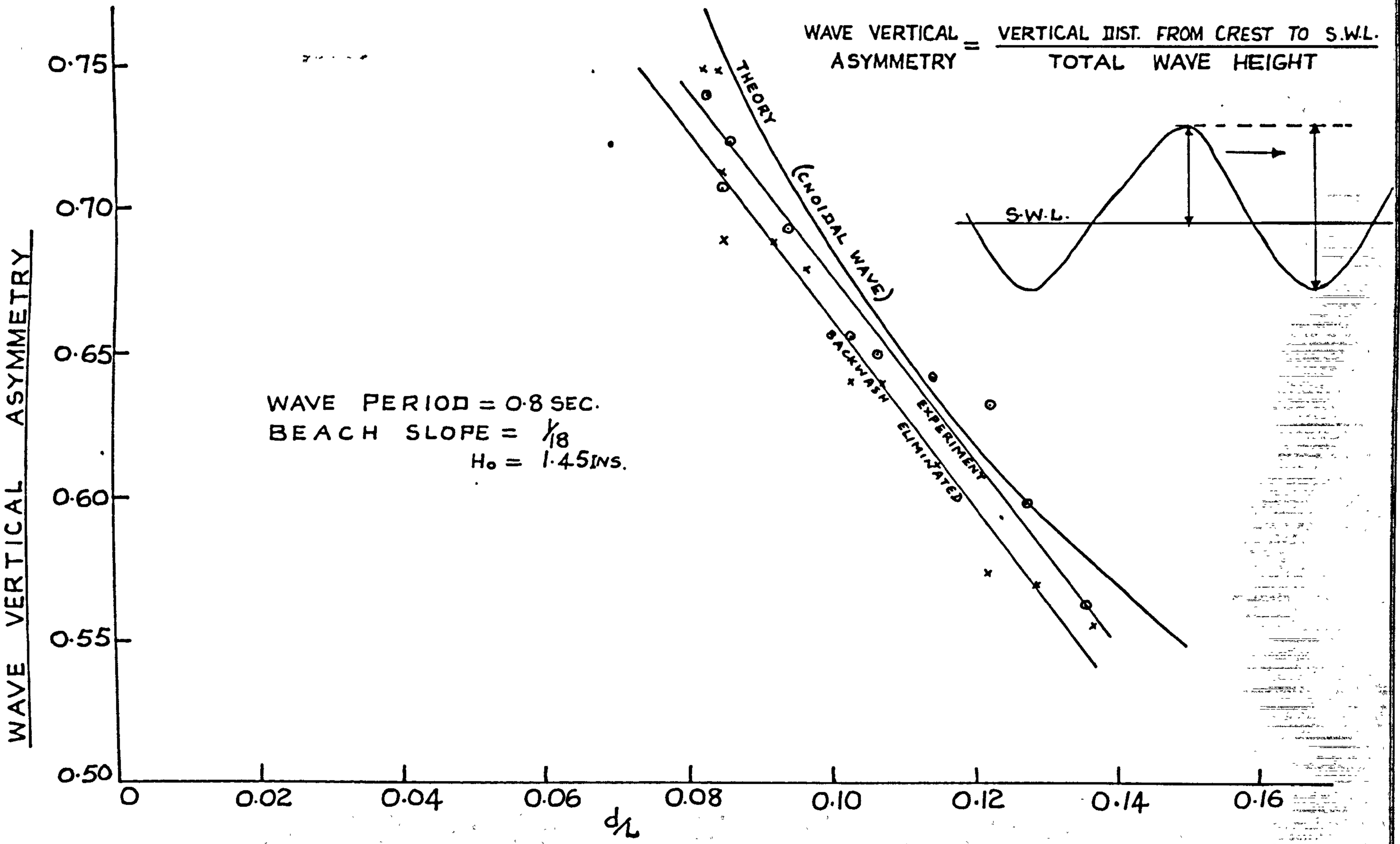

Fig. 3.7 Wave Vertical Asymmetry: Experimental & Theoretical Results.

WAVE PERIOD = 0·8 SEC.
H_o = 1·45 INS

THE VALUES SHOWN ON THE CURVES ARE THE BEACH SLOPES.

$$\text{WAVE VERTICAL ASYMMETRY} = \frac{\text{VERTICAL DIST. FROM CREST TO S.W.L.}}{\text{TOTAL WAVE HEIGHT}}$$

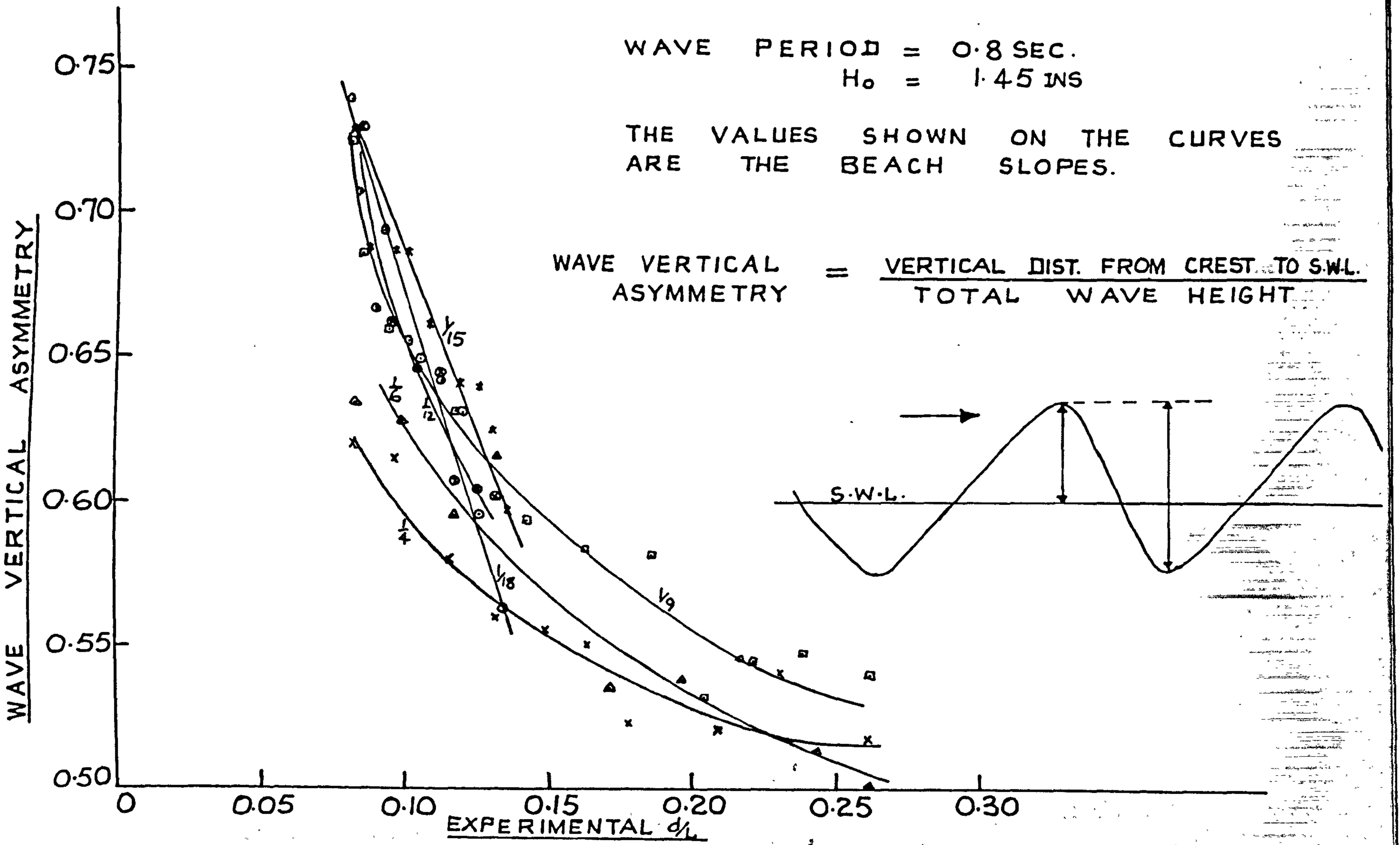

Fig. 3.8 Effect of Beach Slope on Wave Vertical Asymmetry

3.4 Experimental Results on Wave Horizontal Asymmetry

The smaller the numerical value of HA and HA' compared with unity the more asymmetric the wave is, on the basis of the wave horizontal asymmetry definition. On all beach slopes, the graphs of HA and HA' against $\frac{d}{L}$ showed that the numerical values of HA and HA' were decreasing and so the wave was becoming more asymmetric as the wave advanced into shallower water up to and including the break-point.

The graph of HA and HA' against $\frac{d}{L}$ on the beach slope of $\frac{1}{4}$ is shown in figure 3.9. The value of the wave horizontal asymmetry HA at the break-point was about 0.2, which meant that at the breaker position, the horizontal distance from the wave crest to the wave front face at still water level, was $\frac{1}{5}$ of the horizontal distance from the crest to the rear face. At a $\frac{d}{L}$ value of 0.15, the value of HA was 0.80 and so the wave was not really very asymmetric at that stage. The most rapid change in HA and HA' was found to take place at $\frac{d}{L} < 0.15$. The graph of HA' against $\frac{d}{L}$ was quite similar to that of HA against $\frac{d}{L}$. This was, however, in line with expectation as both HA and HA' are measures of wave horizontal asymmetry. It was found however that HA' indicated a higher asymmetry than HA.

The graphs of HA and HA' against $\frac{d}{L}$ for the beach slopes of $\frac{1}{6}$, $\frac{1}{9}$, $\frac{1}{12}$, $\frac{1}{15}$ and $\frac{1}{18}$ are shown

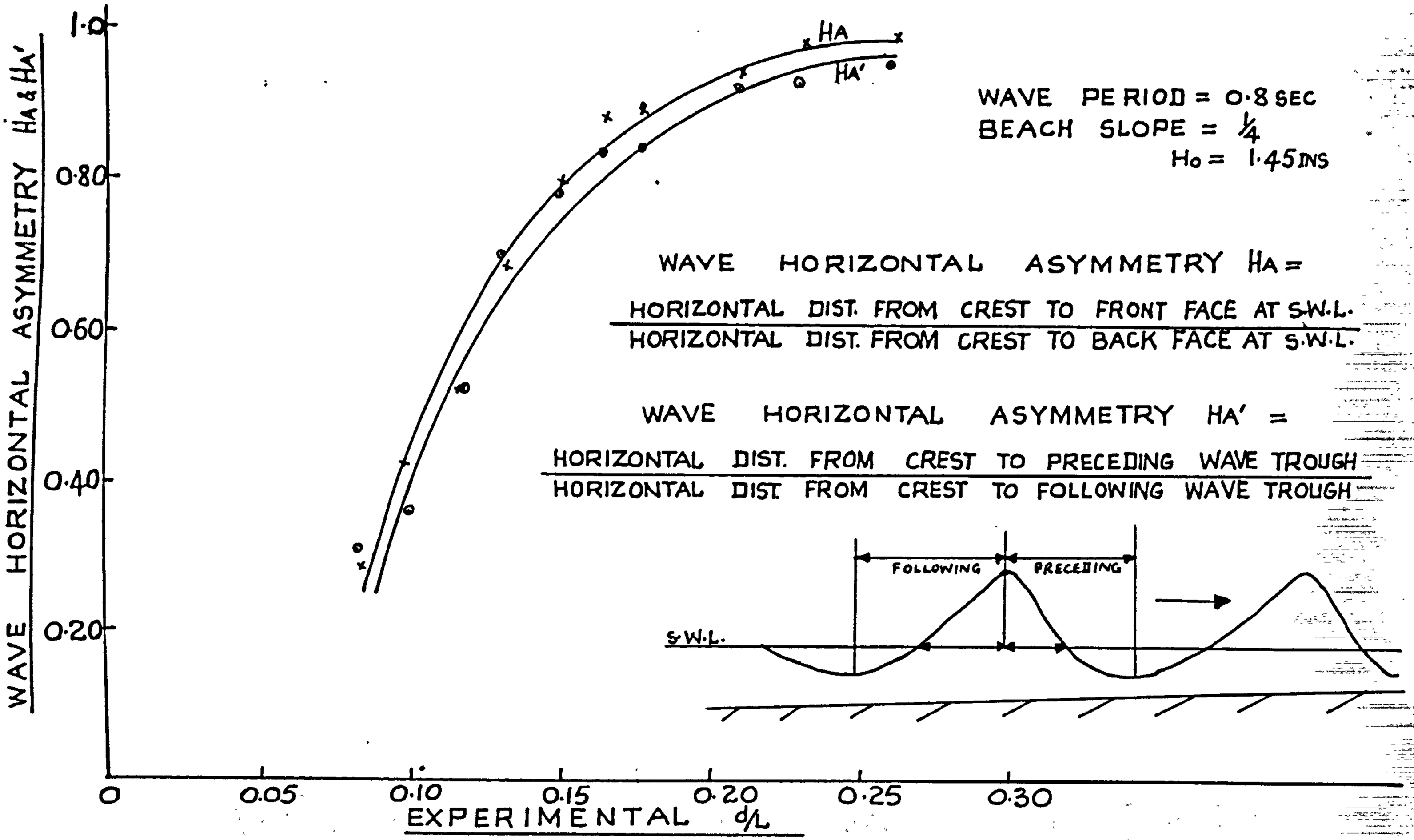

Figure 3.9 Graph of Wave Horizontal Asymmetry HA and HA'

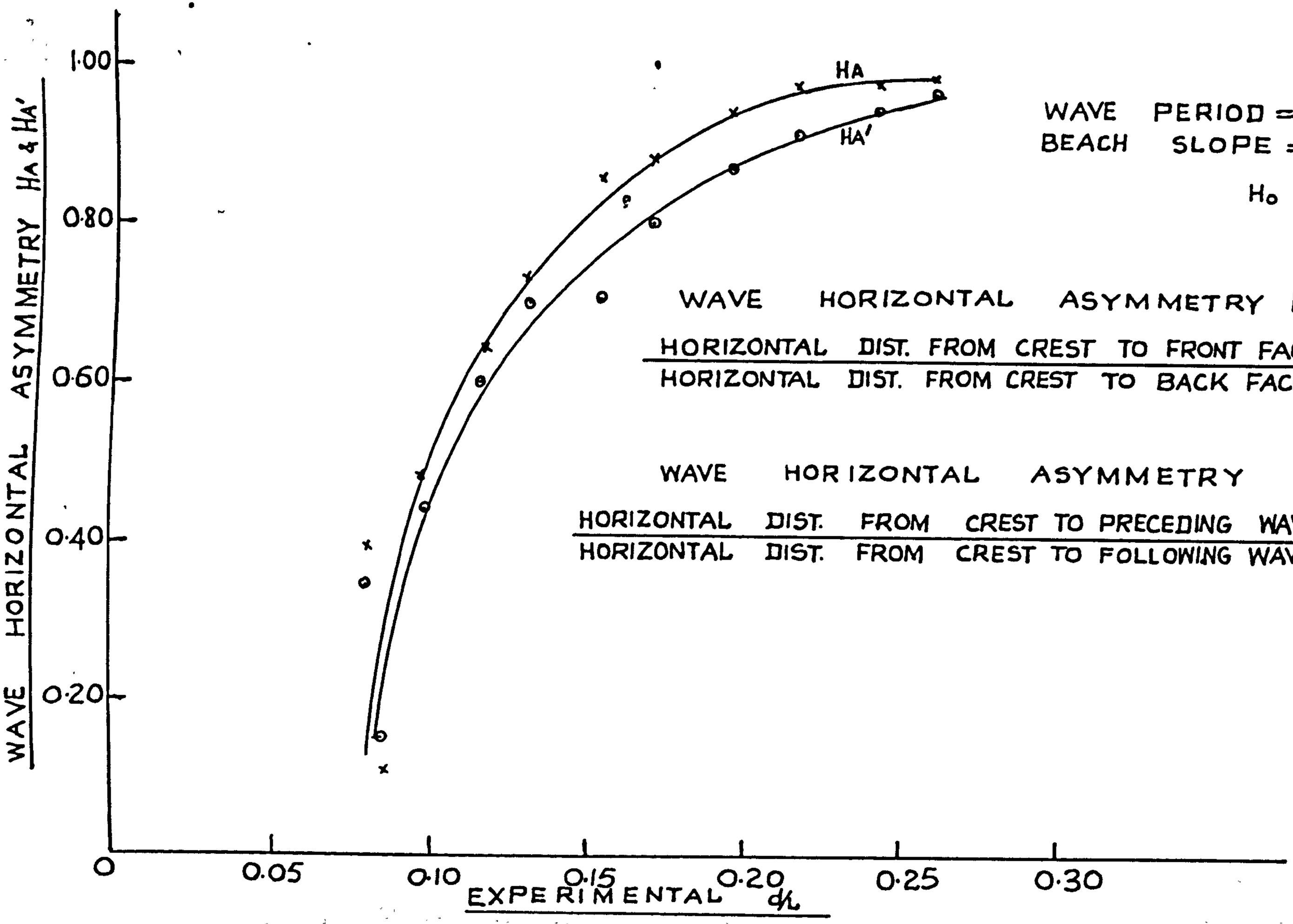

Figure 3.10 Graph of Wave Horizontal Asymmetry HA and HA'

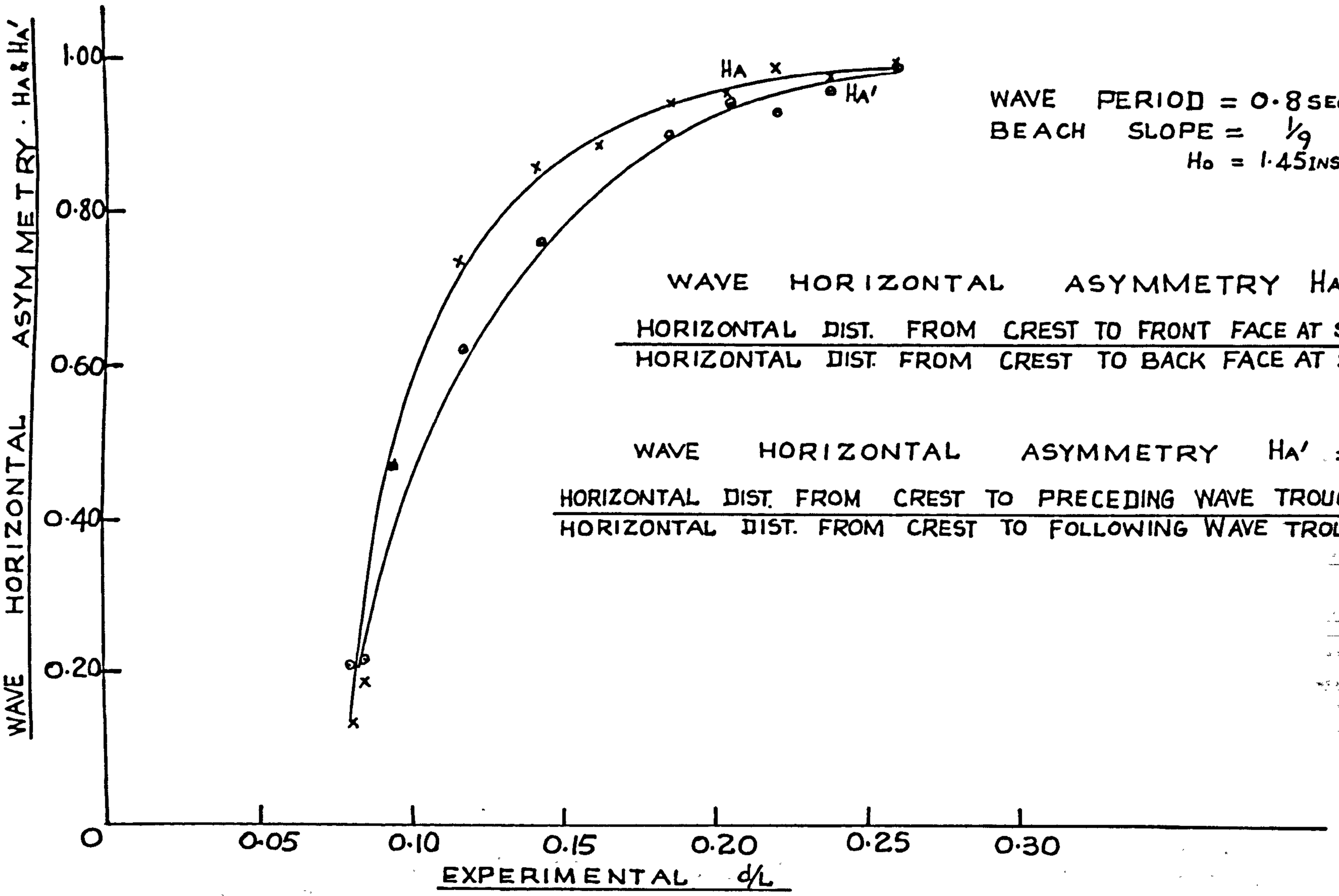

Figure 3.11 Graph of Wave Horizontal Asymmetry HA and HA'

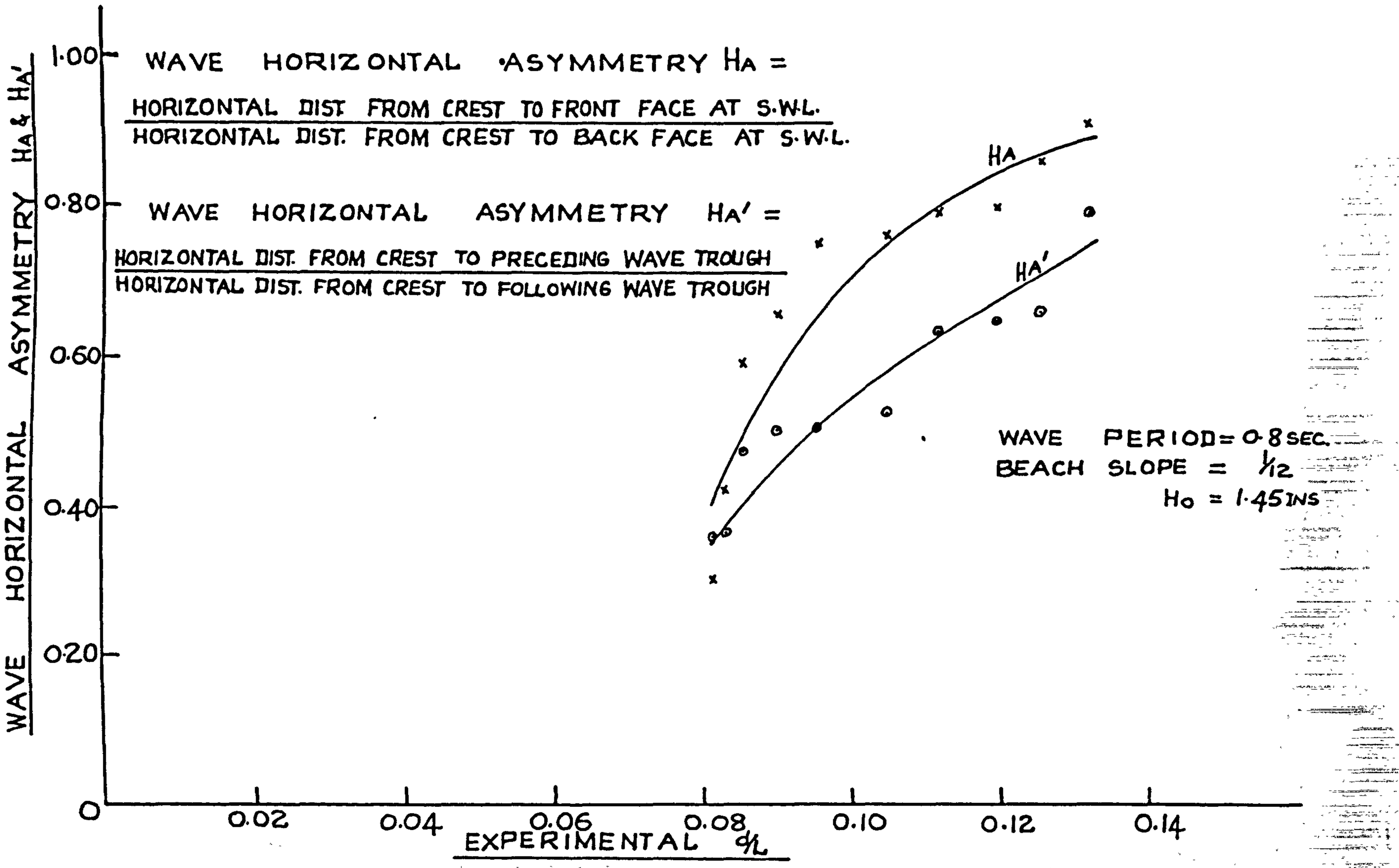

Figure 3.12 Graph of Wave Horizontal Asymmetry HA and HA'

WAVE HORIZONTAL ASYMMETRY HA & HA'

1.00
0.80
0.60
0.40
0.20
0

WAVE HORIZONTAL ASYMMETRY HA =

$$\frac{\text{HORIZONTAL DIST. FROM CREST TO FRONT FACE AT S.W.L.}}{\text{HORIZONTAL DIST. FROM CREST TO BACK FACE AT S.W.L.}}$$

WAVE HORIZONTAL ASYMMETRY HA' =

$$\frac{\text{HORIZONTAL DIST. FROM CREST TO PRECEDING WAVE TROUGH}}{\text{HORIZONTAL DIST. FROM CREST TO FOLLOWING WAVE TROUGH}} \times$$

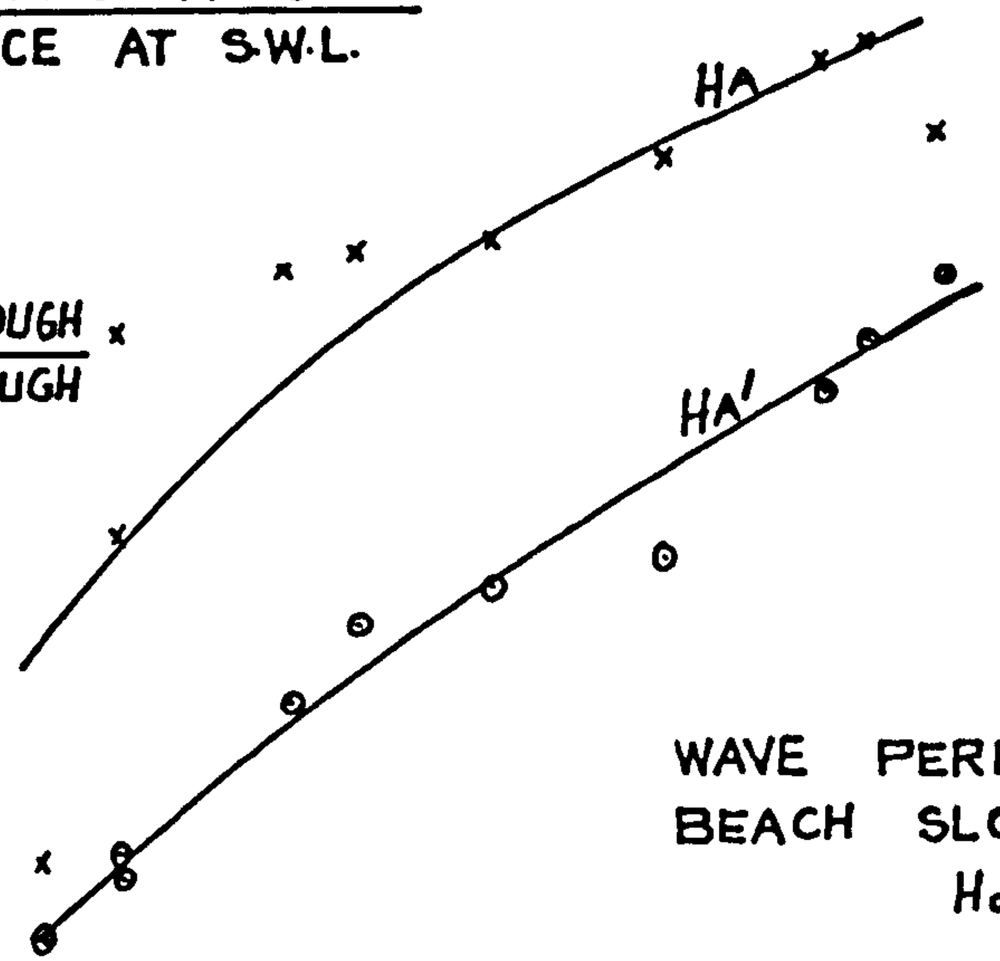

WAVE PERIOD = 0·8SEC.
BEACH SLOPE = 1/5
H_o = 1·45INS

0 0.02 0.04 0.06 0.08 0.10 0.12 0.14

EXPERIMENTAL d/L

Figure 3.13 Graph of Wave Horizontal Asymmetry HA and HA'

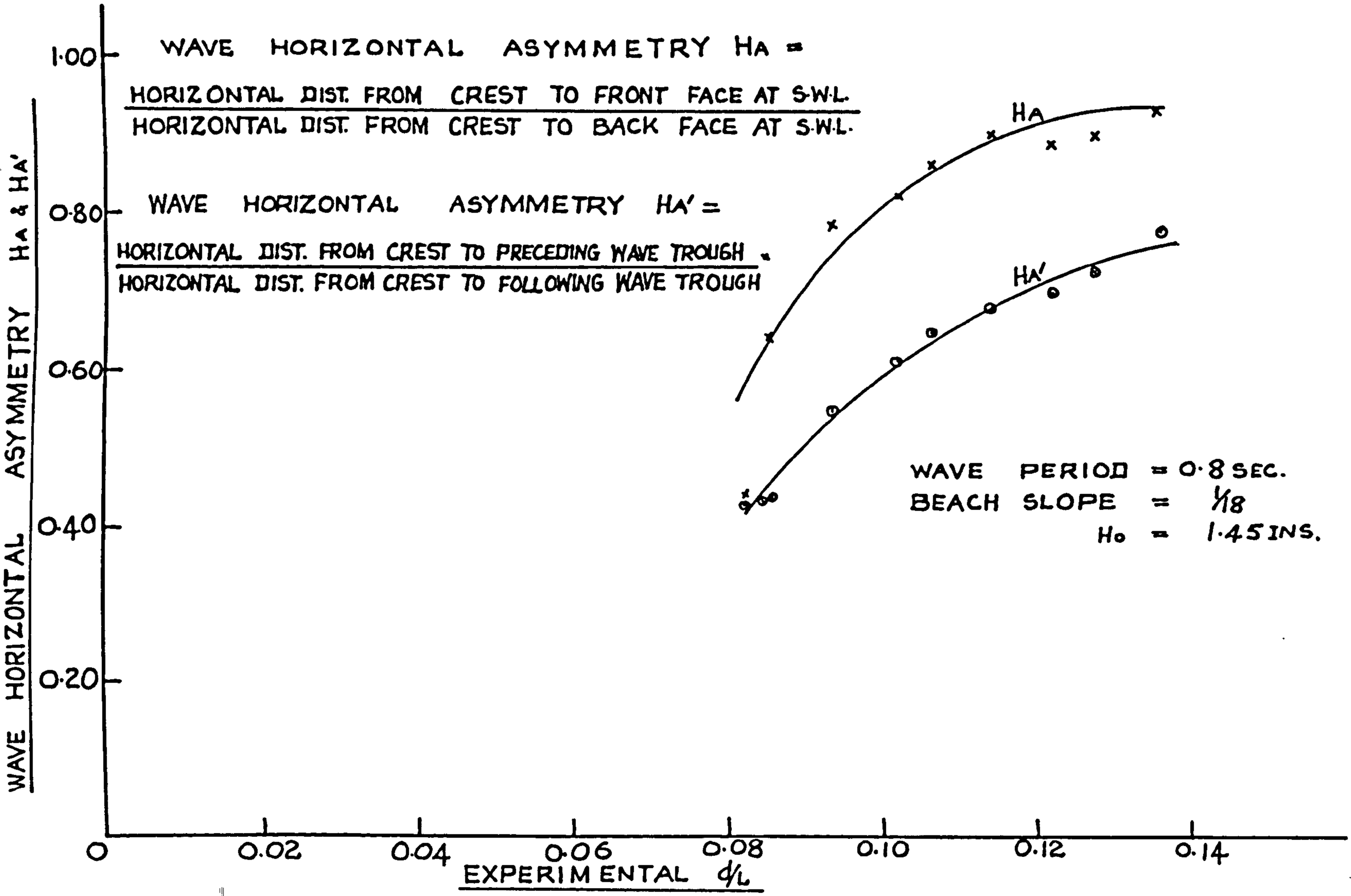

Figure 3.14 Graph of Wave Horizontal Asymmetry HA and HA'

in figures 3.10, 3.11, 3.12, 3.13 and 3.14. and follow the same trend as that on the beach slope of $\frac{1}{4}$ discussed above.

Figure 3.15 and 3.16 show the effect of beach slope on the wave horizontal asymmetry HA and HA'. It is evident from the figures that the horizontal asymmetry of the wave increases as the beach slope gets steeper, whereas it will be remembered that in very shallow water in the case of wave vertical asymmetry, the vertical asymmetry decreases as the beach slope gets steeper.

As can be seen that Figure 3.17, which shows the graph of HA and HA' for the different beach slopes, establishes a correlation between the two types of wave horizontal asymmetry HA and HA'. This is not unexpected, but it is quite useful, in that it does mean that observations or calculations in wave studies can be made in terms of either parameter.

3.5 Experimental Results on Wave Slope Asymmetry

The wave slope asymmetry as noted in section 2.4.4 chapter 2 was defined as

$$\frac{1}{2}\left\{\begin{array}{l}\text{Front face slope at still water level} + \\ \qquad\qquad \text{back face slope at still water level}\end{array}\right\}.$$

Both the front face and the rear face slopes are measured in radians. The front face slope was taken as negative and the back face slope as positive, thus the mean value

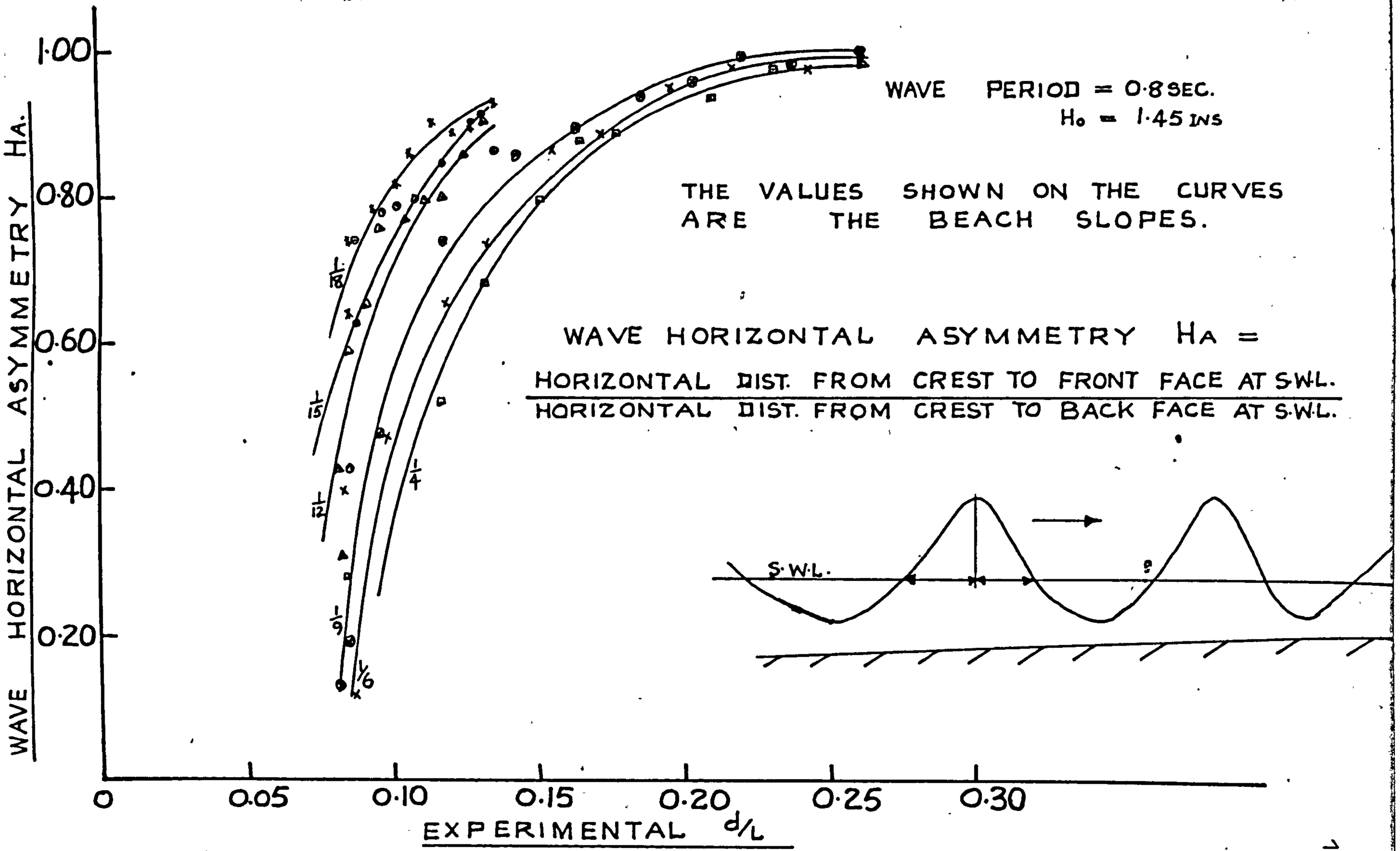

Figure 3.15 Effect of Beach Slope on Wave Horizontal Asymmetry HA

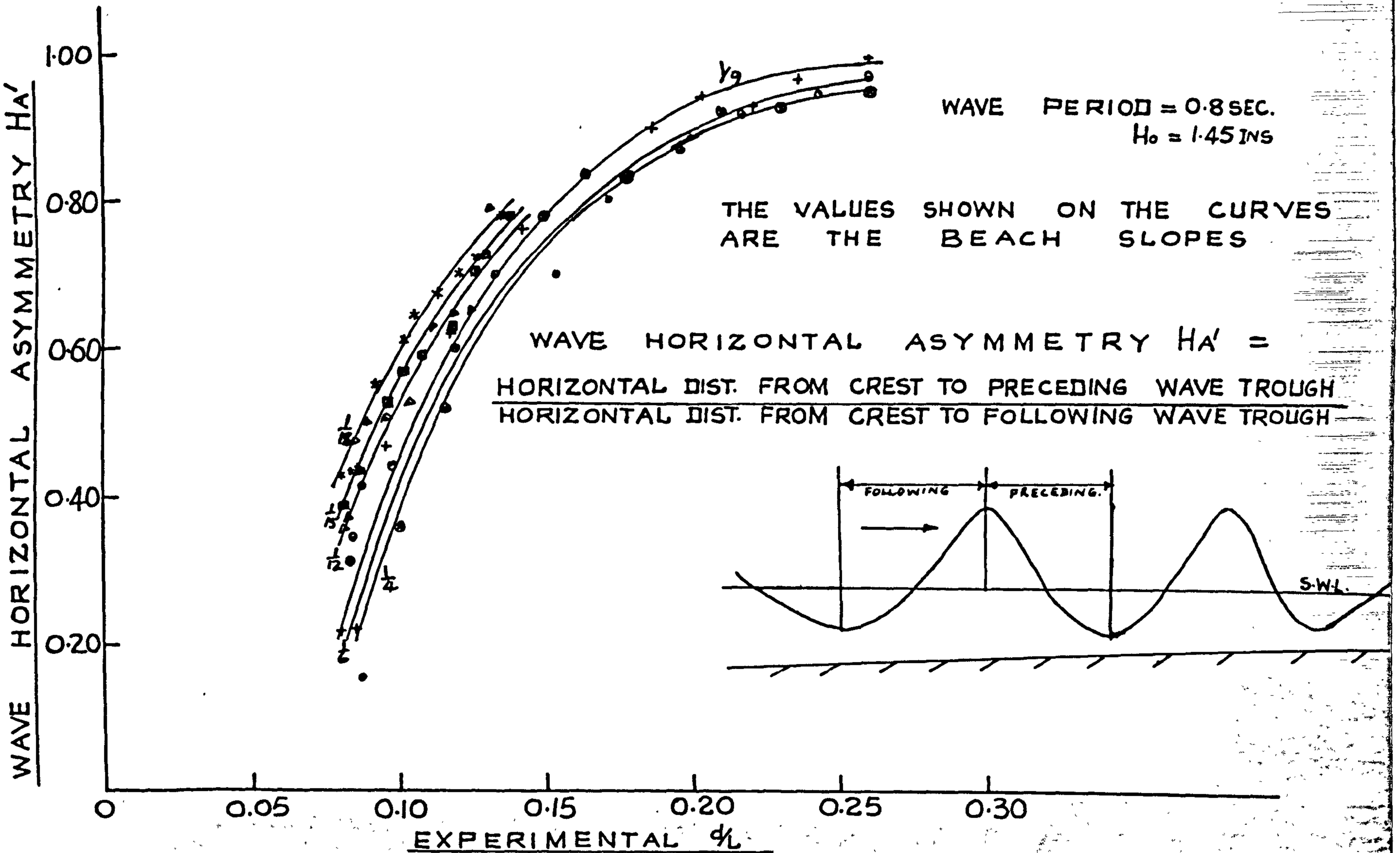

Figure 3.16 Effect of Beach Slope on Wave Horizontal Asymmetry HA'

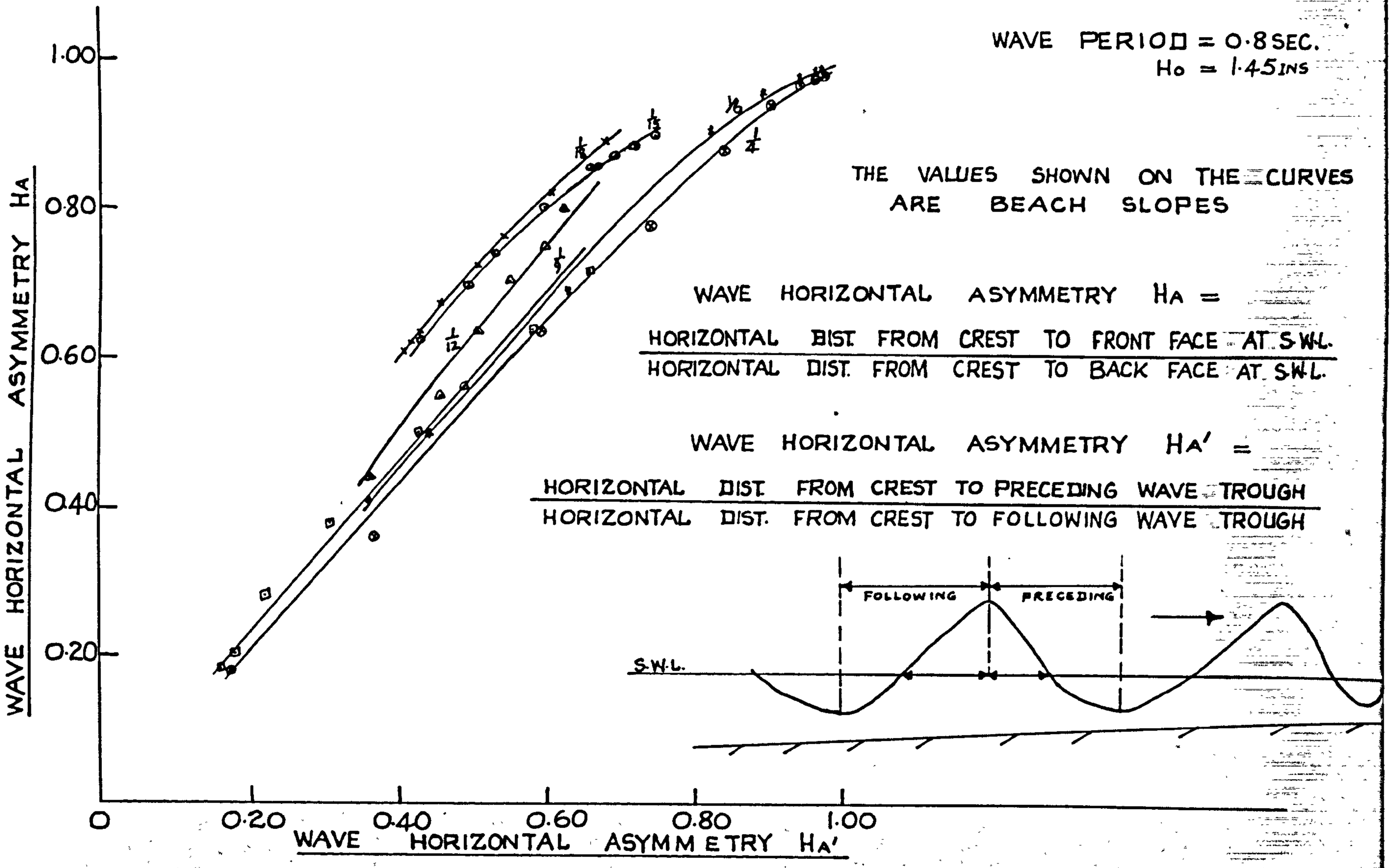

Fig. 3.17 Graph of Wave Horizontal Asymmetry HA against HA'

is a measure of the extent to which the wave front is steeper than the rear face of the wave. This is thus a measure of the asymmetry of the wave. An increasing numerical value of the wave slope asymmetry therefore denotes increasing asymmetry.

On the beach slope of $\frac{1}{4}$, the graph of wave slope asymmetry against $\frac{d}{L}$ (see figure 3.18) showed that the wave slope asymmetry increased as the wave advanced into shallower water. The wave slope asymmetry was negligible at $\frac{d}{L}$ value of 0.26 whereas at $\frac{d}{L}$ value of 0.15 the value of the wave slope asymmetry was -0.007. The most rapid change in wave slope asymmetry took place at $\frac{d}{L} < 0.15$. For instance, at $\frac{d}{L}$ value of 0.10 the value of the wave slope asymmetry became -0.037. At the breaker position where the wave was most asymmetric the value of the wave slope asymmetry was -0.083. The theoretical curve based on the theory of Biesel[5] gave results rather lower than the experimental results.

On the beach slope of $\frac{1}{6}$ (see fig. 3.19), it was again found that the most rapid change in wave slope asymmetry took place at $\frac{d}{L} < 0.15$. The theoretical curve agreed quite well with the experimental results. The maximum divergence between the theory and the experimental results was about 7% of the theoretical prediction. The results for beach slopes of $\frac{1}{9}$, $\frac{1}{12}$,

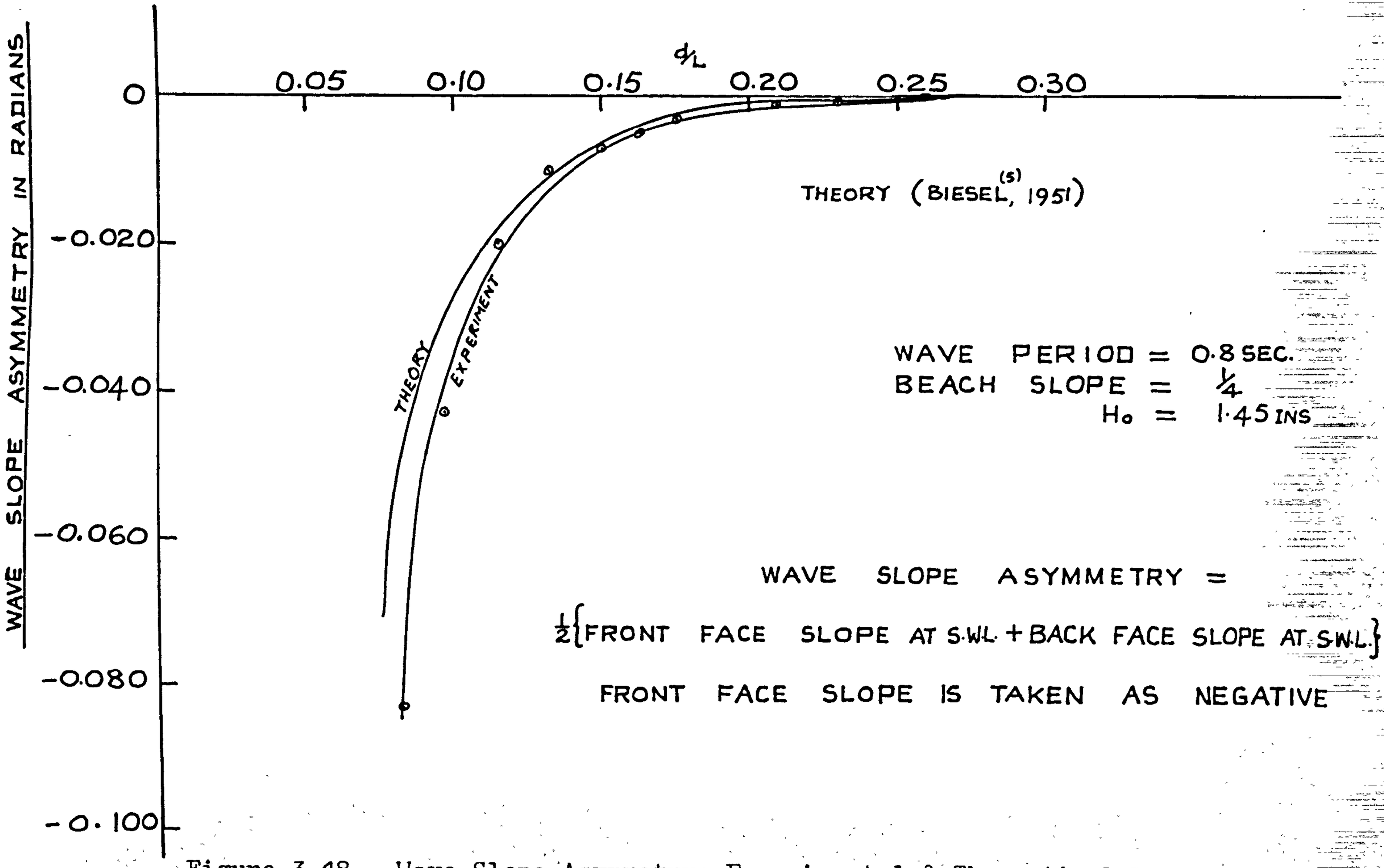

Figure 3.18 Wave Slope Asymmetry: Experimental & Theoretical Results.

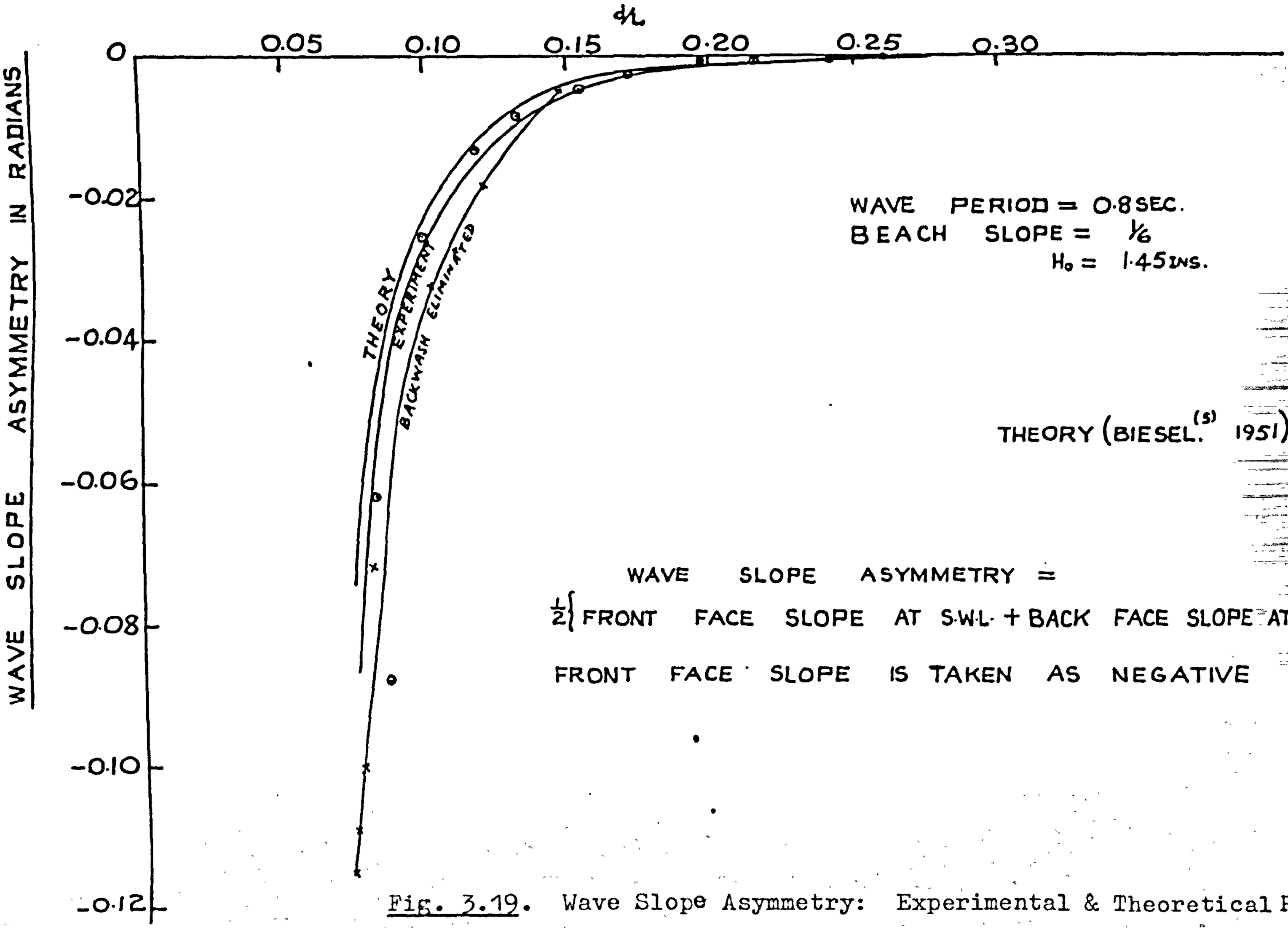

Fig. 3.19. Wave Slope Asymmetry: Experimental & Theoretical Results

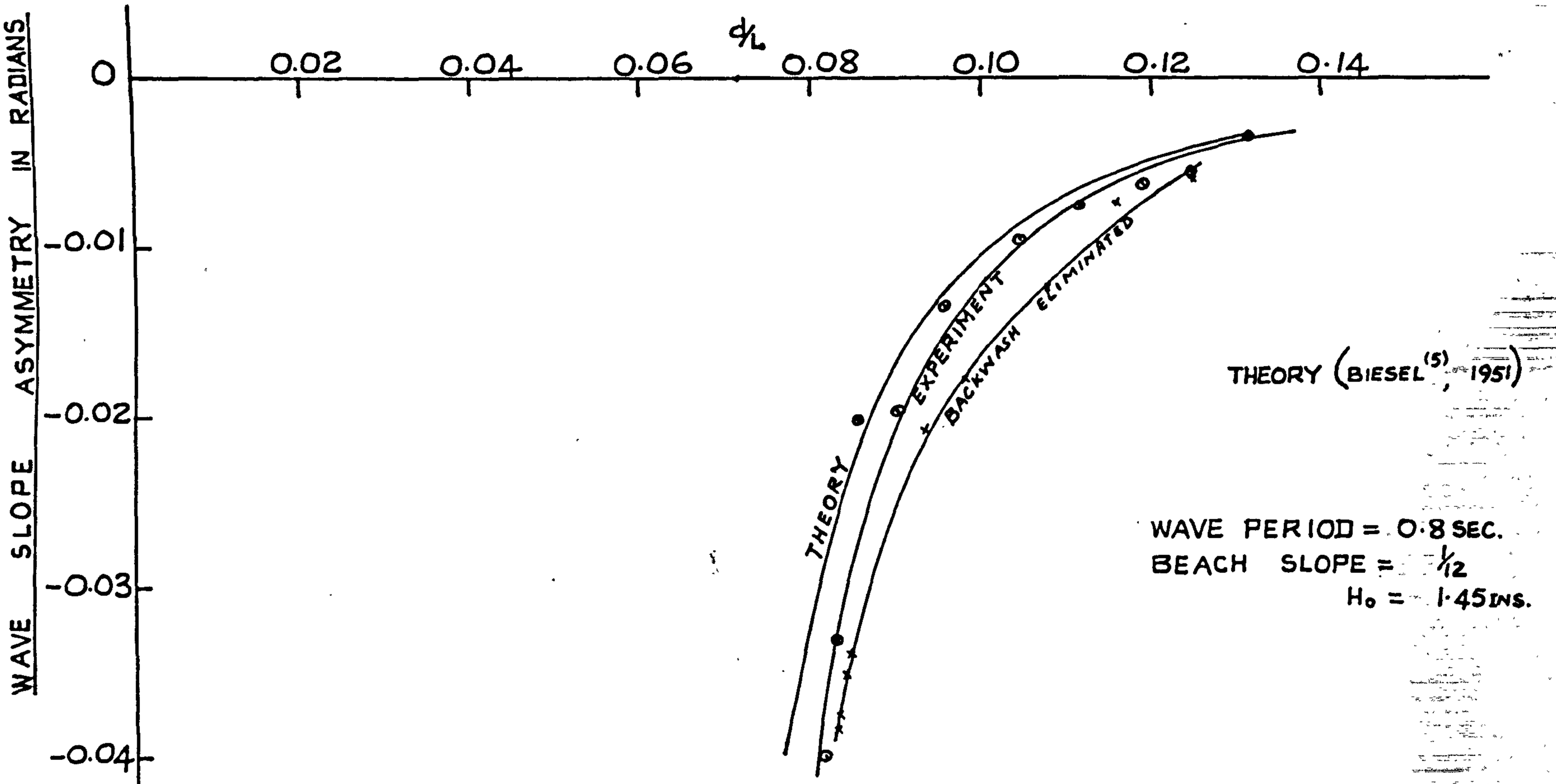

WAVE SLOPE ASYMMETRY =
$\frac{1}{2}$ {FRONT FACE SLOPE AT S.W.L. + BACK FACE SLOPE AT S.W.L.}

FRONT FACE SLOPE IS TAKEN AS NEGATIVE

Fig. 3.20 Wave Slope Asymmetry: Experimental and Theoretical Results

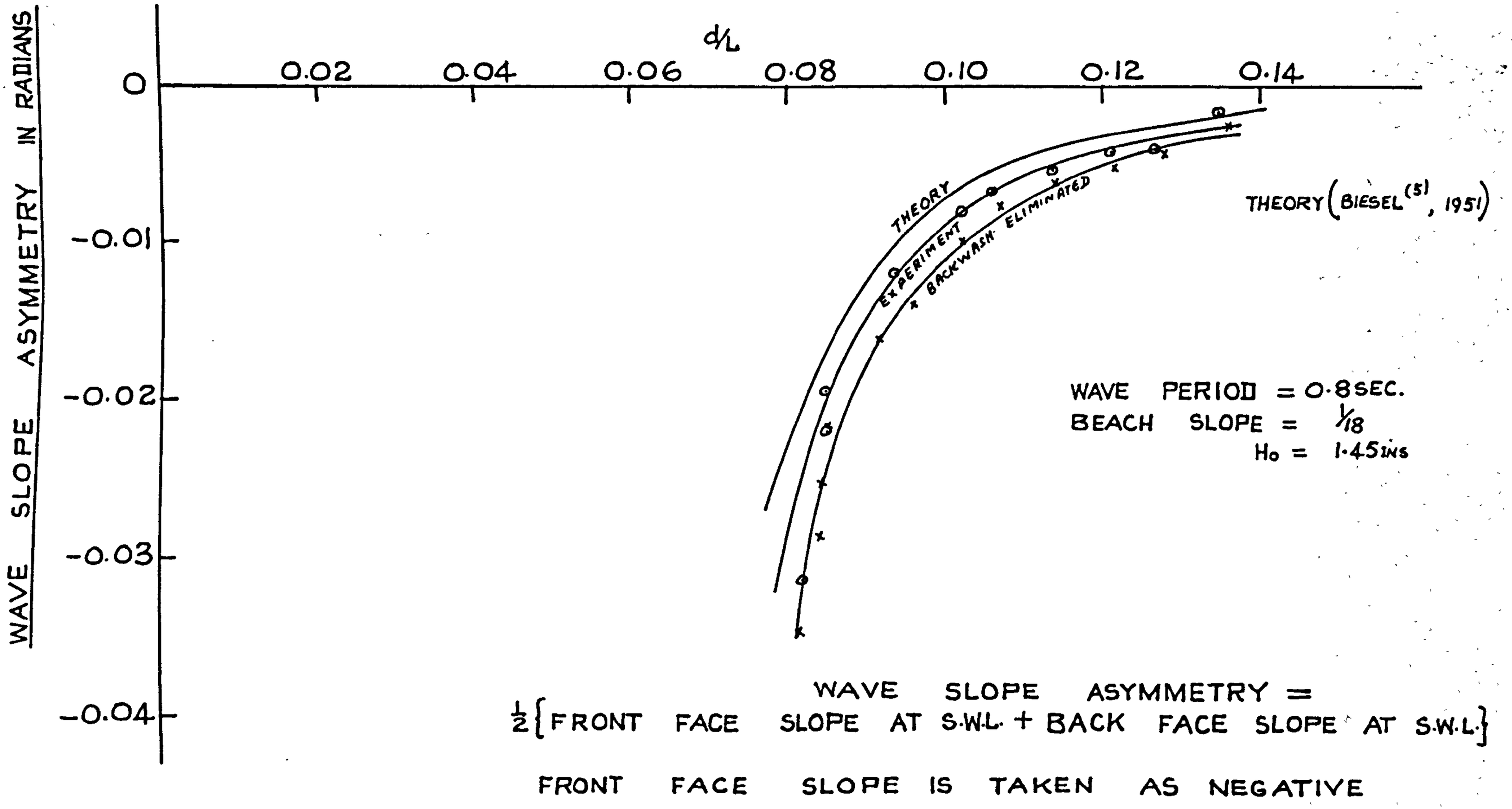

Fig. 3.21 Wave Slope Asymmetry: Experimental & Theoretical Results

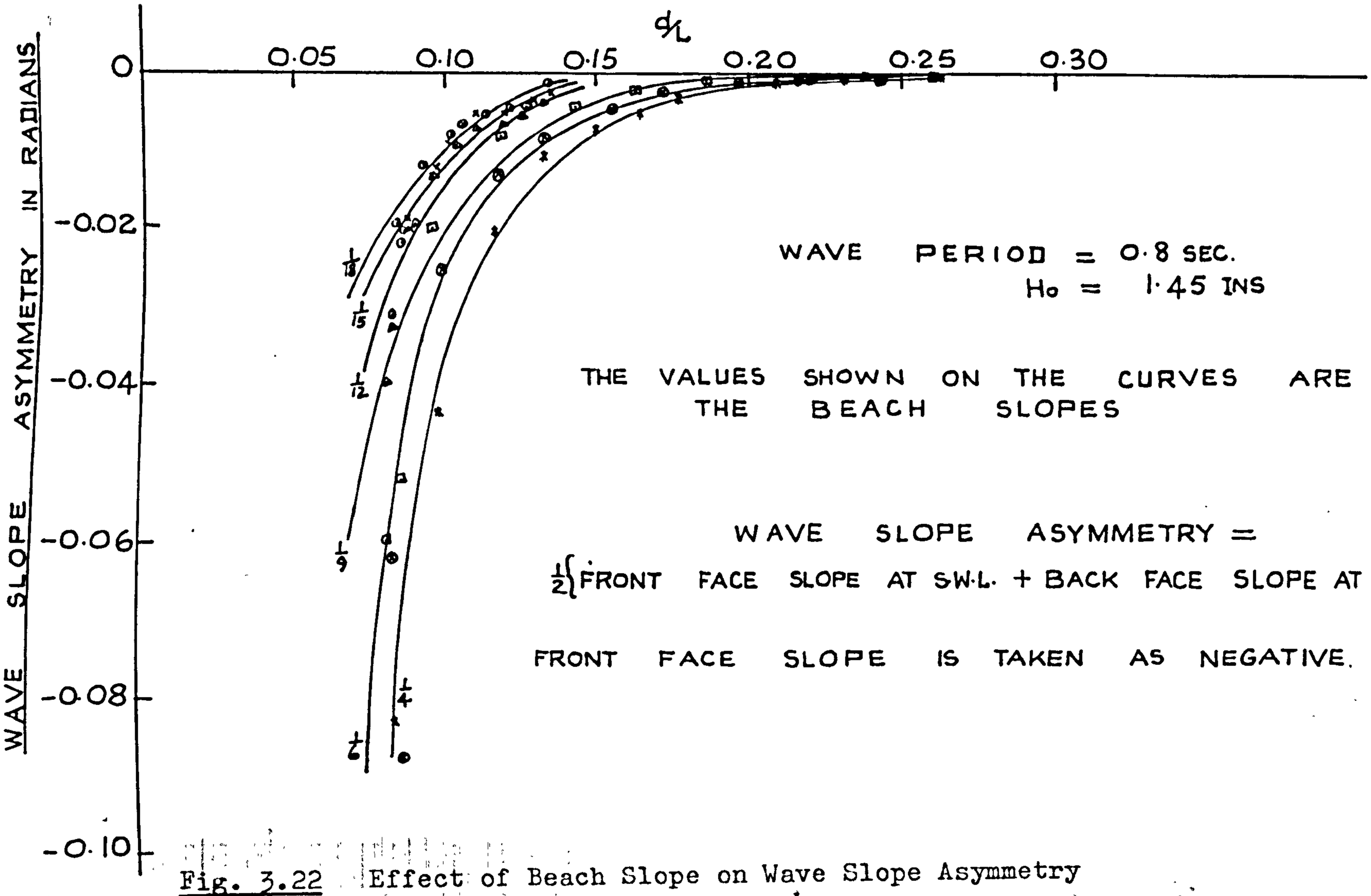

Fig. 3.22 Effect of Beach Slope on Wave Slope Asymmetry

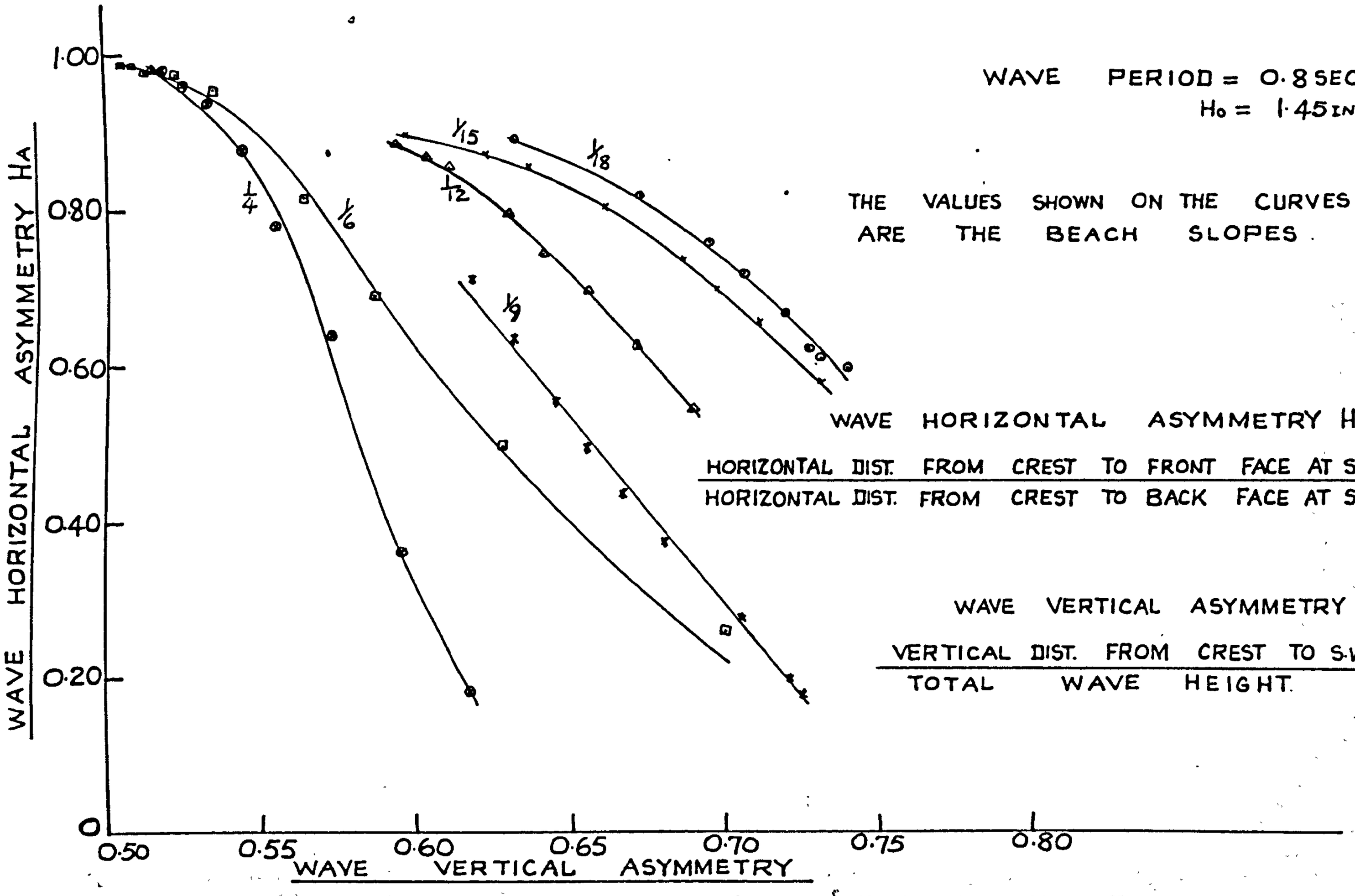

Fig. 3.23 Graph of Wave Horizontal Asymmetry HA against Wave Vertical Asymmetry

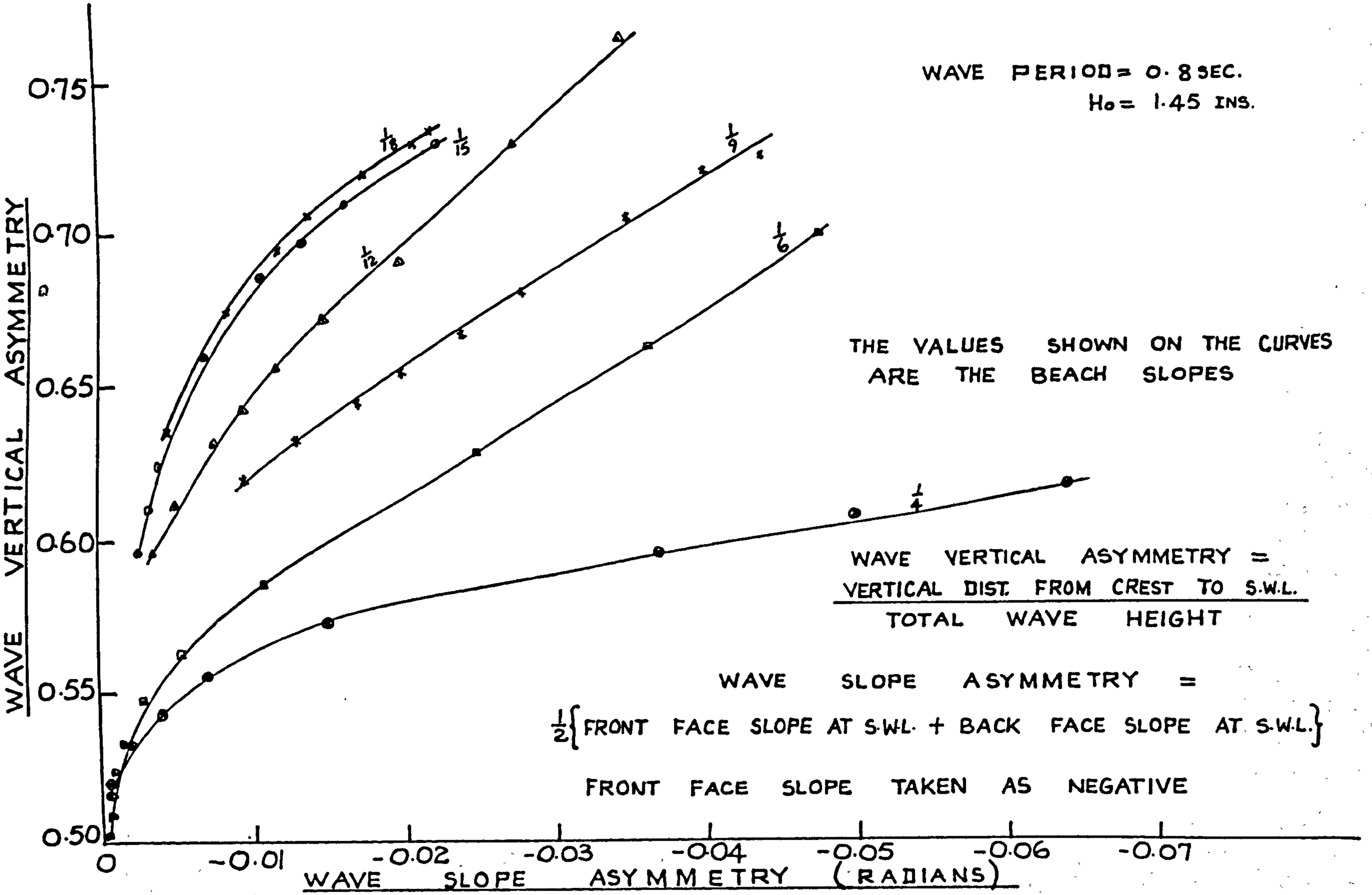

Fig. 3.24 Graph of Wave Vertical Asymmetry against Wave Slope Asymmetry

$\frac{1}{15}$ and $\frac{1}{18}$ indicated a similar trend to those discussed above, and the results for slopes of $\frac{1}{12}$ and $\frac{1}{18}$ are shown in figures 3.20 and 3.21.

As can be seen from Figure 3.22 showing the effect of beach slope on wave slope asymmetry, the wave slope asymmetry increases as the beach slope gets steeper. This is in marked contrast with the wave vertical asymmetry which decreases as the beach slope gets steeper. On the other hand the wave horizontal asymmetry increases with increasing beach slope.

Figure 3.23 and 3.24 show however that all of the asymmetries, 'slope', 'vertical', and 'horizontal', are correlated and as will be shown later on, the orbital velocity field at the bed is also correlated with all three asymmetries.

3.6 Conclusions

The wave asymmetry defined in all of the three ways increases as the wave advances into shallower water and the wave is most asymmetric at the wave break-point. The most rapid change in wave asymmetry takes place in the region $\frac{d}{L} < 0.15$.

The cnoidal wave theory is adequate for predicting wave vertical asymmetry. However, whereas, the cnoidal theory indicates a non-linear curve throughout, the

experimental curves of the wave vertical asymmetry against $\frac{d}{L}$ became linear for slopes $< \frac{1}{12}$. The linearity of the curve will be considered again in the next chapter, when considering the effect of the backwash of the wave.

The work on the wave slope asymmetry showed good agreement with the theory of Biesel[5]. The results of the experiments for the beach slopes $\frac{1}{4}$, $\frac{1}{6}$ and $\frac{1}{9}$ indicated that the wave slope asymmetry ceases at $\frac{d}{L} = 0.26$. The theory of Biesel[5] predicted that the wave slope asymmetry ceases at $\frac{d}{L} = 0.27$. This is a useful and interesting agreement with theory especially as no previous comparison or verification of this theory has been made.

The wave horizontal asymmetry (both HA and HA') and the wave slope asymmetry increase as the beach slope gets steeper, whereas the wave vertical asymmetry is greater for flat slopes when the wave is in very shallow water. The rule of thumb that the trough is a quarter of the breaker height below the undisturbed water level, whatever the beach slope is not quite correct.

A correlation was found to exist between the two types of wave horizontal asymmetry HA and HA'. Further they both show the same trend, thus any studies connected with the wave horizontal asymmetry could be made using

either HA or HA'. As shallow water waves tend towards the characteristics of long waves, it is evident that measurement of HA would be more precise than HA'.

Apart from the correlation between the two types of wave horizontal asymmetry HA and HA' a[illegible] correlation was also found to exist between the wave slope asymmetry, wave horizontal asymmetry and the wave vertical asymmetry. The correlation between the wave asymmetry and the resulting orbital velocity fields at the bed will be discussed in Chapter 5. where the empirical relationships connecting the velocity asymmetry, the wave vertical asymmetry, wave slope asymmetry and the wave horizontal asymmetry will be presented.

CHAPTER 4

EFFECT OF THE BACKWASH OF THE WAVE ON WAVE ASYMMETRY

4.1 Introduction

When the wave breaks, the motion becomes translatory and the water rushes up the beach face moving some sediment along with it. However owing to percolation friction and gravity, the uprush gradually slows down, and soon reaches its limit of uprush. At this maximum landward limit on sandy beaches, a thin line of sand grains (called a swash mark) is deposited Wiegel[56]. When the motion up the beach face has ceased, the water which has not percolated returns down the beach face as a backwash, again moving sediment with it. A fairly large backwash induces erosion of a natural beach and churning up of the sediment within the surf zone. On the other hand a weak backwash may be substantially reduced through percolation and thus the sediment brought up by the swash is slowly added to the beach. Wiegel[56] cautioned that a cursory inspection of a beach immediately following a storm when rapid changes have been taking place may lead to conclusions that would not be substantiated a few days later.

In addition to the importance of the bed slope, wave characteristics are certainly affected by the

backwash of the preceding wave. To the best of the author's knowledge the work reported in this thesis is the first detailed study of the effect of the backwash of the wave on the asymmetry of the wave seaward of the breakers. In the present chapter, the effect of the backwash of the wave on wave asymmetry will be considered, and in Chapter 5 the effect of the backwash of the wave on the orbital velocity asymmetry will be dealt with, while discussing the velocity asymmetry in the breaker zone.

Various comments on the backwash have been made from time to time in the literature. Ippen and Kulin[15] commented that the backwash from preceding waves undoubtedly plays an important role in the breaking process. Iversen[16] also considered the backwash an important factor in the breaking action. Scott[44] in a study of sand movement by waves noted that the sand deposited on the foreshore was flung up the beach by the swash and rolled part way down again by the backwash. He observed that the grains which were packed tightly in place remained on the foreshore while loose grains were rolled back down the beach face by the backwash. He then concluded that the continual action of the swash and backwash reworked the surface layer of the beach, fitting the grains tightly in place as they were deposited.

Mason[36] in an experiment on breaking waves observed that as the wave approached the area of breaking there was a reduction in the speed of advance of the forward face and consequent overtaking of the forward face by the seaward face of the crest, and that the deceleration of the forward face appeared to be related to the speed and depth of the backwash from the preceding broken wave. He commented that there seemed to be an area of limited extent around the intersection of the forward face of the advancing wave and the backwash within which the backwash flow was halted and the water surface rose rapidly, suggesting a conversion of the kinertic energy of the backwash to potential energy in the form of a rise in water surface elevation.

Eagleson and Dean[9] remarked that the onshore motion is more and more opposed by the backwash from the preceding waves in the vicinity of the breaker.

As noted above, the studies discussed in this chapter are concerned with the effect of the elimination of the backwash of the wave on the wave vertical asymmetry, wave horizontal asymmetry and wave slope asymmetry. The work was carried out over five beach slopes and the wave conditions were the same as in the previous study on the effect of beach slope and shoaling on wave asymmetry.

4.2 Results of Experiments on the Effect of Backwash on Wave Vertical Asymmetry

On the beach slope of $\frac{1}{6}$ the graph of wave vertical asymmetry against $\frac{d}{L}$ showed that the effect of eliminating the backwash of the wave was to cause a reduction in the wave vertical asymmetry. As the wave progressed shoreward the wave vertical asymmetry increased but the value of the wave vertical asymmetry was much reduced compared with the case when there was normal backwash. For instance, at a $\frac{d}{L}$ value of 0.14 while the value of the wave vertical asymmetry with backwash was 0.573, the value when the backwash was eliminated was 0.538. At a $\frac{d}{L}$ value of 0.10 the corresponding values of the wave vertical asymmetry were 0.630 and 0.55. Furthermore, it was found that the wave broke in shallower water when the backwash was eliminated, which indicated that the presence of the backwash induces early breaking of the wave, although its presence is not a necessary condition for wave breaking. At the break-point where the wave was most asymmetric the value of the wave vertical asymmetry without the backwash was 0.573 which showed the vertical asymmetry was much reduced when compared with a corresponding value of 0.707 for the wave vertical asymmetry at the break-point with backwash. (See Figure 3.6)

The results for the slopes of $\frac{1}{9}$ and $\frac{1}{12}$ are shown in Figure 4.1 and 4.2 and follow the same trend.

For the beach slope of $\frac{1}{15}$ the graph of wave vertical asymmetry against $\frac{d}{L}$ is shown in figure 4.3. As noted in the last Chapter in a study in which there was normal backwash, the graph of wave vertical asymmetry against $\frac{d}{L}$ was found to be linear on the beach slopes$<\frac{1}{12}$. It was found when the backwash was eliminated that the graph of wave vertical asymmetry against $\frac{d}{L}$ became non linear on the beach slope of $\frac{1}{15}$ as on the steeper slopes of $\frac{1}{6}$, $\frac{1}{9}$ and $\frac{1}{12}$. This seems to show that the linear relationship when the back-wash was present was due to the flat beach slope and the backwash. However, it was found contrary to expectations that for all the beach slopes the theoretical predictions of the wave vertical asymmetry were nearer the experimental results in the case when there was backwash than when the backwash was eliminated. On the beach slope of $\frac{1}{18}$ which was the flattest beach slope considered in this work, the graph of the wave vertical asymmetry against $\frac{d}{L}$ still gave a linear curve when the backwash of the wave was eliminated. Further, the reduction in the wave vertical asymmetry was less on this flat slope as compared with the steeper slopes. For instance, at the $\frac{d}{L}$ value of 0.13 the value of the wave vertical asymmetry was found to be 0.562, when the backwash was eliminated compared with 0.580 when there was backwash. At the $\frac{d}{L}$ value of 0.10 the corresponding values were 0.660 and 0.675.

WAVE PERIOD = 0·8SEC.
BEACH SLOPE = 1/9
Ho = 1·45INS.

WAVE VERTICAL ASYMMETRY = VERTICAL DIST. FROM CREST TO S.W.L. / TOTAL WAVE HEIGHT

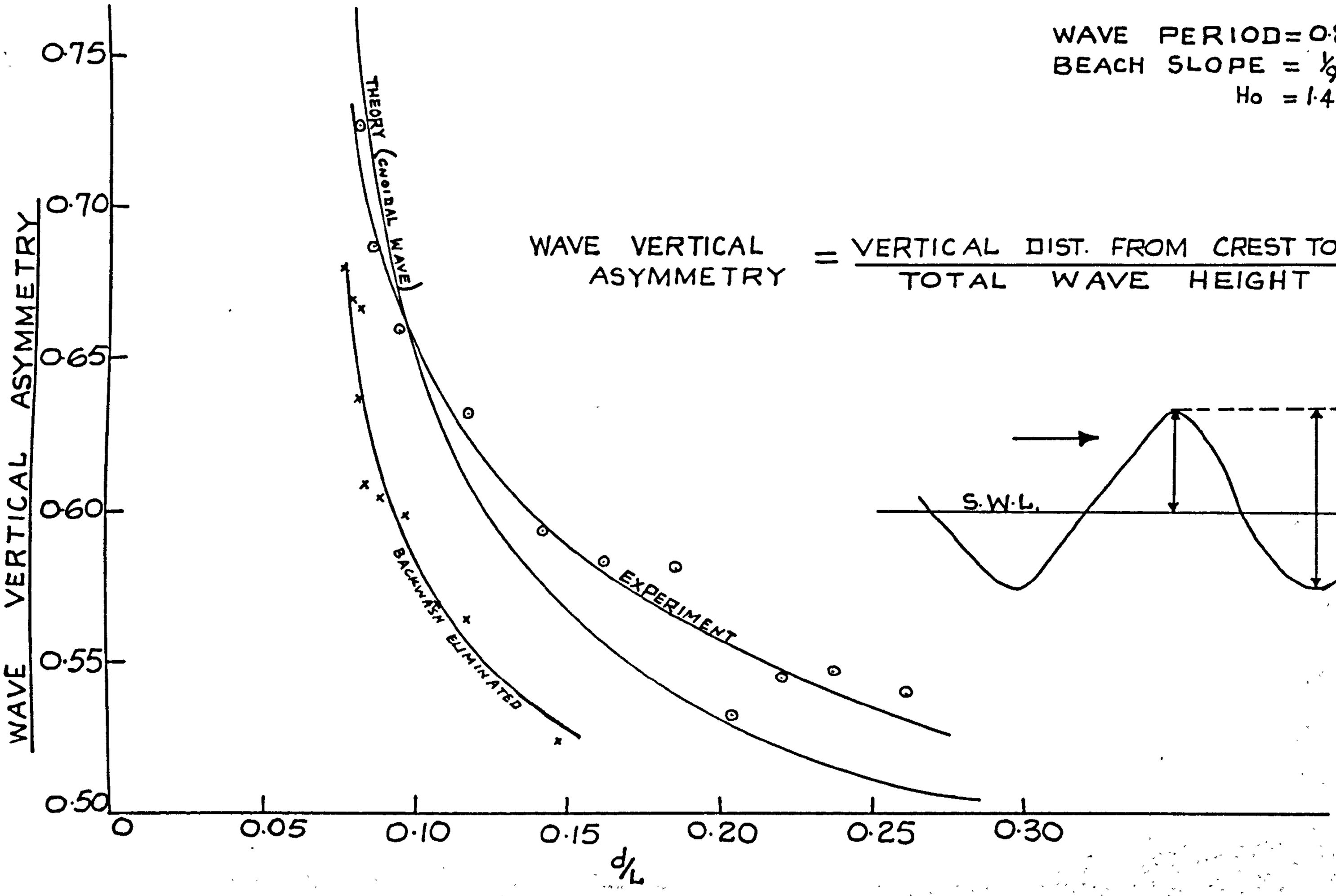

Fig. 4.1 Wave Vertical Asymmetry: Experimental & Theoretical Results.

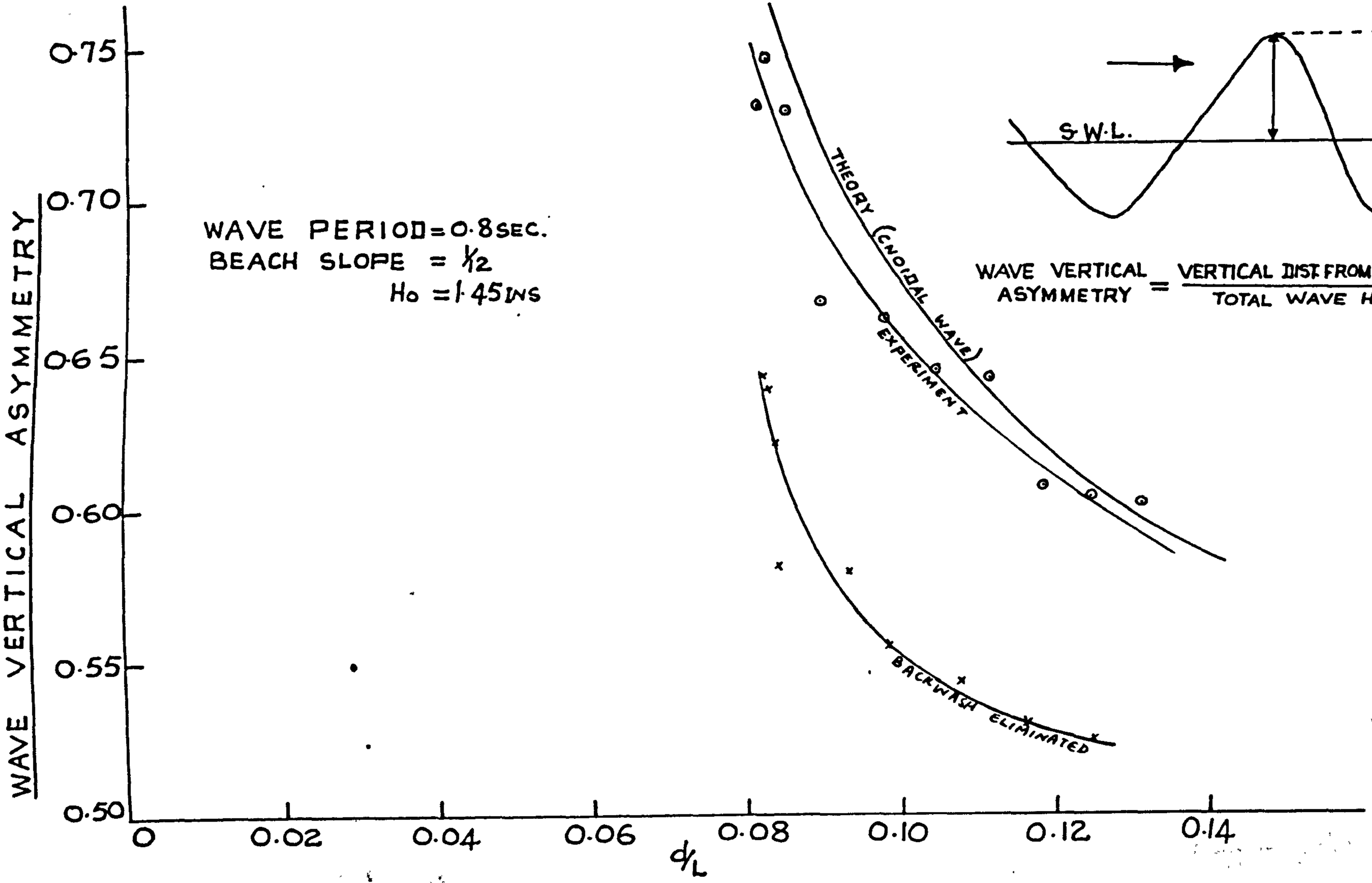

$$\text{WAVE VERTICAL ASYMMETRY} = \frac{\text{VERTICAL DIST. FROM CREST TO S.W.L.}}{\text{TOTAL WAVE HEIGHT.}}$$

Fig. 4.2 Wave Vertical Asymmetry: Experimental and Theoretical Results.

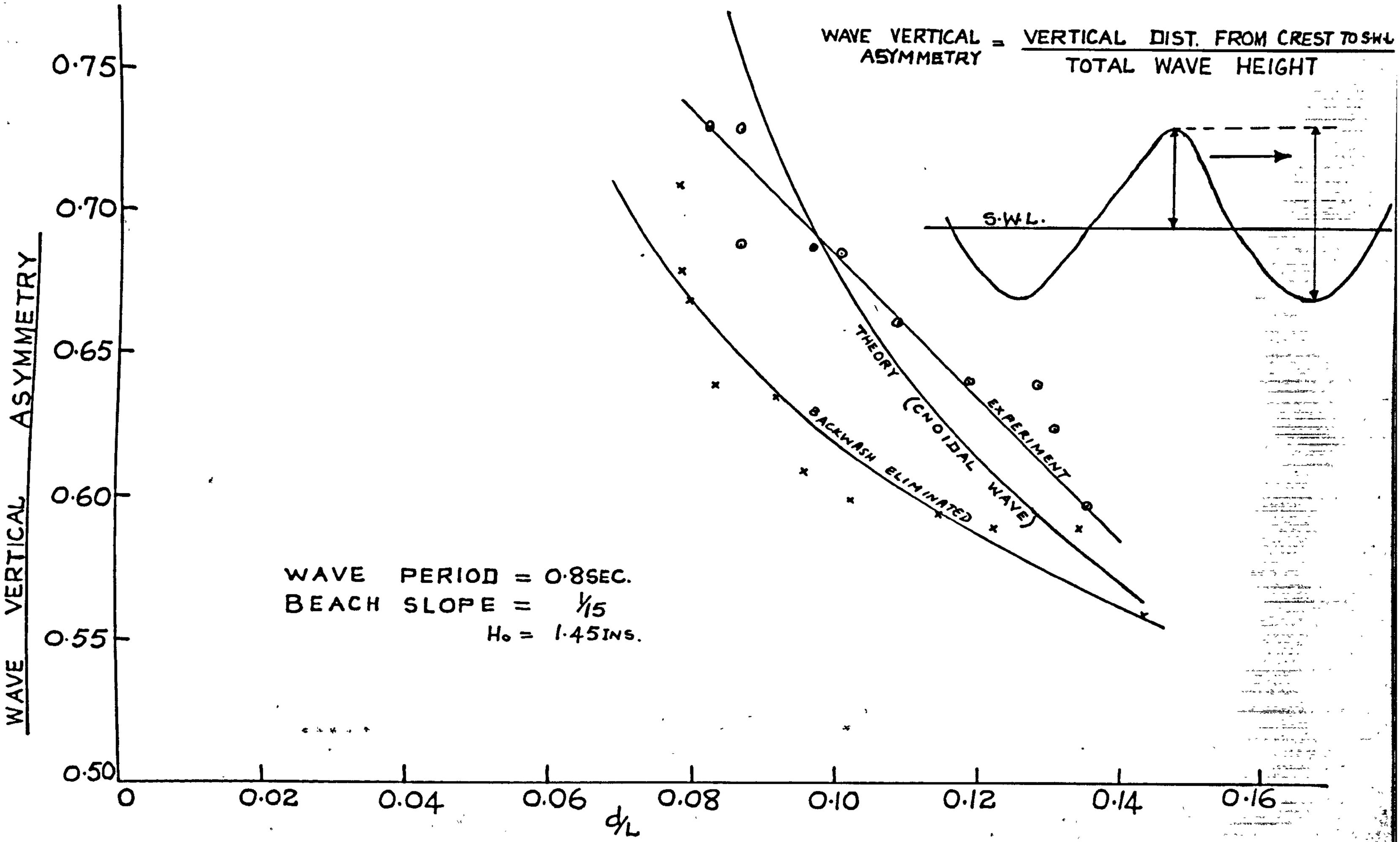

Fig. 4.3 Wave Vertical Asymmetry: Experimental and Theoretical Results

4.3 Results of Experiments on the Effect of Backwash on Wave Slope Asymmetry

The graph of wave slope asymmetry against $\frac{d}{L}$ for the beach slope of $\frac{1}{6}$ (see Figure 3.19) shows that the effect of eliminating the backwash of the wave was to increase the wave slope asymmetry. At a $\frac{d}{L}$ value of 0.15 the effect of the backwash on slope asymmetry did not seem to be significant. At a $\frac{d}{L}$ value of 0.12, values were -0.019 and -0.013, whereas at the $\frac{d}{L}$ value of 0.10 these became -0.036 and -0.025. At the wave breakpoint where the wave was most asymmetric, the value of the wave slope asymmetry when the backwash was eliminated was found to be -0.115, whilst when there was backwash the corresponding value was -0.060. Thus the increase was quite substantial at the breaker position.

Figure 4.4 shows the graph of wave slope asymmetry against $\frac{d}{L}$ for the beach slope of $\frac{1}{9}$ and shows that at the breaker position, the value of the wave slope asymmetry when the backwash was eliminated was -0.066 as against -0.04 with backwash. Further, it must be remembered that on the beach slope of $\frac{1}{6}$ the value of the wave slope asymmetry at the breakpoint when the backwash was eliminated

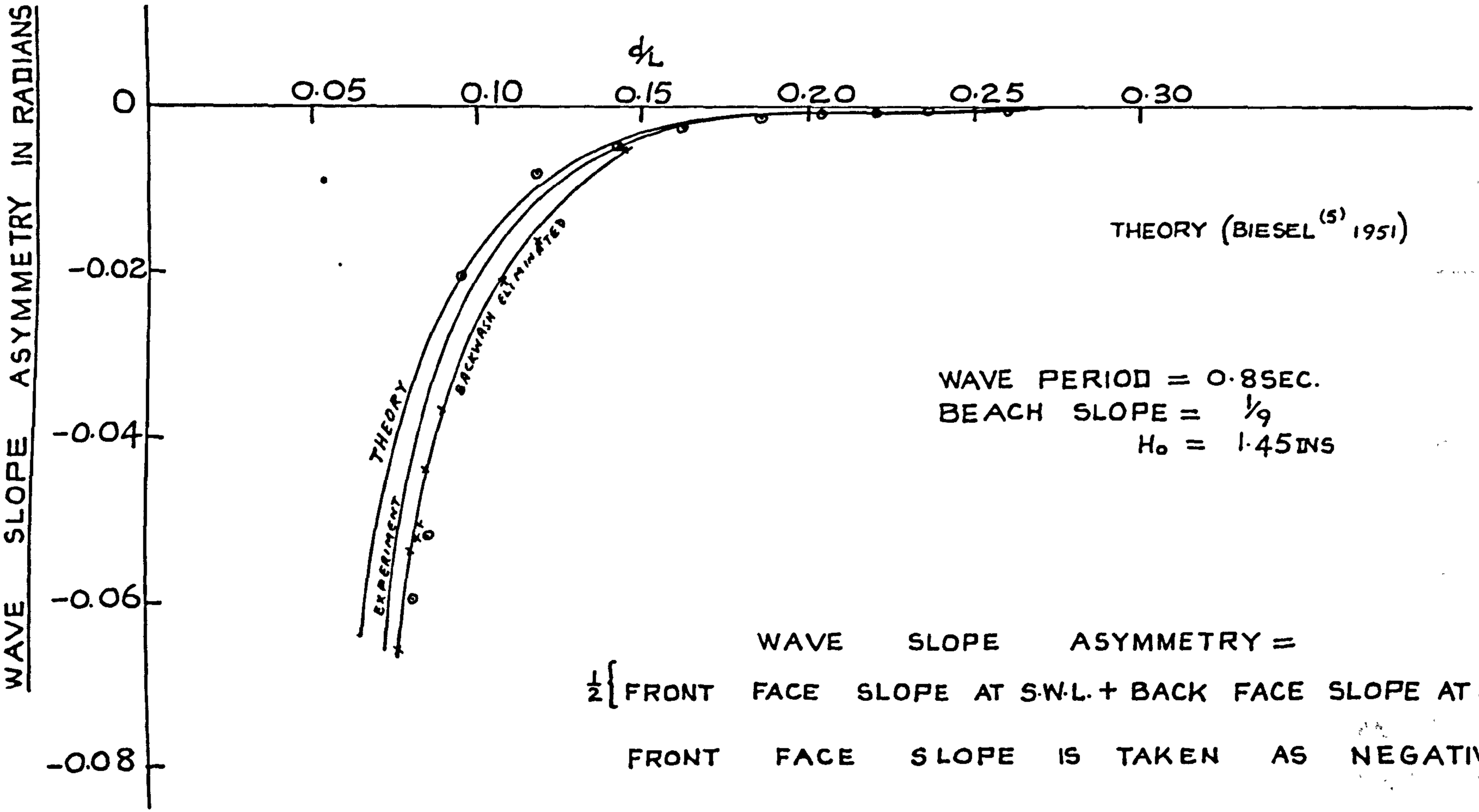

Fig. 4.4 Wave Slope Asymmetry: Experimental & Theoretical Results

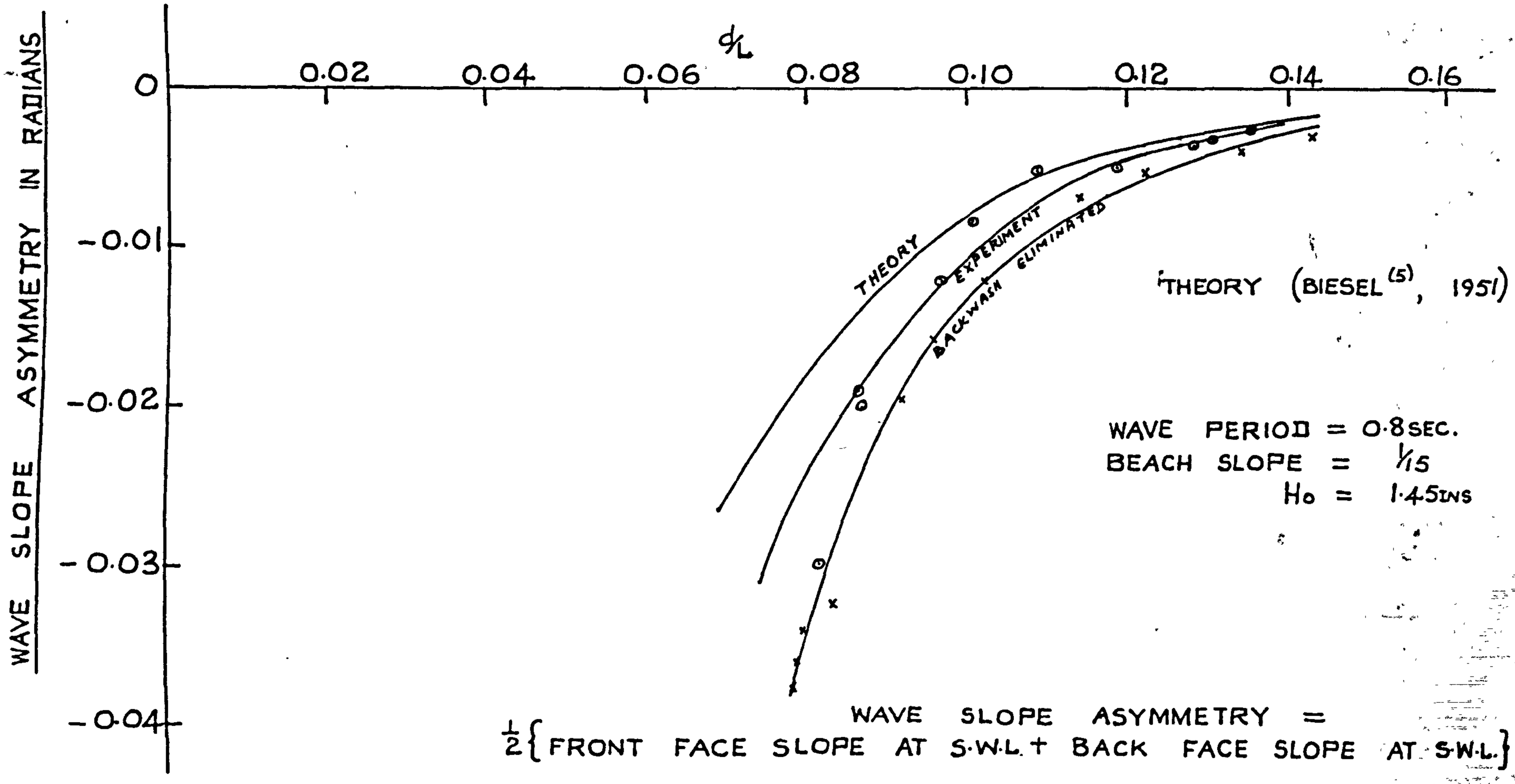

Fig. 4.5 Wave Slope Asymmetry: Experimental & Theoretical Results.

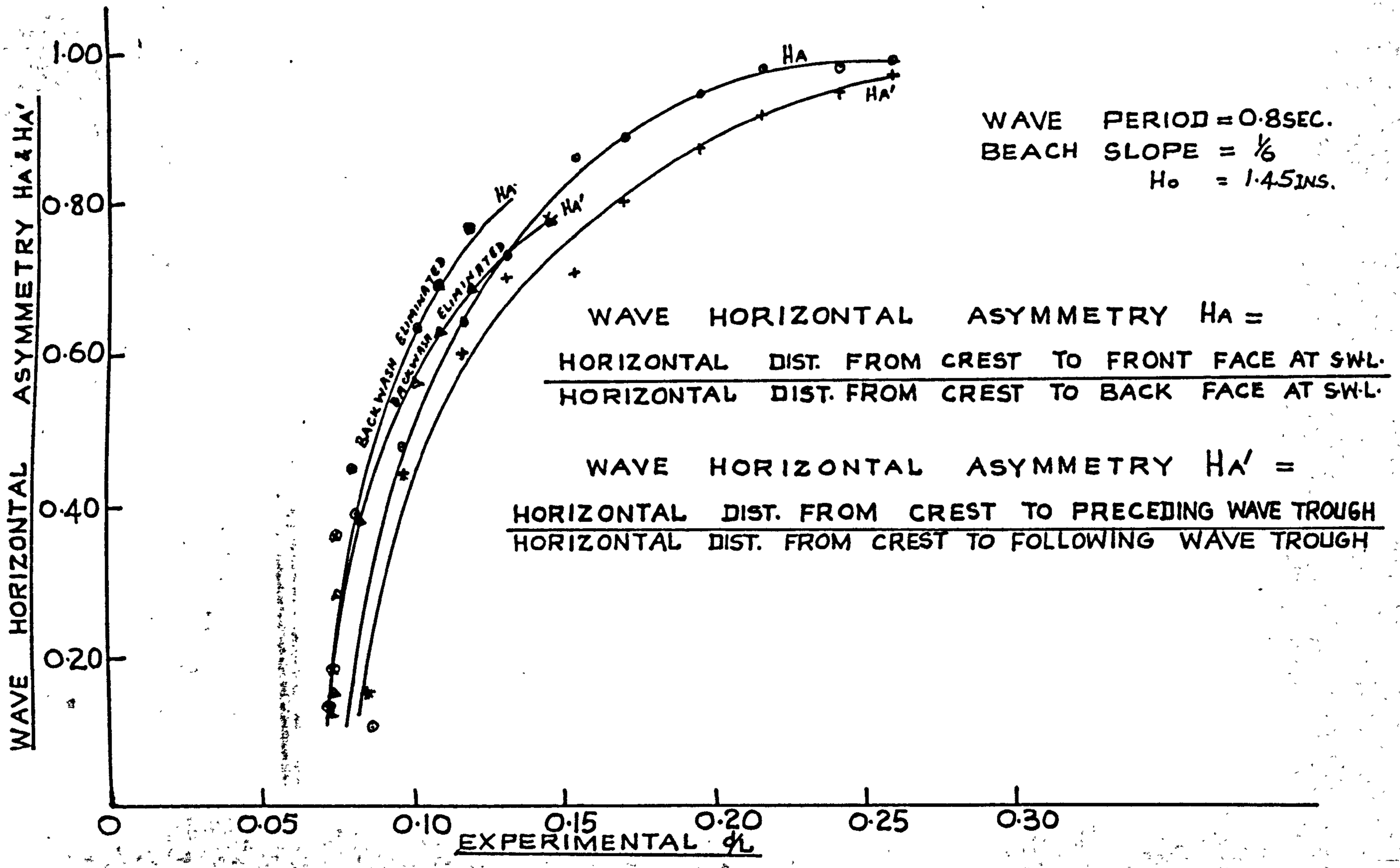

Fig. 4.6 Effect of Eliminating Backwash on Wave Horizontal Asymmetry HA and HA'

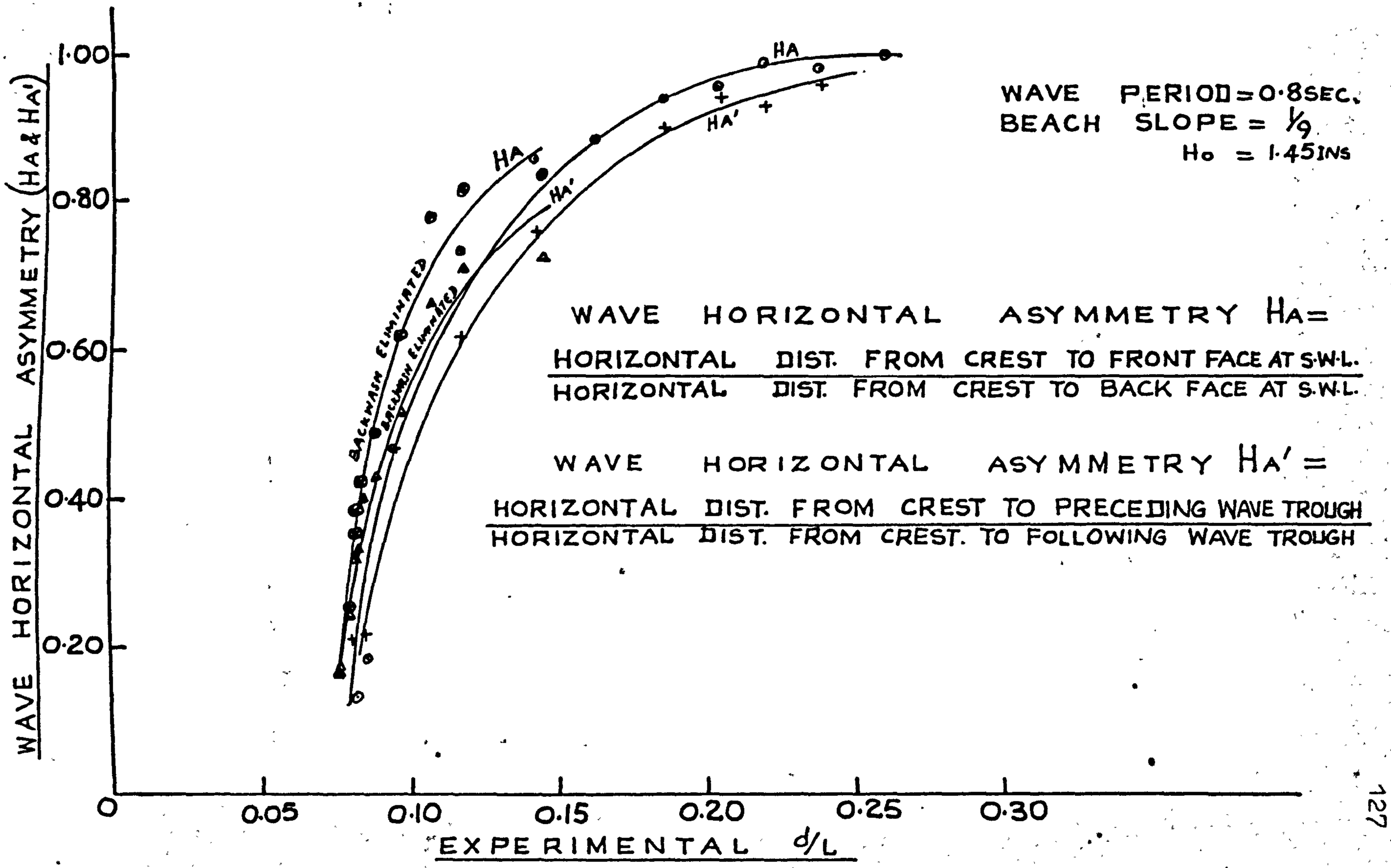

Figure 4.7 Effect of Eliminating Backwash on Wave Horizontal Asymmetry HA and HA'

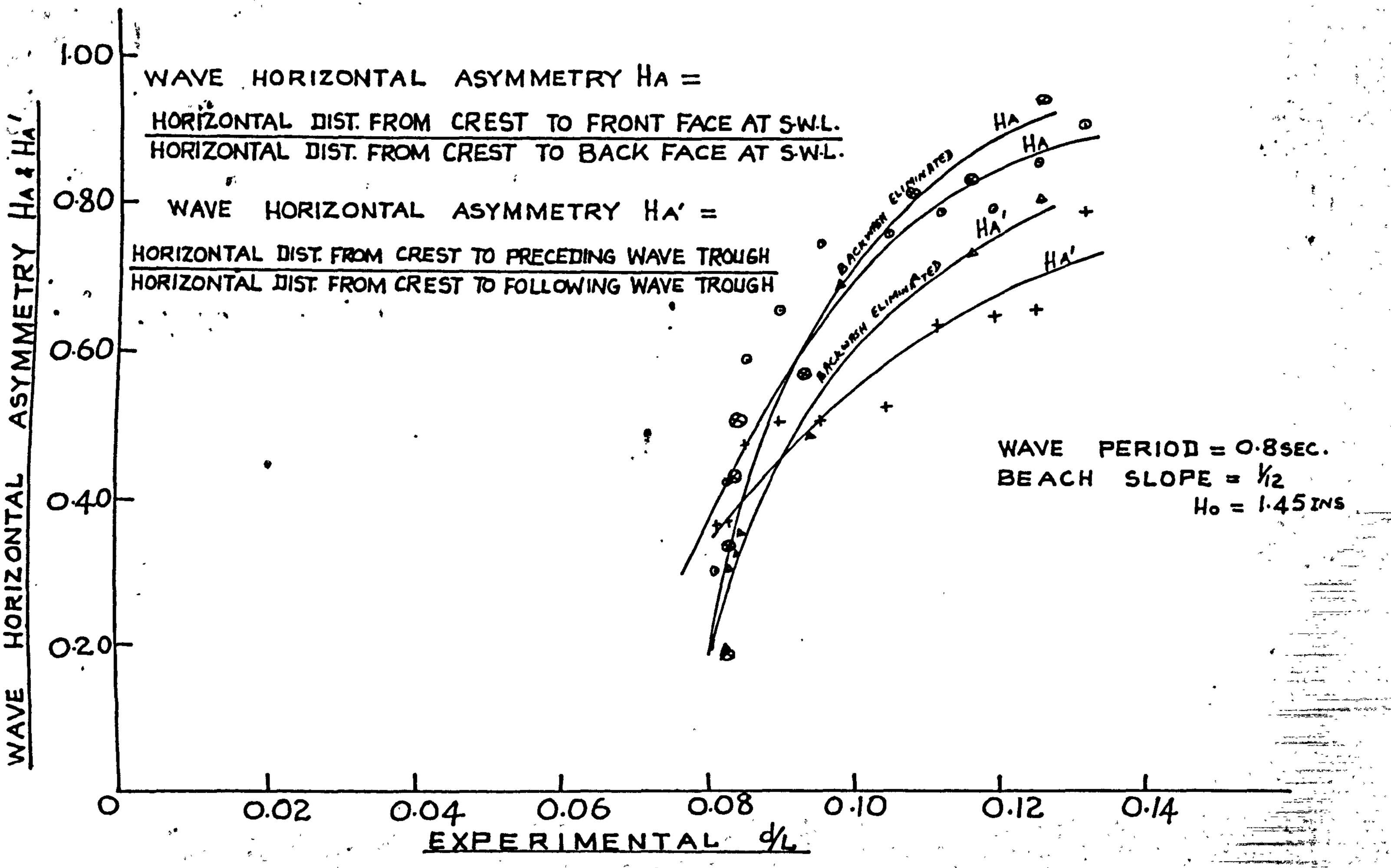

Figure 4.8 Effect of Eliminating Backwash on Wave Horizontal Asymmetry HA and HA'

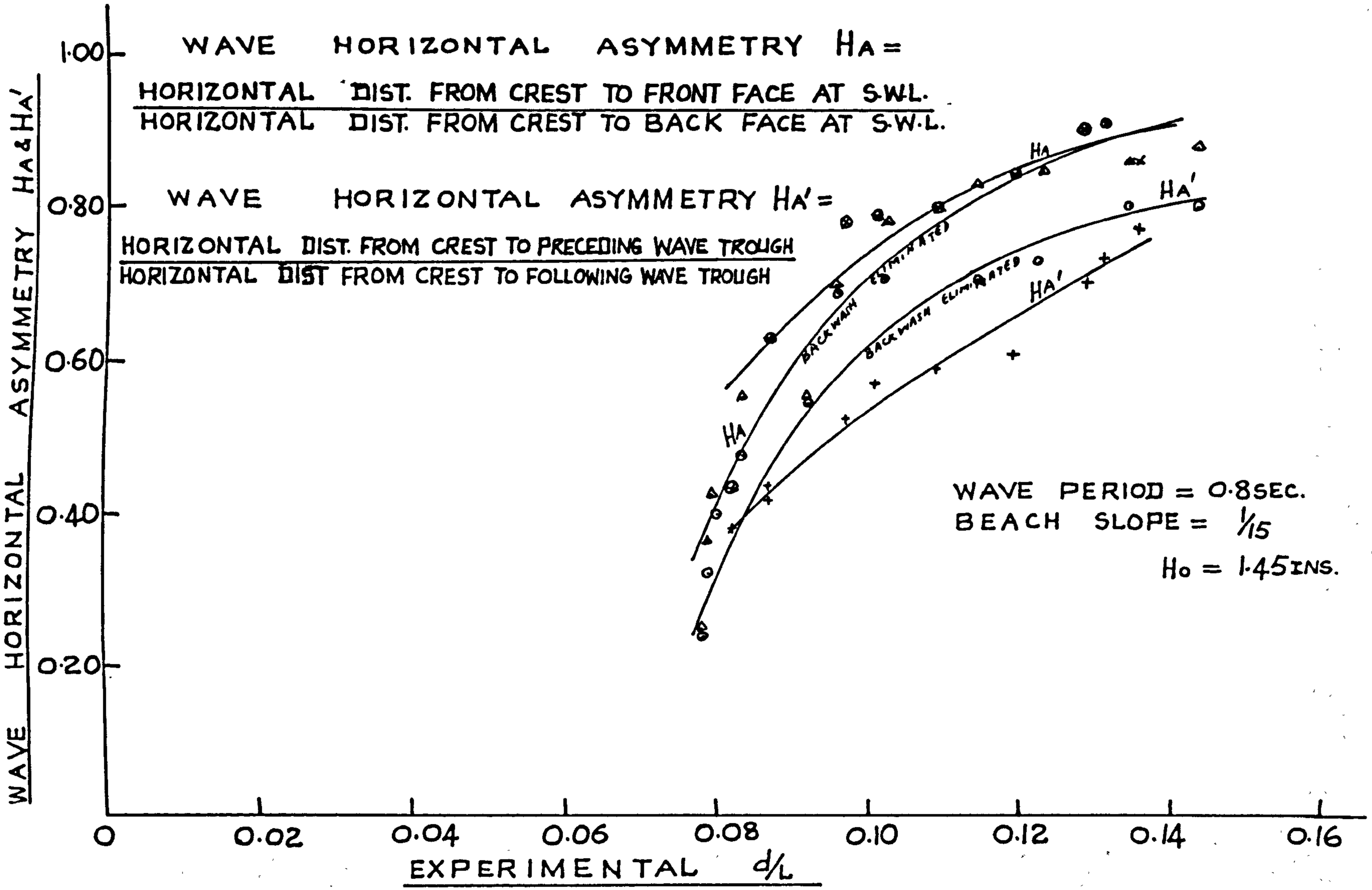

Fig. 4.9 Effect of Eliminating Backwash on Wave Horizontal Assymmetry HA and HA'

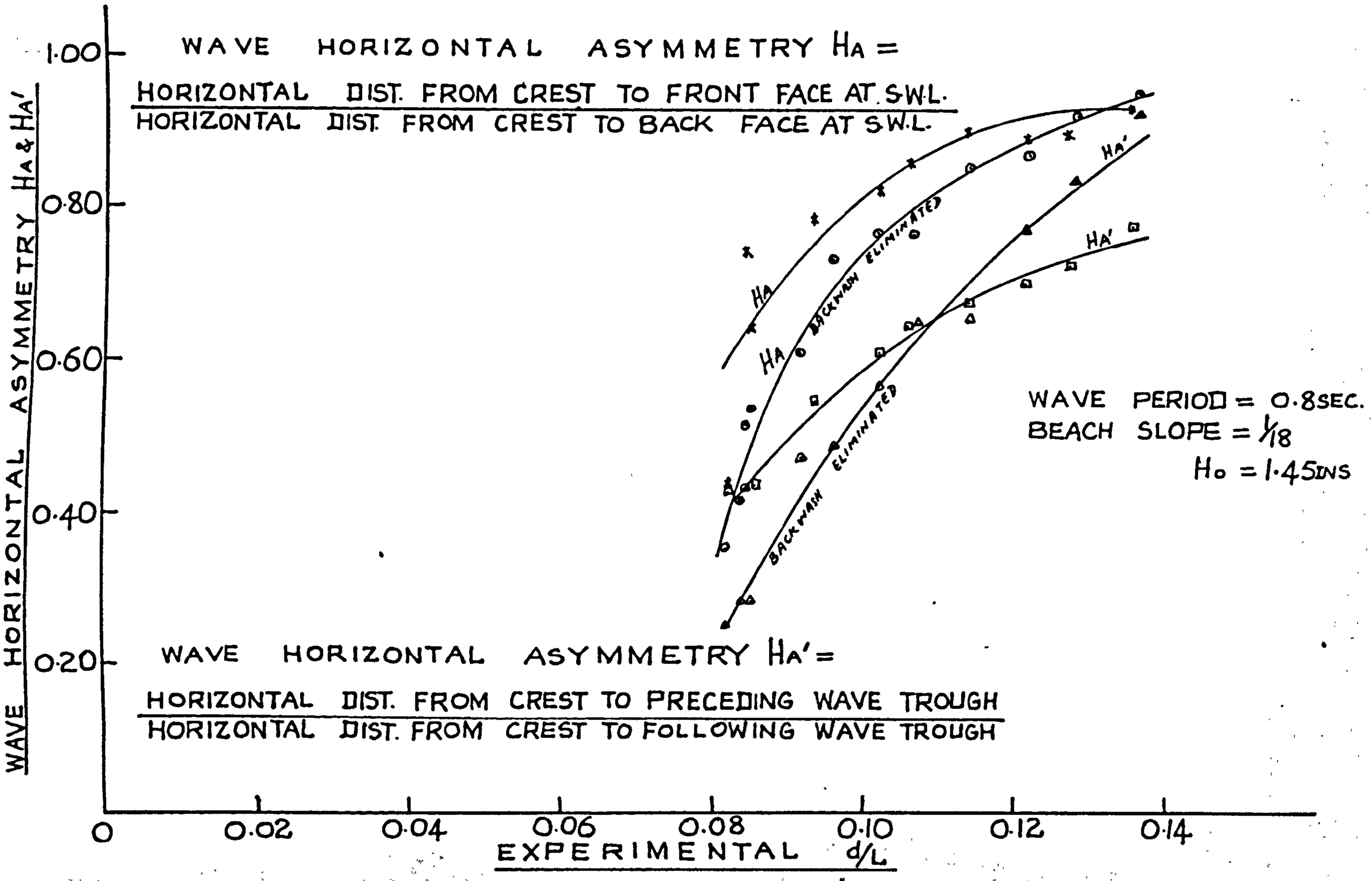

Fig.4.10 Effect of Eliminating Backwash on Wave Horizontal Asymmetry HA & HA'

was -0.115 which was higher than the corresponding value on the beach slope of $\frac{1}{9}$, indicating that the wave slope asymmetry increases with the beach slope.

The graph of wave slope asymmetry against $\frac{d}{L}$ for the beach slope of $\frac{1}{12}$ also shows the same effects (see fig. 3.20).

The corresponding results for slopes of $\frac{1}{15}$ and $\frac{1}{18}$ are shown in figs. 4.5 and 3.21 respectively. It was considered that the increase in the wave slope asymmetry when the backwash of the wave was eliminated might possibly be due to the reduction of any reflected wave, but this was not substantiated by any trend in the variation with the beach slope.

4.4 Experimental Results on the Effect of Backwash on Wave Horizontal Asymmetry

The work on the effect of the backwash on the wave horizontal asymmetry did not show a general trend for all the beach slopes treated. For instance, on the beach slopes of $\frac{1}{6}$ and $\frac{1}{9}$ (see Figs. 4.6 and 4.7) the effect of eliminating the backwash was to reduce the wave horizontal asymmetry, while the trends are inconclusive for the beach slopes of $\frac{1}{12}$ $\frac{1}{15}$, and $\frac{1}{18}$ see figures 4.8, 4.9 and 4.10.

4.5 Conclusions

The work discussed in this chapter on the effect of the backwash of the wave on wave asymmetry was carried out over five beach slopes. The wave conditions were the same as in the previous study on the effect of beach slope and shoaling on wave asymmetry.

On all the beach slopes ($\frac{1}{6}$, $\frac{1}{9}$, $\frac{1}{12}$, $\frac{1}{15}$, $\frac{1}{18}$) covered in this aspect of the work, it was found that the effect of eliminating the backwash of the wave was to cause a reduction in the value of the wave vertical asymmetry. The graph of wave vertical asymmetry against $\frac{d}{L}$ for the flattest beach slope in the work ($\frac{1}{18}$) still showed a linear relationship after the elimination of the backwash, whereas the results for the beach slope of $\frac{1}{15}$ after the elimination of the backwash gave a non-linear curve as for the remaining slopes of $\frac{1}{6}$, $\frac{1}{9}$ and $\frac{1}{12}$. It was found in the work reported in the last chapter that the graphs of wave vertical asymmetry against $\frac{d}{L}$ when there was backwash became linear for slopes $< \frac{1}{12}$. The non-linearity of the curve on the beach slope of $\frac{1}{15}$ when the backwash of the wave was eliminated seems to show that the linear relationship when the backwash was present was due to the backwash and the flat beach slope.

The results of eliminating the backwash in all the cases of the beach slopes covered ($\frac{1}{6}$, $\frac{1}{9}$, $\frac{1}{12}$, $\frac{1}{15}$, and $\frac{1}{18}$) was to increase the wave slope asymmetry when the backwash

was eliminated, the increase being more pronounced near the breakers. Further offshore from the breakers, the divergence of the results with and without backwash became small and tended to disappear at about $\frac{d}{L} = 0.14$. The possibility that the increase in the wave slope asymmetry when the backwash of the wave was eliminated might be due to the reduction of any reflected wave was not substantiated by any trend in the variation with beach slope. However, model studies of waves breaking on mobile beaches indicate that the current from the backwash influences the upper layers of the water seaward of the breakers. This effect is noticeable in the distortion of the mass transport velocity curve close to the shore, the upper layers having a seaward velocity component impressed upon them. Such a current could also be assumed to reduce the shoreward distortion of the wave crest close to the breakers, thus reducing the wave asymmetry.

Eliminating the backwash on the plain beaches used in this study would in nature correspond to wave absorption on highly permeable beaches.

The effect of eliminating the backwash of the wave was to reduce the wave horizontal asymmetry on the steep beach slopes $\frac{1}{6}$ and $\frac{1}{9}$, whereas the trends are inconclusive for the flatter beaches $\frac{1}{12}$ $\frac{1}{15}$ and $\frac{1}{18}$.

It was found that the wave was breaking in shallower water when the backwash of the wave was eliminated, indicating that the presence of the backwash induces early breaking of the wave, although its presence is not a necessary condition for wave breaking.

CHAPTER 5

VELOCITY ASYMMETRY IN THE BREAKER ZONE

5.1 Introduction

In deep water ($\frac{d}{L} > \frac{1}{2}$) the water particle motion associated with wave action becomes negligibly small at a depth from the surface equal to about half the wave length. As the wave advances shoreward into shallower water the bottom begins to feel the effect of the wave as the water particle velocity at the bed increases. The greatesthorizontal water particle velocity occurs at the wave breaker position. The region of interest in this work is the shallow water zone of about $\frac{d}{L} < 0.15$, including the breaker zone.

The horizontal velocity at the bottom is however neither uniform nor steady, but periodic and reversing. In fairly deep water, the water particle horizontal velocities at the bottom are approximately equal for the shoreward and seaward motions, but as the wave moves into progressively shallower water, the asymmetry of the wave gives rise to the velocity differential of the water particles in the beachward and seaward directions, the onshore velocity of the water particle being greater in magnitude and of shorter duration than the offshore

velocity. The two types of horizontal velocity asymmetry have already been defined in paragraph 1.6, one based on the magnitude of the onshore-offshore velocities and the other on duration.

Measurements of the fluid particle horizontal velocity were made at a height of 0.2 ins. from the bed. The measurements were made on two beach slopes of $\frac{1}{9}$ and $\frac{1}{18}$. These two beach slopes were chosen as it had been found from the earlier work reported in the thesis that the slope of $\frac{1}{9}$ was characteristics of the steeper slopes and $\frac{1}{18}$ of the flatter slopes. Further, the two slopes produced different types of breaker, the slope of $\frac{1}{9}$ produced plunging breakers, and the slope of $\frac{1}{18}$ gave spilling breakers. The effect of eliminating the backwash of the wave on the velocity field was also investigated. The wave conditions used were the same as those used in the study on wave asymmetry. The correlation of the wave asymmetry and the asymmetry of the orbital velocity field will be discussed later in this chapter.

A review of previous work on velocity studies of water particles under the action of waves is given below.

5.2 Review of Previous Work

Iversen[16] examined the kinematics of the water movement in breakers. He used particles of a mixture of xylene, carbon tetra chloride and zinc oxide for flow visualization. The movement of the particles was recorded on cine film, from which each particle velocity was obtained by noting the distance moved on the projected frames and the time interval of movement. The velocities obtained were plotted as vectors as shown in Figure 5.1. Iversen, in addition, measured the backwash and crest velocities. He obtained the backwash velocities by averaging all particle velocities in the region of minimum depth in the backwash and the crest velocities were obtained from the gradient of the crest position-time history. His results of the backwash and the crest velocities are shown in figure 5.2 where Y_b is the distance from the bed to the wave creat at the wave break-point. Iversen found that the backwash velocity was higher on a steep beach as compared to a flat beach. This was to be expected.

Hamada[12] studied the particle velocity in wave motion in the region of the breakers. The velocity of flow was measured by means of a current meter which had several propellers driven by the action of water flow.

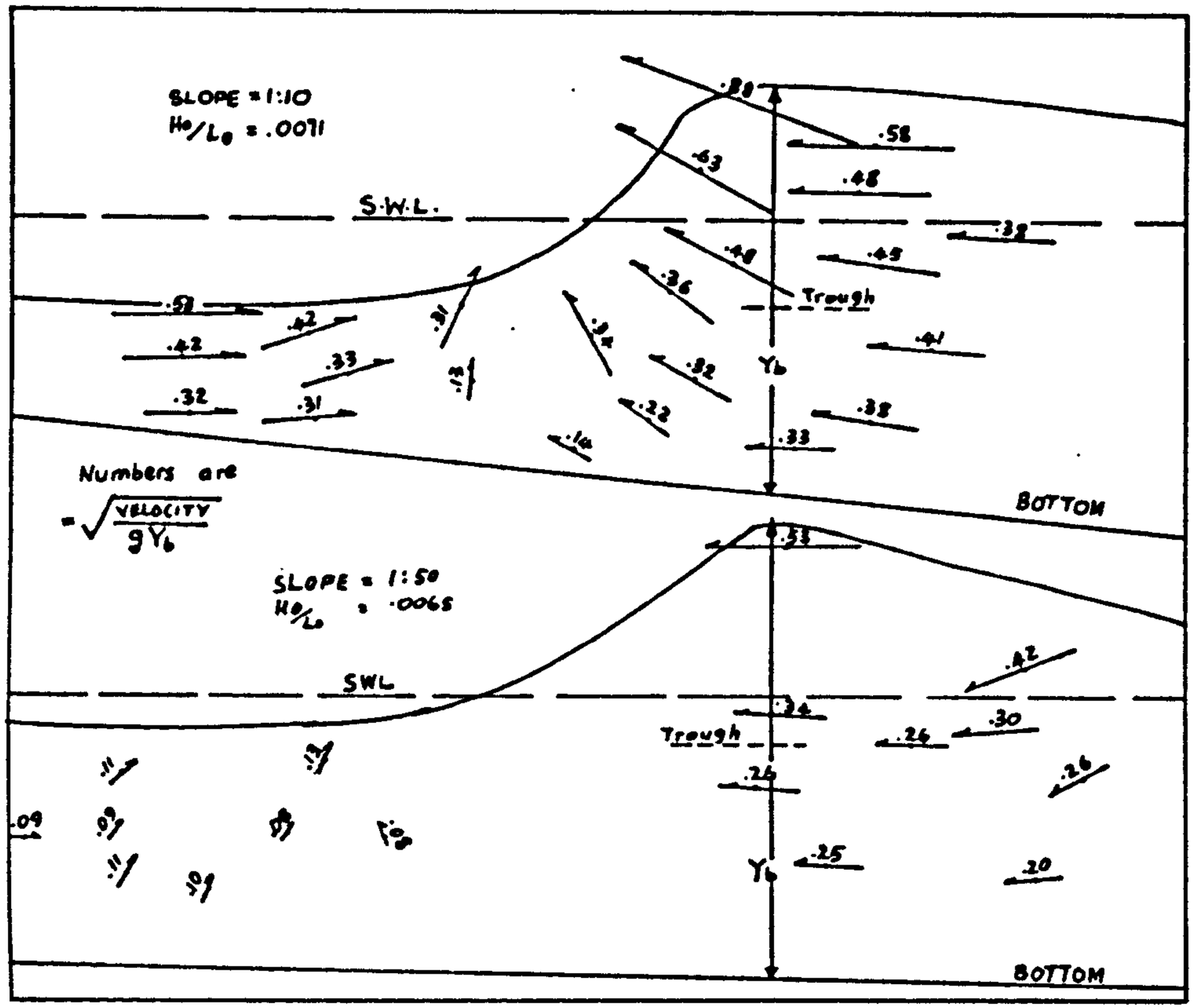

Fig. 5.1 Kinematics of a Breaking Wave (after Iversen[16] (1953)

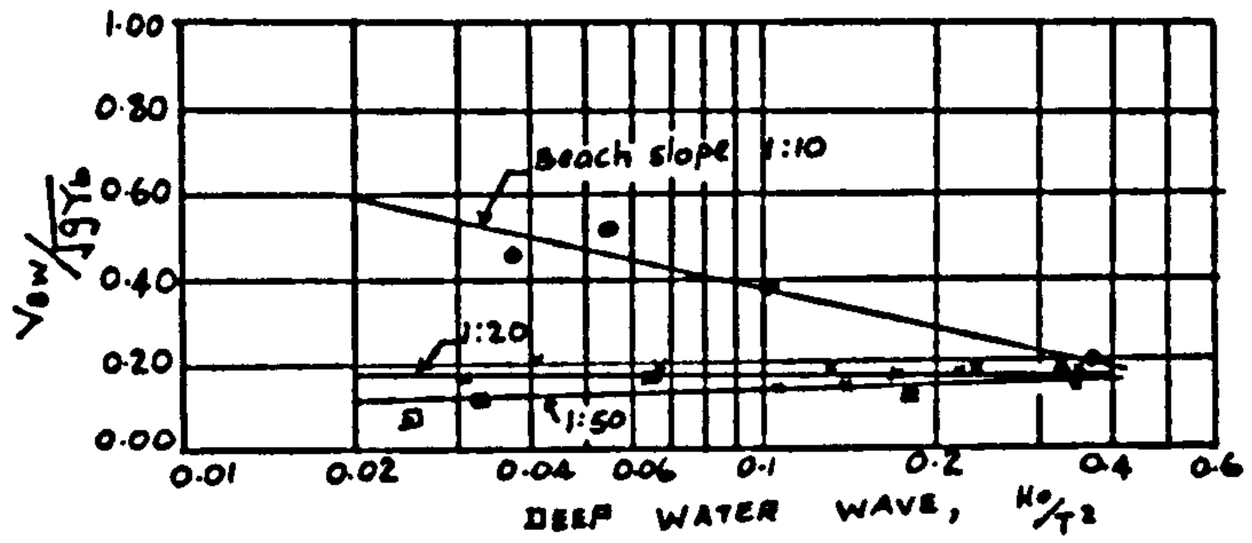

BACKWASH VELOCITY INDEX

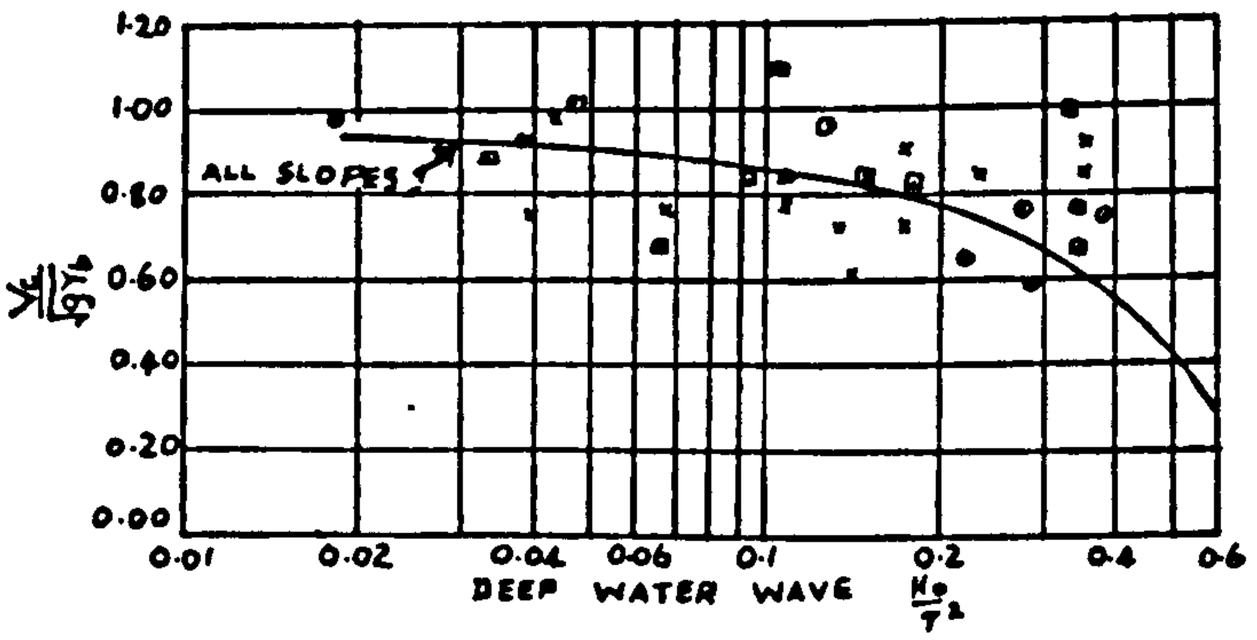

CREST VELOCITY INDEX

Figure 5.2 After Iversen[16] (1953)

A direct electric current in the circuit connected the current meter to an oscillograph, with one element of the oscillograph corresponding to one of the propellers. Hamada made orbital velocity measurments 3 cm. from the bed. He noted the differential velocity in the shoreward and seaward directions. He found the ratio of backward velocity to forward velocity to vary between 1 : 1.16 to 1 : 1.29. However, his theoretical approach was to calculate the orbital velocity by the Airy theory and to add an estimated "residual" velocity (equivalent to the mass transport velocity). Since this was always positive, the resulting values gave a differential between the forward and backward velocities. His measurements are of interest, but his theoretical evaluation neglects the existence of orbital velocity asymmetry even in the absence of mass transport.

Inman and Nasu[14] made a study of orbital velocity in shallow water at La Jolla California. The measurements were made near the bottom and just seaward of the breaker zone in water depths ranging from about five to fifteen feet and wave heights of up to seven and a half feet. The orbital current meter consisted in the main of a cylindrical rod fixed rigidly at one end like a cantilever, and the system was arranged such that the orbital velocity could be interpreted from the bending of the rod caused by the force exerted by the

moving water. A pressure type wave meter was used with the current meter, and both the wave meter and the current meter were mounted on a tripod. The current meter was mounted 0.82 ft. above the bottom. The bed had an average slope of about $\frac{1}{35}$ in the region where the orbital velocities were measured.

Inman and Nasu commented that the graph of the horizontal component of orbital velocity as a function of time resembled that of the wave pressure and they noted that the horizontal velocity seemed to be more dependent on the rate of change in level of the water surface during the passage of the wave than on the actual height of the wave. With reference to Fig. 5.3 after Inman and Nasu[14] they noted that in the figure, the fourth wave was almost as high as those preceding it, but showed a more gradual rise in level from the preceding trough to the crest. The result was a very low crest velocity. In terms of the work reported in this thesis, the statement of Inman and Nasu could be condensed into the statement that for waves of the same height, greater velocities are associated with greater wave slope asymmetry.

Inman and Nasu remarked that the maximum velocity under the wave crest was always onshore and that for almost all the waves analysed the mean onshore maximum

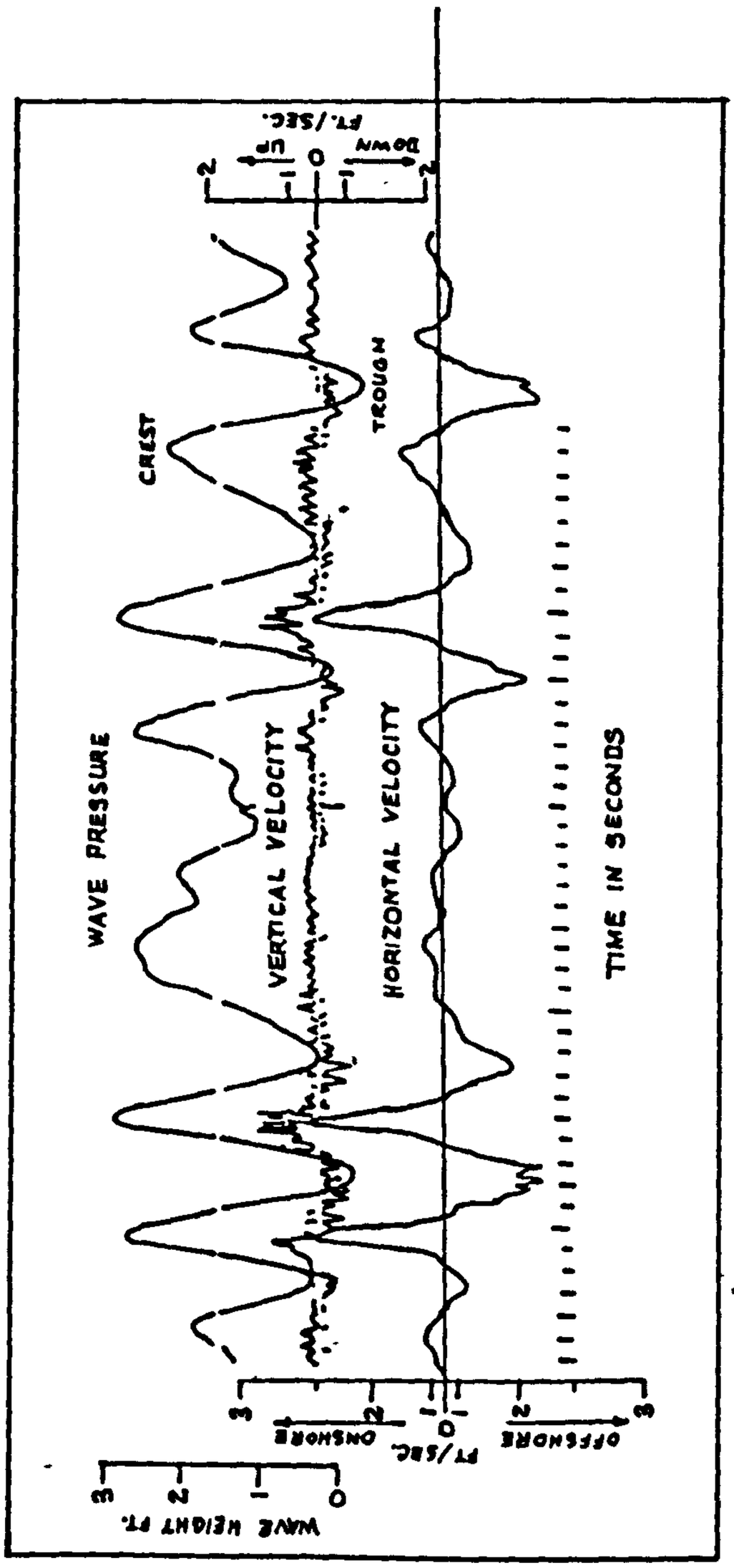

Figure 5.3 After Inman and Nasu (1956)

velocity exceeded the offshore velocity. They compared the maximum orbital velocities with solitary and Airy-Stokes waves. They gave the sum of the crest and trough velocities along the bottom aU for both Airy and Stokes waves as :

$$aU = |U_{crest}| + |U_{trough}| = \frac{2\pi H}{T} \frac{1}{\sinh \frac{2\pi d}{L}} \quad \cdots (5.1)$$

For the solitary wave, they gave the maximum orbital velocity at the bottom sU as :

$$sU = \frac{1}{2} NC \quad \cdots (5.2)$$

where $C = \sqrt{g(H+d)}$ is the velocity of propagation of the wave crest. H is wave height and d water depth.

N is defined by the equations

$$N = \frac{2}{3} \sin^2 \left[M\left(1 + \frac{2H}{3d}\right) \right] \quad \cdots (5.3)$$

and

$$\frac{H}{d} = \frac{N}{M} \tan \frac{1}{2} \left[M\left(1 + \frac{H}{d}\right) \right]. \quad \cdots (5.4)$$

Inman and Nasu[14] remarked that the measured velocities were on the average in better agreement with the solitary wave than with the Airy-Stokes relations.

Scott[44] in a study of sand movement by waves made velocity measurements using a mixture of xylene carbon tetrachloride and zinc oxide having the same specific gravity as water. He injected small droplets of the mixture into the water and used a cine camera to trace the movements. The particle motion was analysed by measuring the time taken by the particle to cover an arbitrary horizontal distance in the seaward or beachward portion of the orbit. Scott found that the velocities and accelerations of the water motion were higher in the beachward direction than in the seaward direction in relatively shallow water.

Miller and Zeigler[38] made a field study of the horizontal velocity of the water motion inside breaking waves. The velocity measurements were made using an acoustic flowmeter, the basic operation of which consisted of two simultaneous acoustic signals sent in opposite directions between a pair of probes spaced 8 inches apart. The meter was in the shape of a tuning fork, and the instrument so positioned so that an imaginary line between the tips of the probes was parallel to the velocity component to be measured. The data was received in the form of continuous records on a Sanborn recorder. The wave

trace was also recorded on the same instrument.

Miller and Zeigler selected about 200 breaker traces from the very many recorded, and plotted each separate breaker on a dimensionless graph. The absicissa had its zero at the centre of the graph and units of $\frac{t}{T_B}$ increasing both to the left and to the right of this centre mark. T_B was defined as the breaker period and t was the time variable. The ordinate consisted of units of $\frac{z}{B_d}$ where z was the observed water height above the bottom and B_d the height of the breaker crest above the bottom. By comparing the breaker profiles plotted on the dimensionless graph as described above Miller and Zeigler considered that the breaker forms fell into three major categories, which they referred to as 'symmetric', 'asymmetric' and 'very asymmetric' breakers. They then averaged the individual breaker traces for each class to obtain a single trace. The single trace was then plotted with ordinates $\frac{z}{B_d}$ and absicissa $\frac{t}{T_B}$ as explained above, and in a similar manner, the velocity values were plotted on a single graph for each of the three breaker classes. The velocity values were entered in the form $\frac{U}{U_{max}}$ where U was the observed velocity and U_{max} the maximum velocity for the individual breaker. Commenting on the class of breaker they classified as symmetric, Miller and Zeigler

noted a lack of symmetry in the velocity field of the lower portion of the breakers. Comparing the breaker they classed as asymmetric breaker with the "near breaking wave", i.e the mean profile just seaward of the break-point they commented that the profile of the asymmetric breaker was more peaked. With respect to the internal velocity field they noted that the distribution of the magnitudes and directions was less complicated in the asymmetric breaker than in the class they referred to as symmetric. They commented that the class referred to as the 'extreme asymmetric' breaker was the least complicated of the three categories. The measurements of all the three classes were made on a single bottom slope.

The author would like to comment that from the study made in the work reported in this thesis, the breaker Miller and Zeigler referred to as a symmetric breaker in fact possessed a distinct vertical asymmetry and some wave horizontal and wave slope asymmetry. Miller and Zeigler themselves remarked that the transition from the profile and velocity field of the "near-breaking wave" which already possessed asymmetry to the symmetric breaker, was difficult to appreciate. On the whole their classification seems to be based on visual judgement of the wave trace with a bias towards what is referred to in the present work as wave slope asymmetry. It was however, very surprising that Miller and Zeigler

considered that the breaker type they referred to as the symmetric breaker was possibly analogous to the plunging type and the very asymmetric breaker was similar to the spilling type; the author considers that, if anything, a plunging breaker ought to correspond to a very asymmetric breaker.

Ippen and Kulin[15] studied the internal velocities of the solitary wave at the break-point. They used droplets of a solution of xylene and n-butyl phthalate. The motion picture camera they employed was operated at 20 frames per second and they placed an auxiliary grid in the plane of the particles so that on the photographs the grid lines could be projected down into the wave itself. They conducted their studies on two types of breakers; the plunging breaker on a slope of 0.065 and the spilling breaker on a slope of 0.023. Their result is shown on Figure 5.4. They found that on the slope of 0.023 the maximum particle velocity was 3.3 ft/s while the wave celerity was 3.9 ft/s, and on the slope of 0.065 they found the celerity was 4.3 ft./s. while the maximum particle velocity was 3.6 ft/s. They commented that on the slope of 0.023 with a spilling breaker the maximum velocity was nearly equal to the crest celerity at the wave breakpoint, and they noted that the maximum particle velocity seemed to occur just

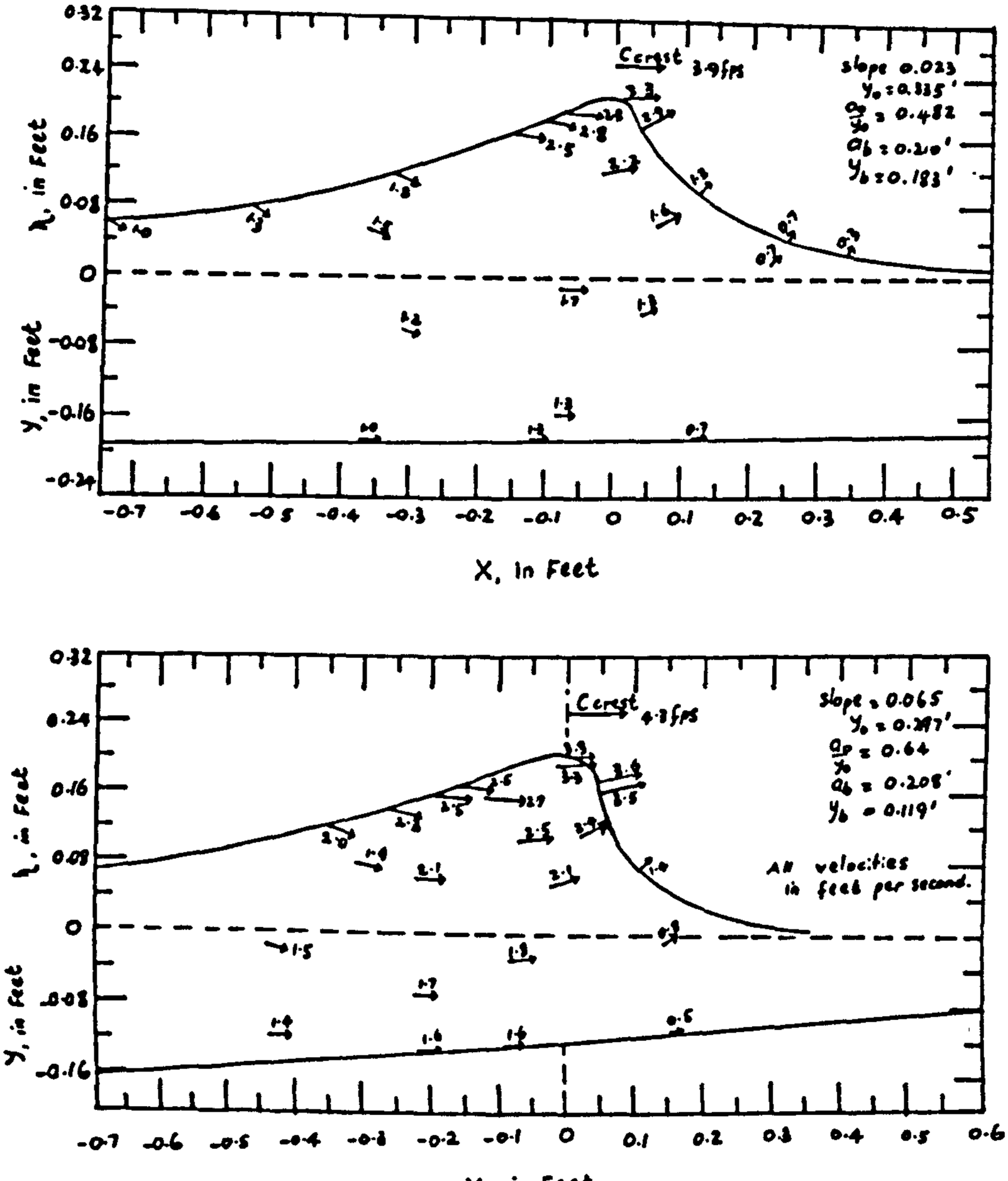

Figure 5.4 Internal velocities at breaking (After Ippen and Kulin[15] (1955)

slightly shoreward of the highest point of the crest.

Some velocity studies were also carried out by Morison and Crooke[39] in a study of deep water, shallow water and breaking waves. They used a mixture of carbon-tetra chloride, xylene and zinc oxide having approximately the same specific gravity as water. Droplets of the mixture were injected into the water and the resulting motion photographed with a cine camera. They found that the greatest horizontal particle velocity occurred when the wave was breaking, and they noted a velocity differential between the shoreward and seaward horizontal velocities. They concluded that the maximum horizontal particle velocity at the crest of the wave might attain the wave celerity as the wave broke, but that the phenomenon was confined to a very narrow region of water at the crest of the wave. This was not borne out by Miller and Zeigler's observations.

The difficulty which arises in comparing laboratory observations with field measurements is referred to in the final conclusion to the thesis.

5.3 Effect of Shoaling on Orbital Velocity Asymmetry

As mentioned in section 1.6 chapter 1, two types of horizontal velocity asymmetry were defined in the present work, one based on the magnitude of the shoreward-seaward velocities and referred to as the horizontal velocity (magnitude) asymmetry, and the other based on duration of the shoreward-seaward motion and referred to as the horizontal velocity (time) asymmetry. In order to obtain both the horizontal velocity (magnitude) asymmetry and the horizontal velocity (time) asymmetry, the velocity-time history at the different positions along the beach had to be obtained from the analysis of the cine films of hydrogen bubble blocks emitted from a wire positioned at varying distances from the breakers. The resulting curves are shown superimposed in Figures 5.5 and 5.6 and the separate curves are shown in the appendix. All measurements were made from the separate curves.

Figures 5.5 and 5.6 show how the curve changes in form as the wave progresses into shallower water. It can also be seen from the figures that the horizontal velocities increased as the wave advanced into shallower water, and for slopes of $\frac{1}{9}$ and $\frac{1}{18}$ the greatest horizontal velocities occurred at the wave

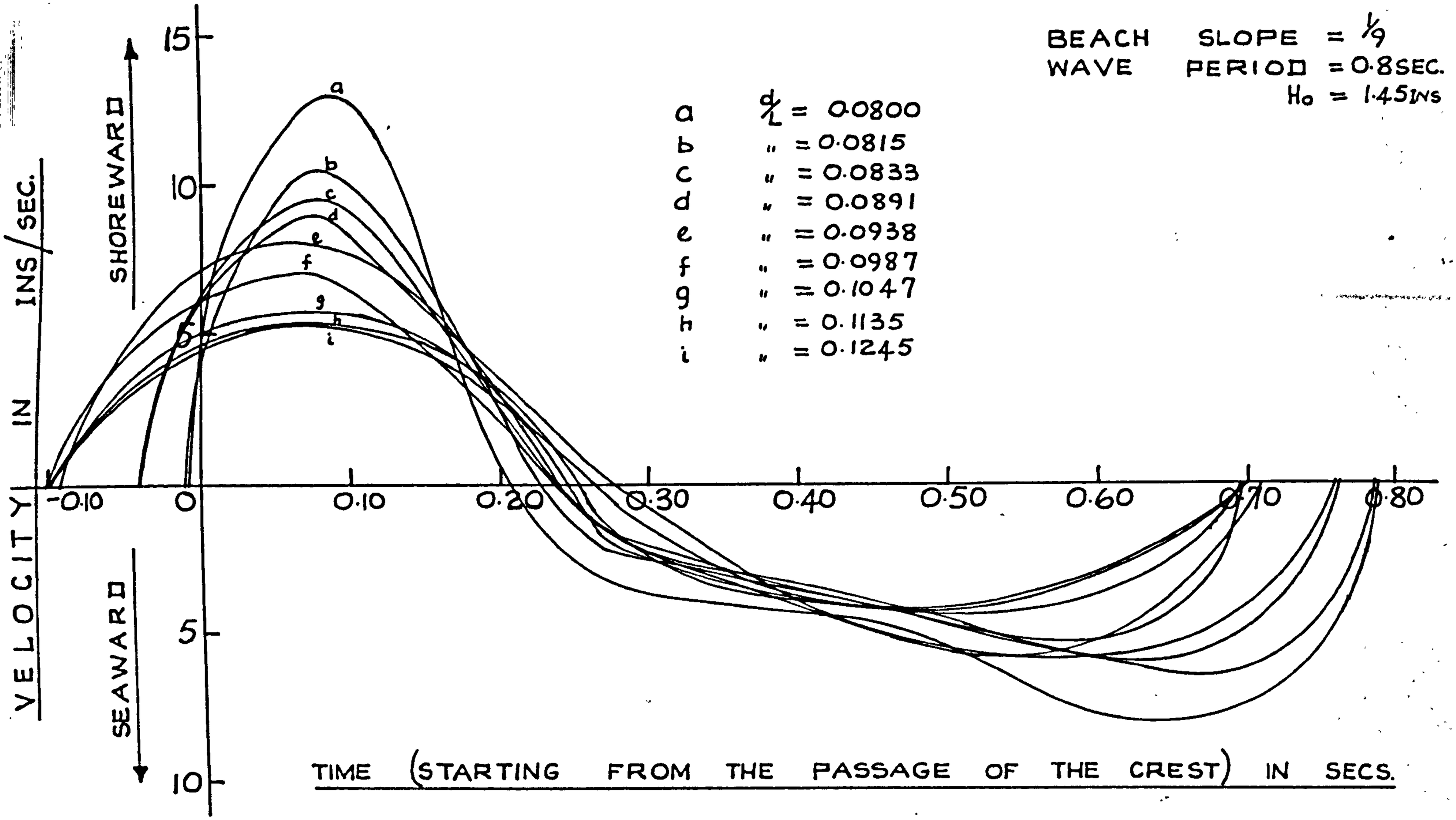

Fig. 5.5 The Superposed Graphs of Horizontal Orbital Velocity Against Time

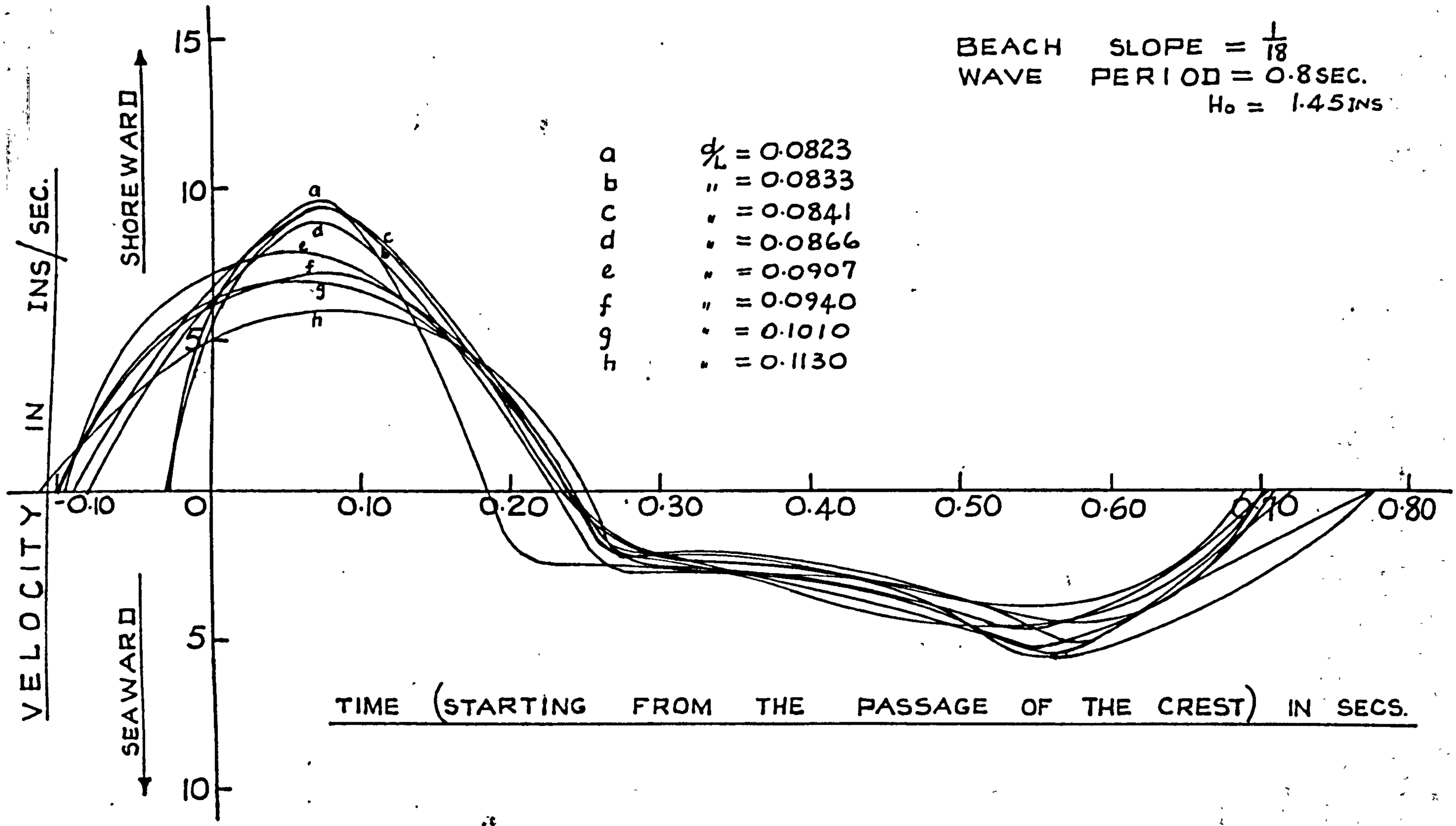

Fig. 5.6 The Superposed Graphs of Horizontal Velocity Against Time

breaker position. It is interesting to note that the curves are closer together on the beach slope of $\frac{1}{18}$ than on the beach slope of $\frac{1}{9}$ but that on each beach slope, the velocity seems to have a constant value at all positions along the beach 0.4 secs i.e. half the wave period after the passage of the wave crest, although the constant velocity varies in magnitude from one slope to another. It is evident from Figures 5.5 and 5.6 that for each position on the beach, the maximum horizontal shoreward velocity did not occur directly under the wave crest but at a time 0.09T seconds after the passage of the crest.

The graphs of horizontal velocity (magnitude) asymmetry against $\frac{d}{L}$ are shown in Figure 5.7. It was found that for slopes of $\frac{1}{9}$ and $\frac{1}{18}$ the horizontal velocity (magnitude) asymmetry increased as the wave advanced into shoaling water and in each case was highest at the wave breaker position. At the $\frac{d}{L}$ value of 0.10 on the beach slope of $\frac{1}{9}$ this asymmetry was found to be 1.37 while on the beach slope of $\frac{1}{18}$ it was found to be 1.585. At the wave break-point on the beach slope of $\frac{1}{9}$ the value of this asymmetry was found to be 1.63 while the corresponding value on the beach slope of $\frac{1}{18}$ was 1.77.

In terms of absolute values of the horizontal velocities, the values on the steeper slope of $\frac{1}{9}$

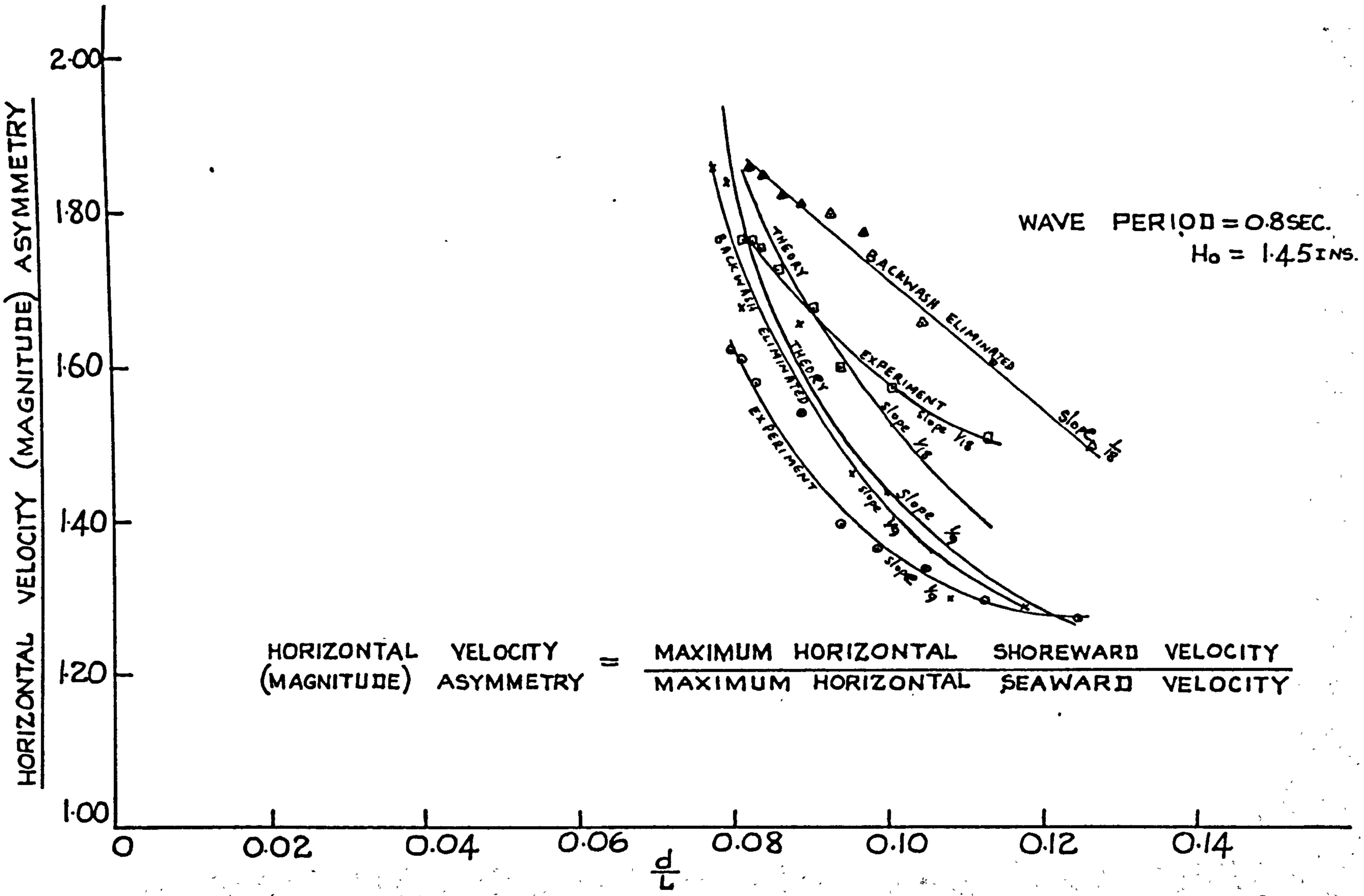

Fig. 5.7 Graph of Horizontal Velocity (Magnitude) Asymmetry against $^{d}/_{L}$

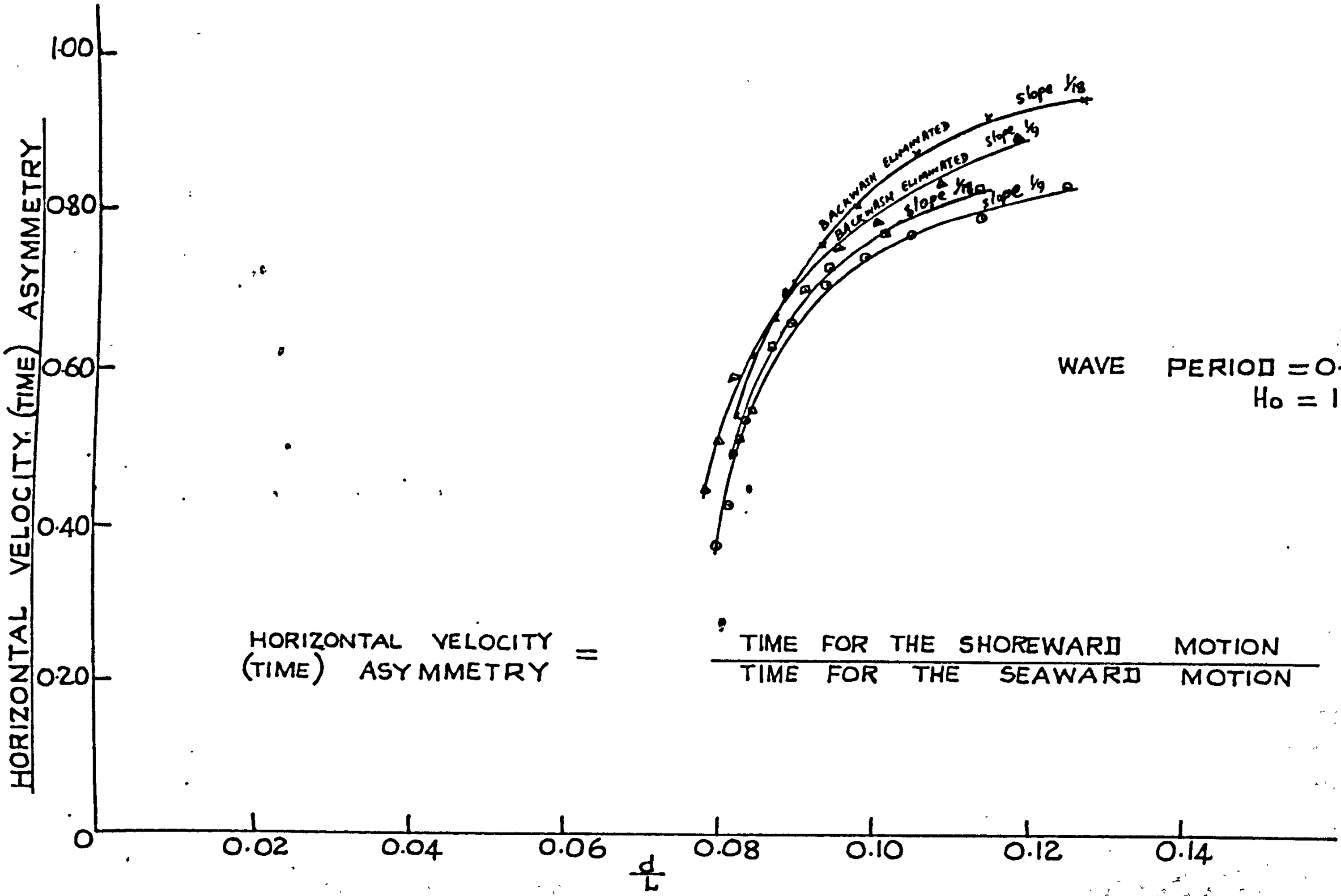

Fig. 5.8 Graph of Horizontal Velocity (time) asymmetry Against d/L

were found to be higher than those on the flatter slope of $\frac{1}{18}$, especially in the neighbourhood of the breakers, but the graph of the horizontal velocity (magnitude) asymmetry against $\frac{d}{L}$ figure 5.7 indicated that the asymmetry values were higher on the flatter slope. In other words larger beach material could be set in motion on the steep slope, but a greater shoreward-to-seaward differential would act on material on the flatter slope.

The graphs of horizontal velocity (time) asymmetry against $\frac{d}{L}$ are shown in Figure 5.8. These show increasing asymmetry as the wave advances into shallower water. As noted in section 1.6, the horizontal velocity (time) asymmetry was defined as the ratio of the time for the shoreward motion to the time for the seaward motion, thus a small numerical value compared with unity denotes increasing asymmetry.

It was found that at the $\frac{d}{L}$ value of 0.10 the value of this asymmetry on the beach slope of $\frac{1}{9}$ was 0.76 while on the beach slope of $\frac{1}{18}$ the value was found to be 0.78. At the wave breaker position on the beach slope of $\frac{1}{9}$ the asymmetry became 0.37 while the corresponding value on the beach slope of $\frac{1}{18}$ was 0.49. Thus the shoreward motion takes a longer time on the flatter slope.

Both the actual magnitude of the maximum bed velocity and the asymmetry of the velocity field are very important in sediment movement under wave action. The magnitude of the maximum velocity is associated with initiating the motion and the asymmetry of the velocity fields the direction and magnitude of the net movement. These will be discussed in greater detail in the next chapter.

Figure 5.9 illustrates the comparison between Stokes theoretical wave profile based on his third approximation, and a typical profile obtained in the present study. It can be seen that the Stokes Wave is less peaked than the experimental wave, and also, by virtue of its mathematical description, does not possess asymmetry about the vertical axis.

Figures 5.10 and 5.11 which compare the orbital velocities based on Stokes theory with those obtained experimentally, show that at a $\frac{d}{L}$ value of 0.0833, which is very close to the breakers, the theory clearly does not agree with the measurements (see Figure 5.11). Farther seaward from the break-point, at a $\frac{d}{L}$ value of 0.1135, (figure 5.10), although the theoretical values were still much higher than the experimental values, for instance, by as much as 73% of the experimental value under the crest, and there was

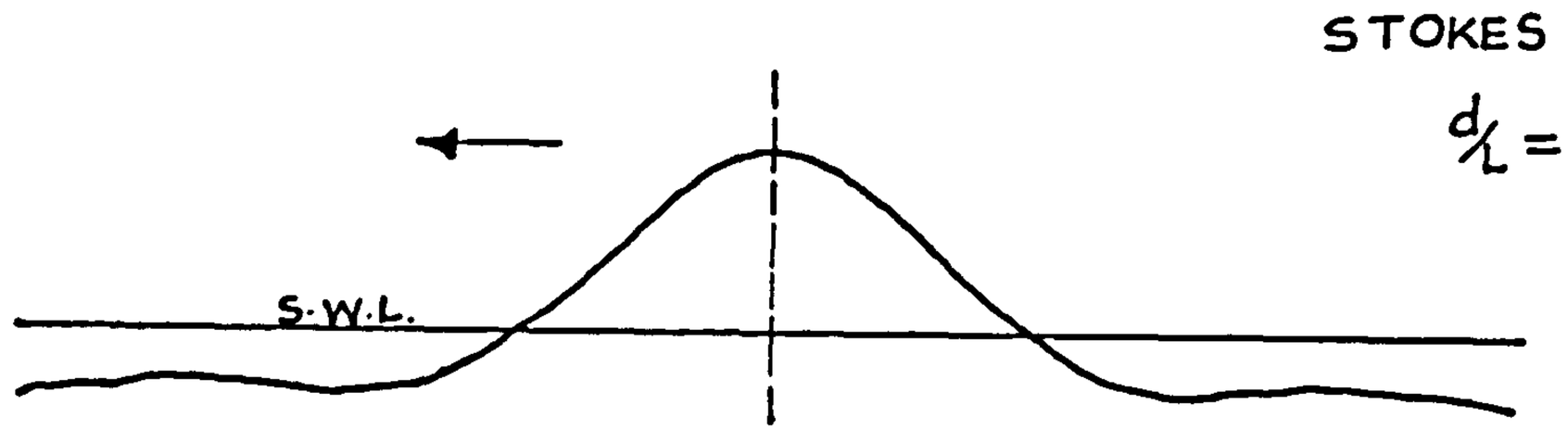

Theoretical Near-Breaking Wave: Stokes Finite Amplitude Wave, Third Approximation (after Miller & Zeigler[38]).

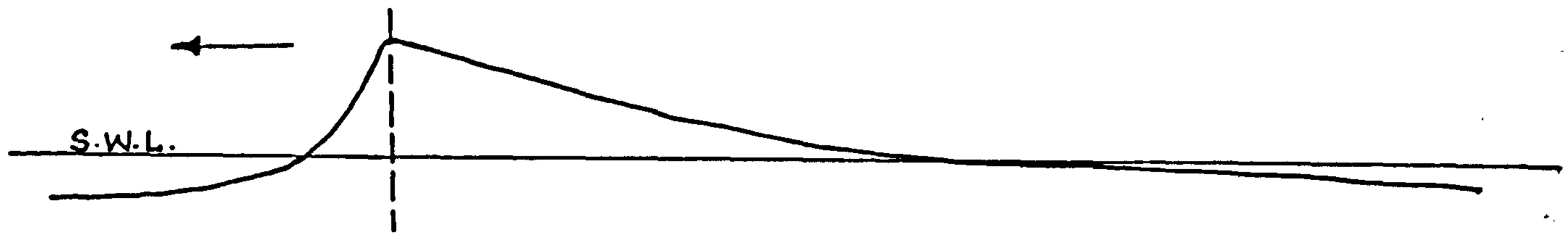

Typical Experimental Profile Near the Break-point.

Figure 5.9.

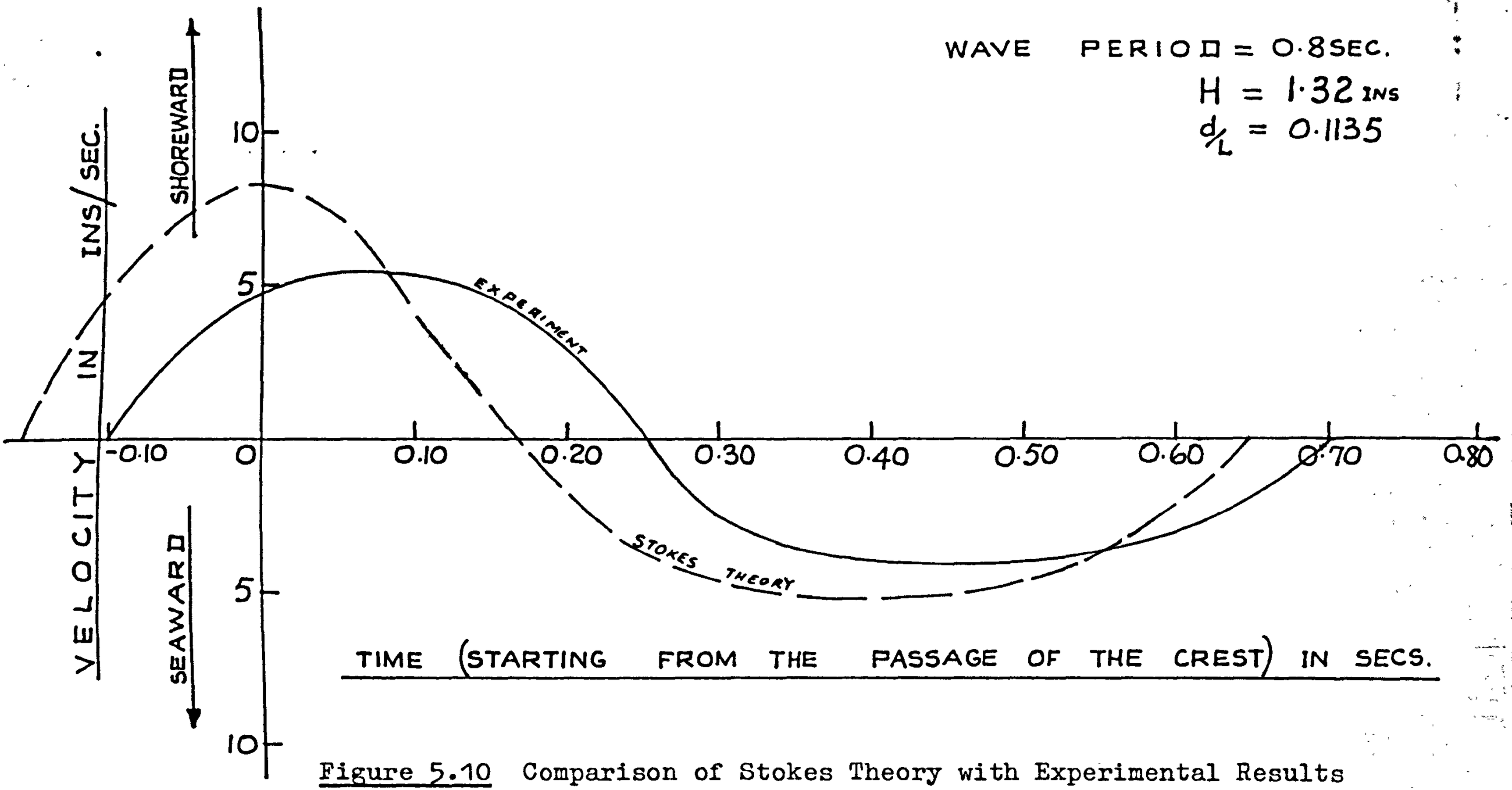

Figure 5.10 Comparison of Stokes Theory with Experimental Results

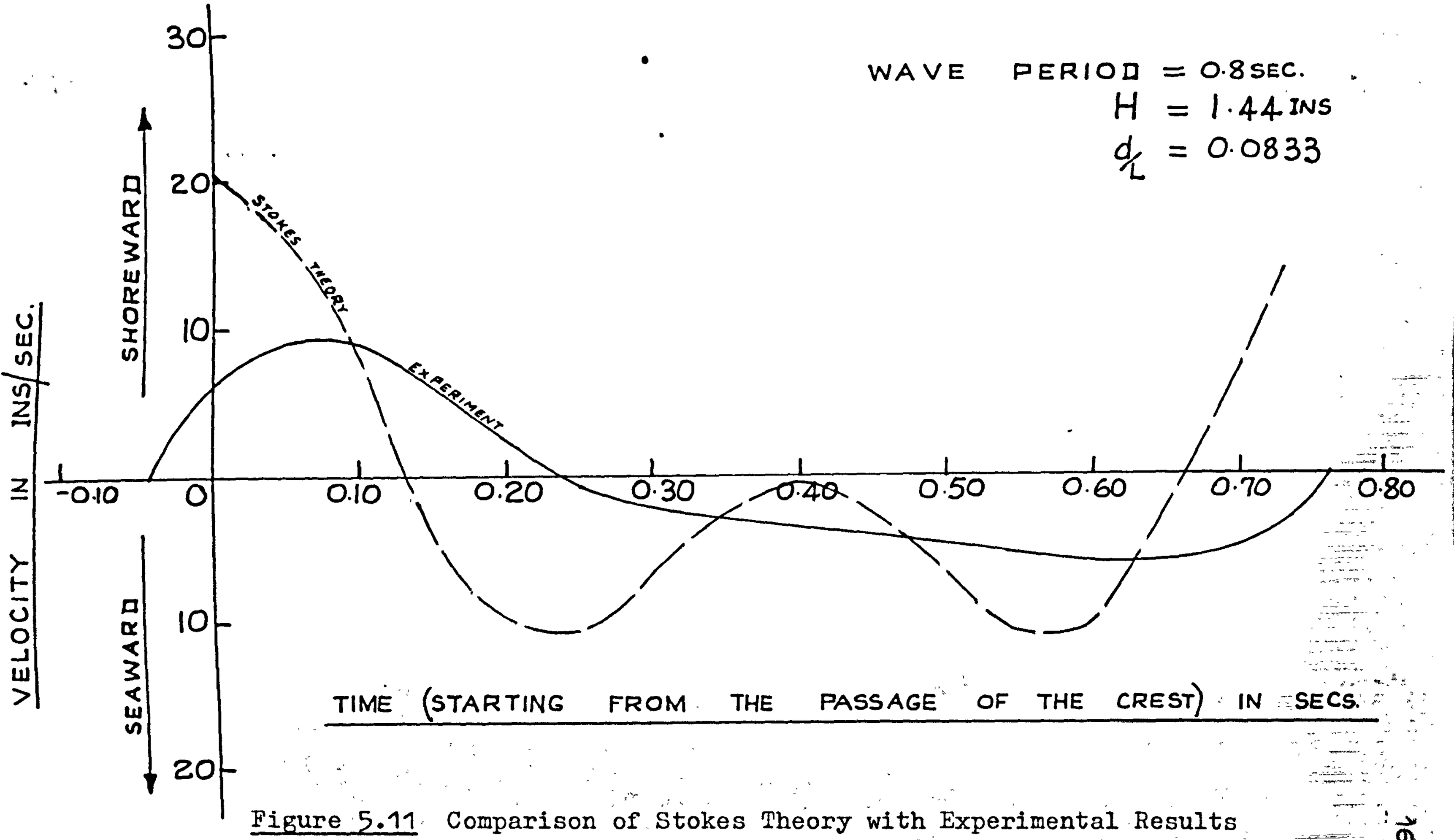

Figure 5.11 Comparison of Stokes Theory with Experimental Results

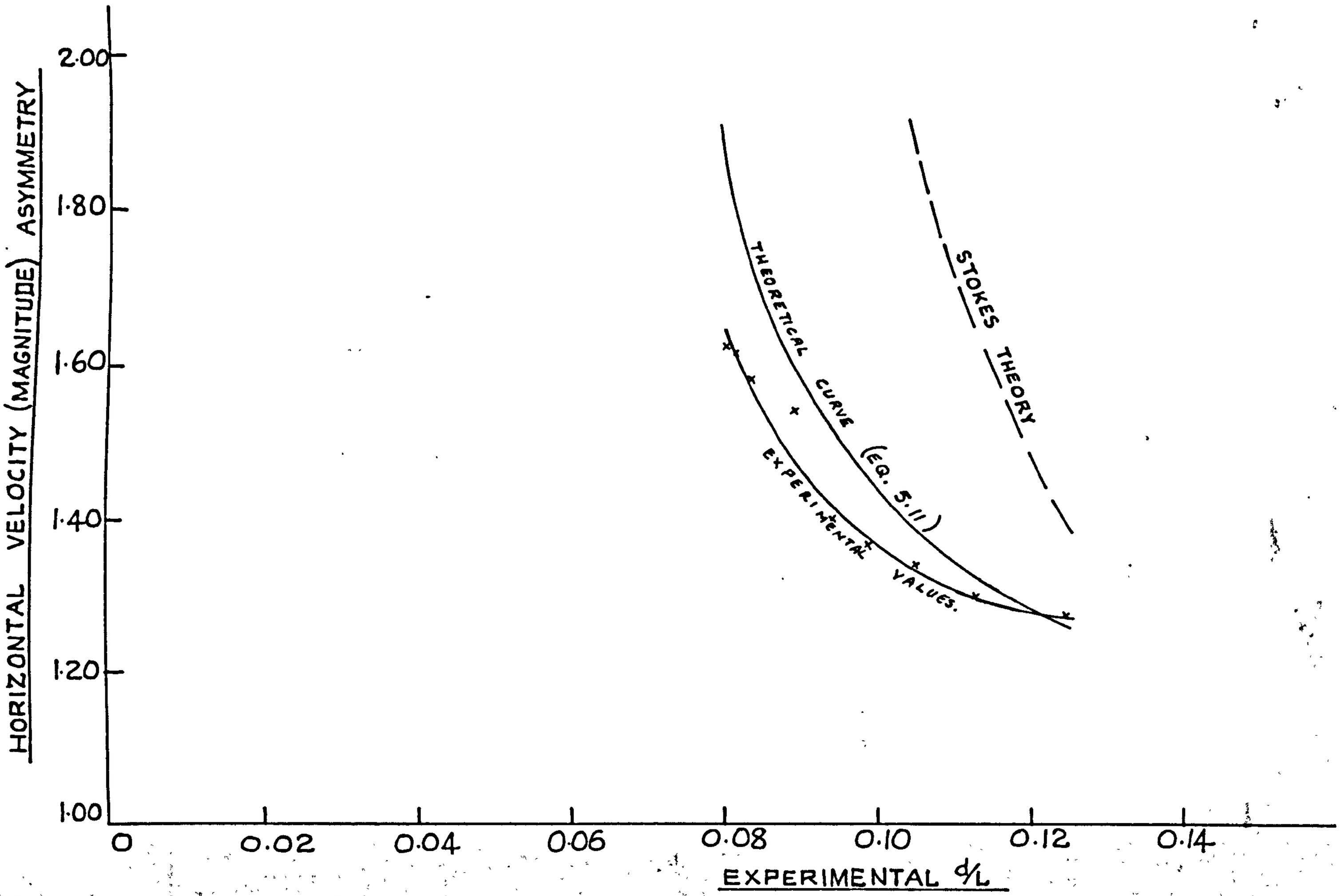

Figure 5.12 Comparison of Stokes Theory with Experimental Results

in addition a phase lag in the profile, nevertheless the comparison was better than in figure 5.11. Figure 5.12 compares the values of the horizontal velocity (magnitude) asymmetry given by the Stokes theory equation 1.1. with the experimental results, and the theoretical values from equation 5.11. It can be seen that the divergence between the Stokes prediction and the experimental results was about 32% at a $\frac{d}{L}$ value of 0.11, with the divergence increasing shoreward but improving seaward.

For these reasons, one can conclude that Stokes theory is not directly applicable to the study of the pattern of velocities in the near breaker zone.

5.4 Correlation Between Wave Asymmetry and Velocity Asymmetry

An important aspect of the work reported in this thesis is the study of the correlation between the different types of wave asymmetry and the correlation between these and the resulting velocity asymmetry as the wave progressed into shallow water. The first aspect has been reported in chapter 3.

Figure 5.13 shows the graphs of both the horizontal velocity (magnitude) asymmetry and the horizontal velocity (time) asymmetry plotted against the wave

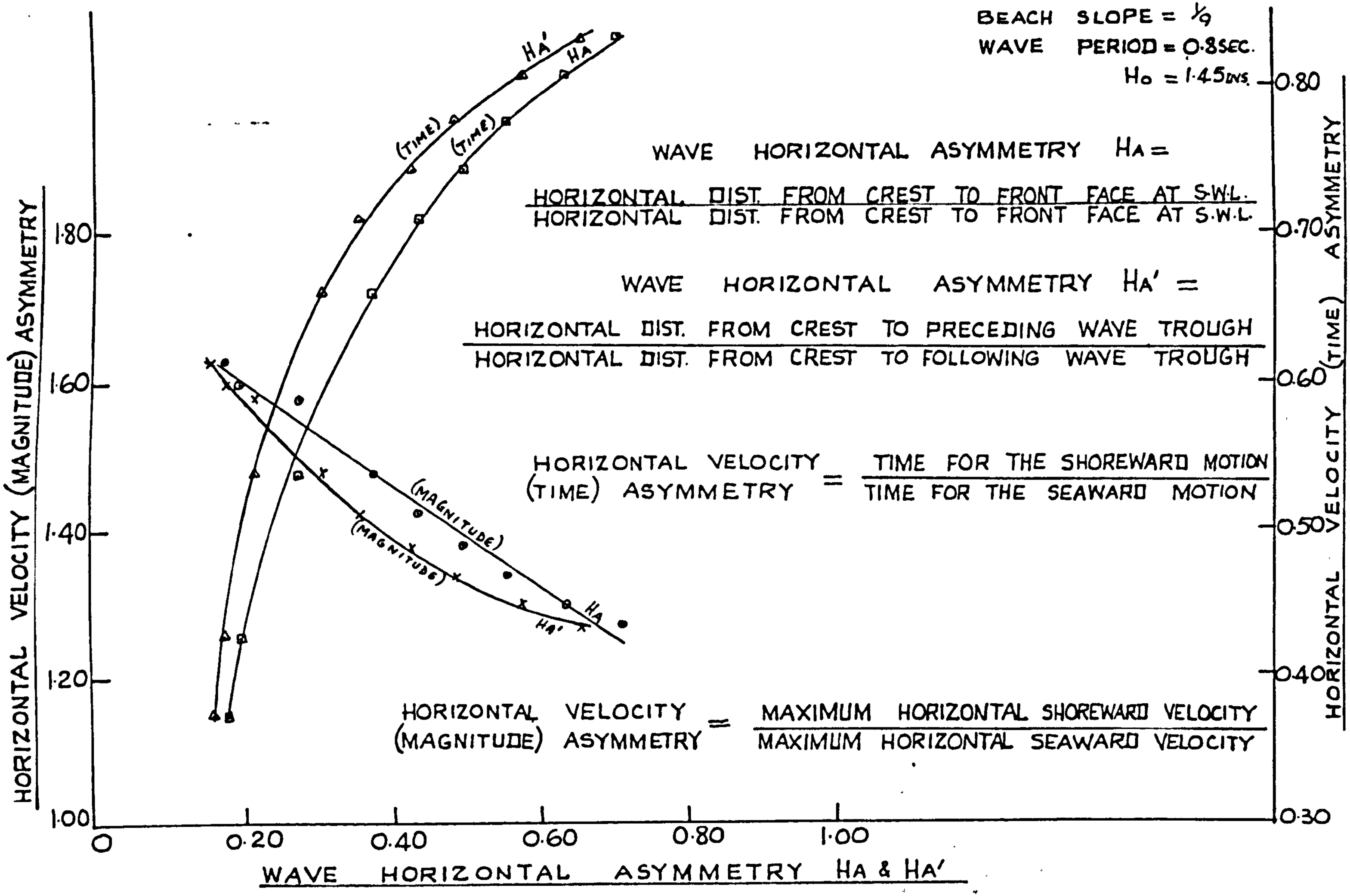

Figure 5.13 Graph of Velocity Asymmetry Against Wave Asymmetry

HORIZONTAL VELOCITY (MAGNITUDE) ASYMMETRY

1·80
1·60
1·40
1·20
1·00

HORIZONTAL VELOCITY (TIME) ASYMMETRY

0·80
0·70
0·60
0·50
0·40
0·30

0·50 0·55 0·60 0·65 0·70 0·75 0·80

WAVE VERTICAL ASYMMETRY

HORIZONTAL VELOCITY (TIME) ASYMMETRY = TIME FOR THE SHOREWARD MOTION / TIME FOR THE SEAWARD MOTION

WAVE VERTICAL ASYMMETRY = VERTICAL DIST FROM CREST TO S.W.L. / TOTAL WAVE HEIGHT

HORIZONTAL VELOCITY (MAGN.TUDE) ASYMMETRY = MAXIMUM HORIZONTAL SHOREWARD VELOCITY / MAXIMUM HORIZONTAL SEAWARD VELOCITY

BEACH SLOPE = 1/9
WAVE PERIOD = 0 8SEC
H_o = 1 45INS

(MAGNITUDE)

(TIME)

Figure 5.14 Graph of Velocity Asymmetry Against Wave Asymmetry

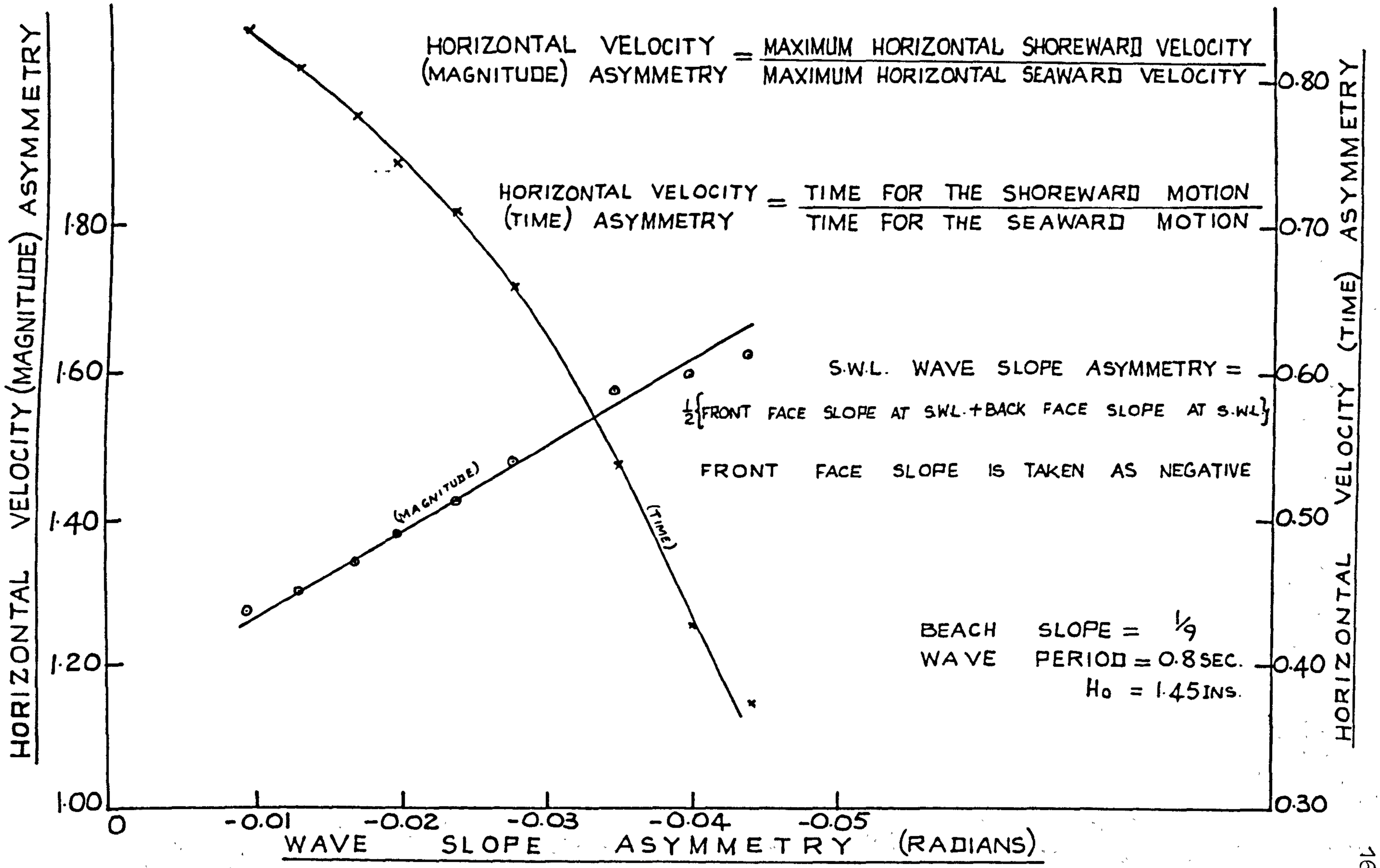

Figure 5.15 Graph of Velocity Asymmetry Against Wave Asymmetry

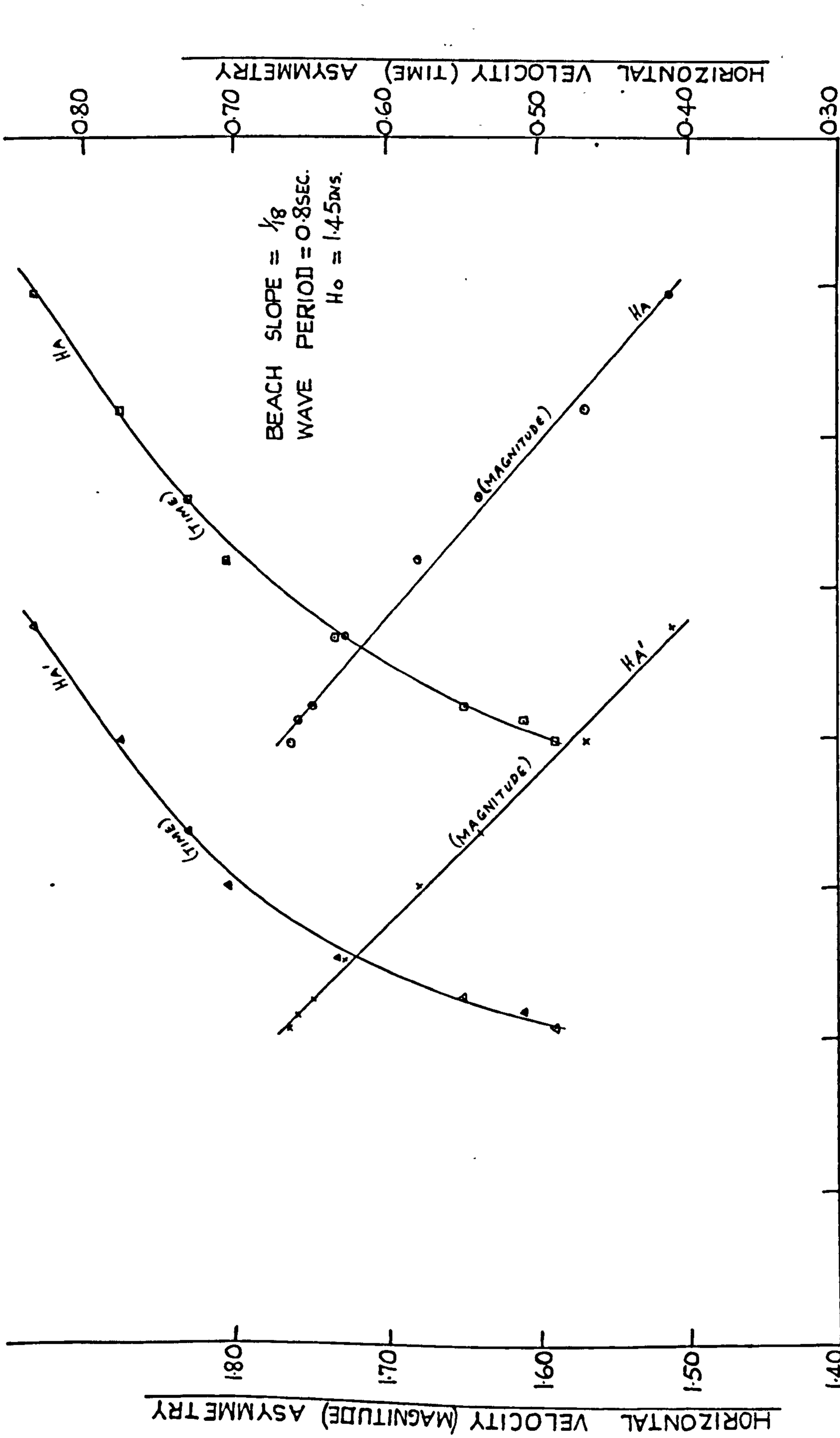

Figure 5.16 Graph of Velocity Asymmetry Against Wave Asymmetry HA & HA'

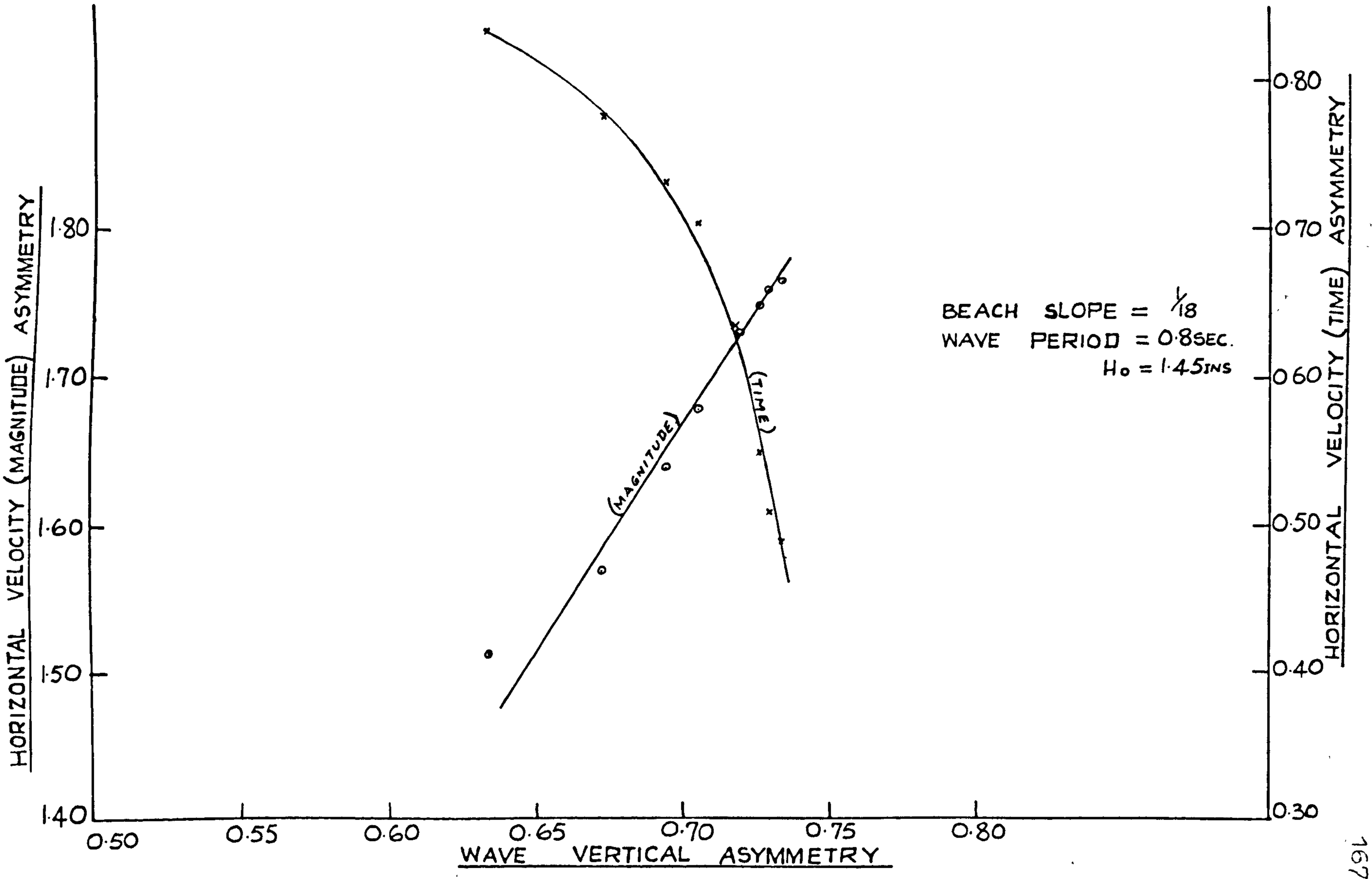

Figure 5.17 Graph of Velocity Asymmetry Against Wave Asymmetry

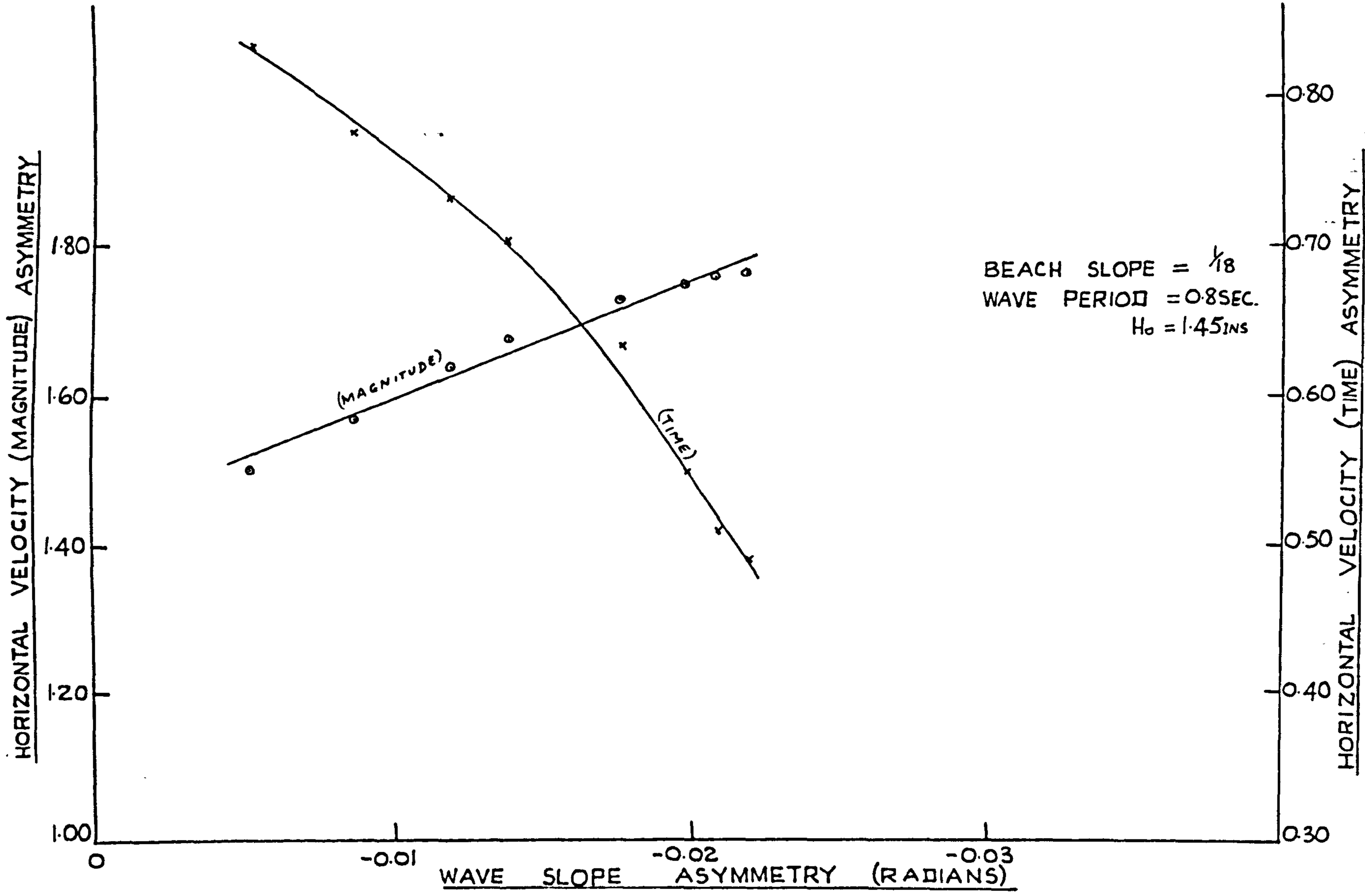

Figure 5.18 Graph of Velocity Asymmetry Against Wave Asymmetry

horizontal asymmetry HA and HA' for the beach slope of $\frac{1}{9}$. The graphs show that a correlation exists between the velocity asymmetry and the wave asymmetry. The graph of horizontal velocity (magnitude) asymmetry against wave horizontal asymmetry HA indicated that as the wave progressed into shallower water and the value of HA decreased, indicating increased asymmetry, the horizontal velocity (magnitude) asymmetry also increased. For instance, when the value of the wave horizontal asymmetry HA is 0.70 the value of the horizontal velocity (magnitude) asymmetry is 1.26, whereas when the value of HA becomes 0.50 the value of the horizontal velocity (magnitude) asymmetry increased to 1.40. Very near the wave break-point, the value of the wave horizontal asymmetry HA becomes 0.20, the value of the horizontal velocity (magnitude) asymmetry is found to be 1.605. The graph of the horizontal velocity (magnitude) asymmetry against HA' followed a trend fairly similar to the graph of the horizontal velocity (magnitude) asymmetry against HA. The graphs of the horizontal velocity (time) asymmetry against HA and HA' also show good correlations. The remaining graphs of the horizontal velocity (Magnitude) asymmetry and the horizontal velocity (time) asymmetry against the different types of wave

asymmetry are shown in figures 5.14, 5.15, 5.16, 5.17 and 5.18. They all show reasonably good correlation between the velocity asymmetry and the wave asymmetry.

As a result of the observations of the wave asymmetry and the velocity asymmetry the following relationships were obtained: -

Let Av = wave vertical asymmetry

s = wave slope asymmetry

|s| = modulus of s

γ = beach slope

VHMA = Horizontal velocity (magnitude) asymmetry

HA & HA' = wave horizontal asymmetry

$$HA = \frac{\text{Horizontal distance from crest to front face at s.w.l}}{\text{Horizontal distance from crest to back face at s.w.l}}$$

$$HA' = \frac{\text{Horizontal distance from crest to preceding wave trough}}{\text{Horizontal distance from crest to following wave trough}}$$

The empirical relationships between VHMA, s, γ, Av, HA and HA' are:

$$H_A = \frac{1.31}{e^{\gamma/2}} \tanh H_A' \qquad \ldots(5.5)$$

$$H_A = \frac{1.52}{e^{\gamma}} \left\{ 1.18 - \sinh A_V \right\} \qquad \ldots(5.6)$$

$$V_{HMA} = 3.4 A_V - 0.78 \qquad \ldots(5.7)$$

$$A_V = \frac{8.8}{e^{\gamma}} \tanh |s| + 0.5 \qquad \ldots(5.8)$$

From the cnoidal wave theory as developed by Korteweg and de Vries[24] , the wave vertical asymmetry Av is given by

$$A_v = \frac{y_c - d}{H} = \frac{16d^3}{3L^2H}\left\{K(k)\left[K(k) - E(k)\right]\right\} \quad \cdots(5.9)$$

where Yc = distance from the ocean bottom to the wave crest,

d = still water depth,

H = wave height (trough to crest)

L = wave length

K(k) = complete elliptic integral of the first kind,

E(k) = complete elliptic integral of the second kind,

k = modulus of the elliptic integral.

From (5.6) and (5.9)

$$H_A = \frac{1.52}{e^{\delta}}\left\{1.18 - \sinh\left(\frac{16d^3}{3L^2H}\left[K(k)\left\{K(k) - E(k)\right\}\right]\right)\right\} \quad \cdots(5.10)$$

From (5.9) and (5.7) we have

$$V_{HMA} = \left[\frac{18.1\,d^3}{L^2H}\left\{K(k)\left[K(k) - E(k)\right]\right\} - 0.78\right] \quad \cdots(5.11)$$

Substituting for Av from 5.8 into (5.7) gives

$$V_{HMA} = 3.4\left\{\frac{8.8}{e^{\delta}}\tanh|S| + 0.271\right\} \quad \cdots(5.12)$$

Also from the work of Biesel [5] , the wave slope asymmetry s is given by

$$s = m^2\left(\frac{H_o}{2}\right)^2 \gamma\left\{ \frac{3 + \frac{md}{\tanh md} - 3md\tanh md}{D^2(\sinh md)^2 \tanh md} \right\} \quad \cdots (5.13)$$

where $D = 1 + \left[\frac{md}{\sinh md \cosh md}\right]$

and $m = \frac{2\pi}{L}$.

Substituting for s from (5.13) into (5.12) gives

$$V_{HMA} = 3{\cdot}4\left\{\frac{8{\cdot}8}{e^{\delta}} \tanh\left[m^2\left(\frac{H_o}{2}\right)^2 \gamma\left\{ \frac{3 + \left(\frac{md}{\tanh md}\right) - 3md\tanh md}{D^2(\sinh md)^2 \tanh md} \right\}\right] + 0{\cdot}271\right\} \cdots (5{\cdot}14)$$

Thus equations (5.11) and (5.14) give expressions for VHMA. However, of the two, equation (5.11) gives closer values to the experimental results in this work, and is the theoretical curve shown on figure 5.7. Values of K(k) and E(k) are tabulated in Masch and Wiegel [34] (1961).

Comment

Figure 5.7 gives the impression that the theoretical predictions of horizontal velocity asymmetry are closer to the experimental values, for

the steeper beach slope category. The correspondence is to within 5% in the region of $\frac{d}{L}$ 0.10 to 0.13, and shows a difference of about 8% very close to the breakers where $\frac{d}{L}$ is approximately 0.08. In fact, similar percentages apply in the case of the flatter beach slope, but the difference in the slope of the curves is more apparent and has the effect of offsetting the correlation.

5.5 Effect of Backwash on Velocity Asymmetry

A study of the effect of the backwash on the velocity asymmetry was made by eliminating the backwash of the wave and studying the resulting velocity fields. The wave conditions were the same as in the previous velocity studies with backwash, and the study was carried out on the beach slopes of $\frac{1}{9}$ and $\frac{1}{18}$.

It was found that although the values of the velocities were reduced when there was no backwash the horizontal velocity (magnitude) asymmetry was found to be higher. The shoreward motion was also found to take a longer time. By referring to paragraph 5.3 it can be deduced that the elimination of backwash is equivalent to reducing the value of the beach slope. A discussion on the effect of backwash in relation

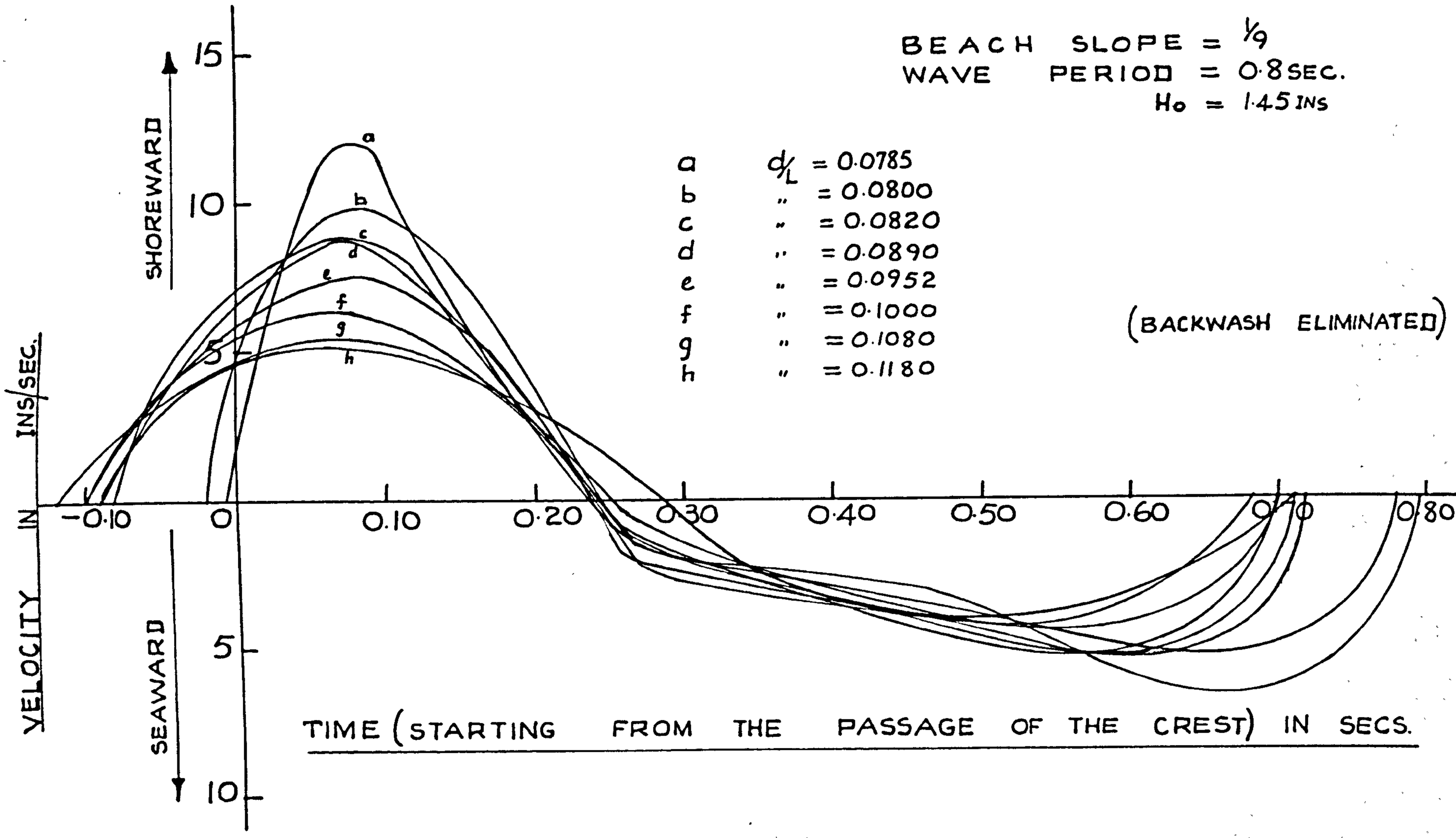

Fig. 5.19 The Superposed Graphs of Horizontal Orbital Velocity Against Time

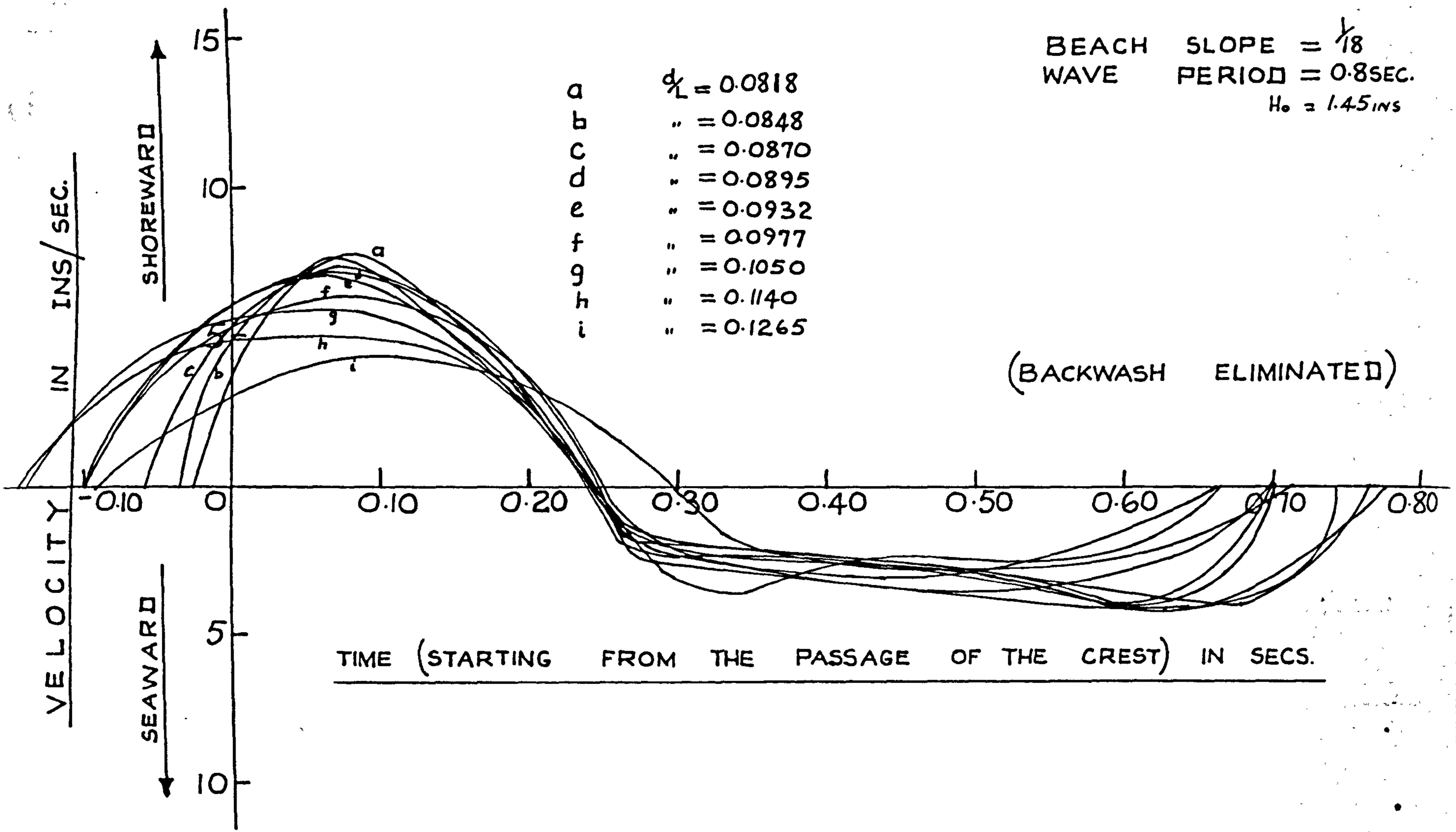

Fig. 5.20 The Superposed Graphs of Horizontal Orbital Velocity against Time.

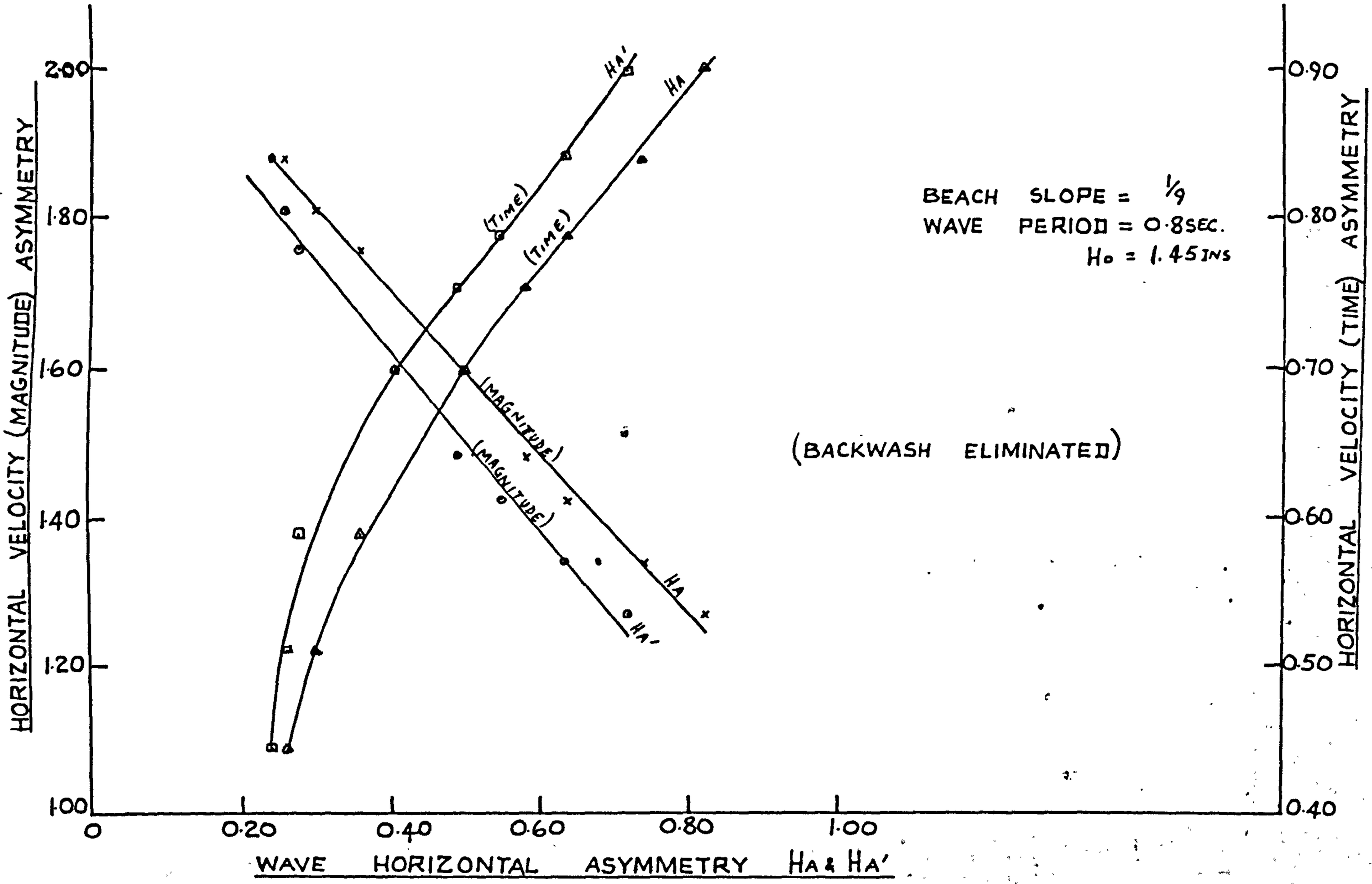
BEACH SLOPE = 1/9
WAVE PERIOD = 0·8SEC.
Ho = 1.45INS
(BACKWASH ELIMINATED)
HORIZONTAL VELOCITY (MAGNITUDE) ASYMMETRY
HORIZONTAL VELOCITY (TIME) ASYMMETRY
2·00
1·80
1·60
1·40
1·20
1·00
0·90
0·80
0·70
0·60
0·50
0·40
0
0·20
0·40
0·60
0·80
1·00
WAVE HORIZONTAL ASYMMETRY HA & HA'
HA'
HA
(TIME)
(TIME)
(MAGNITUDE)
(MAGNITUDE)
HA
HA'

Figure 5.21

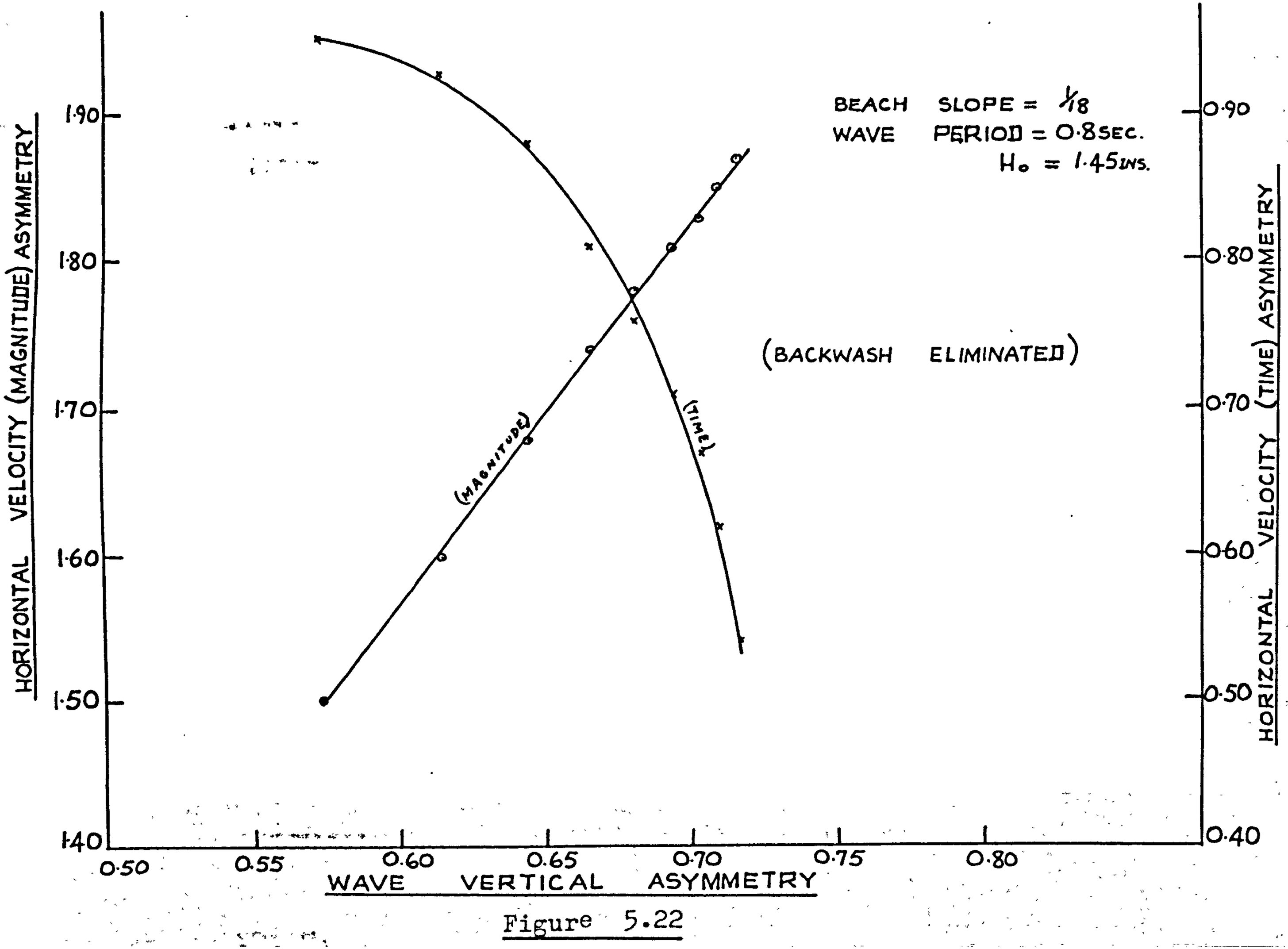
BEACH SLOPE = 1/18
WAVE PERIOD = 0.8 SEC.
H_o = 1.45 INS.
(BACKWASH ELIMINATED)
(MAGNITUDE)
(TIME)
HORIZONTAL VELOCITY (MAGNITUDE) ASYMMETRY
HORIZONTAL VELOCITY (TIME) ASYMMETRY
WAVE VERTICAL ASYMMETRY
1.90
1.80
1.70
1.60
1.50
1.40
0.90
0.80
0.70
0.60
0.50
0.40
0.50
0.55
0.60
0.65
0.70
0.75
0.80

Figure 5.22

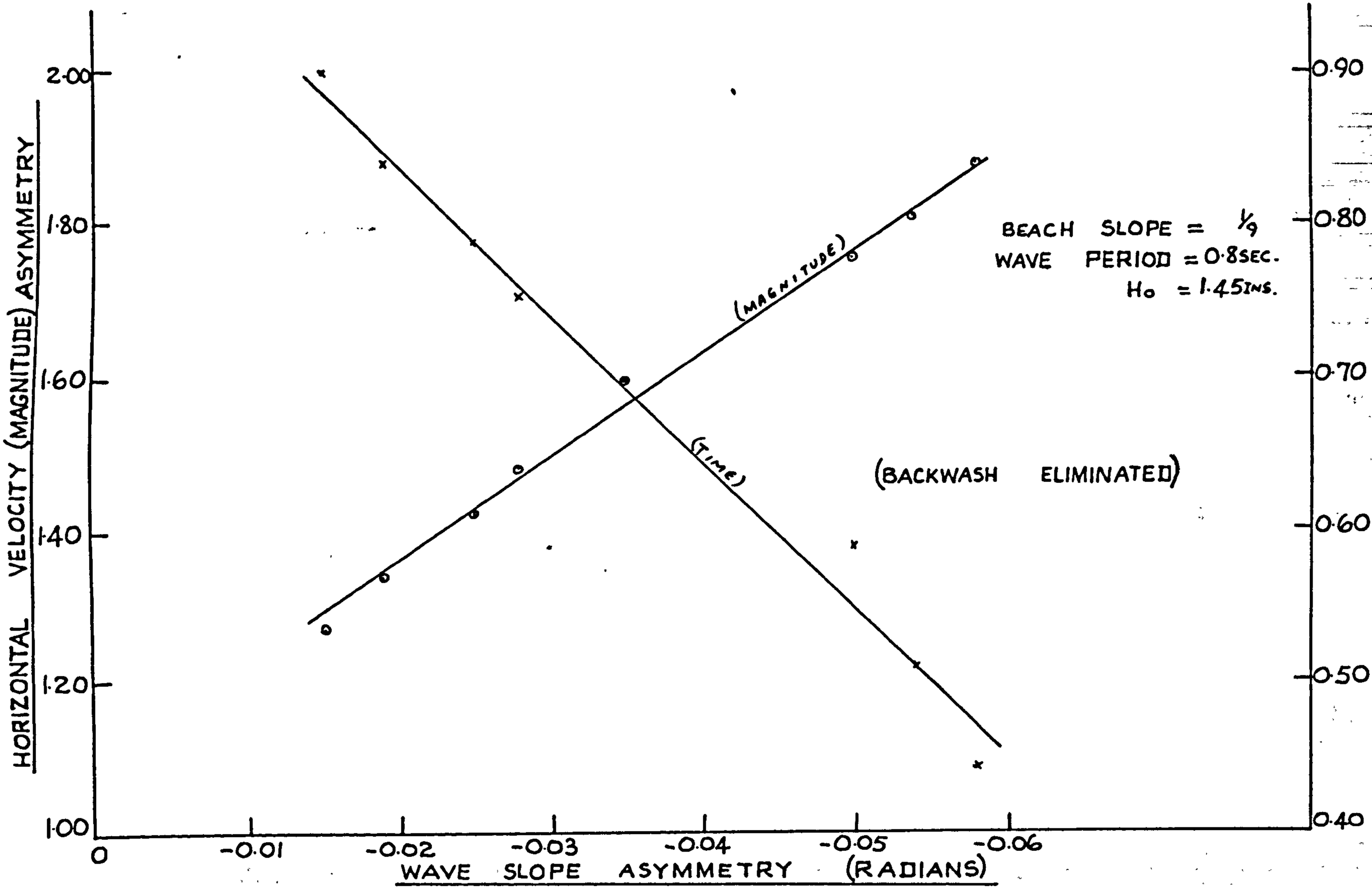
BEACH SLOPE = 1/9
WAVE PERIOD = 0.8SEC.
Ho = 1.45INS.
(MAGNITUDE)
(TIME)
(BACKWASH ELIMINATED)
HORIZONTAL VELOCITY (MAGNITUDE) ASYMMETRY
HORIZONTAL VELOCITY (TIME) ASYMMETRY
WAVE SLOPE ASYMMETRY (RADIANS)
2.00
1.80
1.60
1.40
1.20
1.00
0.90
0.80
0.70
0.60
0.50
0.40
0
-0.01
-0.02
-0.03
-0.04
-0.05
-0.06

Figure 5.23

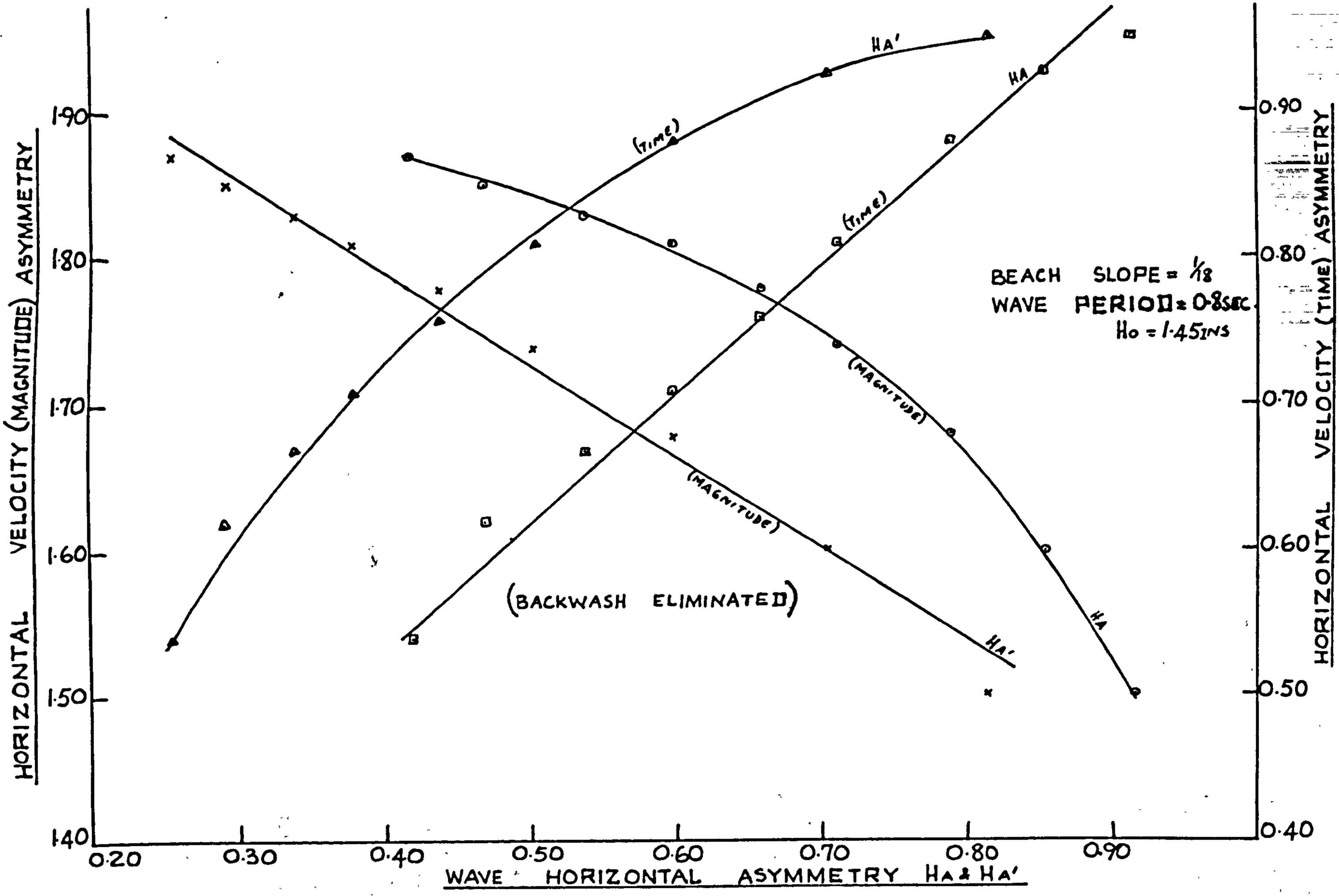
HA'
HA
(TIME)
(TIME)
(MAGNITUDE)
(MAGNITUDE)
(BACKWASH ELIMINATED)
BEACH SLOPE = 1/18
WAVE PERIOD = 0·8SEC.
Ho = 1·45INS
HORIZONTAL VELOCITY (MAGNITUDE) ASYMMETRY
HORIZONTAL VELOCITY (TIME) ASYMMETRY
1·90
1·80
1·70
1·60
1·50
1·40
0·90
0·80
0·70
0·60
0·50
0·40
0·20
0·30
0·40
0·50
0·60
0·70
0·80
0·90
WAVE HORIZONTAL ASYMMETRY HA & HA'

Figure 5.24

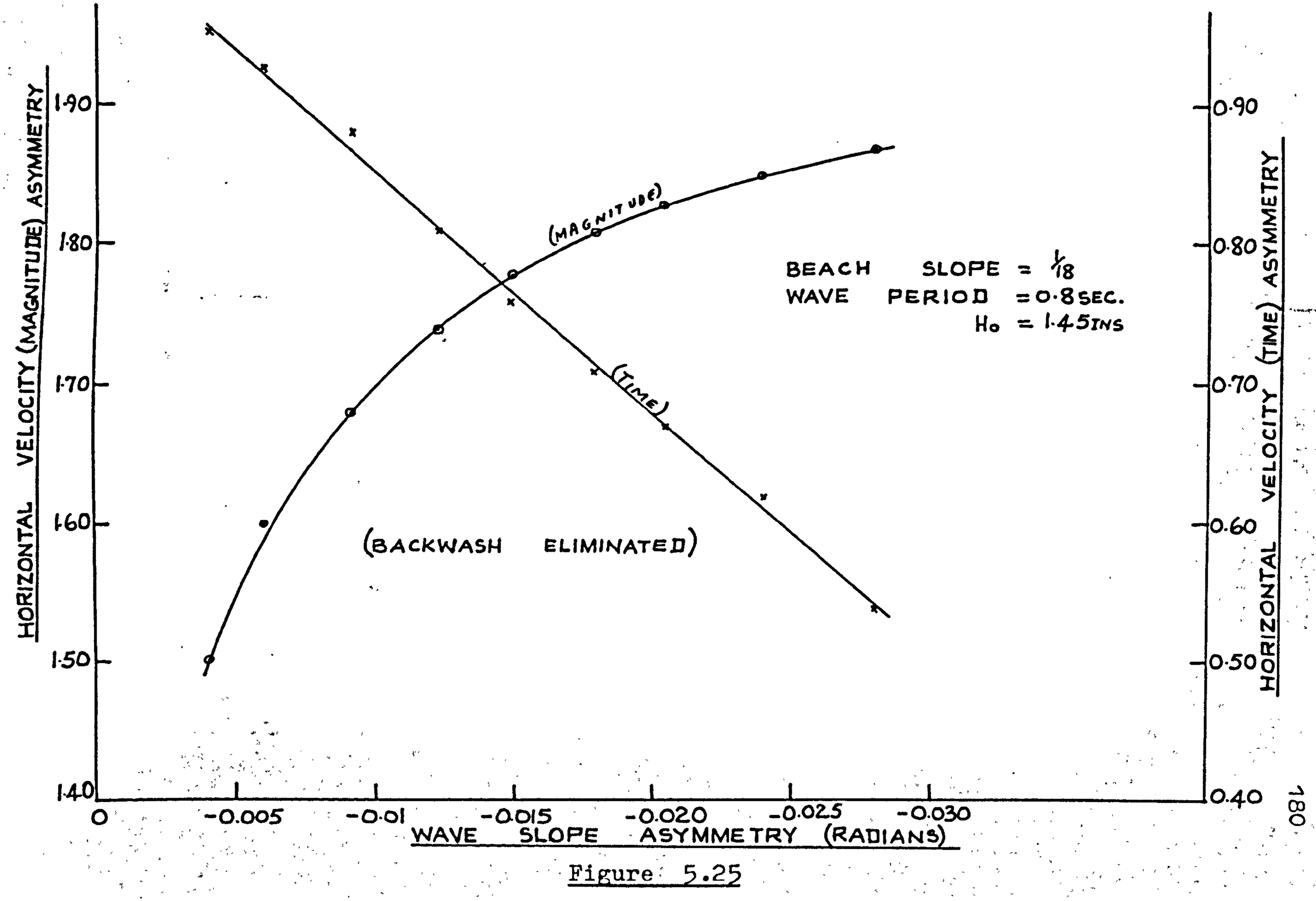
HORIZONTAL VELOCITY (MAGNITUDE) ASYMMETRY
1·90
1·80
1·70
1·60
1·50
1·40
(MAGNITUDE)
(TIME)
BEACH SLOPE = 1/18
WAVE PERIOD = 0·8 SEC.
Ho = 1·45 INS
(BACKWASH ELIMINATED)
0·90
0·80
0·70
0·60
0·50
0·40
HORIZONTAL VELOCITY (TIME) ASYMMETRY
0
-0.005
-0.01
-0.015
-0.020
-0.025
-0.030
WAVE SLOPE ASYMMETRY (RADIANS)

Figure 5.25

to sediment movement will be given in the next chapter.

Figures 5.7 and 5.8 show the graphs of the horizontal velocity (magnitude) asymmetry and the horizontal velocity (time) asymmetry against $\frac{d}{L}$ when the backwash was eliminated and in addition the graphs under backwash conditions. On the beach slope of $\frac{1}{9}$, figure 5.7 seems to indicate that the effect of the backwash becomes quite small at $\frac{d}{L} > 0.12$.

The curves of the velocity-time history at the various positions along the beach when the backwash was eliminated are shown superposed in figures 5.19 and 5.20 and the separate curves are shown in appendix 5. It is quite evident from figures 5.19 and 5.20 that the velocity curves are changing form and showing more asymmetry as the wave advances into shallower water.

Figures 5.21 — 5.25 show the graphs of the horizontal velocity (magnitude) asymmetry and the horizontal velocity (time) asymmetry against the wave asymmetry for the case when the backwash of the wave was eliminated. All the graphs indicate that the velocity field produced when the backwash was eliminated is associated with values of the wave asymmetry under the same conditions.

5.6 Conclusions

The results demonstrate the way in which the horizontal velocities increase in shallow water, and that for both slopes of $\frac{1}{9}$ and $\frac{1}{18}$ the greatest horizontal velocities occurred at the wave breaker position. The curves of the velocity-time history Figures 5.5 and 5.6 show that the curves were closer together on the beach slope of $\frac{1}{18}$ than on the slope of $\frac{1}{9}$. It was however found that the velocity seems to have a constant value on each beach slope at all positions along the beach 0.4 seconds after the passage of the wave crest; although the constant varies from slope to slope.

It was found that the maximum horizontal shoreward velocity did not occur directly under the wave crest but at a time 0.09T seconds after the passage of the crest. In terms of the values of the horizontal velocities, the values on the steeper slope of $\frac{1}{9}$ were higher than those on the flatter slope of $\frac{1}{18}$ especially in the neighbourhood of the breakers, but it was found that the values of the horizontal velocity (magnitude) asymmetry were higher on the flatter slope. Also the graph of the horizontal velocity (time) asymmetry against $\frac{d}{L}$ showed that the shoreward motion takes a longer time on the flatter slope. Both the

actual magnitude of the maximum bed velocity and the asymmetry of the velocity field are very important in sediment movement under wave action, the former being associated with initial grain motion, and the latter with the extent of the motion.

The results of each of the two horizontal velocity asymmetries were plotted against each of the three main types of wave shape asymmetry. All the graphs showed that the resulting velocity asymmetry is very closely associated with the wave asymmetry. Expressions for the wave horizontal asymmetry and the horizontal velocity (magnitude) asymmetry were established on the basis of existing wave theory.

The effect of eliminating the backwash on the velocity studies was also investigated. It was found that the absolute values of the magnitude of the velocities decreased but the horizontal velocity (magnitude) asymmetry was found to be higher than under backwash conditions. The elimination of backwash had an effect equivalent to the lowering of the beach slope. The velocity asymmetry produced when the backwash was eliminated also showed close association with the wave asymmetry under the same conditions, lending more weight to the earlier statement that the resulting velocity asymmetry is

closely associated with the wave asymmetry.

All the experiments, with and without backwash gave quantitative confirmation of the observation that as the waves progress into shallower water, the wave asymmetry and the resulting velocity asymmetry increase up to the break-point.

CHAPTER 6

MECHANICS OF SEDIMENT MOVEMENT UNDER THE ACTION OF WAVES

6.1 Introduction

The understanding of the mechanics of the movement of sediment is of paramount importance in the success of many if not all coastal projects. Further, it is well recognised that waves play a major role in the coastal sediment movement which is reflected in the accretion or erosion of the coast, but as yet too little is known about the mechanics of this movement. The author considers that investigations of the flow structure very close to the bed should eventually provide a quantitative basis for evaluating the accretion and depletion of sediment under wave action.

The existence of differential velocities at the bottom under oscillatory waves was discussed in the last chapter. Later in this chapter, the use of the time history of the velocity curve as a criterion for predicting the onshore-offshore sediment motion is discussed.

Two main types of sediment movement are well recognised on the coast; the longshore movement and the

onshore-offshore movement. The main interest in this thesis is in connection with the onshore-offshore sediment movement. A review of previous work on the mechanics of sediment movement under wave action is given below:

6.2.1 Review of Previous Work

In view of the widely divergent nature of previous studies in this field, representative works have been chosen.

In an investigation of California beaches Grant[11] remarked that the large variation in the amount of sand on a beach and on the adjacent shallow sea floor appeared to be directly related to the magnitude and type of wave action. For instance, ground swells approaching a beach would reach a position where the water particle orbital motion at the bottom was of sufficient velocity to shift the sediment
If the forward motion is more rapid than the reverse movement, then some particles may be of just the proper size and weight to be moved shoreward by the high velocity in that direction but not shifted back again by the slower reverse flow. Commenting on very large particles and very small ones he concluded that some large particles may not move at all, while

very small ones may move in both directions. Grant considered that large waves would transport larger particles to the beach from the adjacent sea floor than small waves. The author considers that in fact, it is not simply the absolute magnitude of the orbital velocity in the shoreward direction that governs the mode of motion of the sediment but the velocity asymmetry of the orbital velocity field. This includes both the velocity magnitude asymmetry, and the velocity time asymmetry.

Grant remarked on a very detailed experiment carried out by La Fond[25] and also some of the work of the Beach Erosion Board[3,35]. La Fond[25] described the changing profile of the beach at the Scripps Institution of Oceanography California in relation to the variations in wave size and type. Lafond's observations were quantitative and included such items as tides, variation in mean sea level, and longshore currents. Summarizing part of Lafond's results bearing on wave action, he found that high waves having maximum height of between seven and twelve feet caused a considerable removal of sand from the beach and the adjacent sea floor to a depth of about ten feet below mean sea level, the removed sand being

deposited in most cases on the sea floor between depths of ten and eighteen feet. On the other hand Lafond recorded smaller waves having a height of between two and a half to three feet that caused deposition of sand from a depth of about twelve to fourteen feet below mean sea level shoreward to a region including the beach and a height of three or four feet above sea level. He found a narrow zone of non-deposition where the waves were breaking.

Grant noted the importance of rip currents as a factor in the offshore transportation of sediment. He remarked that the onshore movement of sea floor sediment, if not counteracted by some form of removal from the beach and adjacent sea floor would produce continuous progradation. The rip currents and other onshore systems do play a large part in the removal of sediment from the beach and the adjacent offshore zone.

In a study of the relative rates of movement of different sizes of beach pebble carried out by the Hydraulics Research Station, two field experiments were conducted, the first at a site north of Deal, Kent, and the second at Rye. The aim was to gain a better understanding of the movement of pebbles,

bearing in mind that the major problems in coastal engineering, and many physiographic problems, originate from the mobility of sediment on the sea floor in the vicinity of coast lines, Jolliffe[18]. The work related to longshore movement, but a very striking feature of the results obtained was the differential movement according to particle size. The larger pebbles moved at a different speed and sometimes even in a different direction from that of the smaller pebbles. An increase in wave height on breaking, and therefore a corresponding increase in the amount of energy available at the shoreline, accentuated the differences in the movement of the large and small particles.

A comprehensive survey of coastal processes in connection with sediment movement was made by Silvester[45], he included such things as storm, swell, onshore zone, offshore zone, wind, tides, littoral drift, water elevation, meteorological effects, groynes and estuaries. He noted in particular the selective sorting of beach materials by wave action as a result of rapid forward motion of the water and a slower backward motion.

The work of Wells[53] included single wave trains a small ensemble of wave trains, and random wave trains.

The purpose was to study the probability density distribution and a measure of its asymmetry for the horizontal water velocity in shallow water resulting from these wave trains. The skewness which was used as a measure of asymmetry was defined as the third moment of the water velocity divided by the second moment raised to the three halves power, $\left(\frac{\mu_3}{\mu_2^{3/2}}\right)$. The study was made by means of an electrical analogue model. In addition some hydraulic measurements were performed in a shallow water flume at the Delft Hydraulic Laboratory. There is some doubt as to whether the rather large spheres used for flow visualisation gave meaningful results.

The following assumptions were made:-

1. In the mathematical model, the first two terms of the single water wave equation due to Stokes were used. It was assumed that the waves were in water shallow enough to generate an appreciable horizontal asymmetrical component of water velocity on the bed.

2. The effects of breakers, and littoral and rip currents were not studied.

3. Distortion of the waves by wind, or horizontal distortion due to shoaling and breaking was neglected.

From his mathematical model he concluded

a) Since the position of the maxima of the probability density distribution moved towards zero as the number of waves increased this suggested that the heavy particles have a greater chance of being moved by one wave train than by more than one wave train.

b) If the orbital velocity $u = A\cos 2\pi X + B\cos 4\pi X$ (1.1) then for one, two, three and four waves which are identical in A and B, heavy particles are less frequently moved as the number of waves increases.

c) Sorting of the sediments will not undergo such a marked change for further superposition of additional of waves above four in number, compared to the cases for one to four superimposed waves.

On the strength of the last statement Wells therefore considered that to simulate the effects of the statistical characteristics of the time varying water velocity of random wave trains, and their effect on sediment movement and sorting, not less than four simultaneously programmed wave trains should be used.

Scott[44] conducted a laboratory investigation of sand movement and included a study on ripples. On the observation of the individual ripples he found that in shallow water the ripple velocity is high along the upper parts of the profile, and as the crest of the wave passed, the surface layer of sand moved up the back slope of the ripple and over the crest and then slumped down the foreslope. He observed that much more sand is moved to the forward face of the ripple during the passage of the wave crest than is carried seaward in suspension during the passage of the trough, hence the crest of the ripple advances a small amount with the passage of each wave.

In order to study the subject more fully Scott took measurements of the water particle velocity by a series of motion pictures as commented in the last chapter. The pictures were then analysed, the velocity obtained was the running average of the velocity over a given distance, and not the time history of the velocity at a particular location. Scott found that the velocities and accelerations of the water motion are higher in the shoreward direction than in the seaward direction. Moving farther offshore, he found the shoreward and seaward velocities and

accelerations become more nearly equal. He found that the velocity of ripple movement seemed to be dependent upon the ratios of water particle velocity or acceleration shoreward, to velocity or acceleration seaward, and the shape of the ripples developed along the sandy bottom varied with the speed with which the ripples moved; faster moving ripples being more skewed than the slower moving ones. Scott also observed that the sand in the ripples in shallower water was coarser than the undisturbed sand immediately under the ripples and the ripple lengths had a direct relationship with the horizontal amplitude of orbital water motion as previously noted by Bagnold[2]. On general movement of sediments Scott found that there was a tendency for the coarser grains to move shoreward and for the finer grains to move seaward, and the size of the sand found at any point was generally related to the horizontal amplitudes of orbital water motion.

Manohar[32] made an analytical and experimental study of the mechanics of sediment movement in relatively deep water. He carried out his work by making the bed oscillate harmonically in still water. In his analysis, Manohar[32] considered the motion as taking place within the boundary layer and expressed the thickness of the boundary layer δ (ft.) as of the

order of

$$\delta = 2.6\sqrt{\nu T} \qquad (6.1)$$

where ν = kinematic viscosity of fluid (ft^2/sec)

and T = wave period (seconds). Taking the value of ν as 1.41×10^{-5} ft^2/sec, the thickness of the boundary layer in the work reported in this thesis using equation (6.1) is 1.05×10^{-2} inches (0.27 mm).

For transition from a laminar to a turbulent boundary layer, Manohar distinguished three types of flow over oscillating rough surfaces as follows:-

1) $\delta \ggg \varepsilon$

2) $\delta \gg \varepsilon$

3) $\delta > \varepsilon$

where ε is the height of elements of roughness (ft.). In the case where $\delta \ggg \varepsilon$ the presence of elements of roughness has no effect on the flow, and so although small finite disturbances are created in the neighbourhood of the elements, the bottom acts as if it were smooth. By considering the thickness of the boundary layer δ as the length scale, and ωa_b as the characteristic velocity, the Reynolds number at transition from laminar to turbulent flow can be defined

as

$$R_\delta = \frac{U_m \delta}{\nu}$$

or substituting from equation (6.1)

$$R_\delta = \text{constant.} \frac{\omega^{1/2} a'_b}{\nu^{1/2}} \quad \cdots (6.2)$$

where $a'_b = \frac{H}{2 \sinh \frac{2\pi d}{L}}$

and $U_m = \omega a'_b$

In the second case, where the thickness of the laminar boundary layer is much larger than the height of the element of roughness, i.e. $\delta >> \varepsilon$, the critical Reynold's number at transition from laminar to turbulent motion was expressed as

$$R_\varepsilon = \frac{\omega a'_b \varepsilon}{\nu} \quad \cdots (6.3)$$

For the third case, where the thickness of the laminar boundary layer is slightly larger than the height of the elements of roughness i.e. $\delta > \varepsilon$, the critical Reynold's Number at transition from laminar to turbulent motion was expressed as:

$$R_{f(\varepsilon)} = \frac{\omega a'_b f(\varepsilon)}{\nu} \quad \cdots (6.4)$$

$f(\varepsilon)$ being a function of the nature and dimension of the roughness.

Motion of Sediment in a laminar boundary layer

The motion within the laminar boundary layer is normally assumed to be very approximately a uniform shearing flow, and Manohar assumed that similar conditions and forces exist in the case of a carefully smoothed bed consisting of grains whose sizes are very small compared to the thickness of the boundary layer. He considered that two types of motion of grains will precede the formation of bed irregularities such as ripples, namely (a) Initial movement and (b) General movement.

Initial Movement

The basic consideration is that there is a minimum fluid force that will set the sediment in motion. The forces acting are the gravity force which acts to keep the sediment particle in its resting position and the horizontal drag exerted by the moving fluid acting tangentially to the surface, the lift force being negligible. Hence the tangential force F_D required to move a sediment particle subjected to such forces must exceed the value

$$F_D = \propto A_2 (\rho_s - \rho_f) g D^3 \tan\theta \qquad \cdots(6.5)$$

where $(\rho_s - \rho_f)$ = effective density of sediment particle

g = acceleration due to gravity

D = diameter of sediment particle

θ = angle of repose of submerged sediment particle

α = a constant depending upon the point of action of the drag force

A_2 = constant of grain volume.

Therefore, the critical drag force per unit area at initial movement of particles is

$$\tau_c = \alpha C_p A_2 (\rho_s - \rho_f) g D \tan \theta \qquad \cdots(6.6)$$

where C_p is the packing coefficient expressing the closeness of packing of the grains and is defined as D^2 times the number of grains per unit area.

Equation (6.6) can be written as

$$\tau_c = \alpha \rho (\rho_s - \rho_f) g D \tan \theta \qquad \cdots(6.7)$$

where $\rho = C_p A_2$

On the other hand, the critical drag force can also be obtained from the flow velocity distribution in the boundary layer as given by

$$U = \omega a_b' e^{-\beta y} \sin(\omega t - \beta y) \qquad \cdots(6.8)$$

where $\beta = \sqrt{\frac{\omega}{2\nu}}$ and y the co-ordinate in the vertical direction.

The shear stress at the bed is given by

$$\tau_o = \mu \left.\frac{du}{dy}\right|_{y=o} \qquad \cdots (6.9)$$

So from equations (6.8) and (6.9) the maximum shear stress is

$$\tau_{o\,max} = \mu \nu^{-\frac{1}{2}} \omega^{\frac{3}{2}} a'_b \qquad \cdots (6.10)$$

From equations (6.7) and (6.10), the stage of initial movement is given by

$$\mu \nu^{-\frac{1}{2}} \omega^{\frac{3}{2}} a'_b = \alpha \rho (\rho_s - \rho_f) g D \tan\theta \qquad \cdots (6.11)$$

$$\text{i.e.} \quad \omega_c = \left[\frac{\alpha \rho (\rho_s - \rho_f) g D \tan\theta}{a'_b \rho_f \nu^{\frac{1}{2}}} \right]^{\frac{2}{3}} \qquad \ldots (6.12)$$

Thus equation (6.12) defines the angular velocity necessary to start the initial movement. This expression does not correspond very closely with that due to Bagnold given in equation (6.30), which has the support of an analytical approach subsequently made by G.I. Taylor.

General Movement

Manohar defined the general movement as the movement of the entire top layer of grains before the

formation of ripples, and thus the critical velocity at general movement is less than that for the formation of ripples but greater than the critical velocity for initial movement.

General movement ensures when the drag force acting tangentially to the surface, exceeds the frictional resistance of the bed material. Obviously in the case of general movement, the movement of the bed material is more intense and αp is greater than for initial movement. Thus Manohar considered that if αp in equation (6.12) is given a higher value then the same equation provides the criterion for defining the critical angular velocity.

Motion of sediment in a turbulent boundary layer

In the consideration of motion of sediment in a turbulent boundary layer, the lift force is of great significance, as the sediment particles have a tendency to be lifted upward, and the drag is quite small. Thus the lift force acting vertically upward through the centre of gravity of the sediment can be expressed as

$$F_L = C_L \rho_f \frac{u^2}{2} A_1 D^2 \qquad \cdots (6.13)$$

where F_L = lift force (lbf)

C_L = coefficient of lift

A_1 = constant of area of grain

U = velocity of flow at sediment level

D = size of grain

since C_L is a function of Reynolds' number equation (6.13) can be written

$$F_L = X_1 \left(\frac{uD}{\nu}\right) \rho_f A_1 D^2 u^2 \quad \ldots (6.14)$$

The drag force F_D can be expressed as

$$F_D = C_D \rho_f \frac{u^2}{2} A_1 D^2 \quad \ldots (6.15)$$

and as C_D is a function of Reynolds' number, equation (6.15) can be written

$$F_D = X_2 \left(\frac{uD}{\nu}\right) \rho_f A_1 D^2 u^2 \quad \ldots (6.16)$$

Manohar further assumed that the resistance to particle movement is proportional to the weight of the immersed sediment particle, and so we have

$$W_s = (\rho_s - \rho_f) g A_2 D^3 \quad \ldots (6.17)$$

where W_s is the weight of sediment particle (lbf)

A_2 is constant of grain volume.

For initial movement, the moments of the drag force F_D and the lift force F_L just overcome the counter moment due to the weight of the immersed sediment particles, and so by taking moment about the point

of support of particle on the bed and further assuming that C_D is constant as it varies only slightly with Reynold's # number in transitional and turbulent flow Manohar finally obtained

$$A_1 \rho_f D^2 u^2 \left[C_D + X_1\left(\frac{uD}{\nu}\right)\right] = A_2 (\rho_s - \rho_f) g D^3$$

i.e. $$A_1 \rho_f D^2 u^2 f_1\left(\frac{uD}{\nu}\right) = A_2 (\rho_s - \rho_f) g D^3 \quad \ldots (6.18)$$

and so for initial movement

$$\frac{A_1 \rho_f D^2 u^2 f_1\left(\frac{uD}{\nu}\right)}{A_2 (\rho_s - \rho_f) g D^3} > 1$$

The left hand side of the last expression can be expressed as a dimensionless function as

$$\psi_1 = \frac{h \rho_f u^2 f_1\left(\frac{uD}{\nu}\right)}{(\rho_s - \rho_f) g D} \quad \ldots (6.19)$$

and the velocity distribution in turbulent flow above the oscillating bed is of the form

$$u = \omega a'_b e^{-\beta' y} \sin(\omega t - \beta' y) \quad \ldots (6.20)$$

where $\beta' = \sqrt{\frac{\omega}{2\varepsilon}}$

and from this ψ_1 can be written as

$$\psi_1 = h_1 \left[\frac{\omega^2 a'^2_b \rho_f f_2\left(\frac{\omega a'_b D}{\nu}\right)}{(\rho_s - \rho_f) g D}\right] \quad (6.21)$$

Thus initial movement will be a function of the dimensionless function ψ_1.

The function ψ_1 can be modified to yield the criterion for general movement as follows

$$\psi_1 = h_2 \left[\frac{\omega^2 a_b'^2 \rho_f f_2 \left(\frac{\omega a_b' D}{\nu}\right)}{(\rho_s - \rho_f) g D} \right] \quad \cdots (6.22)$$

From the experimental results of Manohar[32] and Huon Li[13] it was found that the bed would be hydraulically smooth if $\frac{\delta}{\epsilon} > 30$ and the transition to turbulence is independent of ϵ and is given by

$$R_\delta = \frac{\omega^{1/2} a_b'}{\nu^{1/2}} = 400$$

when $30 > \frac{\delta}{\epsilon} > 18.5$, transition from laminar to turbulent flow is given by

$$R_\delta = \frac{\omega a_b' \epsilon}{\nu} = 104$$

while a rough boundary exists when $\frac{\delta}{\epsilon} < 18.5$ and the transition from laminar to turbulent flow is given by

$$R_{f(\epsilon)} = \frac{\omega a_b' f(\epsilon)}{\nu} = 1.78 \times 10^4$$

where $f(\epsilon) = \epsilon^{0.2}$

Manohar found that in the case when the boundary layer was laminar, the motion was well predicted by eq. (6.12) with $\alpha\rho = 0.063$ for initial movement and $\alpha\rho = 0.077$ for general movement. For the initial and general movement of sediment in turbulent boundary layer,

Manohar noted that the dimensionless function eq. (6.21) written in the form

$$\psi_1' = \left[\frac{\omega a_b' \rho_f^{0.4}}{(\rho_s - \rho_f)^{0.4} g^{0.4} \nu^{0.2} \Pi^{0.2}}\right] \quad \cdots (6.23)$$

governs the motion. From the experimental results Manohar found ψ_1' to be equal to 7.45 at initial movement and ψ_1' = 8.20 at general movement.

Valembois[15] extrapolated the experimental results of Huon Li[13] which involved using an oscillating plate as used by Manohar. Valembois remarked that it is possible to have both laminar and turbulent boundary layers in nature under natural waves of period between 4 and 20 seconds; but that it would be difficult to attain turbulent boundary layers in hydraulic models with periods of the order of 1 second. A natural seiche will nearly always be turbulent near the bed, and in the case of tides, it is almost impossible for a laminar boundary layer to develop and remain stable.

However, Vincent[52] with a view to explaining the mechanics of sediment transport in the open sea, concluded that the results given by Huon Li regarding the onset of turbulence within the oscillatory boundary layer overestimate the range of laminar conditions. More discussion on the work of Vincent will be given later.

The above discussion of the work of Manohar has been related to the mechanics of sediment movement in fairly deep water. In the consideration of sediment movement in shallow water under the action of waves Manohar[32] used the oscillating plate as used in his study dealing with sediment movement in deep water. He obtained the differential velocities, known to be associated with shallow water waves as discussed in Chapter 5, by such an arrangement that the speed of the drive unit was changed every half revolution. The velocity of movement of the plate at different instances during its forward and backward motion was obtained by means of the oscillograph recorder. Measurements of the velocity of the ripple movement and the rates of transport of sediment in the direction of the forward velocity were made. He noted that increase in the velocity of oscillation up to a certain critical velocity resulted in an increase in the height and length of the ripples, Further increase in velocity after that stage resulted in decrease in height and increase in length of the ripples until they finally disappeared. The velocity of movement of the ripples was found to increase with increase in the forward velocity of the plate, but after the disappearance of the ripples the transportation was in a state of suspension close

to the bed, moving in the direction of the forward velocity.

On the rate of transport of sediment, he found that the following expressions satisfied his experimental results:

$$G = 2.50 \times 10^{-11} \psi_1'^{\,6.90} \qquad \cdots (6.24)$$

and

$$U_r = 9.42 \times 10^{-9} \psi_1'^{\,4.60} \qquad \cdots (6.25)$$

where

$$\psi_1' = \frac{\omega_s a_b' \rho_f^{\,0.4}}{(\rho_s - \rho_f)^{0.4} g^{0.4} \nu^{0.2} D^{0.2}}$$

$\omega_s a_b'$ is the maximum velocity towards the beach

G is the rate of transport of sediment (dry weight in lbf/sec/ft.) and U_r is the velocity of ripple movement (ft/sec). Manohar[32] concluded that in shallow water, sediment motion seems to be taking place in a fictitious horizontal layer along the bed of a thickness

$$\delta_2 = \frac{9.1}{W_1} G^{1/3} \qquad \cdots (6.26)$$

where W_1 is the unit weight of sediment.

It is doubtful whether the oscillating bed as used by Huon Li[13] Bagnold[2] and Manohar[32] can in all circumstances reproduce satisfactorily the properties of a progressive wave, especially the shallow water wave.

It is therefore not very surprising that when Manohar compared his experimental results, supposed to be for shallow water, with theory, the results agreed more with the oscillatory wave theory than the solitary wave theory.

Manohar finally remarked that when differential velocities exist at the bottom, the rate of sediment movement and velocity of ripple movement are related to the greater of the two velocities of oscillation. Thus he considers that a knowledge of the maximum velocity of oscillation is sufficient to determine the rate of sediment movement. The author does not share that view, and considers that the absolute magnitude of the maximum velocity is merely a criterion for whether the sediment will ever move at all throughout the whole wave cycle. A more detailed discussion is given later on in this chapter, but it could still be said here too, that if the absolute magnitude of the maximum water particle velocity is greater than the threshold velocity for a sediment, the sediment will move, and once the sediment starts to move the velocity asymmetry becomes the governing factor determining how far onshore or offshore it will move.

Eagleson and Dean[9] examined the mechanics of sediment movement by dividing the observed motion

into two classifications which they called the incipient sediment motion and the established sediment motion. The two classifications are fairly similar in to the terms initial movement and general movement of Manohar[32] but their approaches are quite different.

Eagleson and Dean remarked that on natural beaches the median sediment size is distributed from coarse to fine in the offshore direction, and under the assumption that the median remaining size is indicated by the size that can be maintained in oscillating equilibrium at the point they derived the relationship

$$D_e^{6/7} \sin\alpha = 7.60 \times 10^{-6} \beta^{3/7} \frac{1}{2} \left(\frac{\pi H}{T}\right)\left(\frac{\pi H}{L}\right) \frac{1}{\sinh^2 \frac{2\pi d}{L}} \quad \cdots(6.27)$$

where D_e is the sand sediment diameter as determined from the oscillating equilibrium criterion.

α is the angle the beach makes with the horizontal in radians,

$$\beta = \sqrt{\frac{\omega}{2\nu}}$$

ω = angular frequency rad/sec.

ν = kinematic viscosity of fluid ft^2/ sec or cm^2/sec.

Eagleson and Dean then commented that if on the other hand, the sediment size satisfying the condition for oscillating equilibrium at all locations cannot be moved by the maximum local fluid velocity, then the

median remaining size will be governed by incipient motion conditions. For this condition they derived the relationship

$$D_i \sin(\alpha \pm 0.92) = 8.0 \times 10^{-6} \frac{f}{\delta} \beta \qquad \cdots(6.28)$$

where D_i is the sand sediment diameter as determined from the "incipient" criterion.

Also $$\frac{f}{\delta} = \frac{H}{2} \frac{\omega}{\sinh \frac{2\pi d}{L}}$$

In conclusion, Eagleson and Dean considered it rather difficult to say with assurance which mechanism controls the natural beach configuration.

Goddet[10] approached the study by assuming that the beginning of movement takes place at a constant ratio of particle weight W_s to drag force F_D. He defined the drag coefficient as a function of the Reynolds Number $\left(\frac{ud}{\nu}\right)$, and as proportional to $\left(\frac{ud}{\nu}\right)^{-1}$ for laminar conditions, $\left(\frac{ud}{\nu}\right)^{-\frac{1}{2}}$ for transition conditions and to a constant value for turbulent flow. Goddet's experiments corresponded to transition conditions, and his critical velocity of oscillatory motion U_c is given as

$$U_c = 27 \rho_1^{\frac{2}{3}} D^{\frac{1}{4}} T^{\frac{3}{8}} \text{ in c.g.s units} \qquad \cdots(6.29)$$

where ρ_1 is the ratio of apparent density = $\left(\frac{\rho_s - \rho_f}{\rho_f}\right)$

ρ_s density of sediment

ρ_f density of fluid

T wave period

D grain diameter

Bagnold[2] conducted an investigation into the mechanics of sediment movement, and as previously remarked he made the bed oscillate harmonically in still water. Bagnold in his study noted a complete absence of turbulence even down to a distance of about one grain diameter. He obtained an expression relating the critical angular speed for initial sediment movement to the grain and fluid characteristics. i.e.

$$\omega = 21.5\ r^{-0.75}\ \rho_1^{0.5}\ D^{0.325} \qquad \ldots(6.30)$$

where r is the semi amplitude of oscillation.

In an appendix to the paper of Bagnold[2], G. I. Taylor followed up the work of Bagnold with a theoretical analysis, and produced a general expression as follows:

$$\omega = r^{-2/3}\ \nu\ D^{-4/3}\ \chi\left(\frac{\rho_1 g D^3}{\nu^2}\right) \qquad \ldots(6.31)$$

where $\chi(\zeta) = [\phi(\zeta)]^{2/3}$

Taylor suggested a particular form of χ i.e. $\phi(\zeta) = B\zeta^{2/3}$ which he considered nearly coincides with Bagnold's empirical relation, this however gives:

$$\omega = \text{constant}\ r^{-0.67} \rho_1^{+0.45} \Pi^{0} \qquad \ldots(6.32)$$

To obtain the indices which most nearly coincide with Bagnold's, Taylor should have assumed $\phi(\zeta) = B\zeta^{5/6}$ and equation (6.31) becomes

$$\omega = \text{constant}\ r^{-2/3} \rho_1^{0.55} \Pi^{0.33} \qquad \ldots(6.33)$$

The expression which gives the critical condition for initial movement on the basis of angular velocity can be written in the general form

$$\omega = \text{constant}\ r^{\alpha_1} \rho_1^{\alpha_2} \Pi^{\alpha_3} \qquad \ldots(6.34)$$

This expression can be used to draw a useful comparison between the results obtained by Goddet, Bagnold and Taylor. The values of α_1, α_2 and α_3 in eq. (6.34) applicable to these authors are as follows:

	α_1	α_2	α_3
G.I. Taylor[2](1946)	- 0.67	+ 0.55	+0.33
R.A.Bagnold[2](1946)	- 0.75	+ 0.50	+0.325
J. Goddet[10](1960)	- 0.73	+ 0.48	+0.18

Vincent[52] made a very extensive study of the mechanics of sediment movement under wave action. He remarked that Huon Li's results in which an oscillating bed in still water was used, tended to exaggerate the relative importance of the laminar regime compared to the conditions actually produced when the oscillatory boundary layer is formed by waves progressing over a stationary bed. He considers that within the body of the fluid, waves are either generally laminar or slightly turbulent, but that they are more often turbulent in the immediate vicinity of the bed.

Considering the evolution of movement in the immediate vicinity of the bed from the appearance of the laminar boundary layer to the instant at which well defined solid transport appears, Vincent observed the following phenomena.

1) Development of the oscillatory laminar boundary layer.
2) Appearance of turbulence in the boundary layer.
3) Onset of grain movement.
4) General grain movement.
5) Appearance of ripples.
6) Slow progression of turbulence towards the fluid mass, i.e. from the bed towards the surface.

7) Signs of transport in suspension in the lower part of the fluid mass, and in the opposite direction to that of wave propagation.

8) Lengthening and gradual disappearance of ripples.

Vincent tried to obtain a relationship between the maximum orbital velocity V_m, corresponding to initial grain movement, the fall velocity W and diameter of sediment D. He found that at low $\frac{D}{\delta}$ the relationship assumes the form

$$\frac{V_m}{W} = \frac{\text{constant}}{D} \qquad \cdots(6.35)$$

but at high $\frac{D}{\delta}$,

$$\frac{V_m}{W} = \text{constant} \qquad \cdots(6.36)$$

These results compare very well with Valembois'[51] comments on the results obtained by Larras[28].

Vincent further found that the critical velocity of fluid particles in the immediate vicinity of the bed at the onset of movement of grains of a given material under wave action is "clearly practically constant".

Vincent found the critical velocities at the onset of movement for sand of various grain sizes, two grades of granulated pumice, and pollopas

(granulated plastic) their specific gravities being 2.65, 1.38 and 1.46 respectively. The results for six of the seven grains are set out in the table below

Sediment	D cm	ρ_s	U_c after Vincent[52] (1958)	U_c from Goddet's expression eq. 6.29
Sand no. 1	0.063	2.65	28.5 cm/s	22 cm/s
Sand no. 2	0.046	2.65	20.5 cm/s	20.3 cm/s
Sand no. 3	0.024	2.65	16.5 cm/s	17.3 cm/s
Pumice No. 1	0.160	1.38	11.0 cm/s	10. 44 cm/s
Pumice No. 2	0.120	1.38	8.5 cm/s	9.7 cn/s
Pollopas	0.039	1.46	7.0 cm/s	8.3 cm/s

The author has compared the experimental results of Vincent for the values of U_c with the expression of Goddet eq. (6.29). The critical velocities on the basis of equation (6.29) are shown in the last column above, and give fairly good agreement with the experimental values of Vincent.

Equation (6.29) is used in this thesis in the section below on the use of the time history of the velocity curve as a criterion for predicting sediment motion. Vincent finally commented that a knowledge of the considerable exchange of solid materials at the bed is of great value when seeking a better understanding

of the movements of solids on a beach profile.

6.2.2. Comments on Previous Work

The work of Wells related to the asymmetrical distribution of particle velocities under the action of composite wave trains. The relevance here is that he considers that simple wave trains produce higher velocities and greater sediment transport than are produced by composite waves. On the other hand Well's work excluded waves of asymmetrical shape.

Scott's observations on velocity asymmetry although related to those made by the author are of a "Lagrangian" nature, whereas the present series involved measurements at a point . So far as initial sediment movement is concerned it is the time history of the velocity over a given grain which determines its movement.

Manohar's work, which is related to previous investigations by Huon Li and Bagnold draws attention to the importance of the boundary layer thickness. This does seem to be a significant factor, for the criteria for first movement of sand particles by Valembois, Vincent and Goddet, also take account of the relative magnitude of the grain diameter and

boundary layer thickness. The interpretation of the author's velocity measurements in terms of sediment movement is made for grain sizes which are equal to or greater than the boundary layer thickness. This is designed to enable a consistent comparison to be made. In addition, the velocities used are those measured close to the boundary but outside the boundary layer.

The emphasis, both for unidirectional flow conditions and for oscillatory flow, has up to the present been placed on mean linear or angular velocities. A study on the relationship between turbulence and sediment movement, should throw more light on the relative importance of the stability of the main flow and the effect of grain roughness, on the velocities close to the grains. Mean flow parameters may still prove to be a useful guide to the stresses at the bed, but may need a new interpretation.

Summarising the works of Bagnold Taylor and Goddet the average of the values of α_1, α_2, and α_3 in equation (6.34) namely: $\omega = (const)\, r^{\alpha_1} \rho_1^{\alpha_2} \Pi^{\alpha_3}$ are

$$\alpha_1 = -0.72$$

$$\alpha_2 = +0.51$$

$$\alpha_3 = +0.28$$

6.3 Use of the Velocity-time Curve as a Criterion for predicting Sediment Motion

As noted in the last chapter, the velocity asymmetry was found to increase with decreasing d/L up to and including the break-point.

In the illustration below, use has been made of the expression of Goddet eq. (6.29) for the values of the critical velocity for initial movement of sediments. The critical velocities and diameter of the grains are shown in fig. 6.1 and are given the numbering system by which they are represented in fig. 6.1 - 6.9.

To use the graphs (fig. 6.1 - 6.9) a line is drawn parallel to the time axis at a value of velocity equal to the U_c for the particular sediment under consideration. This is done on both the onshore motion and offshore motion sides of the velocity curve. The total area enclosed between the horizontal line parallel to the time axis and the part of the curve with values of velocities above the U_c is then measured for both the onshore motion and offshore motion sides of the curve. For instance in Fig.6.1 for Pumice D = 0.28 cm, U_c = 5.32 ins/s and denoted by iii, on the onshore side, the area in question will be the total area enclosed by the line

marked iii and the upper part of the curve, and on the offshore side, the total area enclosed by the line marked iii and the remaining part of the curve in the direction of increasing value of offshore velocity which ever of the areas on the onshore or offshore side is greater indicates the direction of the net sediment movement.

Thus fig. 6.1 indicates that at that particular position which happens to be the break-point all the sediments i to iv would move onshore. The values with the units of sq.ins in the figures are the values of the areas enclosed. On the other hand sediments v and vi will move offshore. The value of velocity for which the areas enclosed on the onshore and the offshore sides of the curve are equal, gives the critical velocity for the null point. i.e. the velocity relating to a sediment that will be in oscillating equilibrium at the point where the time history of the velocity curve is measured. The critical velocity for the null point on figure 6.1 is found to be 3.35 ins/s and using the expression in eq. (6.29) the diameter for the null point for fig. 6.1 is found to be Pumice D = 0.044 cm.

The graphs on Fig. 6.2 is the velocity field for a position seaward of the breaker point, and similarly Fig. 6.3 is the velocity field seaward of fig. 6.2 and

BEACH SLOPE = 1/9
WAVE PERIOD = 0.8 SEC.
H = 1.515 INS
d/L = 0.0800

(i)	Pumice	□ = 4.4 cm	ρs = 1.65	Uc = 10.6 ins/s
(ii)	Pumice	□ = 0.74 cm	ρs = 1.65	Uc = 6.8 ins/s
(iii)	"	□ = 0.28 cm	"	Uc = 5.32 ins/s
(iv)	"	□ = 0.142 cm	"	Uc = 4.50 ins/s
(v)	"	□ = 0.036 cm	"	Uc = 3.20 ins/s
(vi)	"	□ = 0.032 cm	"	Uc = 3.08 ins/s

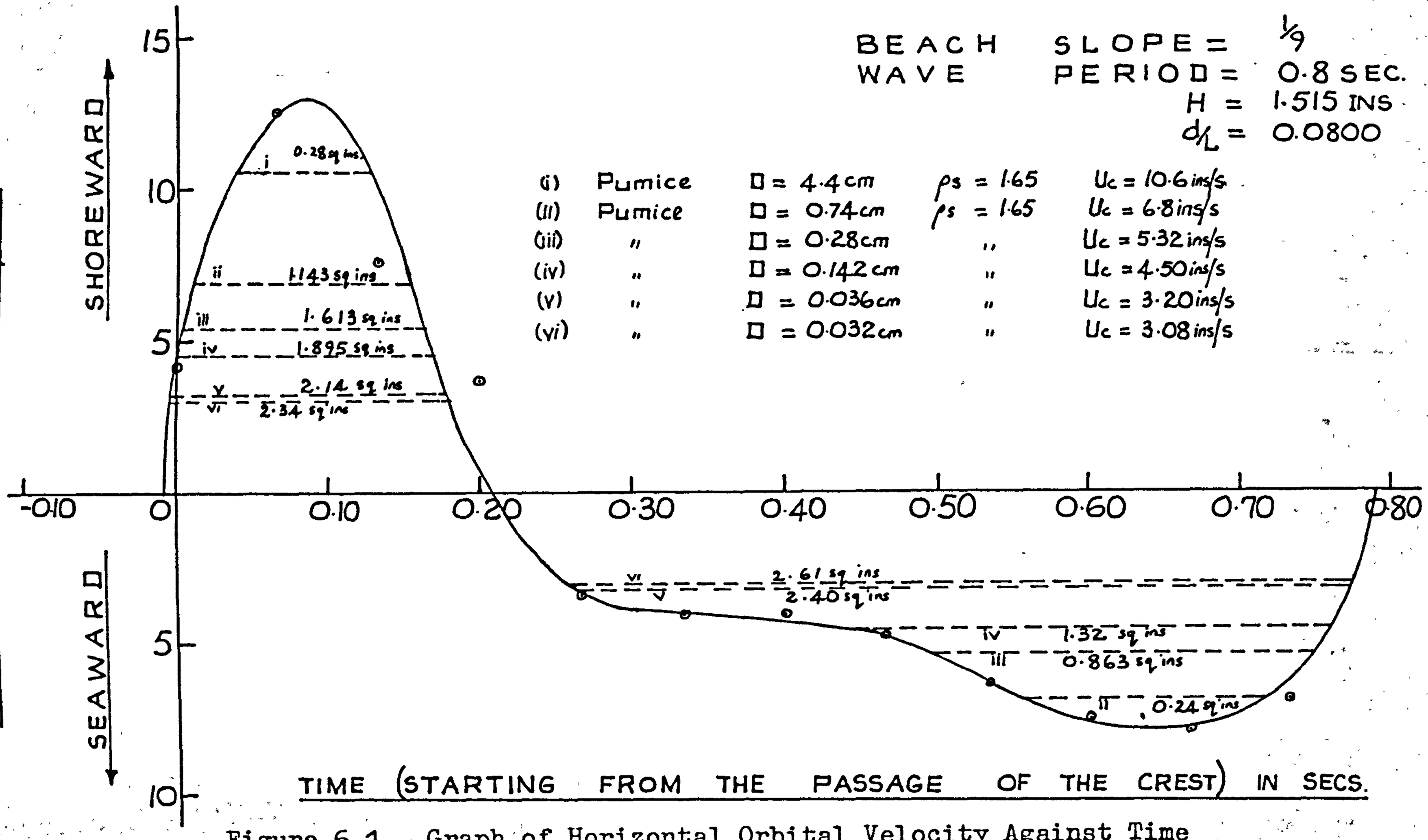

Figure 6.1 Graph of Horizontal Orbital Velocity Against Time

BEACH SLOPE = 1/9
WAVE PERIOD = 0·8 SEC.
H = 1·49 INS
d/L = 0·0815

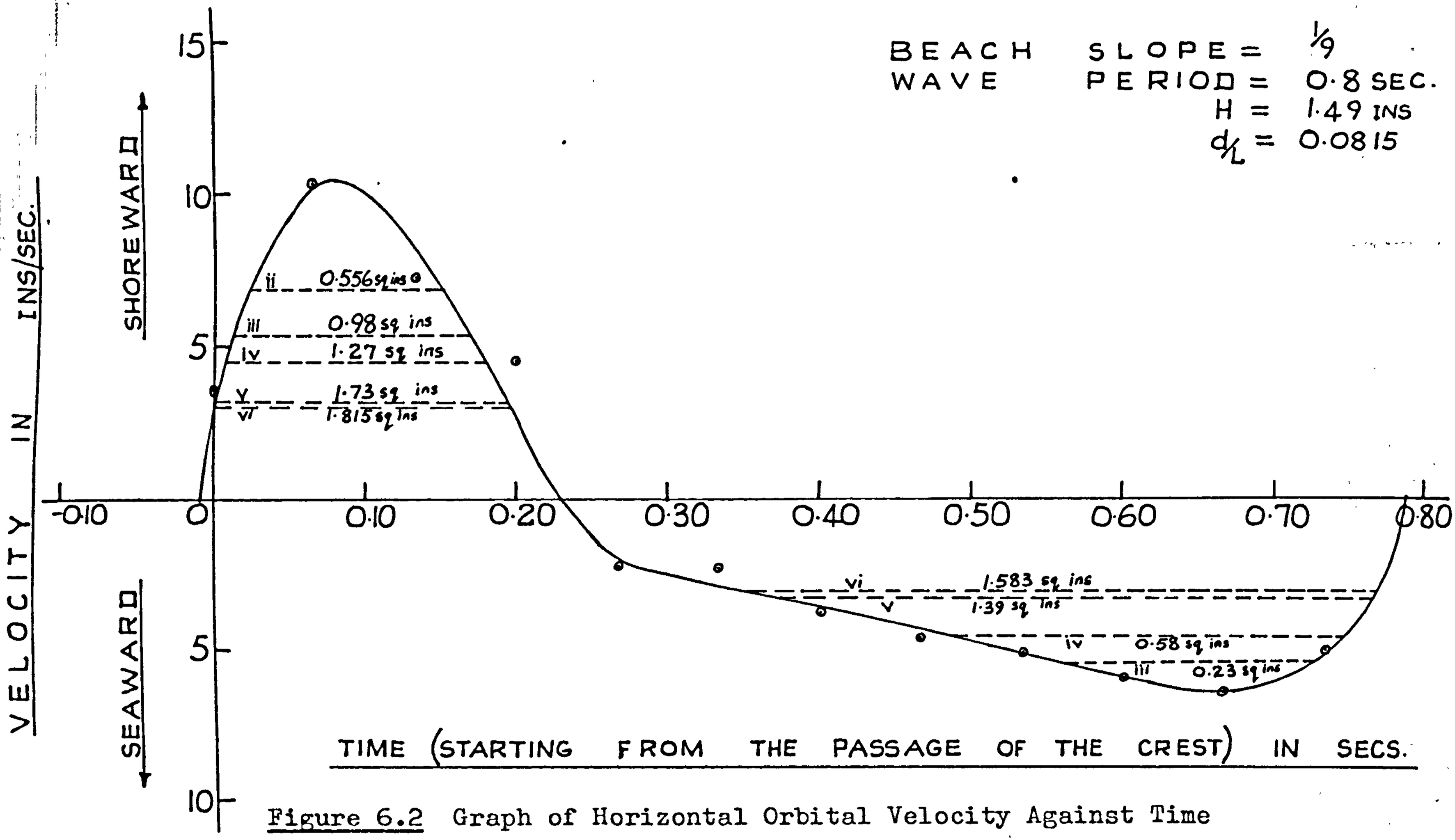

Figure 6.2 Graph of Horizontal Orbital Velocity Against Time

BEACH SLOPE = 1/9
WAVE PERIOD = 0·8 SEC.
H = 1·44 INS
d/L = 0·0833

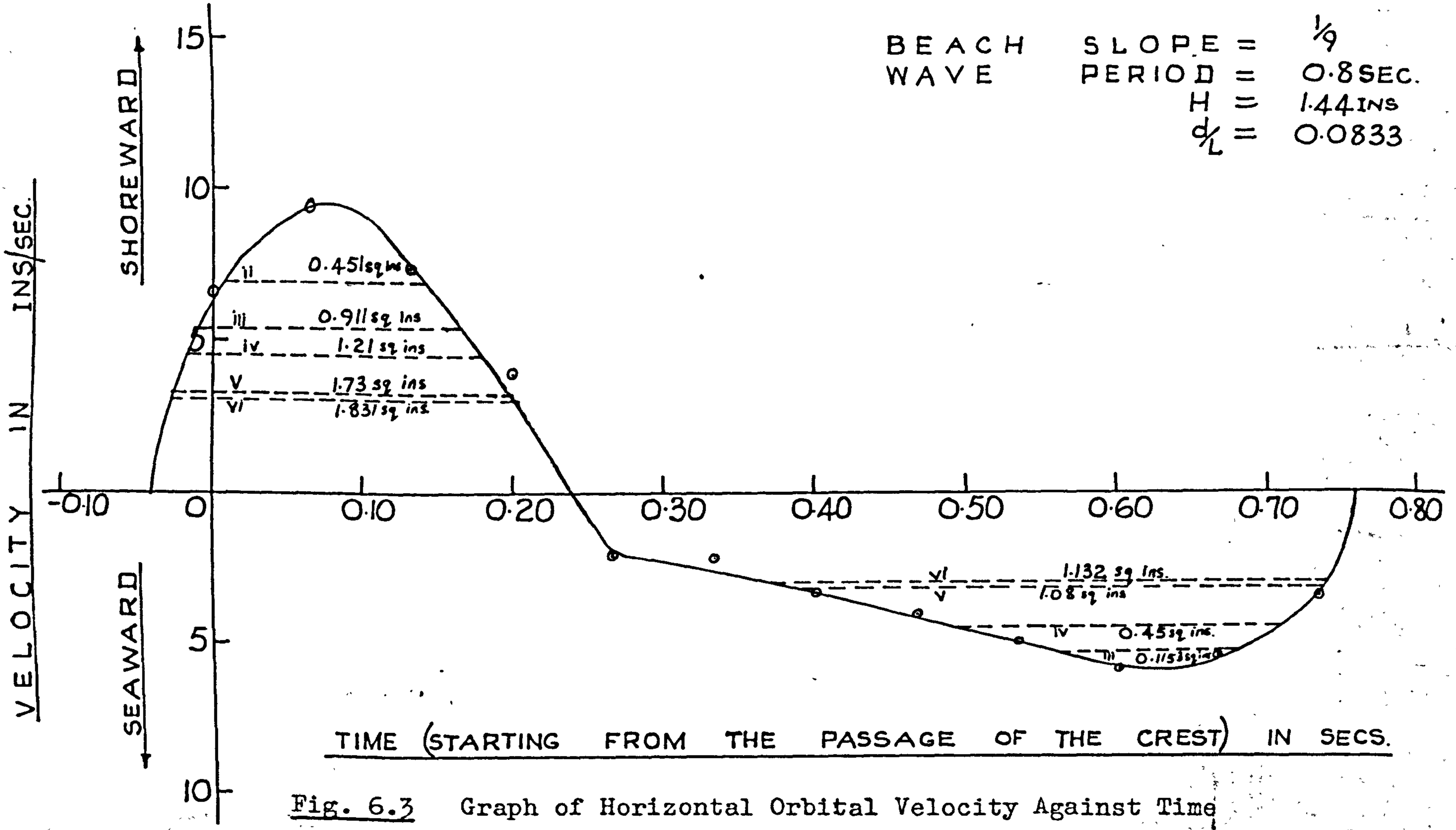

Fig. 6.3 Graph of Horizontal Orbital Velocity Against Time

BEACH SLOPE = 1/9
WAVE PERIOD = 0·8SEC.
H = 1·395 INS
d/L = 0·0891

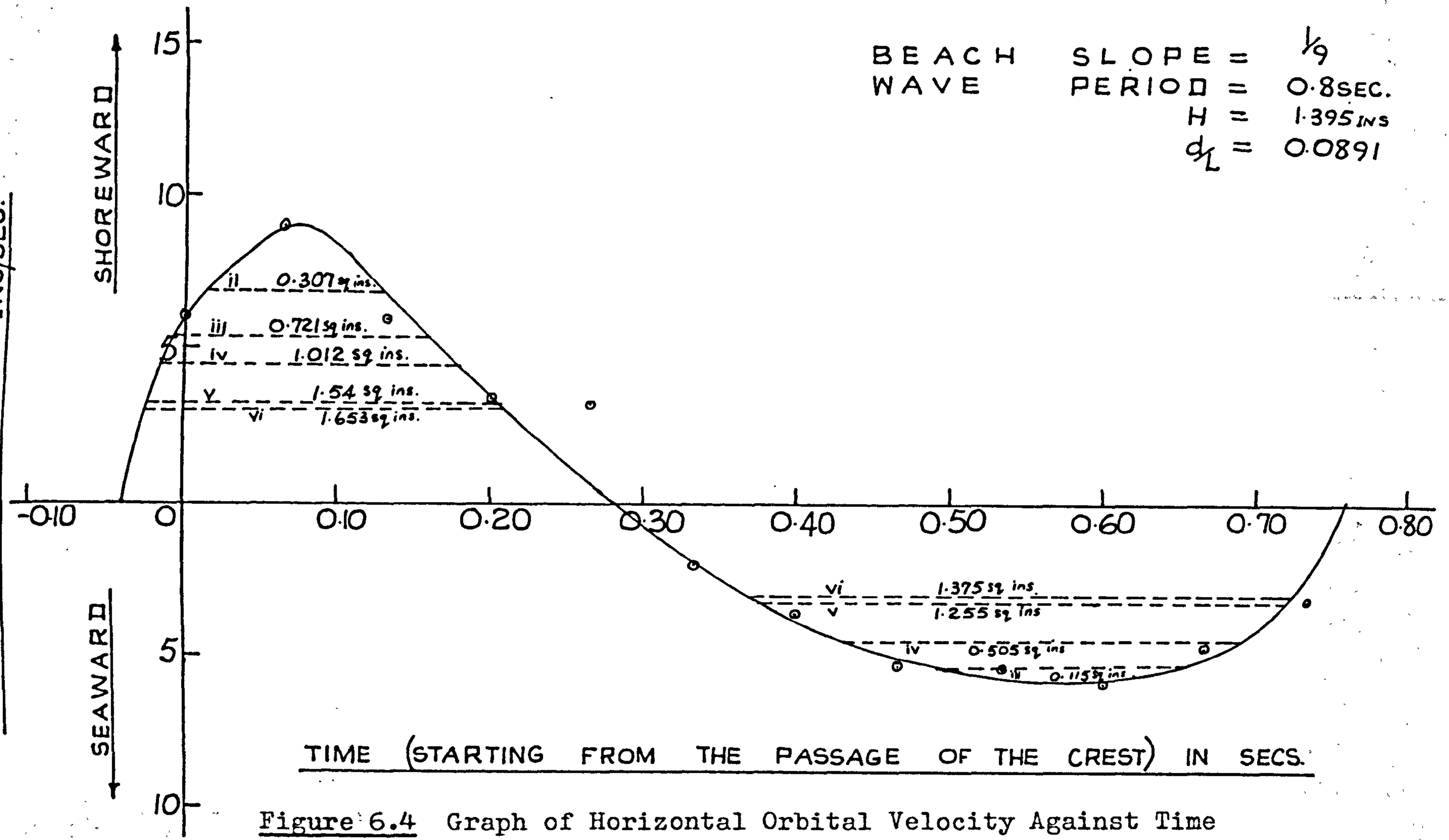

Figure 6.4 Graph of Horizontal Orbital Velocity Against Time

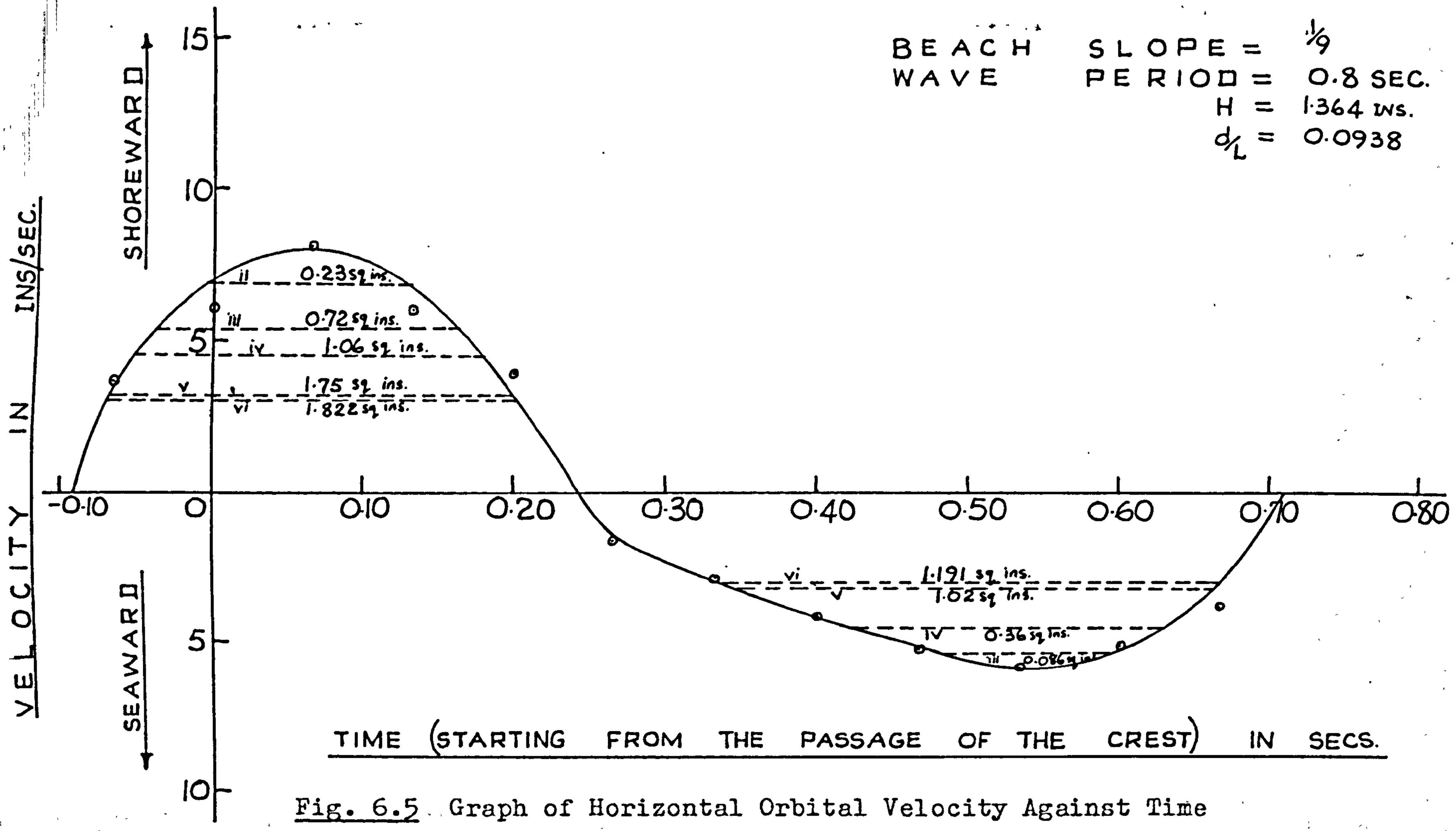

Fig. 6.5 Graph of Horizontal Orbital Velocity Against Time

BEACH SLOPE = 1/9
WAVE PERIOD = 0·8SEC.
H = 1·35 ins
d/L = 0·0987

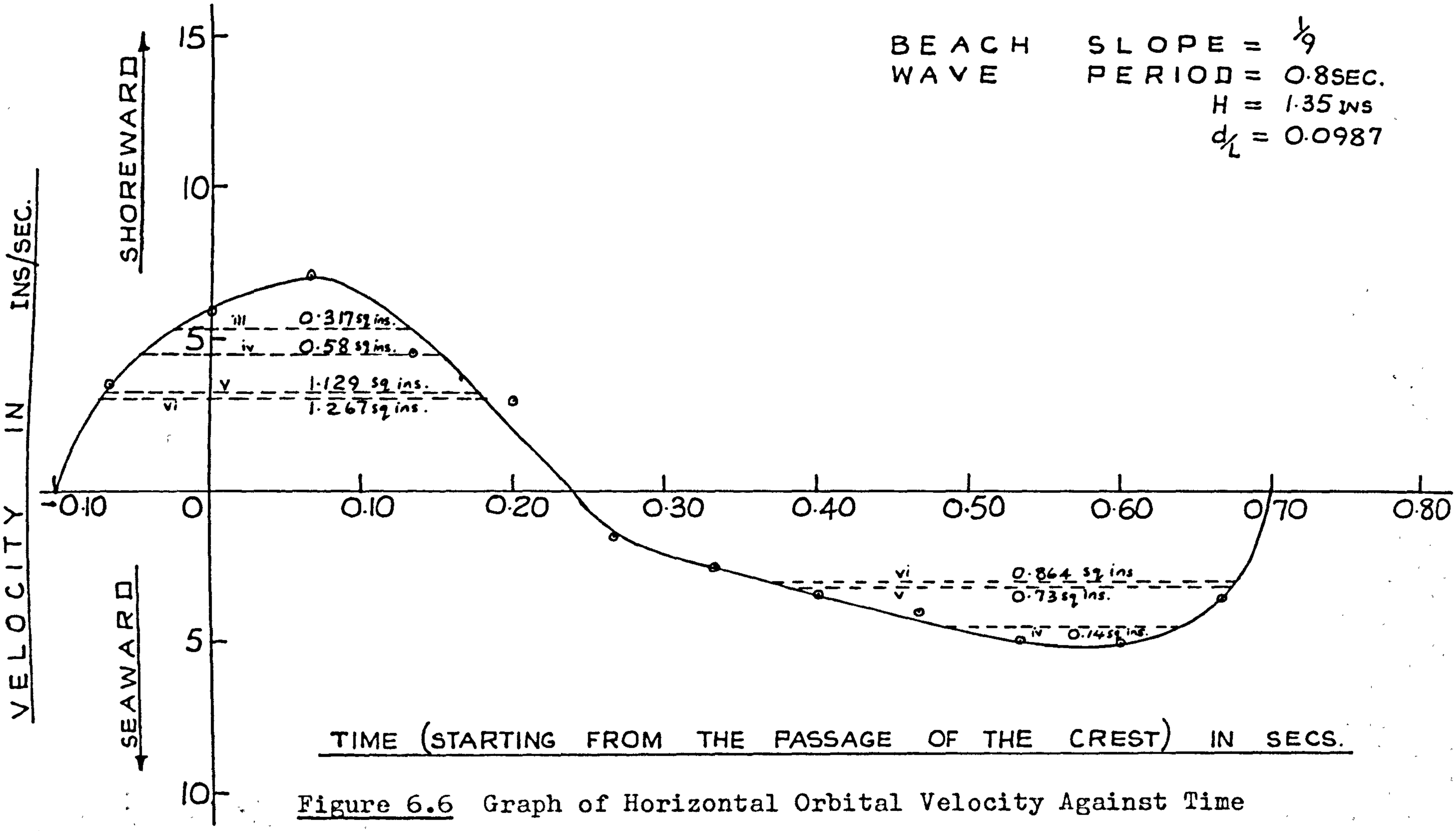

Figure 6.6 Graph of Horizontal Orbital Velocity Against Time

BEACH SLOPE = 1/9
WAVE PERIOD = 0·8 SEC.
H = 1·33 INS
d/L = 0·1047

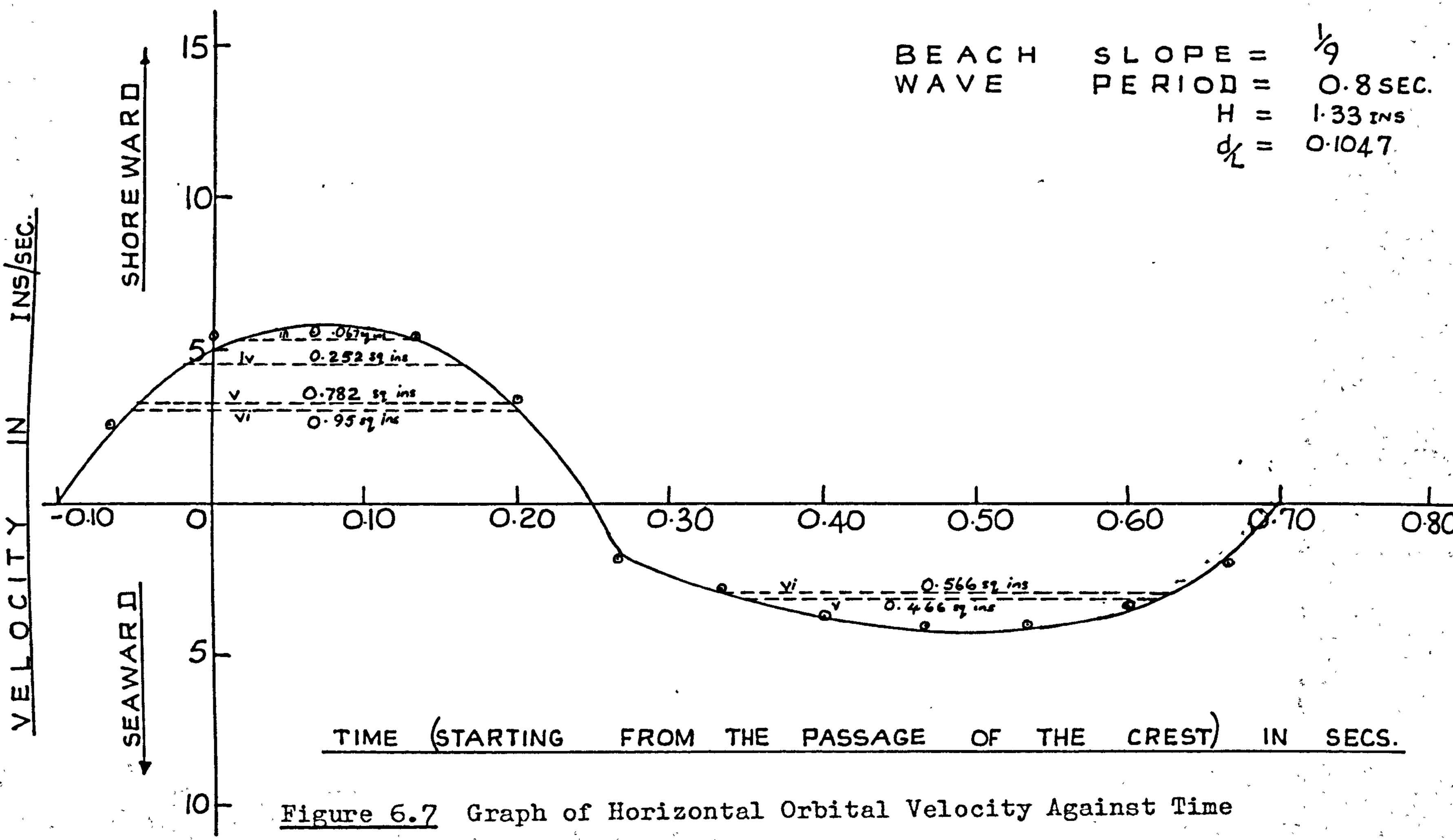

Figure 6.7 Graph of Horizontal Orbital Velocity Against Time

BEACH SLOPE = 1/9
WAVE PERIOD = 0·8SEC.
H = 1·32 INS
d/L = 0·1135

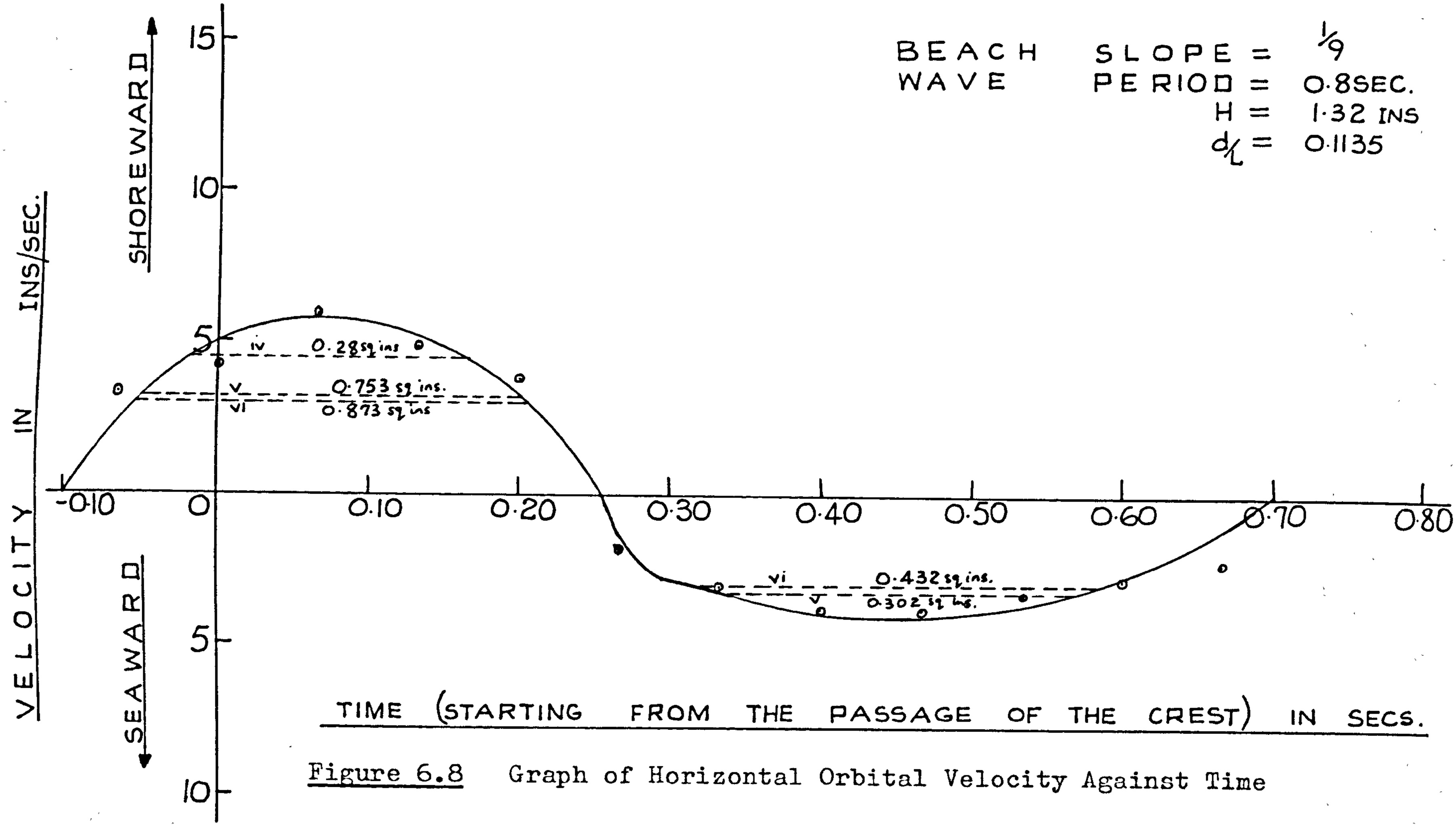

Figure 6.8 Graph of Horizontal Orbital Velocity Against Time

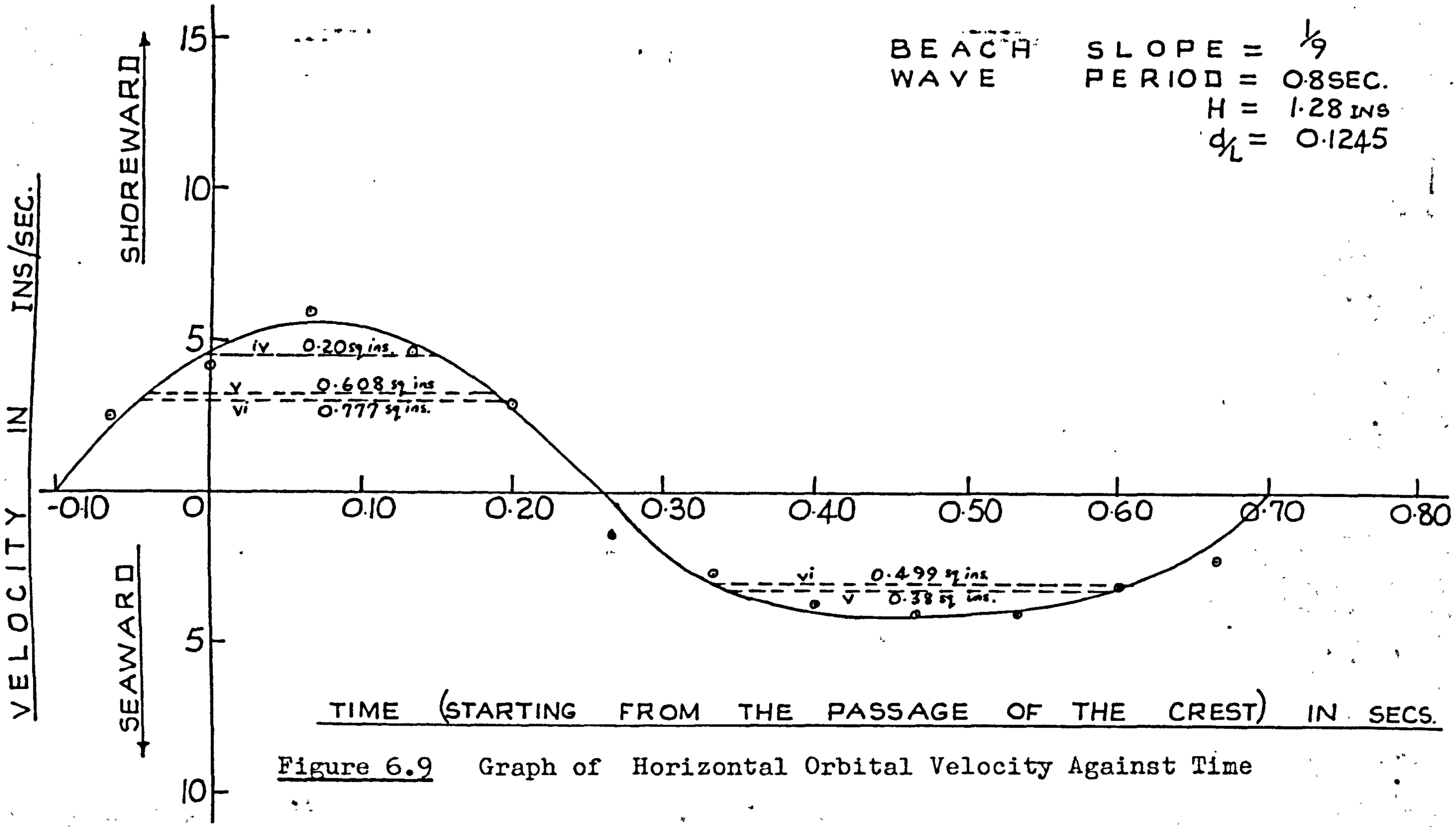

Figure 6.9 Graph of Horizontal Orbital Velocity Against Time

so on up to fig. 6.9. For the velocity fields in fig. 6.2, fig. 6.3 and fig. 6.4 Pumice (i) D = 4.4 cm. would not move at all as the magnitude of the maximum bed velocity in the respective places is less than the threshold velocity for the sediment. Fig. 6.2 indicates that all the other sediments (ii) to (vi) would move shoreward. It is important to note here that sediments v and vi which were moving offshore in the position indicated by fig. 6.1 are now moving onshore in the position indicated by fig. 6.2, thus the null points for sediments v and vi lie somewhere between the positions indicated by figures 6.1 and 6.2. It could therefore be said that shoreward of the null point for a particular sediment, the sediment will be moving seaward, on the other hand seaward of the null point for the sediment, it will be moving shoreward. Thus for the onshore-offshore movement, a sediment if able to move will always move in such a way as to be constantly heading towards its null point. As was commented previously sediment (i) will move shoreward while in the position indicated by fig. 6.1, and will not move at all while in the position indicated by fig. 6.2. All that is happening is that the null point for sediment (i) is not seaward of the breakpoint i.e. fig. 6.1, and so as the sediment is able to move in the position indicated

at the break-point, it moves shoreward as if its null point were still further ahead. However, the sediments on the shore are eventually swept back to the sea by the backwash, wind etc. and the attempt to seek the null point begins all over again. The null point for the velocity field in fig. 6.2 would apply to a Pumice D=0.029cm.

For the position indicated in figures 6.3, 6.4 and 6.5 all the sediments ii to vi move shoreward. And for positions indicated by figures 6.6 and 6.7 sediments i and ii will not move at all, while sediments (iii) to (vi) will move shoreward. As indicated by figures 6.8 and 6.9 sediments (i), (ii) and (iii) will not move at all in these positions, they have found themselves in a relatively weak velocity field, whereas sediments iv, v and vi will move shoreward.

6.4 Conclusions

It can be seen from the above discussion that a great deal of sorting is likely to take place in the breaker zone as a result of the asymmetry of the velocity fields in this region. The absolute values of the maximum bed velocities may be considered to be of extreme importance in determining whether there will

be sediment movement at all i.e. initial movement. Once the initial movement starts, further movement is influenced by the asymmetry of the velocity fields.

On this basis it may be concluded that there will always be a sediment type for which the net transport will be zero at any particular point, or conversely, for any position in shallow water there will always be, for any resulting velocity field at the bed, a size of sediment having that position as its null point. Shoreward of this null point the material is moving seaward and seaward of the point it is moving shoreward. Thus the largest materials moved, which have not reached their null point anywhere seaward of the break-point will continue to be transported shoreward. Each sediment if able to move is thus seeking its own null point. If the conditions of the wave, tide, wind etc. remain fairly constant for some time, then each sediment might eventually reach its null point, and the sediment sizes would then be in oscillating equilibrium with the water motion at every point, and no net transport would occur. This is the condition usually referred to as the equilibrium condition. Thus the tendency for the sediments to maintain their null points governs the attainment

of the equilibrium profile of the shore, such a condition would however be only transitory, as conditions in nature rarely remain stable for very long. Although the variability of wave action, coupled with tidal variations in water level, and tidal and wind generated currents, combine to obscure the single effect of asymmetry, nevertheless the established phenomena of sediment sorting provides the necessary evidence of the differential forces at work.

From the work discussed in the last chapter on the effect of eliminating the backwash of the wave on the resulting velocity fields, it was found that the velocity asymmetry increases when the backwash of the wave is eliminated, although the absolute values of the magnitude of the water particle velocity decreases. It may thus be inferred that some sediments which would move when backwash is present, might not move at all when there is no backwash. It also means that all sediments, large and small, which are able to move in the velocity fields created when there is no backwash would be subject to very rapid sorting, and those nearer the shore would in the absence of any return flow, move continuously shoreward. Sediments moved to the shoreline would be able to remain there

until moved away by forces other than the direct effect of the wave. Eliminating the backwash would in nature correspond to highly permeable beaches, so offering an explanation for the exceptional stability of such beaches, and for the fact that the material is always packed closely against the shore. It may be concluded that elimination of the backwash would help to stabilize the coastline, whereas the presence of strong backwash for instance at the base of sea walls is likely to contribute to the erosion of the beach. The evidence in the previous chapter also explains why beaches flatten in order to achieve stability, since the velocity patterns for flat beaches resemble those which occur in the absence of back wash.

This onshore-offshore sediment movement due to wave asymmetry can therefore be seen to be quite important. Whether or not material once eroded from the shore by storm action will eventually return to the beach is determined by the mechanics of this type of movement, providing the material has not been carried seaward in suspension into rapidly deepening water.

On this picture one must eventually superimpose the effects produced by ripples. The variation in

shear stress over ripples and the convergent-divergent nature of the flow has not yet been evaluated for either unidirectional or oscillating flow conditions.

CHAPTER 7

FLOW IN THE ONSHORE ZONE

7.1 Introduction

As it was established from the work reported in previous chapters that the backwash had a remarkable effect on the wave and velocity asymmetries, it was then considered that a connection between the onshore and offshore asymmetries is very likely to exist. Only a preliminary examination of this possibility could be attempted in the time available.

The effect of the phase-difference of uprush and backwash on the motion at the breaker position was therefore investigated. The phase difference was defined by Kemp[20,21] as the ratio of the time of uprush to the wave period. In the present work the incident wave characteristics were systematically varied in order to obtain different breaker types, and the work was carried out on a beach slope of $\frac{1}{6}$.

A review of previous work on the phase difference of uprush and backwash of the wave is given below.

7.2 Review of Previous Work.

Kemp[20,21] examined the importance of the phase difference in relation to the flow conditions and the beach profile characteristics. He remarked

that although increase in wave height produced an increase in the distance from the breakpoint to limit of uprush, he found that initially the time of uprush remained constant at a value of approximately 0.3T even though the distance from the break-point to limit of uprush increased. He observed that the behaviour of the wave and the beach profile in the initial zone of constant phase-difference resembled the behaviour of a simple pendulum. An increase in amplitude of the incident wave produced an increase in the velocity of the wave surge, the beach crest retreated but the time of the surge remained constant. Kemp referred to the condition as the "surge condition".

Kemp observed that as the distance from the break-point to limit of uprush increased a critical point was reached at which the phase difference ceased to be constant, and thereafter the phase difference increased with increase in wave height, consequently the time available for backwash before the next wave broke was reduced, thus the backwash was not completed before the next wave plunged. Kemp referred to this situation as the transition condition, characterised by some interchange between the water in the zone seaward of the breakers and the near shore zone. Kemp remarked that the instability of the flow pattern

under transition conditions resulted in lateral circulation which could explain the origin of beach cusps.

As the time of uprush increased, Kemp noted that the partly oscillatory nature of the onwash and backwash with limited interchange of water through the breakers gradually gave way to continuous flow into and out of the breakers, the continuous flow conditions becoming fully developed when the time of uprush was equal to the wave period. The bar profile then achieved full development. The flow conditions when the time of uprush was greater than the wave period were referred to as the "surf condition". He commented that cusps did not occur under surge or surf conditions.

In a very recent study Plinston[40] remarked that surging conditions finally broke down at a phase difference of about 0.7 which was in the transition range described by Kemp. Plinston commented that when the breakers were surging, the asymmetry of the motion just offshore of the break-point defined as the ratio of the duration of forward motion to the wave period was the same as the phase difference; and in an attempt to reconcile the work with the solitary wave or Stokes' theory he concluded that

the phase difference could not be predicted satisfactorily by either the solitary wave or Stokes' theories.

7.3 Experimental Study of the Effect of the Phase Difference of Uprush and Backwash on the Wave Motion at the Break-point.

The duration of the shoreward motion and the seaward motion were made by velocity studies using the methods already described. The other measurements taken were the wave height at the breaker position, the time of uprush, and the wave height in the horizontal section of the channel in order to obtain the deep water wave height.

The graph of the phase difference $\frac{t_1}{T}$ against $\frac{H_b}{T}$ is shown in Fig. 7.1. The graph showed a discontinuity between the surging and the plunging breakers. The graph for the surging section was found to be non-linear whereas the plunging section was found to show a linear relationship. Surging was found to break down at a phase difference of about 0.63 and $\frac{H_b}{T}$ = 0.83 ins/sec. Working on a mobile beach D.T. Plinston[40] obtained corresponding values of 0.70 and 1.18 respectively.

Figure 7.2 shows the graph of the phase difference $\frac{t_1}{T}$ against $\frac{H_o}{L_o}$. Again the graph showed a discontinuity between the surging and plunging breakers at a phase difference of about 0.63 and $\frac{H_o}{L_o}$ = 0.0108. The graph

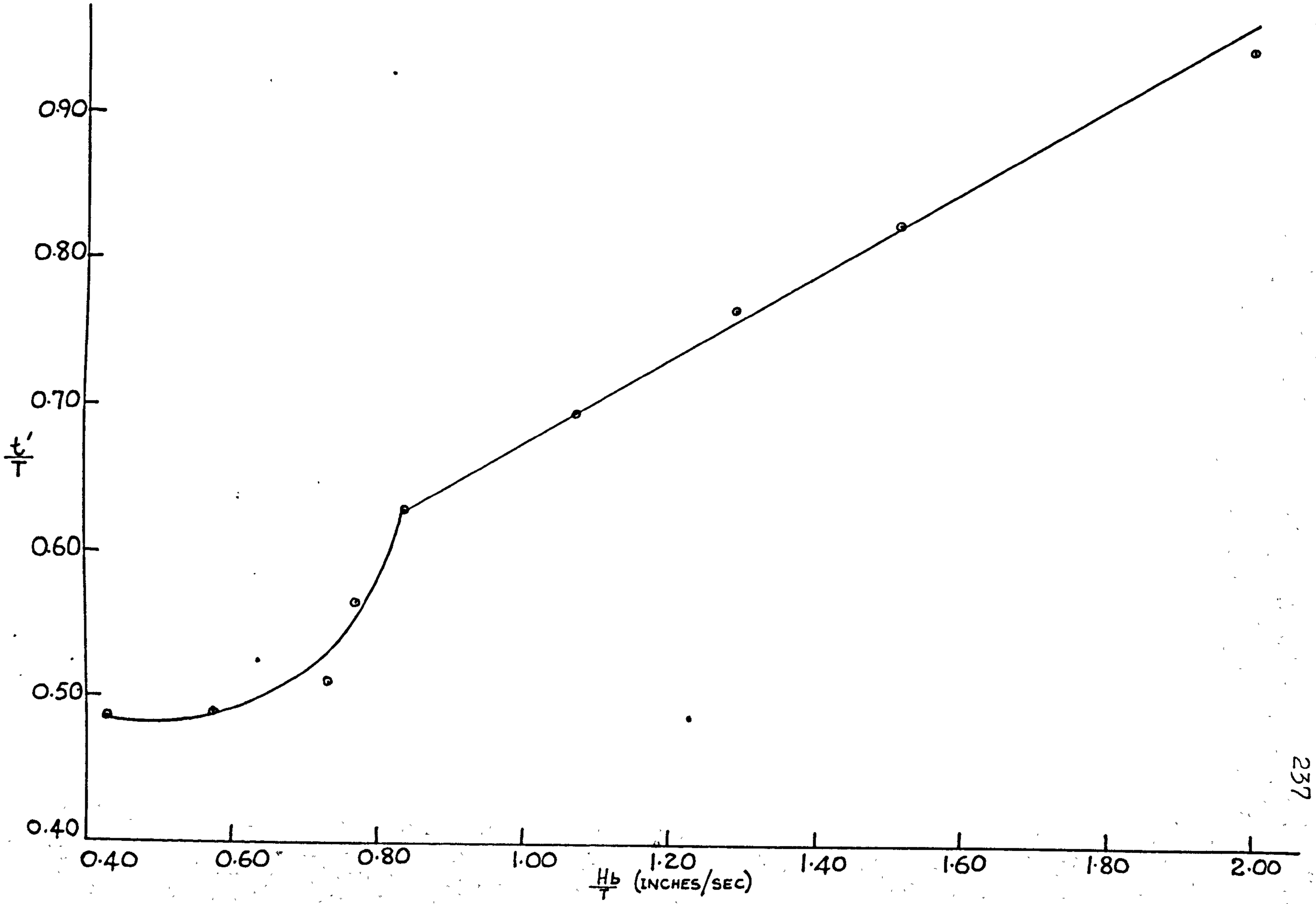

Fig. 7.1 Graph of Phase Difference of Uprush and Backwash of the wave $\frac{t'}{T}$ against $\frac{Hb}{T}$

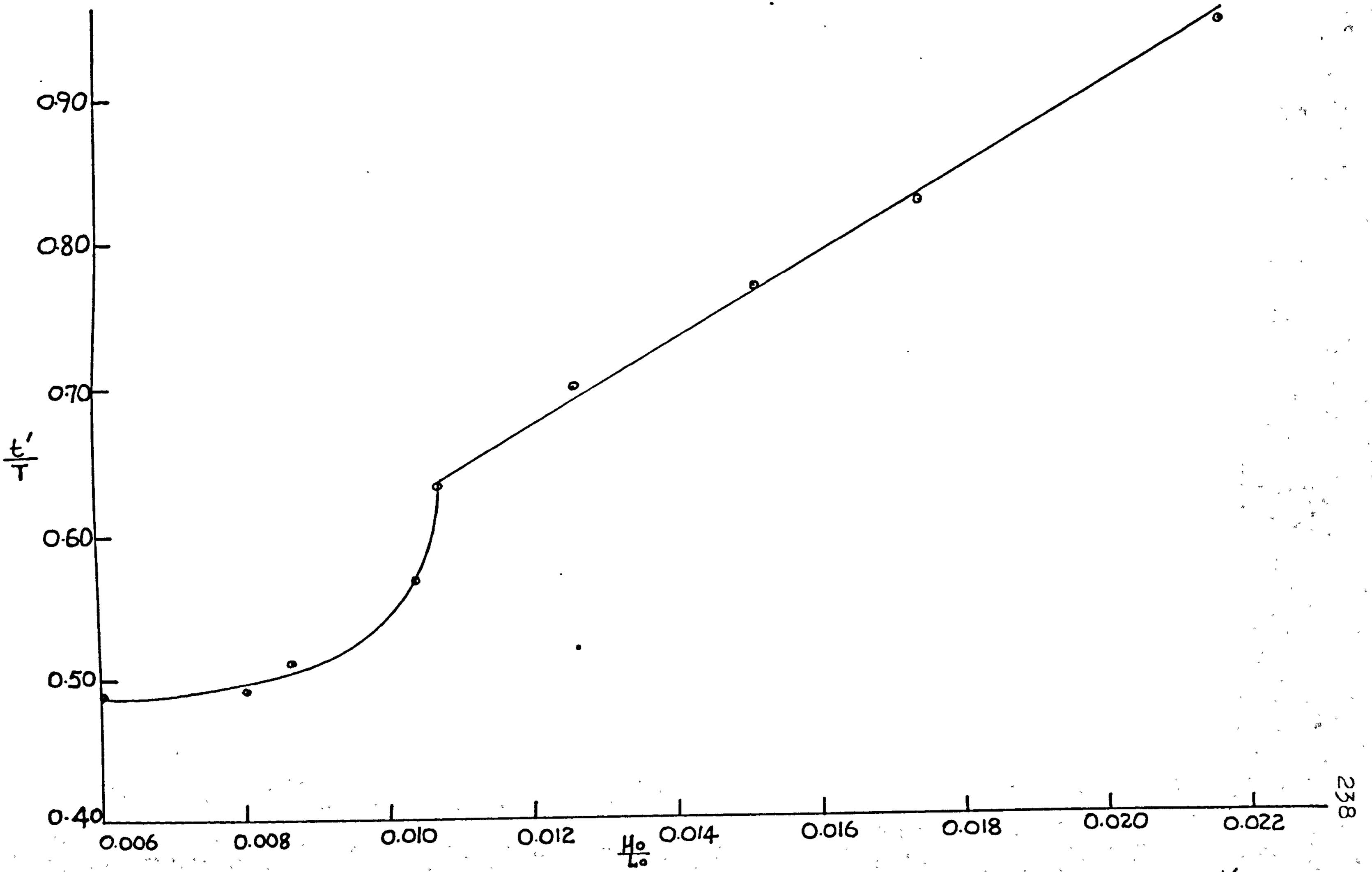

Fig. 7.2 Graph of Phase Difference of Uprush and Backwash of the wave $\frac{t'}{T}$ against $\frac{H_0}{L_0}$

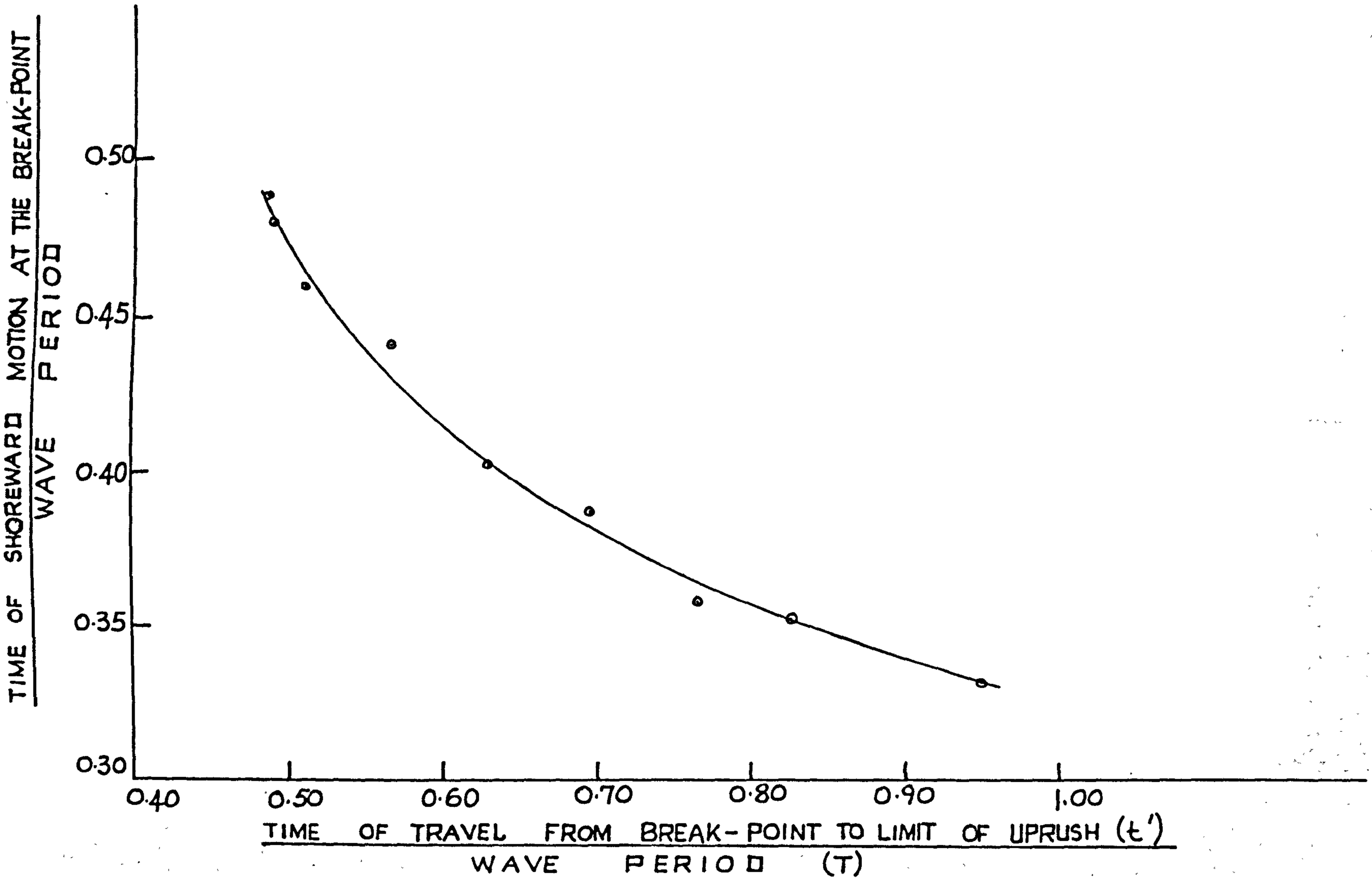

Fig. 7.3 Graph of Time of Shoreward Motion at the Break-point against the Phase Difference of Uprushh and Backwash of the Wave

for the plunging section was again found to be linear.

The graph of the ratio of time of shoreward motion at the wave break-point to the wave period against the phase difference see fig. 7.3 showed a continuous curve without any discontinuity characterising figs. 7.1 and 7.2. The graph gave an indication of a possible connection between the motion at the wave breaker position and the phase difference of uprush and backwash of the wave.

In Fig. 7.3 the duration of the shoreward motion at the wave break-point was found to be equal to the time of travel from the break-point to the limit of uprush at a phase difference value of about 0.487, after which, as the phase difference increased, the duration of the shoreward motion at the wave break-point was found to decrease.

7.4 Conclusions

It is significant that the same type of discontinuity in the relationship between phase difference $\left(\frac{t_1}{T}\right)$ and wave characteristics $\left(\frac{H_b}{T}\right)$ was observed in the present series of experiments using a fixed smooth bed, as was observed by Plinston using a granular beach. The present results show that the simple surging conditions break down at a much lower value of wave height than occurred on a permeable beach. The smooth beach clearly results in a longer run up, and the backwash gets out of step sooner with the oscillatory motion of the next wave. This result emphasises the care which must be taken in translating the results from smooth impermeable slopes, to the case of a natural beach. Bearing in mind that the impermeable plane slope does not adjust its angle of inclination with change in wave characteristics the results can only be comparable for one given value of the natural beach slope.

In examining Figure 7.3 it must be remembered that the "time of shoreward motion" relates to motion close to the bed. The graph implies that for a given period T, the steep waves which produce large values of $\frac{t'}{T}$, have a short duration of shoreward motion at the breakers. This can be clearly observed in nature, for the water

in the uprush zone but close to the breakers can be seen to be moving seaward before the uprush of the wave has been completed.

The lack of discontinuity in the curve of Figure 7.3 suggests that both the oscillatory motion just seaward of the breakers, and the phase difference of uprush to wave period, are interrelated, but the basis of this relationship could only be established from an extension to the present study.

CHAPTER 8

GENERAL SUMMARY AND SUGGESTIONS FOR FURTHER RESEARCH

Note

The general summaries of the results on the various aspects of the work covered are given below. As any study is of necessity bound to be limited in scope, some suggestions for further research are also given.

General Summary

The investigation was designed to identify and correlate a number of possible definitions of wave shape and wave velocity asymmetry, both in the presence and absence of the effect of backwash. It was further intended to provide a basis for the description of the onshore-offshore movement of sediment.

The wave asymmetry defined in all of the three ways varied systematically and could be correlated with one another. In each case the asymmetry increased as the wave advanced into shallower water, reaching a maximum at the wave break-point. The most rapid change in wave asymmetry took place in the region $\frac{d}{L} < 0.15$.

The Cnoidal wave theory was found to be adequate for predicting wave vertical asymmetry. However, whereas the cnoidal theory indicates a non linear curve throughout, the experimental curves of the wave vertical asymmetry against $\frac{d}{L}$ became linear for slopes $< \frac{1}{12}$. The study of the effect of the backwash indicated that this linearity could be attributed to the backwash and to flat beach slopes.

The results of the experiments on the wave slope asymmetry for the beach slopes of $\frac{1}{4}$, $\frac{1}{6}$, $\frac{1}{9}$ showed that the wave slope asymmetry ceases at a value of $\frac{d}{L} = 0.26$. The theory of Biesel[5] (1951) predicted a value of 0.27. This would appear to be a valuable verification of a theory which had not previously been checked experimentally.

The wave horizontal asymmetry (both HA and HA') and the wave slope asymmetry increase as the beach slope gets steeper, whereas the converse is true for wave vertical asymmetry when the wave is in very shallow water.

A quantitative correlation was found to exist between the wave slope asymmetry, wave horizontal asymmetry and the wave vertical asymmetry; as well as between the wave asymmetry and the velocity asymmetry. Expressions for the wave horizontal asymmetry and the horizontal velocity (magnitude)

asymmetry were derived based on existing wave theories.

The elimination of the backwash of the wave resulted in the wave breaking in shallower water. Clearly the presence of the backwash induces early breaking of the wave, although its presence is not a necessary condition for breaking.

The horizontal velocities were found to increase in shallower water, with the greatest horizontal velocities occuring at the wave breaker position. It was found that the maximum horizontal onshore velocity did not occur directly under the wave, but at a time 0.09T seconds after the passage of the crest. In terms of the absolute values of the horizontal velocities, the values on the slope of $\frac{1}{9}$ were higher than those on the flatter slope of $\frac{1}{18}$ especially in the neighbourhood of the breakers. On the other hand it was found that the values of the horizontal velocity (magnitude) asymmetry were higher on the flatter slope. Also, the graph of the horizontal velocity (time) asymmetry against $\frac{d}{L}$ showed that the shoreward motion occupies a longer time on the flatter slope.

When the backwash was eliminated the absolute values of the magnitude of the velocities decreased but the

horizontal velocity (magnitude) asymmetry was found to be higher than when the backwash was present. Thus the velocity patterns for flat beaches resemble those which occur in the absence of backwash, which explains why beaches flatten in order to achieve stability.

In drawing conclusions from the study of the velocity fields associated with asymmetrical waves on varying beach slopes it is important to note that Miller and Zeigler[38] observed three broad classes of wave asymmetry on a beach of only one slope. It is clear, as they suggest, that in nature in addition to the importance of beach slope, breaker shapes are affected by the interaction of different wave trains, and by the timing and magnitude of the backwash. It seems probable that the observations by Inman and Nasu[14] that higher orbital velocities are associated with wave shape asymmetry must be considered in relation to the fact that their measurements were also made in nature, and that more than one wave train was likely to be present.

A consideration of the mechanics of sediment movement by the use of the velocity-time curve showed that a great deal of sorting in the breaker zone could be due to the asymmetry of the velocity fields. The absolute values of the maximum bed velocities are

undoubtedly of importance in determining whether there will be sediment movement at all. However, once the initial movement starts, further movement is governed by the asymmetry of the velocity fields. On this basis for any position in shallow water, there will be a size of sediment having that position as its null point, under given wave conditions. Shoreward of the null point the material will tend to move seaward, and seaward of the point, shoreward. Large materials whose null point is not seaward of the break-point will be transported to the shoreline. If the conditions of the wave, wind and tide etc. remain fairly constant, then each sediment might in the long run reach its null point. The sediment sizes would then be in oscillating equilibrium with the water motion at every point, and practically no net transport would occur. This is the condition usually referred to as the equilibrium condition. Thus the tendency for the sediments to maintain their null points governs the attainment of the equilibrium profile of the shore, a condition that is however only transitory as conditions rarely remain stable for very long in nature.

The graph of the phase-difference $\frac{t_1}{T}$ against $\frac{H_b}{T}$ showed a discontinuity between surging and plunging breakers, surging was found to break down at a phase

difference of about 0.63 and $\frac{H_b}{T}$ = 0.83 ins/sec. Working on a mobile beach D.T. Plinston[40] obtained corresponding values of 0.70 and 1.18 respectively. It is quite significant that the same type of discontinuity in the relationship between phase-difference $\frac{t_1}{T}$ and wave characteristics $\frac{H_b}{T}$ was observed in the present series of experiments using a fixed smooth bed, as was observed by Plinston using a granular beach.

The lack of discontinuity in the curve of Figure 7.3 suggests that both the oscillatory motion just seaward of the breakers, and the phase difference of uprush to wave period, are inter-related, but the basis of this relationship could only be established from an extension to the present study.

Suggestions for further research

The present work has concentrated on the evaluation of the geometrical asymmetry and velocity asymmetry associated with waves acting on plane impermeable beaches. The elimination of backwash has been used as a pointer to the effect of permeability on these characteristics. Inferences have been made from the velocity studies of the behaviour of sediments under asymmetrical waves. The logical extension of the work

would be to examine wave asymmetry in a mobile bed model using grains which would move primarily as bed load.

APPENDIX 1

Symbols

a	constant, also used as wave amplitude (defined in the text in each case.
b	constant
c	constant
C_L	coefficient of lift
C_D	coefficient of drag
C	wave velocity
A_v	wave vertical asymmetry
d	still water depth, also used as constant (defined in the text in each case)
δ	thickness of the boundary layer
D	diameter of sediment
K(k)	complete elliptic integral of the first kind
E(k)	complete elliptic integral of the second kind
k	modulus of elliptic integral
sn, cn, dn, tn, -	elliptic functions
$\bar{u}$	incomplete elliptic integral of the first kind
F_D	drag force
F_L	lift force
L	wave length
H	wave height (trough to crest)

S.W.L.	still water level
H_A and $H_{A'}$	wave horizontal asymmetry
m	$\frac{2\pi}{L}$
g	acceleration due to gravity
r	semi amplitude of oscillation
R	Reynold number, also used as rational function (defined in the text in each case)
s	wave slope asymmetry
t	time variable
t_1	time of travel from wave breakpoint to limit of uprush
T	wave period
u	horizontal component of water particle velocity
v	vertical component of water particle velocity
$\bar{U}$	velocity of mass transport
y_c	vertical distance from bottom to wave crest
y_t	vertical distance from bottom to wave trough
y_s	vertical distance from ocean bottom to wave surface
V_{HMA}	horizontal velocity (magnitude) asymmetry
y	vertical coordinate
x	horizontal coordinate, also used simply as variable (defined in the text in each case)
W	fall velocity

ϕ	velocity potential
α	variable
α_1 α_2 α_3	constant
ω	angular frequency = $\frac{2\pi}{T}$
ε	height of element of roughness
ν	kinematic viscosity of fluid
γ	slope of the bed
ρ_f	density of fluid
ρ_s	density of sediment
ρ_1	ratio of apparent density = $\frac{\rho_s - \rho_f}{\rho_f}$
$\varnothing$	variable
Suffix o	deep water conditions
" c	(other than y_c) critical value
" b	conditions at the break-point
" m	maximum value

APPENDIX 2

GLOSSARY

Break-point - The point in space where the wave breaks.

Backwash - The seaward return of the water following the uprush of the waves.

Limit of Uprush - The furthest point from the breakers which is reached by the uprush.

Phase difference - The ratio of uprush time to wave period.

Wave vertical asymmetry - $\frac{\text{Vertical dist. from crest to S.W.L.}}{\text{Total wave height.}}$

Wave horizontal asymmetry HA - $\frac{\text{Horiz.dist. from crest to front face at S.W.L.}}{\text{Horiz.dist. from crest to back face at S.W.L.}}$

Wave horizontal asymmetry HA′ - $\frac{\text{Horiz.dist. from crest to preceding wave trough.}}{\text{Horiz.dist. from crest to following wave trough.}}$

Wave slope asymmetry (radians) - $\frac{1}{2}\left\{\begin{matrix}(\text{Front face slope at S.W.L.} + \\ \text{Backface slope at S.W.L.})\end{matrix}\right\}$

Horizontal velocity (time) asymmetry - $\frac{\text{Time for shorward motion}}{\text{Time for seaward motion}}$

Horizontal velocity (magnitude) asymmetry - $\frac{\text{Max.horiz.shoreward velocity}}{\text{Max.horiz.seaward velocity}}$

APPENDIX 3

Notes on elliptic integrals in relation to the Cnoidal Wave Theory

Every integral of the type $\int R\left(x, \sqrt[n]{ax+b}\right) dx$ or $\int R\left(x, \sqrt{ax^2+bx+c}\right) dx$, where R is a rational function i.e. quotient of two polynomials of the arguments indicated, can be evaluated in terms of the usual elementary functions (algebraic, trigonometric, inverse trigonometric, exponential and logarithmic)

An important class of integrals which require new functions for their evaluation (Burington and Torrance [7]) are integrals of the type

$$\int R\left(x, \sqrt{ax^3+bx^2+cx+d}\right) dx \qquad \cdots (A.3.1)$$

and

$$\int R\left(x, \sqrt{ax^4+bx^3+cx^2+dx+e}\right) dx \qquad \cdots (A.3.2)$$

The evaluation of (A.3.1) and (A.3.2) can be reduced to the evaluation of the following types of integrals, known as legendre's normal forms

$$\bar{U} \equiv \int_0^x \frac{dz}{\sqrt{(1-z^2)(1-k^2z^2)}} \qquad \cdots (A.3.3)$$

$$\int_0^x \sqrt{\frac{1-k^2z^2}{1-z^2}}\, dz \qquad \ldots(A.3.4)$$

$$\int_0^x \frac{dz}{(z^2-a)\sqrt{(1-z^2)(1-k^2z^2)}} \qquad \ldots(A.3.5)$$

These integrals are called incomplete elliptic integrals of the first, second, and third kind respectively, and k is such that $0<k<1$.

More generally, any integral of the type (A.3.2) in which $ax^4 + bx^3 + cx^2 + dx + e = 0$ has no multiple roots, is called an elliptic integral. The variables x and Z may be either complex or real. Upon substituting $Z = \sin\alpha$ in the integrals (A.3.3) (A.3.4.) and (A.3.5) we obtain, respectively,

$$F(k,\phi) = \int_{\alpha=0}^{\alpha=\phi} \frac{d\alpha}{\sqrt{1-k^2\sin^2\alpha}} \qquad \ldots(A.3.6)$$

$$E(k,\phi) = \int_{\alpha=0}^{\alpha=\phi} \sqrt{(1-k^2\sin^2\alpha)}\, d\alpha \qquad \ldots(A.3.7.)$$

and

$$\int_{\alpha=0}^{\alpha=\phi} \frac{d\alpha}{(\sin^2\alpha-a)\sqrt{1-k^2\sin^2\alpha}} \qquad \ldots(A.3.8)$$

If $\phi = \pi/2$ in integrals (A.3.6) and (A.3.7) the integral (A.3.6) is called the complete elliptic integral of the first kind and is denoted by K(k) or simply as K and integral (A.3.7) is called the complete elliptic integral of the second kind and is denoted by E(k) or simply E. This integral arises in the determination of the length of arc of an ellipse and supplies a reason for use of the term elliptic integral.

The Elliptic Functions

Let the integral in (A.3.6) be denoted by q, then the relation

$$q = F(k, \phi) \qquad \cdots (A.3.9)$$

defines q as a function of k and ϕ. The number ϕ is known as the amplitude of the integral q, and k is the modulus of q. Suppose that k is fixed. Then (A.3.9) defines ϕ as a function of q which we denote by

$$\phi = am\, q$$

Since $x = \sin\phi$ and q is equal to the integral $\bar{u}$ given in (A.3.3)

$$x = Sin\,(am\ \bar{u})$$

or more briefly

$$x = Sn\ \bar{u} \qquad \cdots (A.3.10)$$

The expressions $\sqrt{1-x^2}$ and $\sqrt{1-k^2x^2}$ define the functions cn $\bar{u}$ and dn $\bar{u}$

$$\sqrt{1-Sn^2\bar{u}} = \sqrt{1-x^2} = \cos(am\ \bar{u}) = Cn\,\bar{u} \qquad \cdots (A.3.11)$$

$$\sqrt{1-k^2sn^2\bar{u}} = \sqrt{1-k^2x^2} = dn\,\bar{u} \qquad \cdots (A.3.12)$$

$$\frac{x}{\sqrt{1-x^2}} = \frac{Sn\,\bar{u}}{Cn\,\bar{u}} = tn\,\bar{u} \qquad \cdots (A.3.13)$$

The elliptic functions sn $\bar{u}$, cn $\bar{u}$, dn $\bar{u}$ have , many important properties analogous to those of trigonometric functions.

It is also possible to define inverse elliptic functions; for example, if $x = sn\,\bar{u}$, then $\bar{u} = Sn^{-1}x$. It is worth noting that $\bar{u}$ depends on k. To emphasize this dependence we sometimes write $\bar{u} = Sn^{-1}(x,k)$.

To complete the definitions of these functions we have

sn 0 = 0, cn 0 = 1, dn 0 = 1 tn 0 = 0

and also

$$sn(-\bar{u}) = -sn(\bar{u}) \quad , \qquad cn(-\bar{u}) = cn(\bar{u})$$

$$dn(-\bar{u}) = dn(\bar{u}) \quad , \qquad tn(-\bar{u}) = -tn(\bar{u})$$

The Periods of the Elliptic Functions

The functions sn $\bar{u}$, cn $\bar{u}$, dn $\bar{u}$ are doubly periodic; sn $\bar{u}$ having the periods 4K and 2jk', cn $\bar{u}$ having the periods 2K and 4jk' where

K' is known as the associated elliptic integral of the first kind and defined by

$$K' = \int_0^{\pi/2} \frac{d\alpha}{\sqrt{1-(k')^2 \sin^2\alpha}}$$

and $k' = \sqrt{1-k^2}$

k' is the modulus complementary to the modulus k.

Beach Slope = $\frac{1}{4}$, Wave Period T = 0.8 sec. H_o = 1.45 ins.

WATER DEPTH d INCHES	EXP. WAVE LENGTH L INCHES	THEOR. WAVE LENGTH (CNOIDAL WAVE) INS.	EXP. $\frac{d}{L}$	THEOR. $\frac{d}{L}$ (CNOIDAL WAVE)	$\frac{H}{d}$	$\frac{HL^2}{d^3}$	WAVE — ASYMMETRY					
							WAVE VERT ASYM.		WAVE HORIZ. ASYM. HA	WAVE HORIZ. ASYM. HA'	WAVE SLOPE ASYM.	
							EXP	THEOR			EXP RADIANS	THEOR. BIESEL(1951)
9.50	36.5	-	0.2605	-	0.146	2.16	0.517	0.510	0.980	0.950	.000120	.000095
8.25	35.7	-	0.2310	-	0.152	2.84	0.540	0.520	0.980	0.927	.00070	.00047
7.00	33.5	-	0.2090	-	0.169	3.86	0.520	0.525	0.940	0.927	.00131	.00105
5.75	32.3	-	0.1783	-	0.233	7.35	0.523	0.540	0.882	0.840	.0030	.00252
5.12	31.2	31.9	0.1642	0.1606	0.274	10.20	0.55	0.550	0.880	0.840	.0051	.00382
4.50	30.0	30.6	0.1500	0.1470	0.264	11.76	0.555	0.556	0.790	0.780	.0074	.00582
3.87	29.2	30.2	0.1325	0.1285	0.298	17.10	0.560	0.575	0.680	0.700	.0105	.0095
3.25	28.0	29.4	0.1162	0.1108	0.385	29.0	0.580	0.620	0.512	0.519	.0205	.0158
2.62	26.7	28.8	0.0980	0.0910	0.546	56.80	0.615	0.69	0.417	0.360	.0435	.0303
2.00	24.00	-	0.0833	-	0.80	114.4	0.62	0.76	0.274	0.308	.083	.0618

Beach Slope = 1/6 Wave Period T = 0.8 sec. H_o = 1.45 ins.

WATER DEPTH d INCHES	EXP. WAVE LENGTH L INCHES	THEOR. WAVE LENGTH (CNOIDAL WAVE) INS.	EXP. $\frac{d}{L}$	THEOR. $\frac{d}{L}$ (CNOIDAL WAVE)	$\frac{H}{d}$	$\frac{HL^2}{d^3}$	WAVE — ASYMMETRY.					
							WAVE VERT. ASYM.		WAVE HORIZ. ASYM. HA	WAVE HORIZ. ASYM. HA'	WAVE SLOPE ASYM.	
							EXP.	THEOR.			EXP RADIANS	THEOR. BIESEL(1951)
9.50	36.5	-	0.2605	-	0.121	1.79	0.496	0.505	0.990	0.970	0.00011	-.000062
8.50	35.0	-	0.2430	-	0.149	2.52	0.513	0.515	0.980	0.950	0.0003	-.000199
7.50	34.7	-	0.2165	-	0.166	3.55	0.546	0.525	0.980	0.920	0.0007	-.000527
6.50	33.1	-	0.1965	-	0.169	4.38	0.538	0.530	0.946	0.874	0.00122	-.001003
5.50	32.0	-	0.1720	-	0.23	7.78	0.535	0.540	0.883	0.802	0.00252	-.001985
4.50	29.0	30.7	0.1550	0.1468	0.253	10.5	0.593	0.550	0.861	0.706	0.0047	-.00366
3.83	28.8	30.1	0.1330	0.1280	0.295	17.0	0.615	0.575	0.734	0.702	0.0080	-.00642
3.17	26.9	28.8	0.1178	0.1100	0.413	30.0	0.595	0.625	0.643	0.600	0.0131	-.0110
2.50	25.2	27.6	0.0992	0.0905	0.53	54.0	0.627	0.670	0.480	0.440	0.0254	-.0218
1.83	22.0	25.0	0.832	0.0732	0.737	110.0	0.634	0.750	0.390	0.340	0.062	-.0492
1.50	17.5	-	0.0860	-	1.00	136.0	0.707	0.79	0.104	0.154	0.088	-.0704

Beach Slope = 1/9, Wave Period T = 0.8 sec. Ho = 1.45 ins.

WATER DEPTH d INCHES	EXP. WAVE LENGTH L INCHES	THEOR. WAVE LENGTH (CNOIDAL WAVE) INS.	EXP. $\frac{d}{L}$	THEOR. $\frac{d}{L}$ (CNOIDAL WAVE)	$\frac{H}{d}$	$\frac{HL^2}{d^3}$	WAVE — ASYMMETRY.					
							WAVE VERT. ASYM.		WAVE HORIZ. ASYM. HA	WAVE HORIZ. ASYM. HA'	WAVE SLOPE ASYM.	
							EXP.	THEOR.			EXP RADIANS	THEOR. BIESEL(1951)
9.50	36.5	-	0.2605	-	0.134	1.977	0.540	0.510	1.000	1.000	.00010	.0000422
8.61	36.2	-	0.2380	-	0.153	2.70	0.548	0.520	0.980	0.961	.000210	.0001527
7.72	35.0	-	0.2205	-	0.164	3.37	0.545	0.525	0.990	0.932	.00050	.000306
6.84	33.5	-	0.2042	-	0.191	4.57	0.532	0.530	0.960	0.944	.00072	.000535
5.95	32.0	-	0.1862	-	0.208	6.00	0.582	0.540	0.940	0.900	.0012	.000935
5.06	31.0	32.0	0.1632	0.1580	0.251	9.43	0.584	0.550	0.891	0.900	.0024	.001745
4.17	29.0	30.5	0.1438	0.1368	0.300	14.52	0.594	0.570	0.860	0.760	.0045	.003215
3.28	27.9	29.0	0.1178	0.1132	0.400	28.9	0.632	0.620	0.737	0.620	.00805	.006830
2.40	25.2	27.0	0.0952	0.0888	0.558	61.6	0.660	0.700	0.465	0.467	.0205	.01651
1.50	17.5	-	0.0857	-	0.91	124.0	0.686	0.780	0.188	0.216	.0520	.0478
1.40	17.1	-	0.0819	-	1.02	152.0	0.726	0.810	0.130	0.214	.0600	.0571

Beach Slope = 1/12, Wave Period T = 0.8 sec. H_0 = 1.45 ins.

WATER DEPTH d INCHES	EXP. WAVE LENGTH L INCHES	THEOR. WAVE LENGTH (CNOIDAL WAVE) INS.	EXP. $\frac{d}{L}$	THEOR. $\frac{d}{L}$ (CNOIDAL WAVE)	$\frac{H}{d}$	$\frac{HL^2}{d^3}$	WAVE — ASYMMETRY.					
							WAVE VERT. ASYM.		WAVE HORIZ. ASYM. HA	WAVE HORIZ. ASYM. HA'	WAVE SLOPE ASYM.	
							EXP.	THEOR.			EXP RADIANS	THEOR. BIESEL(1951)
3.70	28.2	29.8	0.1315	0.1242	0.343	19.8	0.602	0.60	0.910	0.792	$\bar{0}$.00349	$\bar{0}$.00347
3.50	28.0	29.7	0.1250	0.1180	0.380	24.3	0.605	0.61	0.860	0.658	$\bar{0}$.0055	$\bar{0}$.00418
3.30	27.8	29.4	0.1188	0.1123	0.412	29.2	0.608	0.62	0.795	0.654	$\bar{0}$.00610	$\bar{0}$.00503
3.00	26.9	29.0	0.1115	0.1035	0.470	37.8	0.644	0.64	0.790	0.638	$\bar{0}$.00750	$\bar{0}$.00661
2.80	26.8	28.8	0.1046	0.0973	0.518	47.5	0.646	0.66	0.760	0.524	$\bar{0}$.00951	$\bar{0}$.00812
2.50	26.2	28.0	0.0954	0.0892	0.60	65.8	0.663	0.71	0.750	0.505	$\bar{0}$.0133	$\bar{0}$.01142
2.25	25.0	27.0	0.0900	0.0834	0.688	85.2	0.668	0.73	0.655	0.504	$\bar{0}$.0196	$\bar{0}$.01498
2.05	24.0	26.0	0.0854	0.0788	0.76	104.1	0.730	0.75	0.593	0.474	$\bar{0}$.0201	$\bar{0}$.0192
1.75	21.0	-	0.0832	-	0.896	129.0	0.746	0.78	0.422	0.365	$\bar{0}$.033	$\bar{0}$.02708
1.55	19.0	-	0.0815	-	1.06	159.1	0.732	0.81	0.30	0.364	$\bar{0}$.0400	$\bar{0}$.0353

Beach Slope = 1/15, Wave Period T = 0.8 sec. H_o = 1.45 ins.

WATER DEPTH d INCHES	EXP. WAVE LENGTH L INCHES	THEOR. WAVE LENGTH (CNOIDAL WAVE) INS.	EXP. $\frac{d}{L}$	THEOR. $\frac{d}{L}$ (CNOIDAL WAVE)	$\frac{H}{d}$	$\frac{HL^2}{d^3}$	WAVE — ASYMMETRY.					
							WAVE VERT. ASYM.		WAVE HORIZ. ASYM. HA	WAVE HORIZ. ASYM. HA'	WAVE SLOPE ASYM.	
							EXP.	THEOR.			EXP RADIANS	THEOR. BIESEL(1951)
3.93	29.0	30.6	0.1355	0.1285	0.343	18.70	0.598	0.58	0.860	0.775	$\bar{0}$.00262	$\bar{0}$.00237
3.73	28.5	30.1	0.1310	0.1240	0.364	21.2	0.625	0.60	0.910	0.737	$\bar{0}$.0033	$\bar{0}$.002758
3.63	28.3	29.8	0.1284	0.1220	0.378	22.9	0.640	0.61	0.900	0.705	$\bar{0}$.00378	$\bar{0}$.002988
3.33	28.0	29.5	0.1190	0.1130	0.412	29.1	0.641	0.62	0.841	0.608	$\bar{0}$.00505	$\bar{0}$.00393
3.03	27.8	29.0	0.1090	0.1044	0.458	38.6	0.662	0.65	0.794	0.590	$\bar{0}$.00524	$\bar{0}$.00532
2.73	27.0	28.1	0.1011	0.0971	0.513	50.2	0.686	0.67	0.790	0.572	$\bar{0}$.00343	$\bar{0}$.00716
2.43	25.0	27.7	0.0971	0.0878	0.578	61.2	0.687	0.70	0.780	0.525	$\bar{0}$.0121	$\bar{0}$.00945
2.13	24.5	27.4	0.0869	0.0778	0.695	92.0	0.688	0.74	0.740	0.436	$\bar{0}$.0190	$\bar{0}$.001391
1.83	21.0	-	0.0871	-	0.844	111.0	0.730	0.76	0.625	0.418	$\bar{0}$.0201	$\bar{0}$.0192
1.53	18.5	-	0.0826	-	1.01	147.5	0.730	0.80	0.430	0.382	$\bar{0}$.030	$\bar{0}$.0286

Beach Slope = 1/18, Wave Period T = 0.8 sec. H_o = 1.45 ins.

WATER DEPTH d INCHES	EXP. WAVE LENGTH L INCHES	THEOR. WAVE LENGTH (CNOIDAL WAVE) INS.	EXP. $\frac{d}{L}$	THEOR. $\frac{d}{L}$ (CNOIDAL WAVE)	$\frac{H}{d}$	$\frac{HL^2}{d^3}$	WAVE — ASYMMETRY.					
							WAVE VERT. ASYM.		WAVE HORIZ. ASYM. HA	WAVE HORIZ. ASYM. HA'	WAVE SLOPE ASYM.	
							EXP.	THEOR.			EXP RADIANS	THEOR. BIESEL (1951)
3.90	28.9	30.5	0.1350	0.1280	0.346	19.0	0.563	0.580	0.931	0.775	0.00175	0.0020
3.60	28.4	30.0	0.1268	0.1200	0.384	23.6	0.598	0.61	0.895	0.722	0.00405	0.0026
3.40	28.0	29.4	0.1215	0.1158	0.403	27.4	0.632	0.62	0.890	0.701	0.0041	0.0031
3.10	27.3	29.2	0.1136	0.1062	0.445	34.5	0.642	0.64	0.902	0.674	0.0055	0.0040
2.85	26.9	28.3	0.1060	0.1007	0.488	43.5	0.650	0.66	0.860	0.643	0.0069	0.0052
2.60	25.5	27.8	0.1020	0.0935	0.534	51.3	0.656	0.67	0.820	0.610	0.0081	0.0065
2.30	24.5	27.4	0.0937	0.0840	0.617	70.0	0.694	0.72	0.785	0.549	0.0120	0.0092
2.00	23.6	26.6	0.0847	0.0752	0.740	106.0	0.708	0.75	0.740	0.432	0.0195	0.0135
1.80	21.0	-	0.0845	-	0.855	116.5	0.725	0.76	0.640	0.437	0.0220	0.0167
1.50	18.2	-	0.0823	-	1.03	150.5	0.740	0.81	0.435	0.429	0.0315	0.1249

Beach Slope = 1/6, Wave Period T = 0.8 sec. H_o = 1.45 ins. (BACKWASH ELIMINATED)

WATER DEPTH d INCHES	EXP WAVE LENGTH L INCHES	THEOR WAVE LENGTH (CNOIDAL WAVE) INS.	EXP. $\frac{d}{L}$	THEOR. $\frac{d}{L}$ (CNOIDAL WAVE)	$\frac{H}{d}$	$\frac{HL^2}{d^3}$	WAVE — ASYMMETRY.				
							WAVE VERT. ASYM.		WAVE HORIZ. ASYM. HA	WAVE HORIZ. ASYM. HA'	WAVE SLOPE ASYM.
							EXP.	THEOR.			EXP. RADIANS
4.20	28.7	29.9	0.1470	0.1406	0.335	19.6	0.540	0.590	0.781	0.775	-0.005
3.40	28.0	29.2	0.1215	0.1165	0.375	25.4	0.540	0.610	0.767	0.690	-0.0180
3.00	27.0	28.5	0.1112	0.1054	0.447	36.1	0.545	0.640	0.697	0.637	-0.02618
2.70	26.5	28.1	0.1020	0.0960	0.515	49.5	0.548	0.665	0.639	0.563	-0.0324
1.90	23.5	26.6	0.0807	0.0714	0.731	112.5	0.557	0.750	0.452	0.391	-0.0720
1.60	20.5	-	0.0780	-	0.90	148.0	0.564	0.800	0.366	0.281	-0.1002
1.30	17.4	-	0.0747	-	1.145	205.0	0.576	0.830	0.181	0.154	-0.1093
1.20	16.5	-	0.0727	-	1.25	236.0	0.580	0.835	0.131	0.135	-0.115

Beach Slope = 1/9, Wave Period T = 0.8 sec. H_o = 1.45 ins. (BACKWASH ELIMINATED)

WATER DEPTH d INCHES	EXP WAVE LENGTH L INCHES	THEOR WAVE LENGTH (CNOIDAL WAVE) INS.	EXP. $\frac{d}{L}$	THEOR. $\frac{d}{L}$ (CNOIDAL WAVE)	$\frac{H}{d}$	$\frac{HL^2}{d^3}$	WAVE — ASYMMETRY.				
							WAVE VERT. ASYM.		WAVE HORIZ. ASYM. HA	WAVE HORIZ. ASYM. HA'	WAVE SLOPE ASYM.
							EXP.	THEOR.			EXP. RADIANS
4.18	28.8	30.0	0.1455	0.1397	0.323	18.5	.525	0.580	.839	.721	-0.0050
3.30	28.0	29.4	0.1180	0.1123	0.387	27.8	.565	0.620	.813	.711	-0.0163
2.90	26.9	28.4	0.1078	0.1022	0.441	38.0	.570	0.650	.783	.663	-0.0212
2.50	25.7	27.6	0.0972	0.0905	0.517	54.8	.600	0.670	.624	.517	-0.0256
2.20	24.5	26.8	0.0897	0.0821	0.616	76.6	.605	0.720	.493	.427	-0.0367
2.00	23.6	26.6	0.0847	0.0752	0.721	100.5	.610	.750	.422	.398	-0.0441
1.70	20.5	-	0.0830	-	0.873	127.0	.638	.78	.391	.329	-0.0509
1.60	19.4	-	0.0825	-	0.931	136.8	.668	.79	.356	.323	-0.0521
1.40	17.5	-	0.0800	-	1.070	167.0	.67	.81	.246	.241	-0.0540
1.30	17.0	-	0.0765	-	1.160	198.0	.68	.83	.162	.170	-0.0662

Beach Slope 1/12, Wave Period T = 0.8 sec. H_0 = 1.45 ins. (BACKWASH ELIMINATED)

WATER DEPTH d INCHES	EXP WAVE LENGTH L INCHES	THEOR WAVE LENGTH (CNOIDAL WAVE) INS.	EXP. $\frac{d}{L}$	THEOR. $\frac{d}{L}$ (CNOIDAL WAVE)	$\frac{H}{d}$	$\frac{HL^2}{d^3}$	WAVE — ASYMMETRY.				
							WAVE VERT. ASYM.		WAVE HORIZ. ASYM. HA	WAVE HORIZ. ASYM. HA'	WAVE SLOPE ASYM.
							EXP.	THEOR.			EXP. RADIANS
3.55	28.4	29.5	0.1250	0.1205	0.342	21.9	.526	0.60	.943	0.807	-0.00612
3.25	28.0	29.4	0.1161	0.1105	0.398	29.5	.53	0.62	.836	0.733	-0.00740
2.90	26.9	28.5	0.1079	0.1018	0.462	39.7	.544	0.65	.818	.703	-0.0124
2.55	26.0	27.3	0.0981	0.0933	0.506	52.6	.557	0.67	.678	.697	-0.0178
2.35	25.1	26.7	0.0935	0.0879	0.534	61.2	.58	0.70	.568	.482	-0.02095
2.05	24.3	26.3	0.0844	0.0780	0.654	91.8	.582	0.74	.508	.357	-0.0340
1.85	22.0	26.0	0.0840	0.0712	0.78	110.7	.623	0.750	.427	.332	-0.0351
1.70	20.4	-	0.0833	-	0.878	126.8	.64	0.78	.339	.304	-0.0375
1.52	18.3	-	0.0830	-	0.986	143.2	.644	0.80	.185	.193	-0.0382

Beach Slope 1/15, Wave Period T = 0.8 sec. H_o = 1.45 ins. (BACKWASH ELIMINATED)

WATER DEPTH d INCHES	EXP WAVE LENGTH L INCHES	THEOR WAVE LENGTH (CNOIDAL WAVE) INS.	EXP. $\frac{d}{L}$	THEOR. $\frac{d}{L}$ (CNOIDAL WAVE)	$\frac{H}{d}$	$\frac{HL^2}{d^3}$	WAVE — ASYMMETRY.				
							WAVE VERT. ASYM.		WAVE HORIZ. ASYM. HA	WAVE HORIZ. ASYM. HA'	WAVE SLOPE ASYM.
							EXP.	THEOR.			EXP. RADIANS
4.30	30.0	31.3	0.1435	0.1375	0.291	14.1	.56	0.570	0.88	0.800	-0.00322
3.90	29.0	30.2	0.1345	0.1295	0.320	17.7	.59	0.575	0.86	0.800	-0.00405
3.45	28.2	29.3	0.1225	0.1180	0.365	24.3	.59	0.610	0.85	0.730	-0.00530
3.20	28.0	28.9	0.1145	0.1110	0.394	30.1	.595	0.625	0.83	0.710	-0.00698
2.80	27.3	28.2	0.1025	0.0993	0.459	43.8	.60	0.660	0.78	0.709	-0.0121
2.50	26.0	27.5	0.0960	0.0910	0.520	56.4	.61	0.690	0.70	0.694	-0.0159
2.30	25	26.9	0.0920	0.0855	0.574	67.8	.636	0.710	0.55	0.543	-0.0197
2.05	24.5	26.5	0.0836	0.0773	0.654	93.6	.64	0.735	0.548	0.475	-0.0325
1.85	23.2	26.2	0.0798	0.0706	0.778	120.0	.67	0.770	0.424	0.400	-0.0341
1.70	21.5	-	0.0790	-	0.882	141.0	.68	0.790	0.370	0.320	-0.0360
1.50	19.1	-	0.0785	-	1.03	160.0	.71	0.810	0.243	0.239	-0.0378

Beach Slope = 1/18 Wave Period, T = 0.8 sec. H_o = 1.45 ins. (BACKWASH ELIMINATED)

WATER DEPTH d INCHES	EXP WAVE LENGTH L INCHES	THEOR WAVE LENGTH (CNOIDAL WAVE) INS.	EXP. $\frac{d}{L}$	THEOR. $\frac{d}{L}$ (CNOIDAL WAVE)	$\frac{H}{d}$	$\frac{HL^2}{d^3}$	WAVE – ASYMMETRY.				
							WAVE VERT. ASYM.		WAVE HORIZ. ASYM. HA	WAVE HORIZ. ASYM. HA'	WAVE SLOPE ASYM.
							EXP.	THEOR.			EXP. RADIANS
3.90	28.7	30.5	0.1360	0.1280	0.321	17.4	0.556	0.575	0.950	0.920	-0.0025
3.65	28.5	29.8	0.1280	0.1225	0.342	20.8	0.570	0.600	0.920	0.837	-0.00429
3.40	28.0	29.4	0.1215	0.1160	0.370	25.1	0.573	0.610	0.870	0.770	-0.00514
3.10	27.2	28.8	0.1140	0.1078	0.434	33.4	0.612	0.640	0.857	0.650	-0.0061
2.85	26.8	28.3	0.1065	0.1008	0.473	41.7	0.64	0.650	0.763	0.648	0. 00786
2.65	26.0	28.0	0.1020	0.0946	0.512	49.2	0.64	0.670	0.766	0.565	-0.0101
2.40	25.0	27.8	0.0960	0.0862	0.591	64.2	0.682	0.710	0.733	0.486	-0.0140
2.25	24.5	27.4	0.0918	0.0821	0.633	75.0	0.690	0.720	0.610	0.470	-0.0161
2.00	23.5	26.6	0.0850	0.0752	0.714	99.0	0.690	0.745	0.536	0.284	-0.0218
1.80	21.3	–	0.0845	–	0.866	121.0	0.714	0.770	0.517	0.288	-0.0253
1.70	20.2	–	0.0840	–	0.958	136.0	0.750	0.790	0.419	0.281	-0.0287
1.48	18.1	–	0.0818	–	1.15	170.0	.750	0.810	0.349	0.250	-0.0349

WAVE SLOPE ASYMMETRY (S)

THEORY BIESEL[5] (1951)

$$S = m^2 a_o^2 \gamma \left\{ \frac{3 + \frac{md}{\tanh md} - 3md \tanh md}{D^2 (\sinh md)^2 \tanh md} \right\}$$

where $D = 1 + \frac{md}{\sinh md \cosh md}$

γ = bottom slope = $\frac{1}{12}$

H_o = 1.45 ins.

d = water depth

a_o = wave amplitude in deep water taken as $\frac{H_o}{2}$

$m = \frac{2\pi}{L}$

L^2 ins^2	$\frac{d}{L}$	$\frac{2\pi d}{L}$	$\tanh \frac{2\pi d}{L}$	$\sinh \frac{2\pi d}{L}$	$\cosh \frac{2\pi d}{L}$	$\frac{\frac{2\pi d}{L}}{\sinh \frac{2\pi d}{L} \cosh \frac{2\pi d}{L}}$	D	$\frac{\frac{2\pi d}{L}}{\tanh \frac{2\pi d}{L}}$	$3 \times \frac{2\pi d}{L} \tanh \frac{2\pi d}{L}$	$3 + \frac{\frac{2\pi d}{L}}{\tanh \frac{2\pi d}{L}} - 3 \times \frac{2\pi d}{L} \tanh \frac{2\pi d}{L}$	$D^2 \left(\sinh \frac{2\pi d}{L}\right)^2 \tanh \frac{2\pi d}{L}$	$\frac{(2\pi)^2 \left(\frac{H_o}{2}\right)^2 \gamma}{L^2}$	S radians	EXPT. VALUE OF S radians
794	0.1315	0.8262	0.6784	0.9235	1.361	0.657	1.657	1.218	1.68	2.538	1.595	0.00218	-0.00347	-0.00349
784	0.1250	0.7854	0.6558	0.8687	1.325	0.682	1.682	1.198	1.543	2.655	1.402	0.002208	-0.00418	-0.0055
771	0.1188	0.7464	0.6330	0.8177	1.292	0.706	1.706	1.178	1.416	2.762	1.232	0.002245	-0.00503	-0.00610
722	0.1115	0.7005	0.6047	0.7593	1.255	0.734	0.734	1.159	1.270	2.889	1.048	0.002395	-0.00661	-0.00750
718	0.1046	0.6572	0.5765	0.7056	1.224	0.762	1.762	1.141	1.135	3.006	0.890	0.002408	-0.00812	-0.00951
685	0.0954	0.5994	0.5366	0.6360	1.186	0.796	1.796	1.118	0.964	3.154	0.698	0.00253	-0.01142	-0.0133
625	0.0900	0.5655	0.5120	0.5961	1.164	0.815	1.815	1.105	0.867	3.238	0.598	0.00277	-0.01498	-0.0196
576	0.0854	0.5366	0.4904	0.5627	1.148	0.829	1.829	1.097	0.788	3.309	0.518	0.00301	-0.0192	-0.0201
441	0.0832	0.5227	0.4799	0.5469	1.139	0.838	1.838	1.090	0.752	3.338	0.484	0.00393	-0.02708	-0.033
361	0.0815	0.5120	0.4715	0.5347	1.134	0.844	1.844	1.085	0.723	3.362	0.457	0.00479	-0.0353	-0.0400

Beach Slope = $^1/_9$, Wave Period T = 0.8 sec. H_o = 1.45 ins

WATER DEPTH d INCHES	EXPT. WAVE LENGTH L INCHES	EXPT. $\frac{d}{L}$	WAVE HT. H INCHES	ORBITAL VELOCITY ASYMMETRY					
				MAX. HORIX. SHOREWARD VELOCITY INS/SEC	MAX HORIX SEAWARD VELOCITY INS/SEC	HORIZ. VEL. (MAG) ASYM.	TIME FOR SHOREWARD MOTION SEC.	TIME FOR SEAWARD MOTION SEC.	HORIZ. VEL. (TIME) ASYM.
3.50	28.2	0.1245	1.28	5.35	4.20	1.275	0.364	0.436	0.834
3.10	27.3	0.1135	1.32	5.50	4.20	1.310	0.355	0.445	0.798
2.70	25:8	0.1047	1.33	5.80	4.35	1.335	0.350	0.450	0.777
2.45	24.8	0.0987	1.35	7.10	5.20	1.367	0.340	0.460	0.740
2.25	24.0	0.0938	1.364	8.10	5.80	1.400	0.333	0.467	0.713
2.05	23.0	0.0891	1.395	9.10	5.90	1.545	0.320	0.480	0.667
1.75	21.0	0.0833	1.44	9.50	6.00	1.585	0.280	0.520	0.538
1.55	19.0	0.0815	1.49	10.50	6.50	1.615	0.240	0.560	0.428
1.40	17.5	0.0800	1.515	13.00	8.00	1.625	0.218	0.582	0.374

Beach Slope = 1/18, Wave Period T = 0.8 sec. H_o = 1.45 ins.

WATER DEPTH d INCHES	EXPT. WAVE LENGTH L INCHES	EXPT. $\frac{d}{L}$	WAVE HT. H INCHES	ORBITAL VELOCITY ASYMMETRY					
				MAX HORIX. SHOREWARD VELOCITY INS/SEC	MAX HORIX SEAWARD VELOCITY INS/SEC	HORIZ. VEL. (MAG) ASYM.	TIME FOR SHOREWARD MOTION SEC.	TIME FOR SEAWARD MOTION SEC.	HORIZ. VEL. (TIME) ASYM
3.10	27.5	0.1130	1.35	6.05	4.00	1.512	0.364	0.436	0.834
2.65	26.3	0.1010	1.382	7.00	4.45	1.575	0.345	0.455	0.758
2.35	25.0	0.0940	1.400	7.20	4.50	1.600	0.340	0.460	0.740
2.15	23.7	0.0907	1.415	7.90	4.70	1.680	0.334	0.466	0.716
1.95	22.5	0.0866	1.455	9.00	5.20	1.730	0.310	0.490	0.632
1.75	20.8	0.0841	1.485	9.30	5.30	1.758	0.275	0.525	0.524
1.65	19.8	0.0833	1.52	9.50	5.40	1.761	0.270	0.530	0.510
1.50	18.2	0.0823	1.545	9.70	5.50	1.765	0.263	0.537	0.490

Beach Slope = 1/9, Wave Period T = 0.8 sec. H_o = 1.45 ins. (Backwash Eliminated)

WATER DEPTH d INCHES	EXPT. WAVE LENGTH L INCHES	EXPT. $\frac{d}{L}$	WAVE HT. H INCHES	ORBITAL VELOCITY			ASYMMETRY		
				MAX HORIX. SHOREWARD VELOCITY INS/SEC	MAX HORIX SEAWARD VELOCITY INS/SEC	HORIZ. VEL. (MAG) ASYM.	TIME FOR SHOREWARD MOTION SEC.	TIME FOR SEAWARD MOTION SEC.	HORIZ. VEL. (TIME) ASYM
3.30	28.0	0.1180	1.276	5.25	4.05	1.290	0.380	0.420	0.905
2.90	26.9	0.1080	1.280	5.50	4.25	1.300	0.364	0.436	0.833
2.60	26.0	0.1000	1.283	6.40	4.45	1.440	0.353	0.447	0.790
2.40	25.2	0.0952	1.285	7.60	5.20	1.462	0.342	0.458	0.746
2.15	24.2	0.0890	1.334	8.75	5.28	1.658	0.330	0.470	0.701
1.85	22.5	0.0820	1.40	8.90	5.30	1.680	0.325	0.475	0.684
1.60	20.0	0.0800	1.495	9.75	5.32	1.840	0.265	0.535	0.495
1.30	16.5	0.0785	1.52	12.1	6.50	1.860	0.246	0.554	0.444

Beach Slope = 1/18, Wave Period T = 0.8 sec. H_o = 1.45 ins. (Backwash Eliminated)

WATER DEPTH d INCHES	EXPT. WAVE LENGTH L INCHES	EXPT. $\frac{d}{L}$	WAVE HT. H INCHES	ORBITAL VELOCITY ASYMMETRY					
				MAX HORIX. SHOREWARD VELOCITY INS/SEC	MAX HORIX SEAWARD VELOCITY INS/SEC	HORIZ. VEL. (MAG) ASYM.	TIME FOR SHOREWARD MOTION SEC.	TIME FOR SEAWARD MOTION SEC.	HORIZ. VEL. (TIME) ASYM.
3.60	28.5	0.1265	1.270	4.35	2.90	1.500	0.390	0.410	0.951
3.15	27.7	0.1140	1.33	5.00	3.10	1.615	0.385	0.415	0.927
2.80	26.7	0.1050	1.35	5.90	3.55	1.660	0.380	0.420	0.905
2.50	25.6	0.0977	1.368	6.40	3.60	1.780	0.352	0.448	0.785
2.30	24.7	0.0932	1.38	7.10	3.95	1.800	0.346	0.454	0.762
2.15	24.0	0.0895	1.42	7.25	4.00	1.810	0.335	0.465	0.720
2.00	23.0	0.0870	1.468	7.30	4.00	1.825	0.308	0.492	0.626
1.85	21.8	0.0848	1.518	7.60	4.10	1.850	0.280	0.520	0.540
1.70	20.7	0.0818	1.56	7.80	4.20	1.860	0.270	0.530	0.510

Beach Slope = 1/6, Wave Period T = 1 sec. L_o = 61.4 ins.

DEEP WATER WAVE HT. H_o INS.	BREAKER HT. H_b INS.	BREAKER DEPTH d_b INS.	TIME OF TRAVEL FROM BREAK-POINT TO LIMIT OF UPRUSH t_1 SEC.	PHASE DIFFERENCE $\frac{t_1}{T}$	TIME OF SHOREWARD MOTION AT THE BREAK-POINT SEC.	TIME OF SHOREWARD MOTION AT THE BREAK-POINT / WAVE PERIOD
0.370	0.429	0.95	0.487	0.487	0.488	0.488
0.495	0.572	0.96	0.490	0.490	0.480	0.480
0.534	0.733	1.05	0.510	0.510	0.460	0.460
0.640	0.770	1.07	0.567	0.567	0.442	0.442
0.660	0.838	1.45	0.630	0.630	0.402	0.402
0.776	1.075	1.50	0.697	0.697	0.388	0.388
0.932	1.290	1.70	0.767	0.767	0.358	0.358
1.07	1.513	1.80	0.827	0.827	0.352	0.352
1.33	2.00	2.30	0.950	0.950	0.332	0.332

COMPARISON OF STOKES VELOCITY EQUATION WITH EXPERIMENTAL RESULTS (see Fig. 5.11)

$$u = \frac{\frac{\pi H}{T}\cosh\frac{2\pi(y+d)}{L}}{\sinh\frac{2\pi d}{L}}\cos 2\pi\left(\frac{x}{L}-\frac{t}{T}\right) + \frac{\frac{3}{4}\left(\frac{\pi H}{T}\right)\left(\frac{\pi H}{L}\right)\cosh\frac{4\pi(y+d)}{L}}{\sinh^4\frac{2\pi d}{L}}\cos 4\pi\left(\frac{x}{L}-\frac{t}{T}\right) \quad \ldots(1.1)$$

i.e.

$u = A\cos\frac{2\pi t}{T} + B\cos\frac{4\pi t}{T}$ for a given position

t = time variable, T = wave period,

T = 0.8 sec., H = 1.44 ins., L = 21.00 ins (measured),

$\frac{d}{L} = 0.0833$, $\frac{\pi H}{T} = 5.65$, $\frac{3}{4}\left(\frac{\pi H}{T}\right)\left(\frac{\pi H}{L}\right) = 0.911$,

$\frac{y+d}{L} = \frac{0.2}{21} = 0.00951.$

$\cosh 2\pi\frac{(y+d)}{L} = 1.0018$, $\cosh 4\pi\frac{(y+d)}{L} = 1.007$

$\sinh\frac{2\pi d}{L} = 0.5479$, $\sinh^4\frac{2\pi d}{L} = 0.09$

i.e. $A = \frac{5.65 \times 1.0018}{.5479} = 10.32$

$B = \frac{.911 \times 1.007}{0.09} = 10.20$

t/T	$\cos 2\pi t/T$	$\cos 4\pi t/T$	$10.32\cos\frac{2\pi t}{T}$	$10.2\cos\frac{4\pi t}{T}$	U(Stokes) ins/sec	U (Expmt) ins/sec.
0	1	1	+10.32	+10.2	+20.52	+6.573
$\frac{1}{12}$	0.8660	+0.5	+8.93	+ 5.1	+14.03	+9.40
$\frac{1}{6}$	0.5	-0.5	+5.16	- 5.1	+ 0.06	+7.427
$\frac{1}{4}$	0	-1	0	-10.2	-10.2	+3.80
0.29	-0.254	-0.87	-2.62	- 8.86	-11.48	+0.60
$\frac{1}{3}$	-0.5	-0.5	-5.16	- 5.1	-10.26	-2.15
$\frac{5}{12}$	-0.8660	+0.5	-8.93	+ 5.1	- 3.83	-2.203
$\frac{1}{2}$	-1	+1	-10.32	+10.2	- 0.12	-3.31
$\frac{7}{12}$	-0.8660	+0.5	- 8.93	+ 5.1	- 3.83	-4.09
$\frac{2}{3}$	-0.5	-0.5	- 5.16	- 5.1	-10.26	-5.077
$\frac{3}{4}$	0	-1	0	-10.2	-10.20	-5.983
$\frac{5}{6}$	+0.5	-0.5	+5.16	- 5.1	+ 0.06	-5.56
$\frac{11}{12}$	+0.8660	+0.5	+8.93	+ 5.1	+14.03	-3.583
1	1	+1	+10.32	+10.2	+20.52	+6.573

Determination of maxima and minima of Stokes Velocity

Equation Figure 5.11.

$$u = A\cos\frac{2\pi t}{T} + B\cos\frac{4\pi t}{T}$$

For either maximum or minimum

$$\frac{du}{dt} = -\frac{2\pi A}{T}\sin\frac{2\pi t}{T} - \frac{4\pi B}{T}\sin\frac{4\pi t}{T} = 0 \qquad \cdots(A.4.1)$$

i.e. $$A\sin\frac{2\pi t}{T} + 4B\sin\frac{2\pi t}{T}\cos\frac{2\pi t}{T} = 0$$

$$\sin\frac{2\pi t}{T}\left\{ A + 4B\cos\frac{2\pi t}{T} \right\} = 0 \qquad \cdots(A.4.2)$$

which is satisfied by

$$\sin\frac{2\pi t}{T} = 0 \quad \text{i.e.} \quad \frac{2\pi t}{T} = n\pi \quad \text{where} \quad n = 0,\ 1,\ 2\ \ldots\ldots$$

In particular when $n = 0$ and 1, $\frac{t}{T} = 0$ and $\frac{1}{2}$ respectively.

Eq. A.4.2 is also satisfied by

$$A = -4B\cos\frac{2\pi t}{T}$$

i.e. $$\cos\frac{2\pi t}{T} = -\frac{A}{4B}$$

By substituting values we have

$$\cos\frac{2\pi t}{T} = \frac{-10.32}{4 \times 10.20} = -0.254$$

i.e. $\frac{2\pi t}{T} = 0.58\pi$ so $\frac{t}{T} = 0.29$

and $\frac{2\pi t}{T} = 1.42\pi$ i.e. $\frac{t}{T} = 0.71$

By differentiating equation A.4.1 and substituting these values of $\frac{t}{T}$ it is easily seen that u is maximum for $\frac{t}{T} = 0$ and $\frac{1}{2}$ and minimum for $\frac{t}{T} = 0.29$ and 0.71.

BEACH SLOPE = $\frac{1}{18}$
WAVE PERIOD = 0·8 SEC.
H = 1·545 INS.
d/L = 0·0823

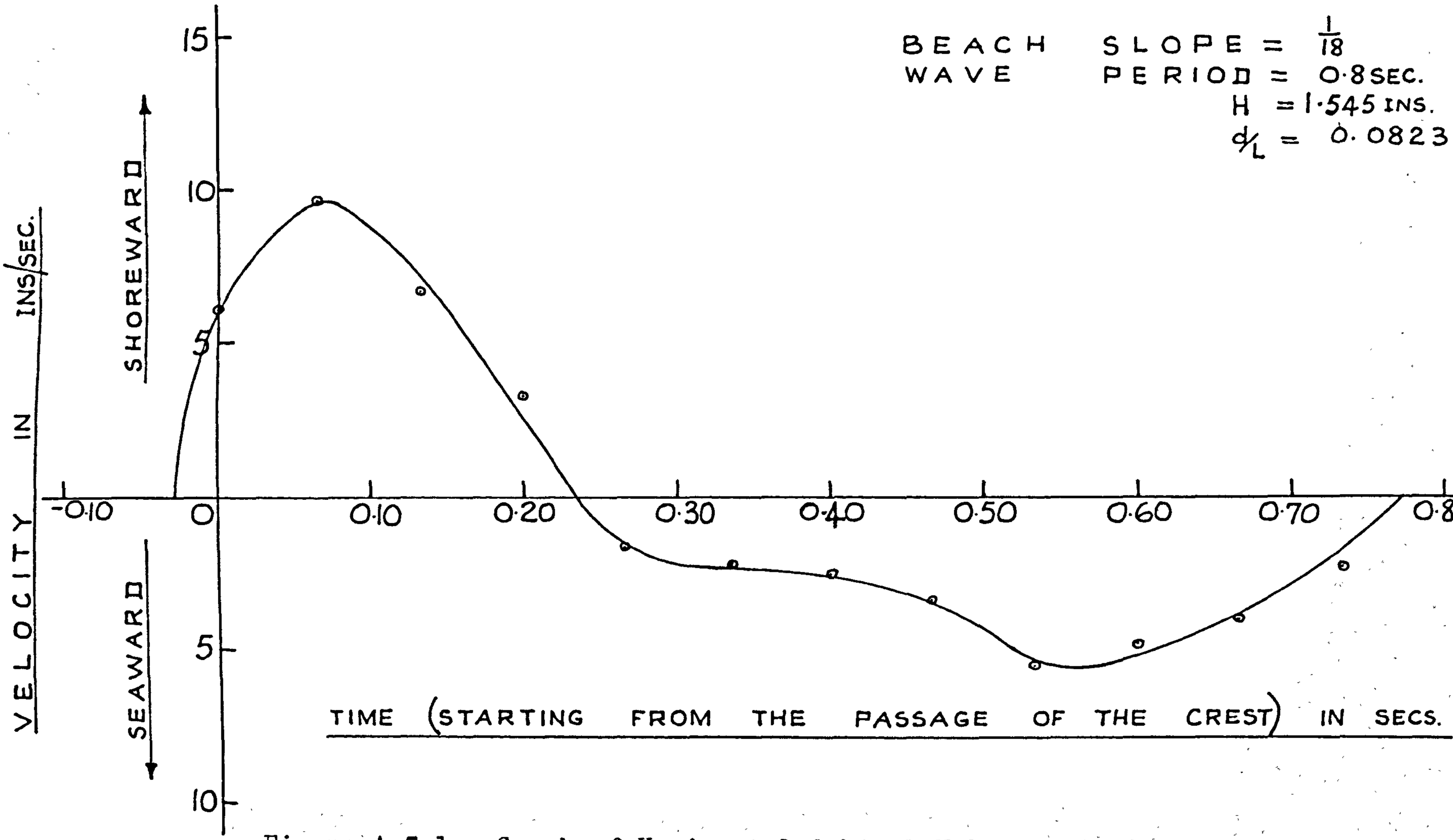

Figure A.5.1 Graph of Horizontal Orbital Velocity Against Time

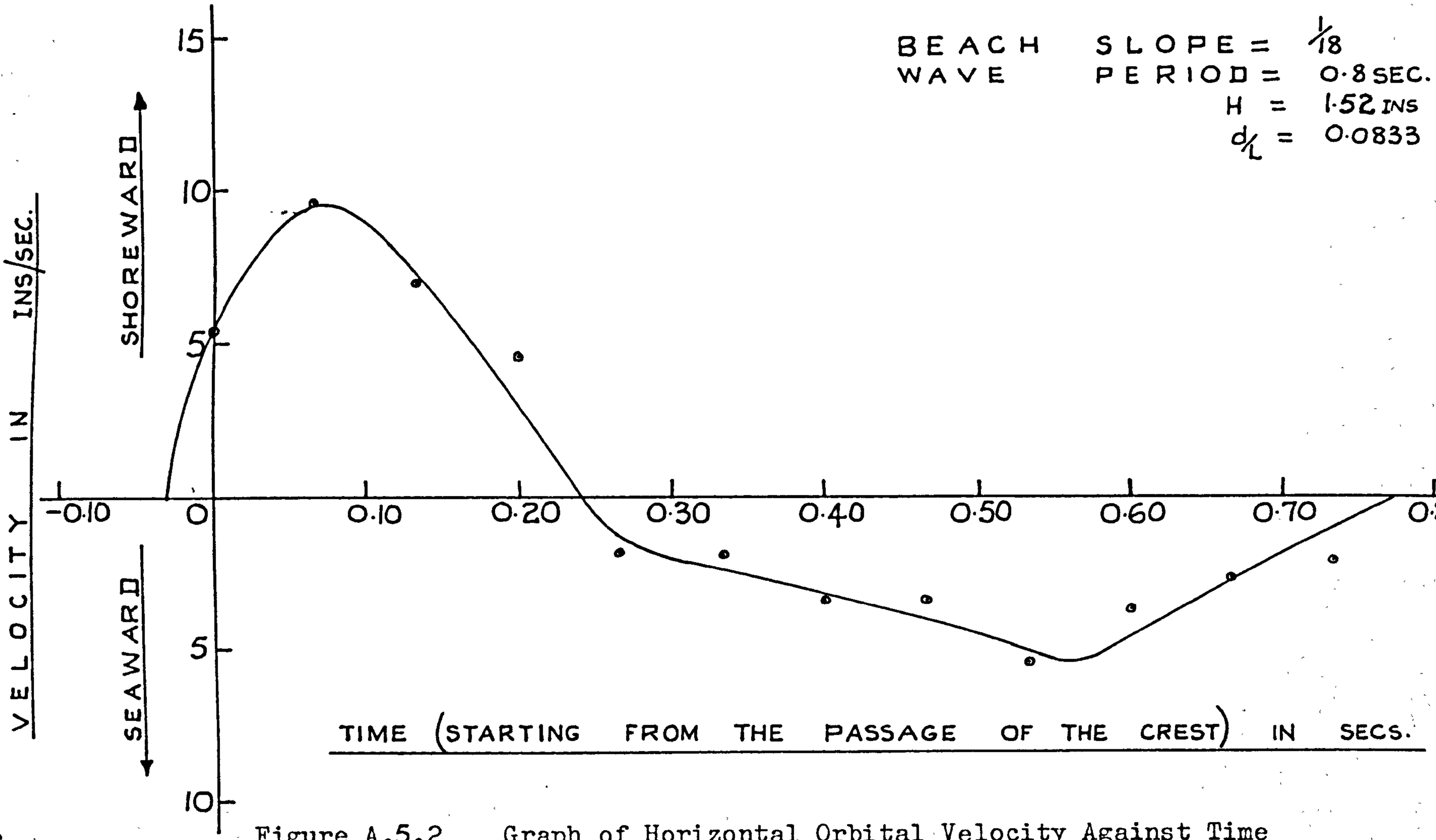

Figure A.5.2 Graph of Horizontal Orbital Velocity Against Time

BEACH SLOPE = $\frac{1}{18}$
WAVE PERIOD = 0·8 SEC.
H = 1·485 INS
d/L = 0·0841

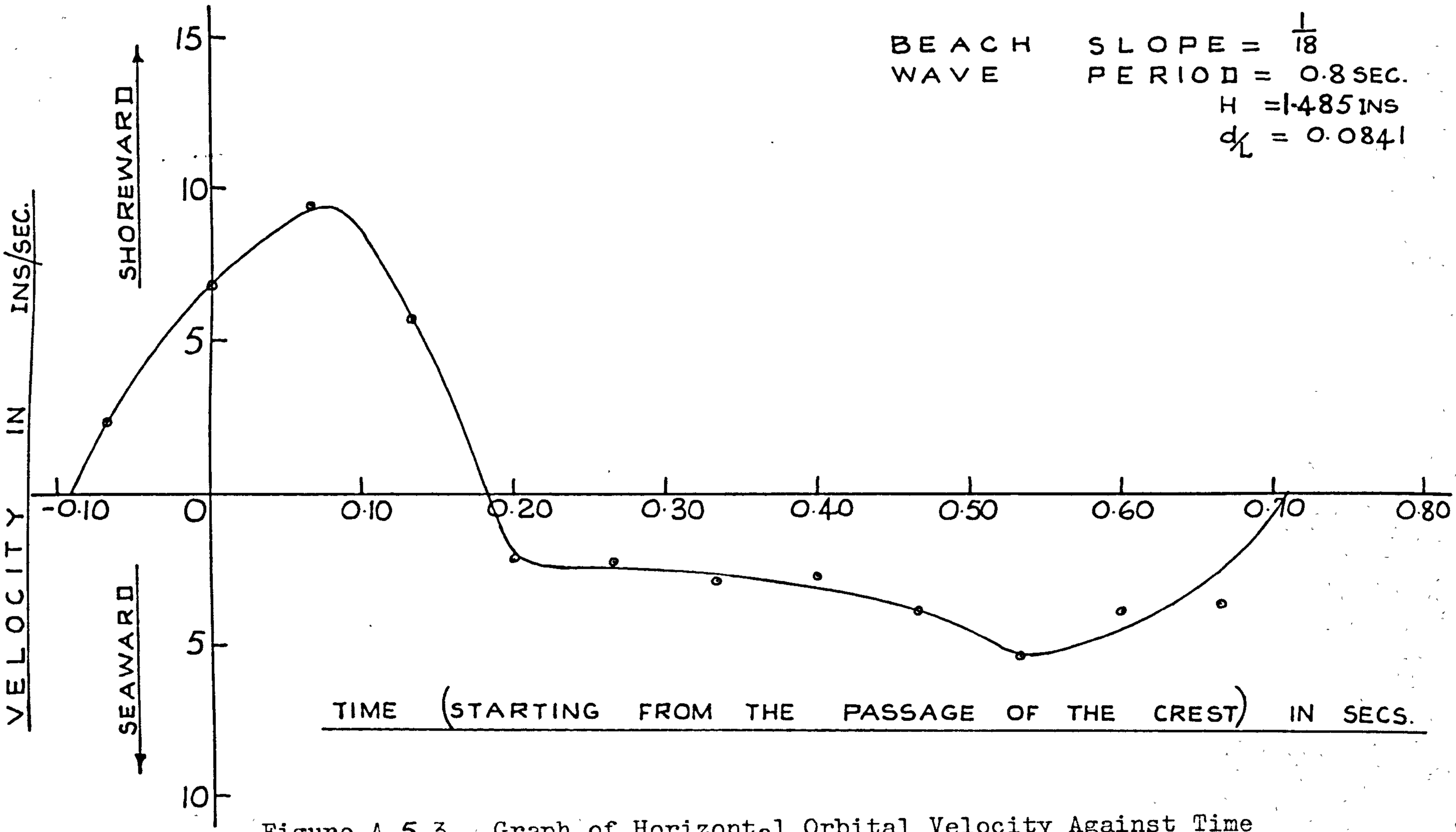

Figure A.5.3 Graph of Horizontal Orbital Velocity Against Time

BEACH SLOPE = $\frac{1}{18}$
WAVE PERIOD = 0·8 SEC.
H = 1·455 INS
d/L = 0·0866

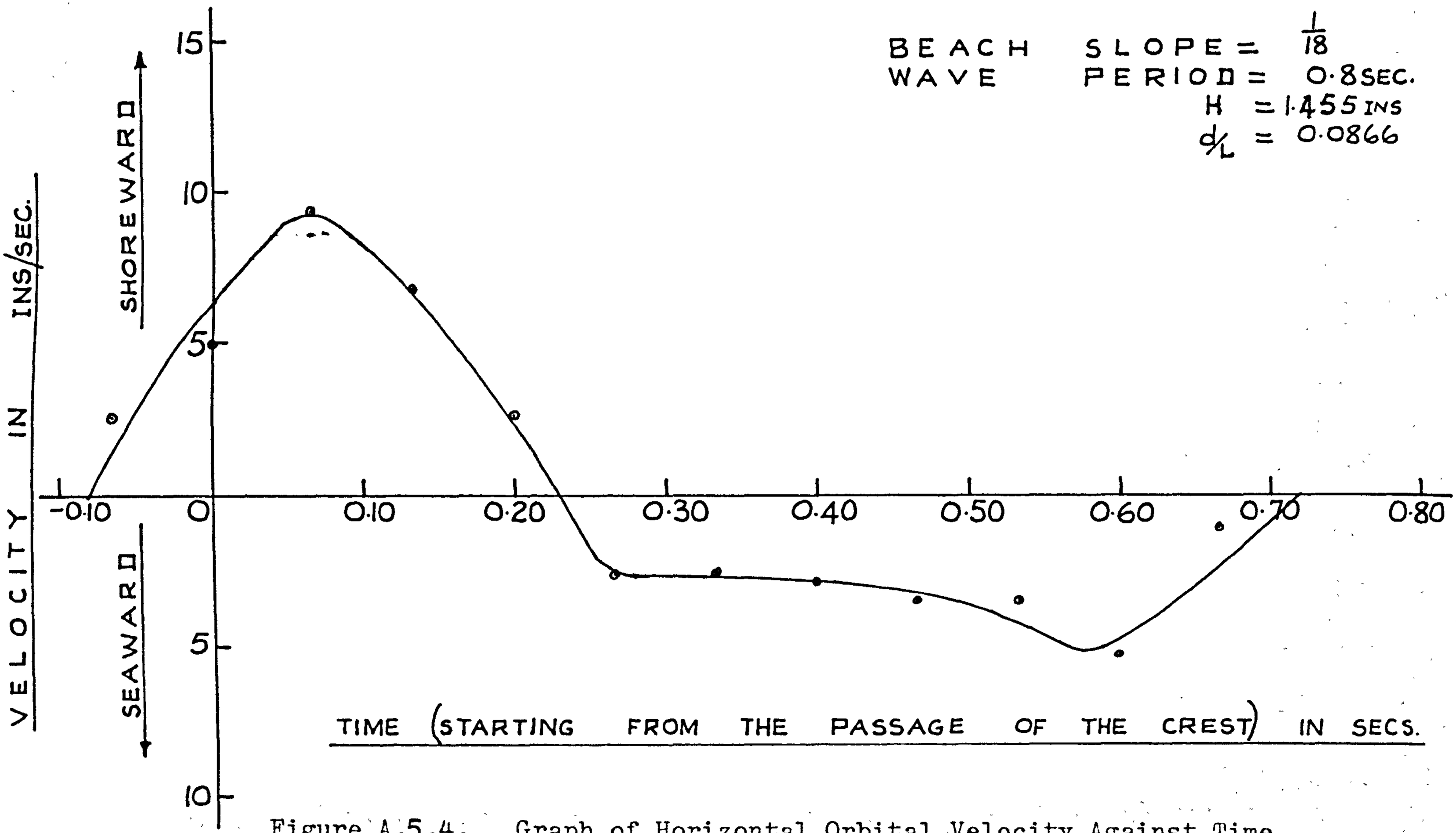

Figure A.5.4. Graph of Horizontal Orbital Velocity Against Time

BEACH SLOPE = $\frac{1}{18}$
WAVE PERIOD = 0·8 SEC.
H = 1·415 INS
d/L = 0.0907

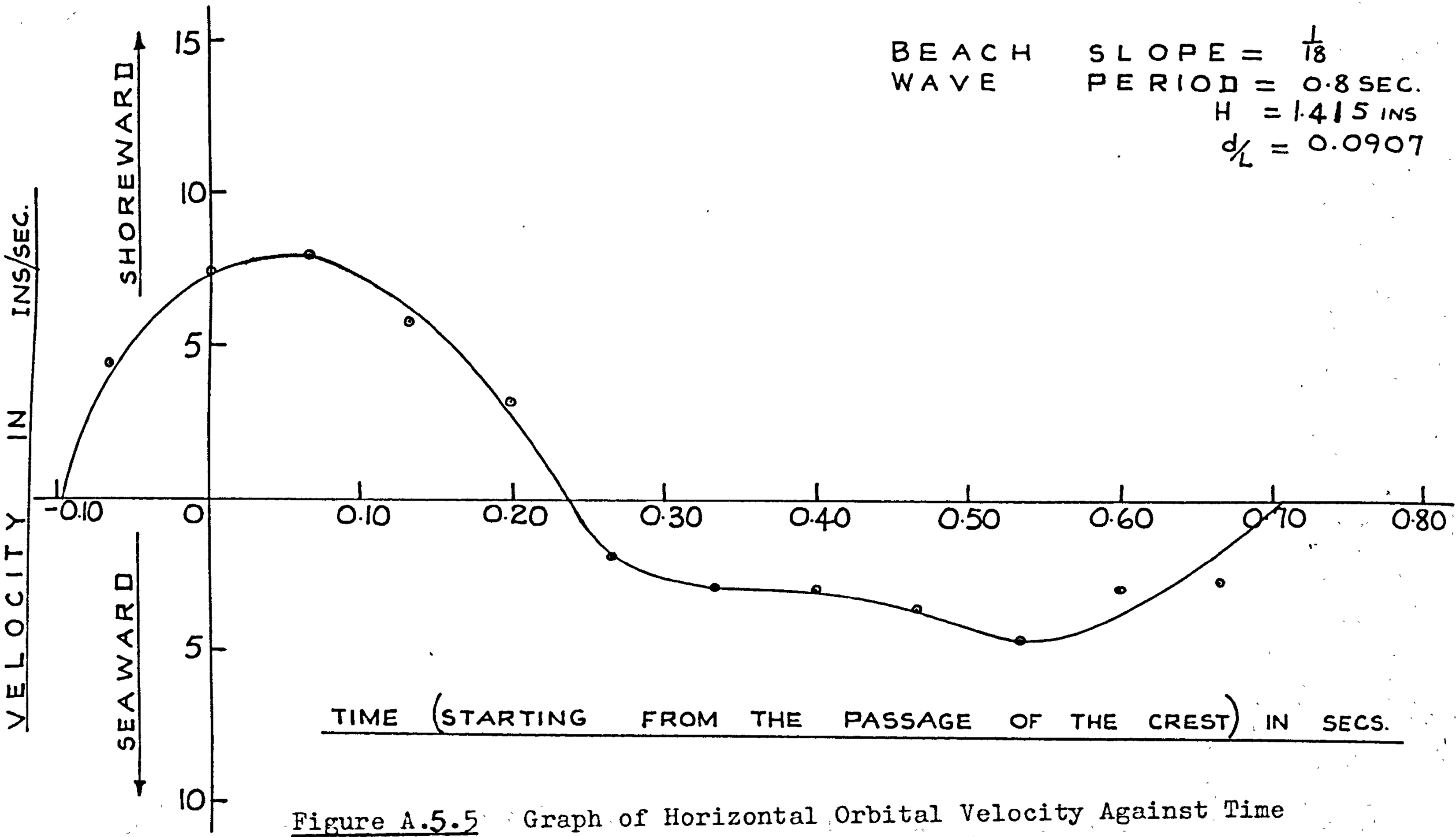

Figure A.5.5 Graph of Horizontal Orbital Velocity Against Time

BEACH SLOPE = $\frac{1}{18}$
WAVE PERIOD = 0.8 SEC.
H = 1.40 INS
d/L = 0.0940

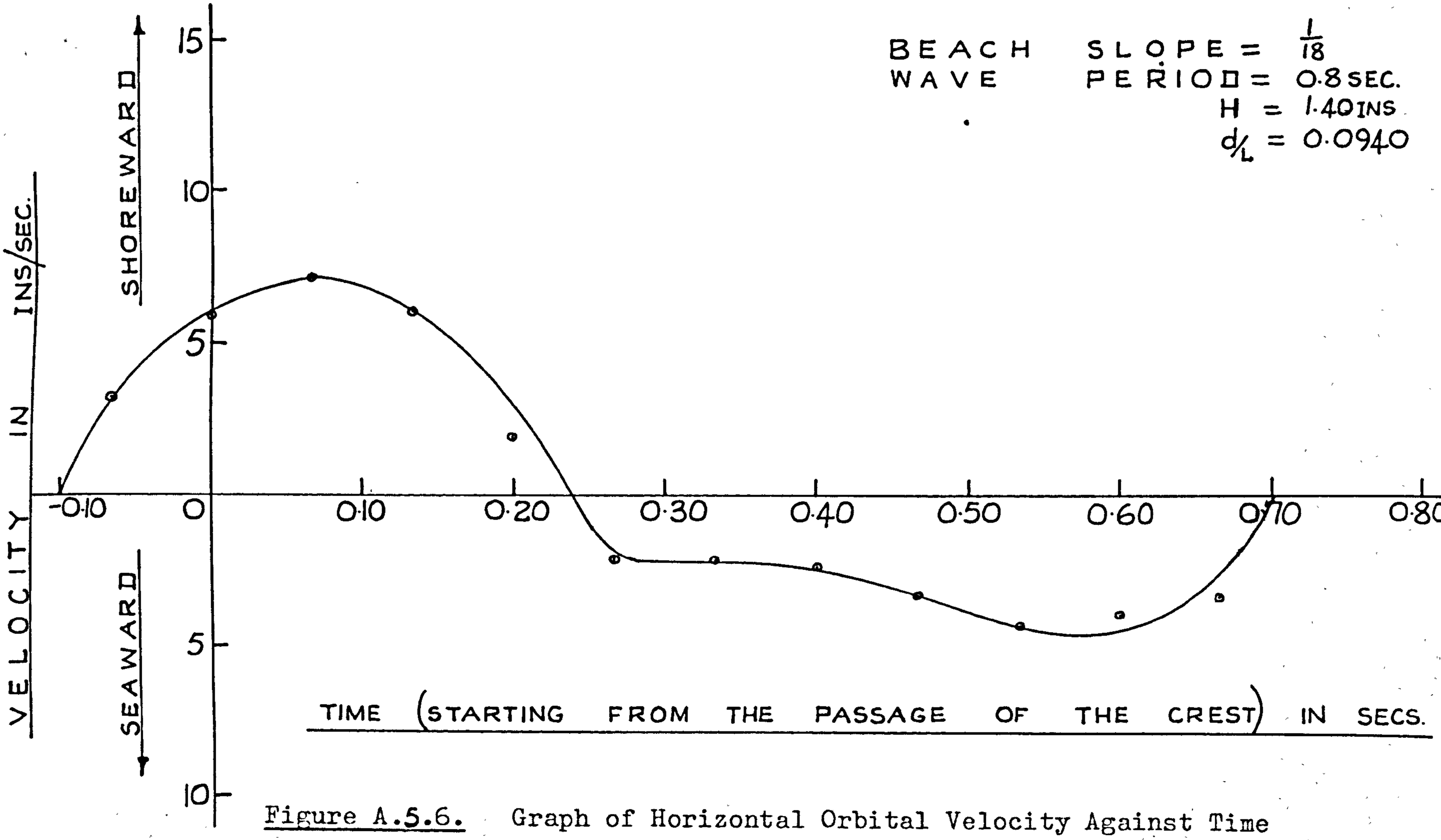

Figure A.5.6. Graph of Horizontal Orbital Velocity Against Time

BEACH SLOPE = $\frac{1}{18}$
WAVE PERIOD = 0·8 SEC.
H = 1·382 INS
d/L = 0·1010

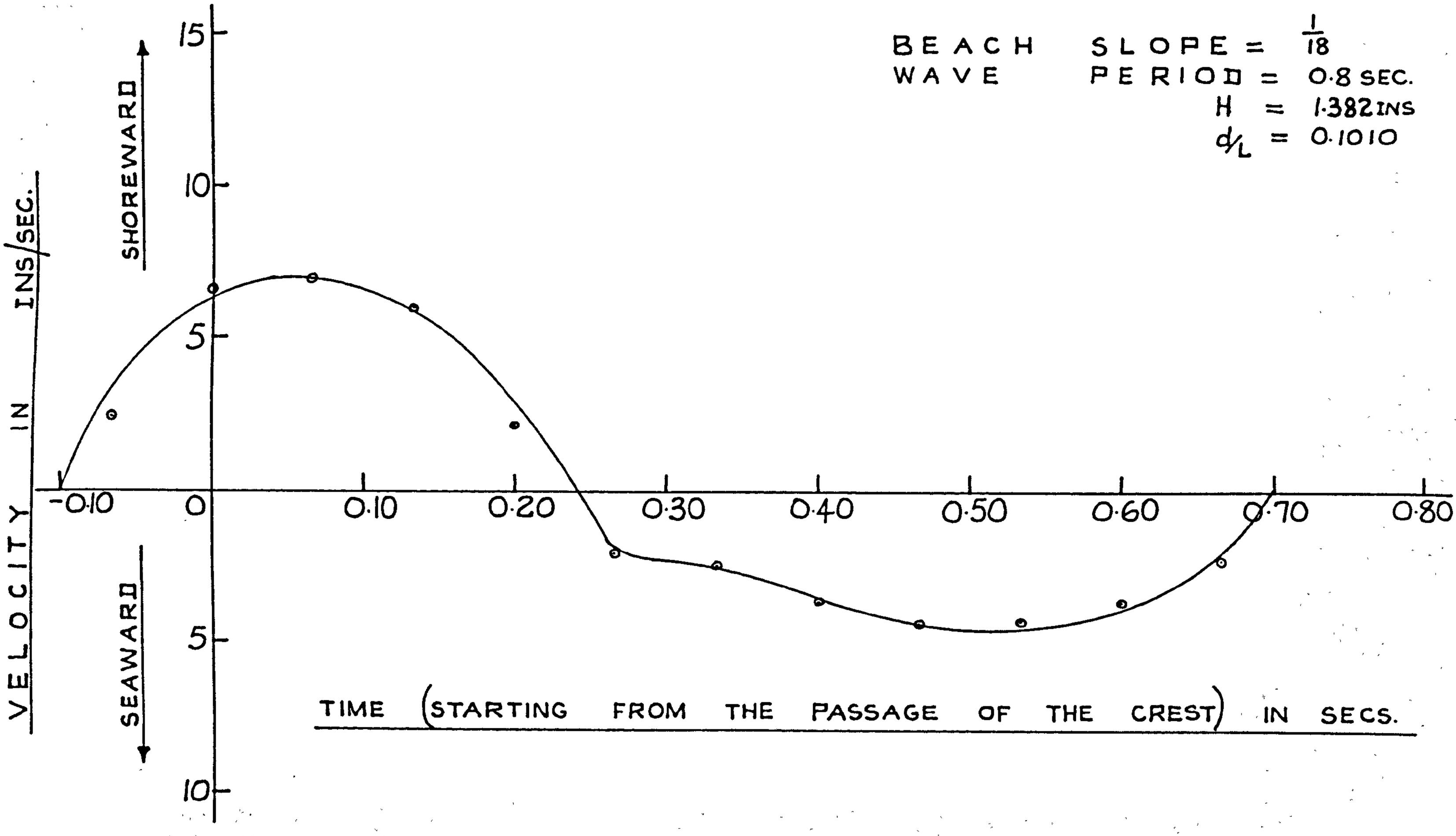

Figure A.5.7 Graph of Horizontal Orbital Velocity Against Time

BEACH SLOPE = $\frac{1}{18}$
WAVE PERIOD = 0·8SEC.
H = 1·35INS
d/L = 0·1130

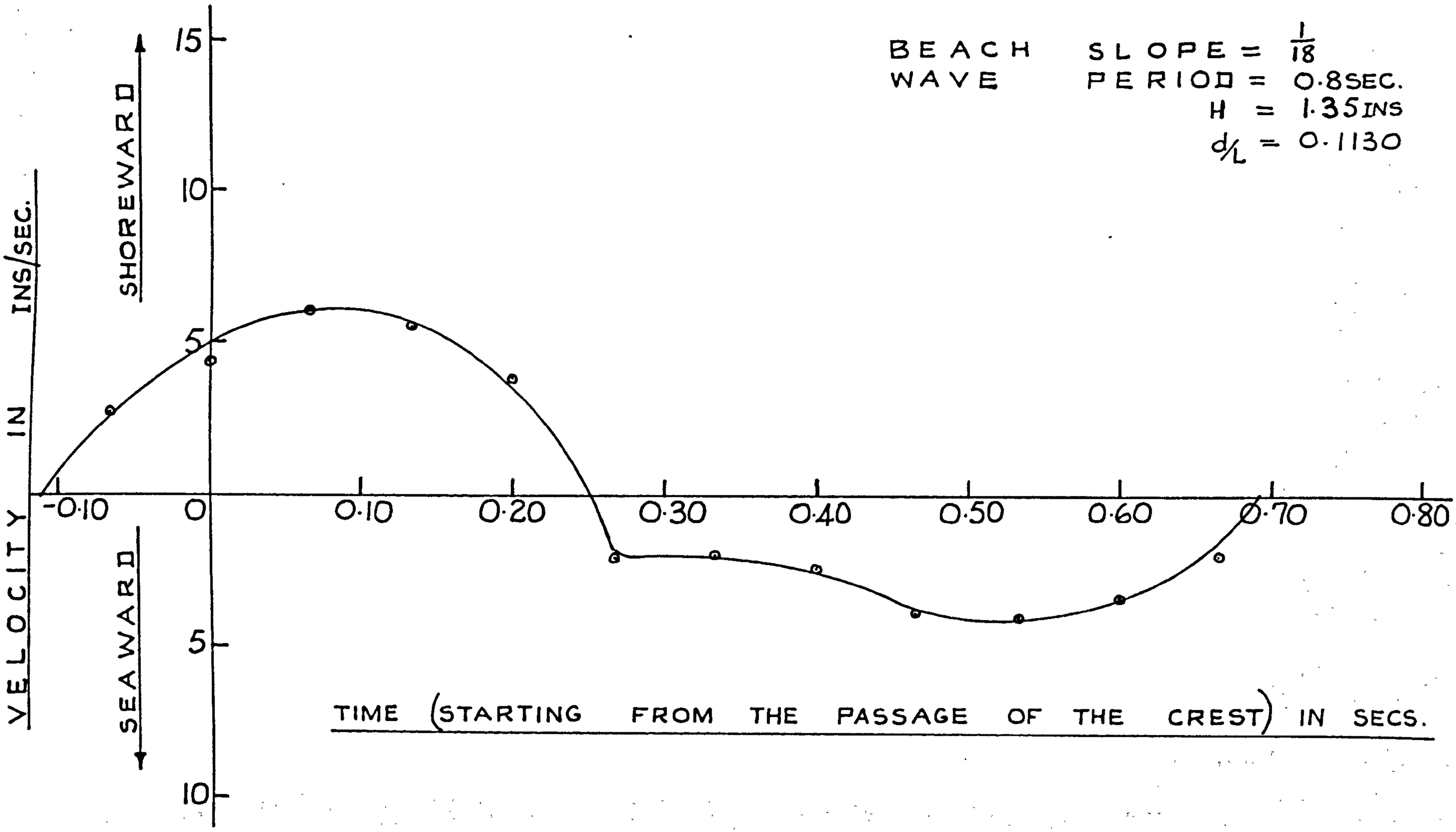

Figure A.5.8 Graph of Horizontal Orbital Velocity Against Time

BEACH SLOPE = 1/9
WAVE PERIOD = 0·8 SEC.
H = 1·52 INS
d/L = 0·0785

(BACKWASH ELIMINATED)

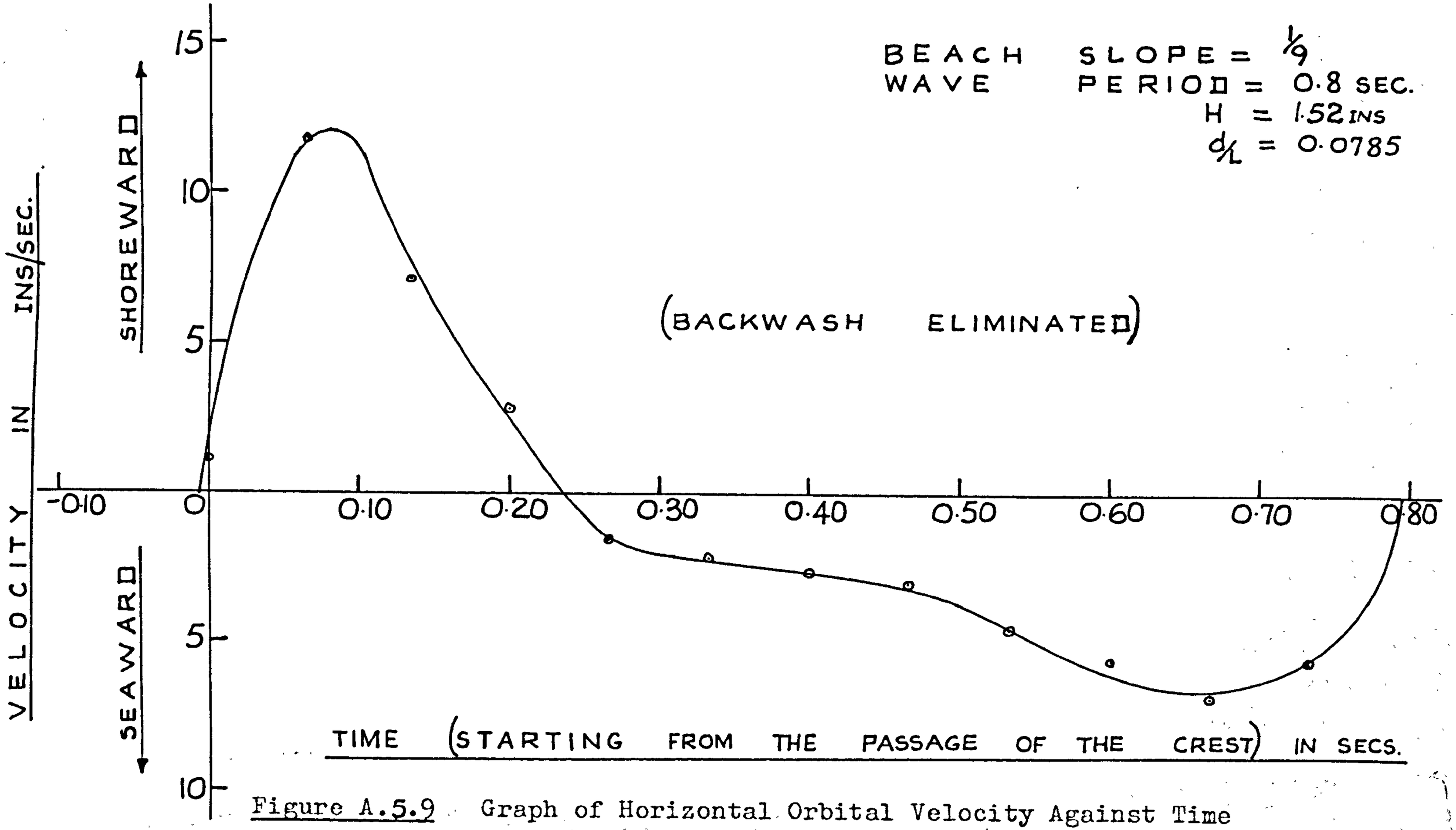

Figure A.5.9 Graph of Horizontal Orbital Velocity Against Time

BEACH SLOPE = 1/9
WAVE PERIOD = 0.8 SEC.
H = 1.495 INS
d/L = 0.0800

(BACKWASH ELIMINATED)

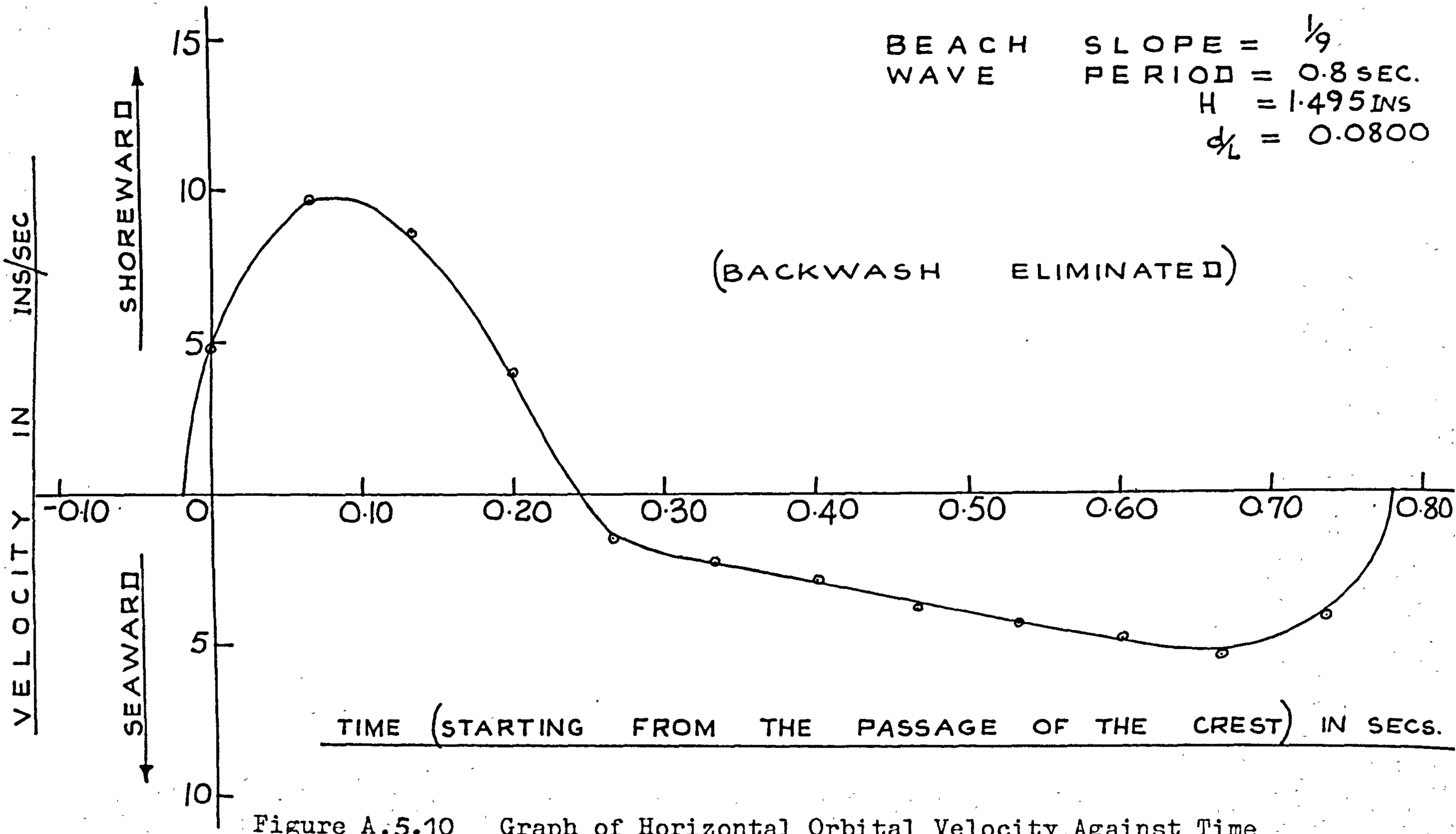

Figure A.5.10 Graph of Horizontal Orbital Velocity Against Time

BEACH SLOPE = 1/9
WAVE PERIOD = 0·8 SEC.
H = 1·40 INS
d/L = 0·0820

(BACKWASH ELIMINATED)

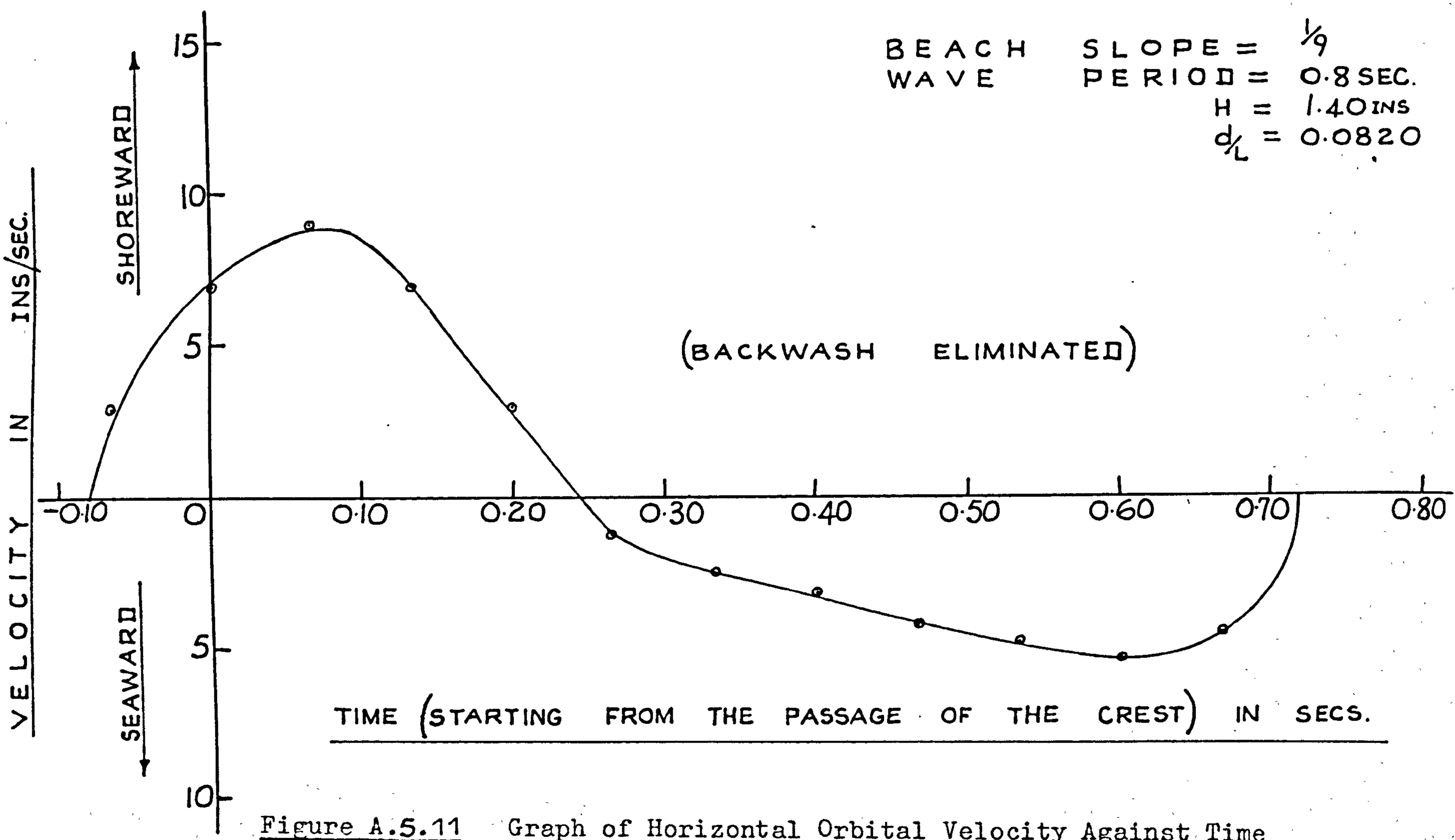

Figure A.5.11 Graph of Horizontal Orbital Velocity Against Time

BEACH SLOPE = 1/9
WAVE PERIOD = 0.8 SEC.
H = 1.334 INS
d/L = 0.0890

(BACKWASH ELIMINATED)

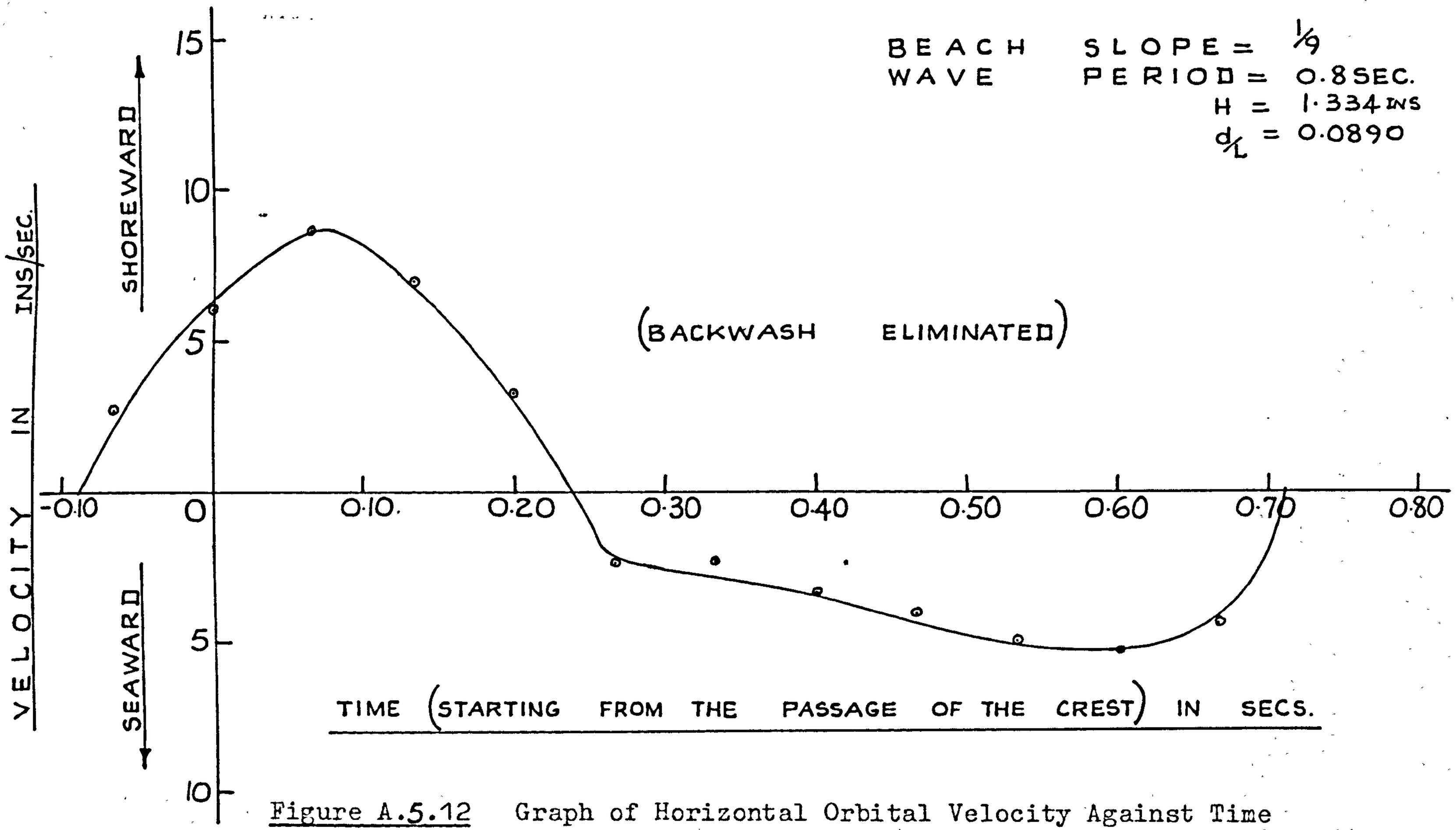

Figure A.5.12 Graph of Horizontal Orbital Velocity Against Time

BEACH SLOPE = 1/9
WAVE PERIOD = 0·8 SEC.
H = 1·285 INS
d/L = 0·0952

(BACKWASH ELIMINATED)

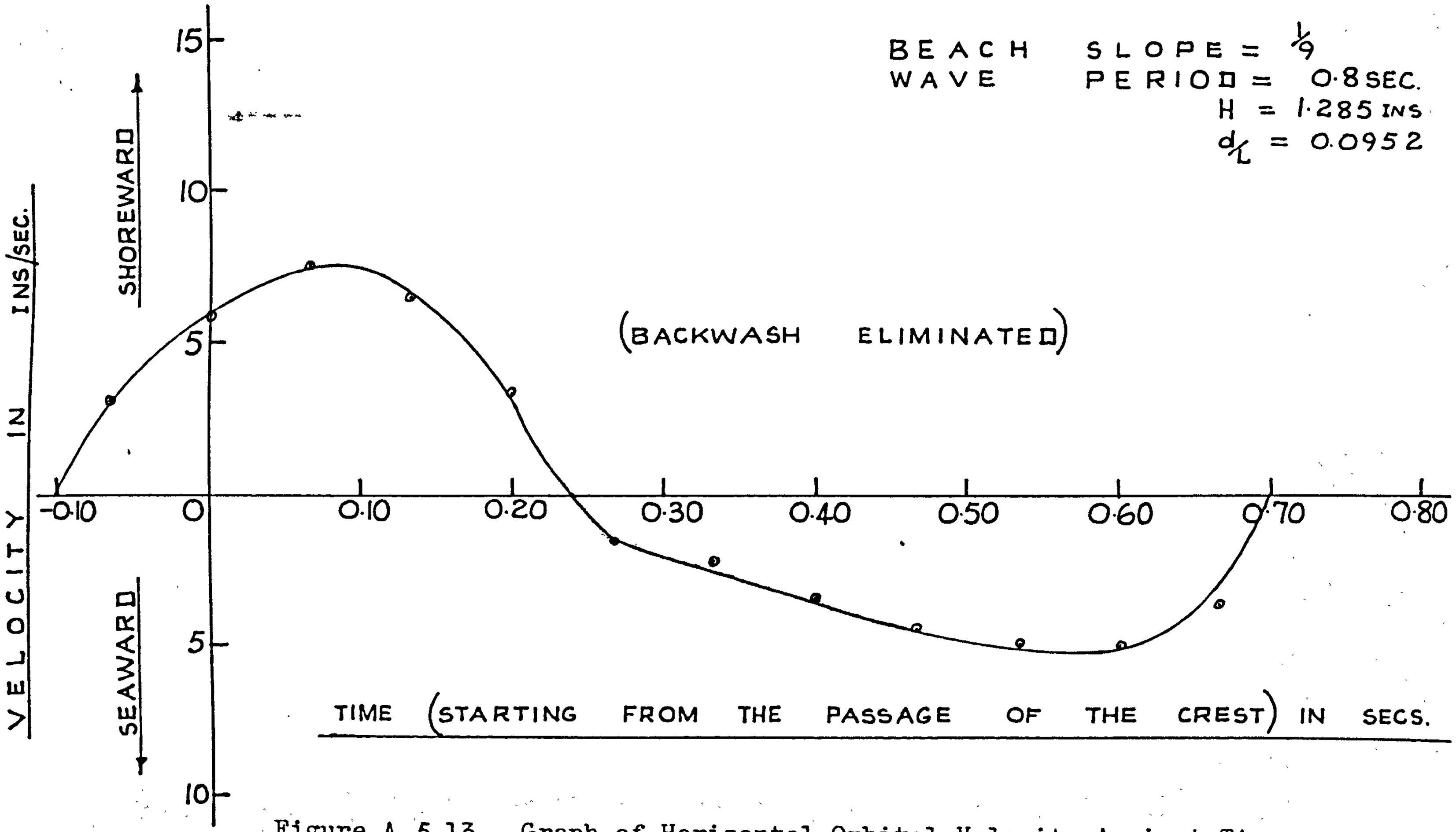

Figure A.5.13 Graph of Horizontal Orbital Velocity Against Time

BEACH SLOPE = 1/9
WAVE PERIOD = 0.8 SEC.
H = 1.283 INS
d/L = 0.1000

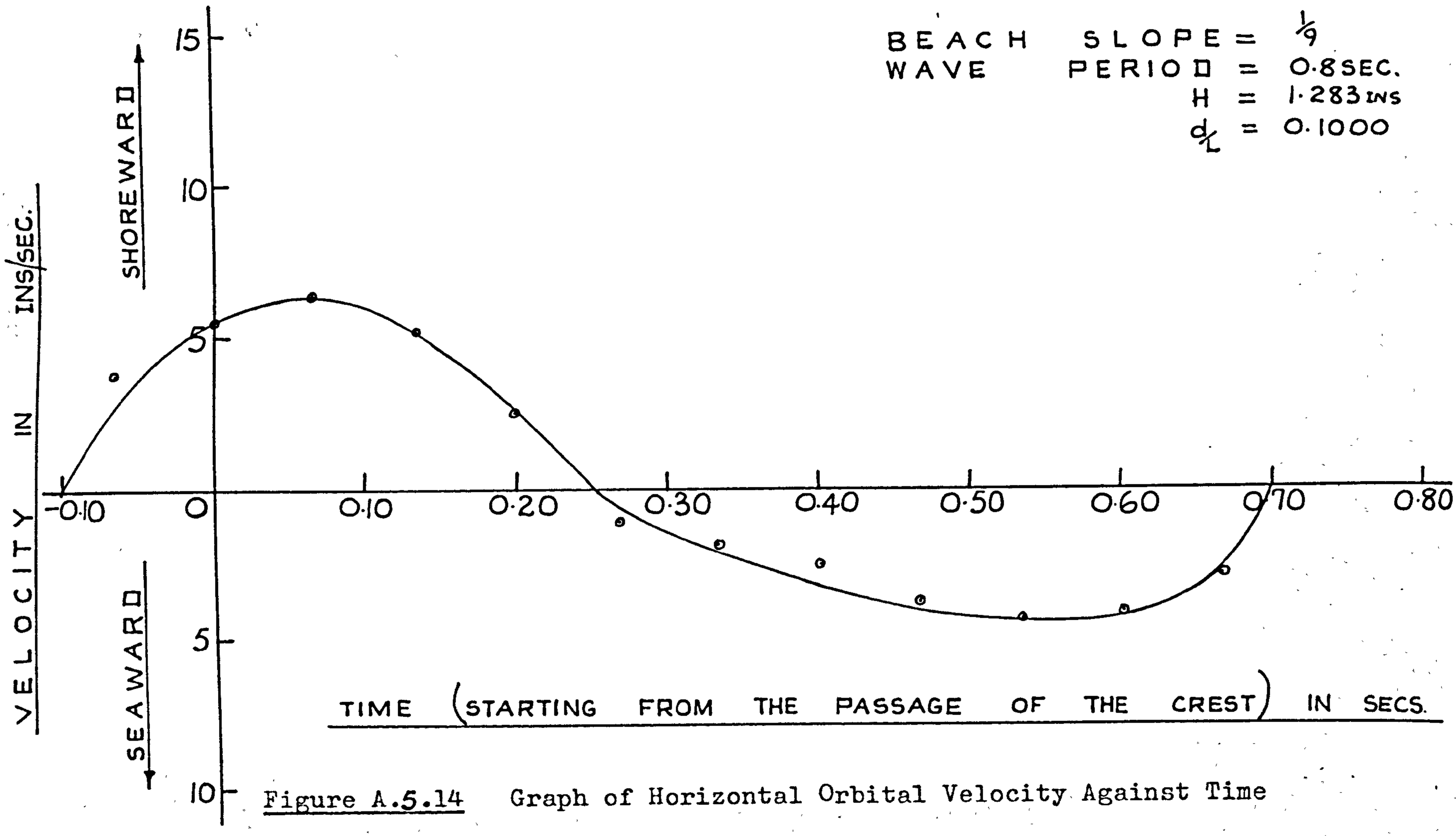

Figure A.5.14 Graph of Horizontal Orbital Velocity Against Time

BEACH SLOPE = 1/9
WAVE PERIOD = 0·8SEC.
H = 1·280INS
d/L = 0·1080

(BACKWASH ELIMINATED)

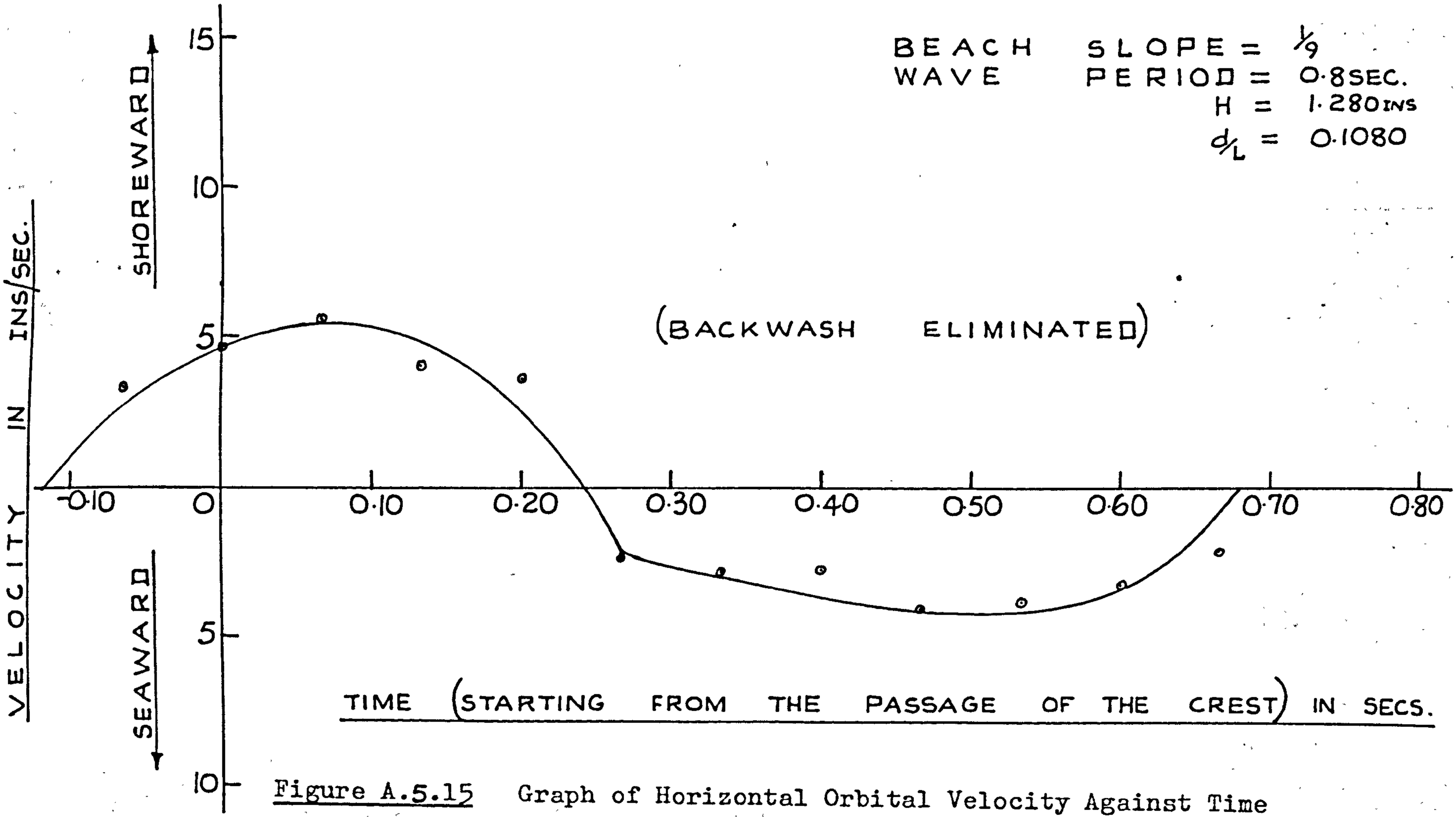

Figure A.5.15 Graph of Horizontal Orbital Velocity Against Time

BEACH SLOPE = 1/9
WAVE PERIOD = 0·8SEC.
H = 1·276 INS
d/L = 0·1180

(BACKWASH ELIMINATED)

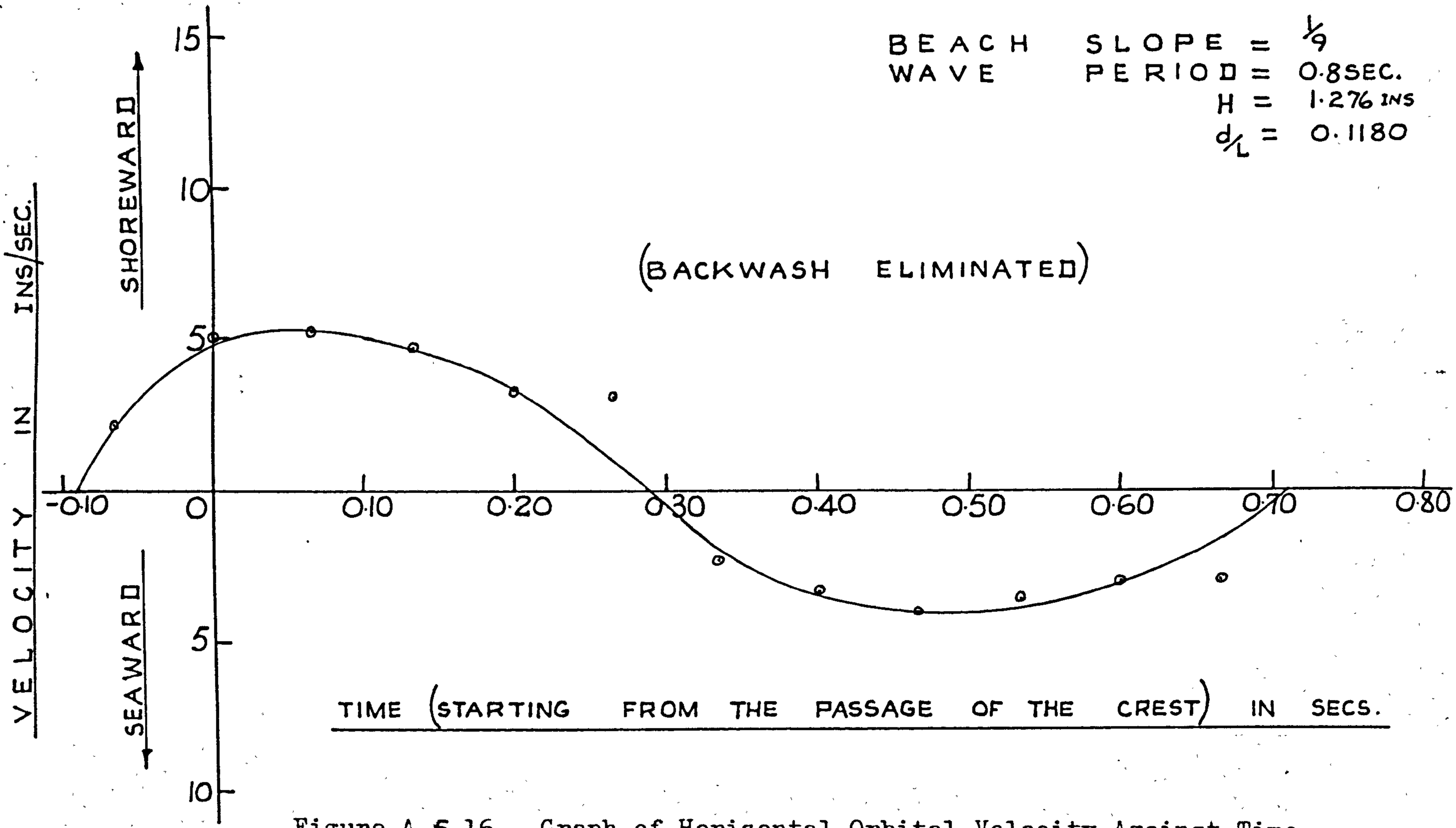

Figure A.5.16 Graph of Horizontal Orbital Velocity Against Time

BEACH SLOPE = $\frac{1}{18}$
WAVE PERIOD = 0·8 SEC.
H = 1·56 INS
d/L = 0·0818

(BACKWASH ELIMINATED)

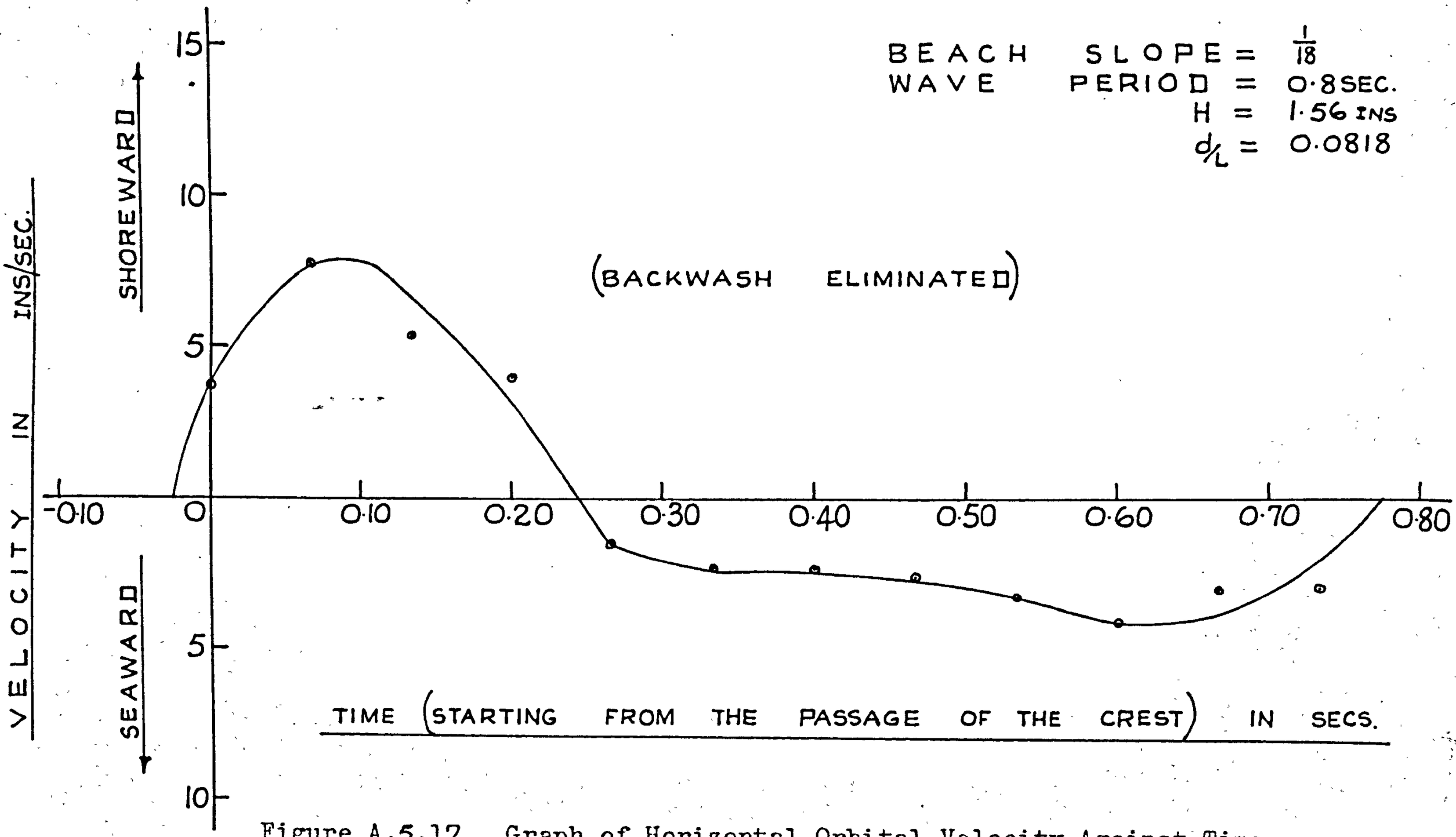

Figure A.5.17 Graph of Horizontal Orbital Velocity Against Time

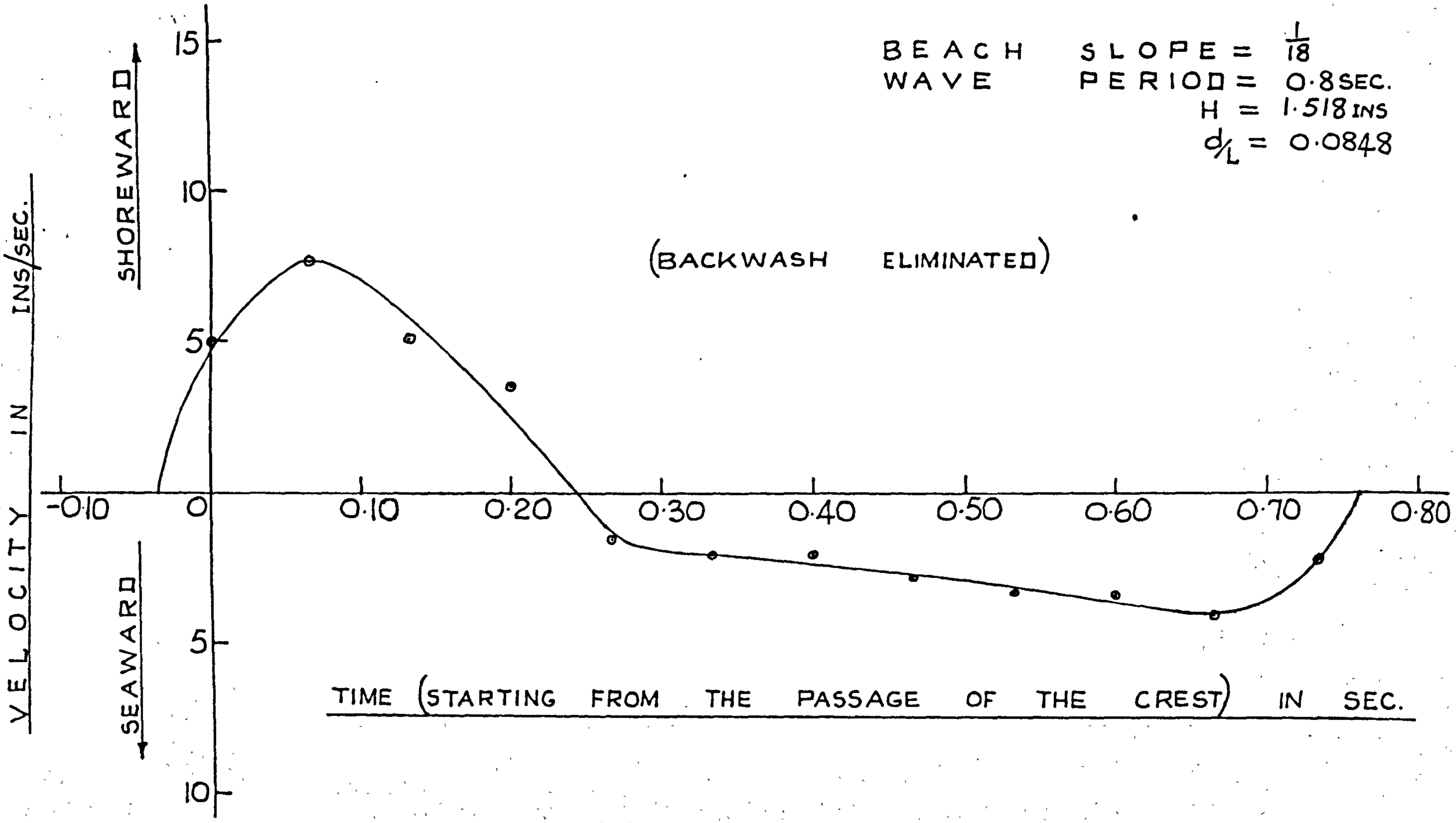

Figure A.5.18 Graph of Horizontal Orbital Velocity Against Time

BEACH SLOPE = 1/18
WAVE PERIOD = 0·8 SEC.
H = 1·468 INS.
d/L = 0·0870

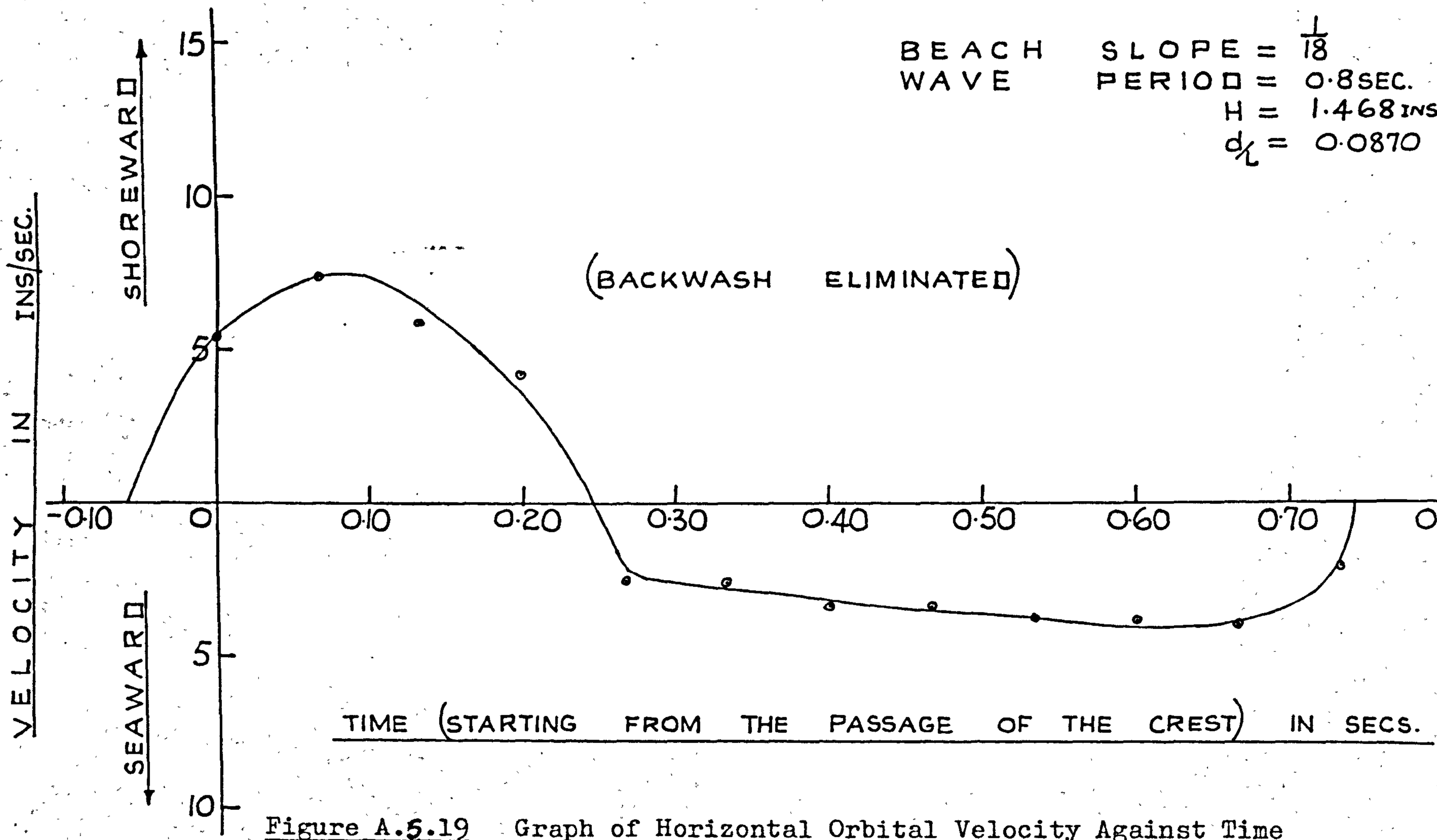

Figure A.5.19 Graph of Horizontal Orbital Velocity Against Time

BEACH SLOPE = 1/18
WAVE PERIOD = 0·8SEC.
H = 1·42 INS.
d/L = 0·0895

(BACKWASH ELIMINATED)

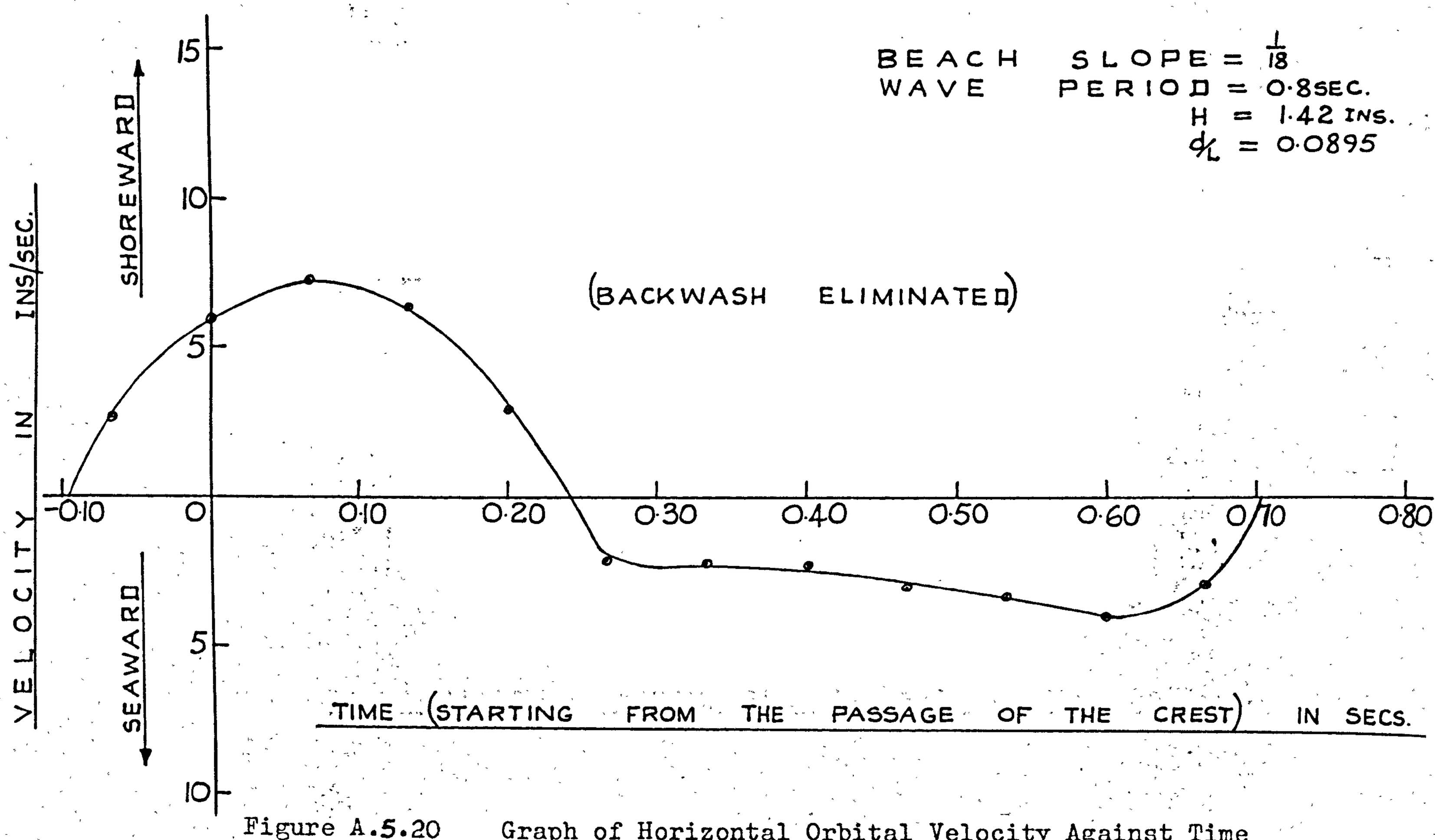

Figure A.5.20 Graph of Horizontal Orbital Velocity Against Time

BEACH SLOPE = 1/18
WAVE PERIOD = 0·8SEC.
H = 1·38 INS.
d/L = 0·0932

(BACKWASH ELIMINATED)

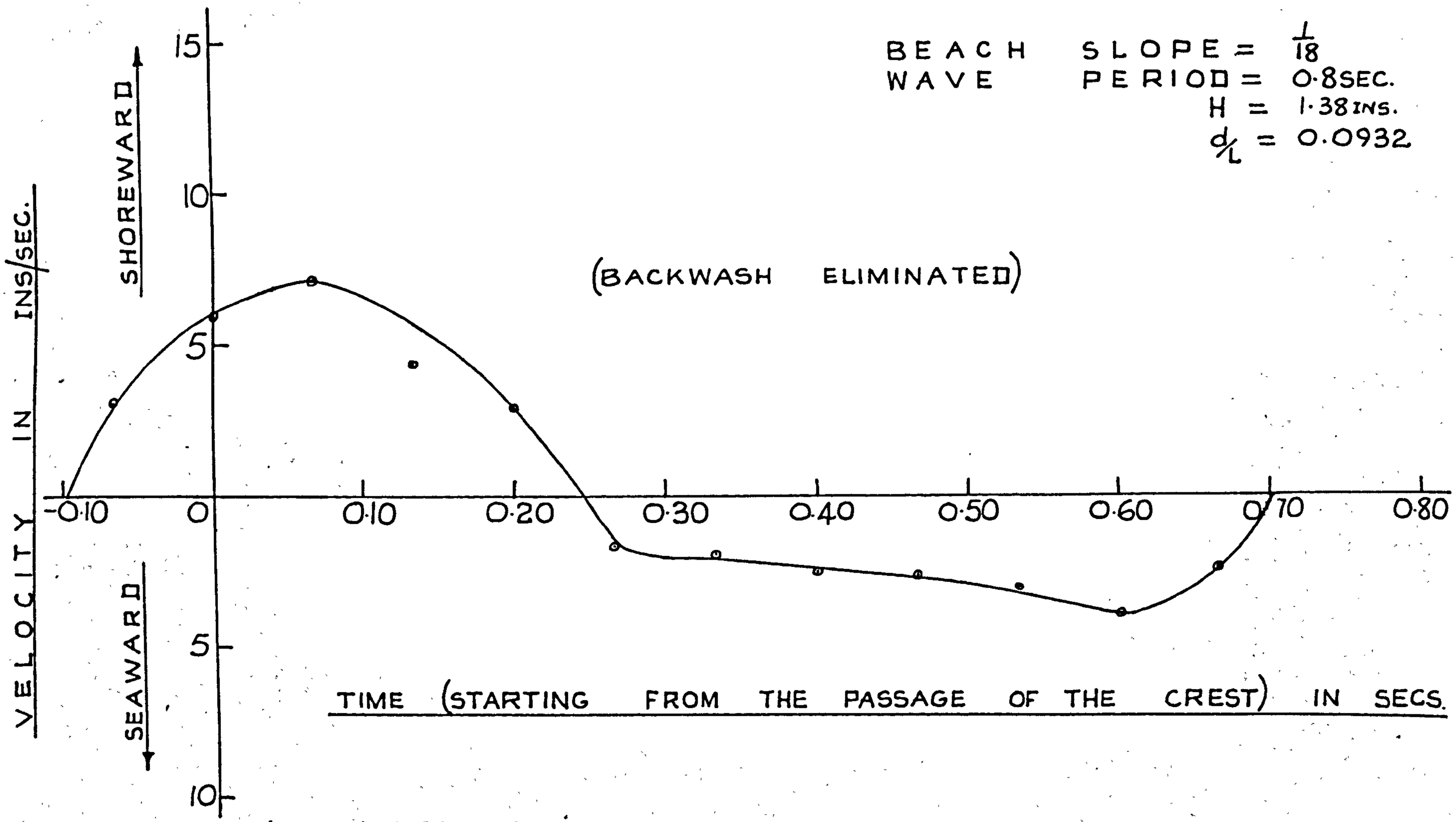

Figure A.5.21 Graph of Horizontal Orbital Velocity Against Time

BEACH SLOPE = 1/18
WAVE PERIOD = 0·8 SEC.
H = 1·368 INS.
d/L = 0·0977

(BACKWASH ELIMINATED)

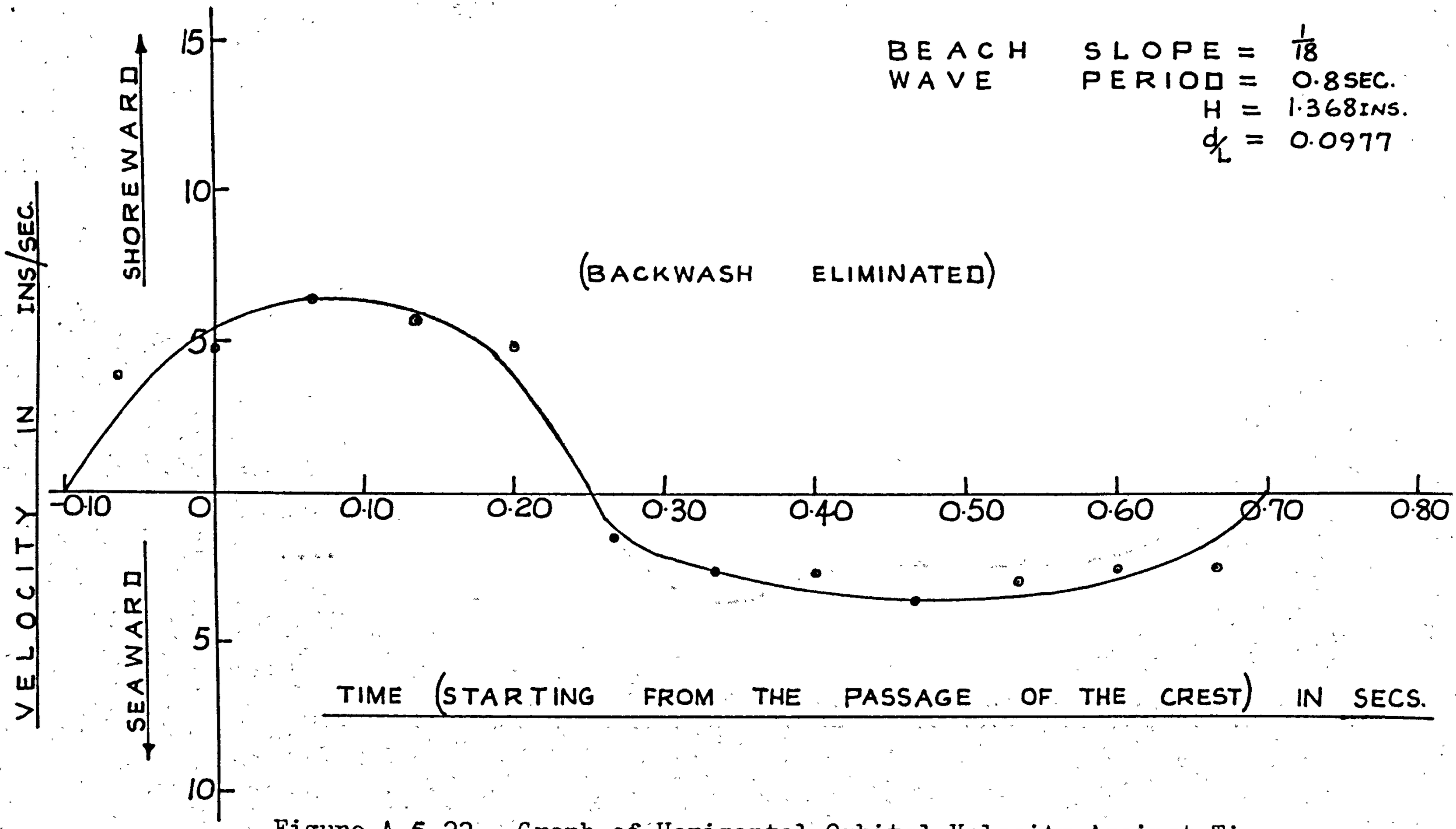

Figure A.5.22 Graph of Horizontal Orbital Velocity Against Time

BEACH SLOPE = $\frac{1}{18}$
WAVE PERIOD = 0·8 SEC.
H = 1·35 INS.
d/L = 0·1050

(BACKWASH ELIMINATED)

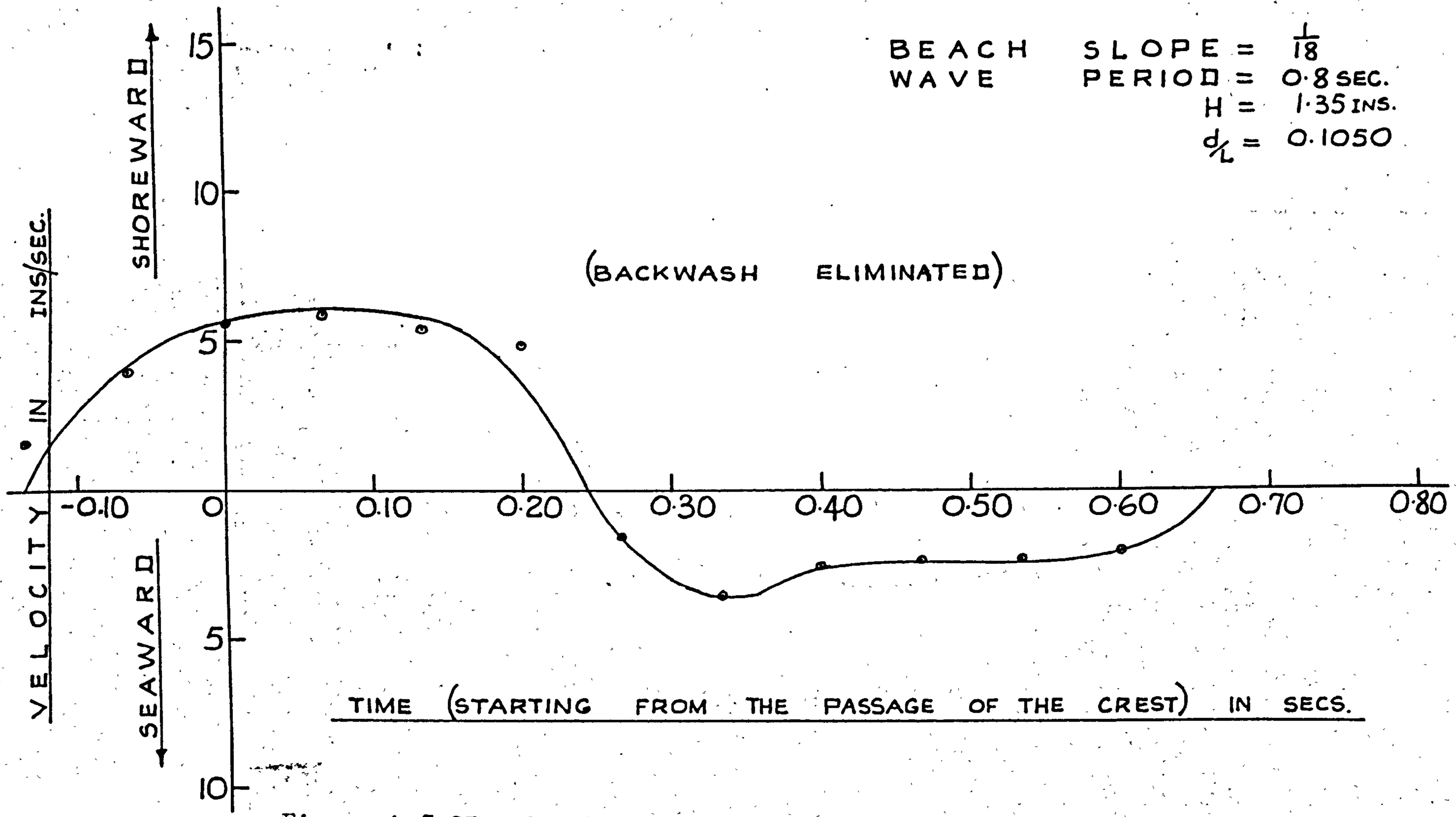

Figure A.5.23 Graph of Horizontal Orbital Velocity Against Time

BEACH SLOPE = 1/18
WAVE PERIOD = 0·8SEC.
H = 1·33INS.
d/L = 0·1140

(BACKWASH ELIMINATED)

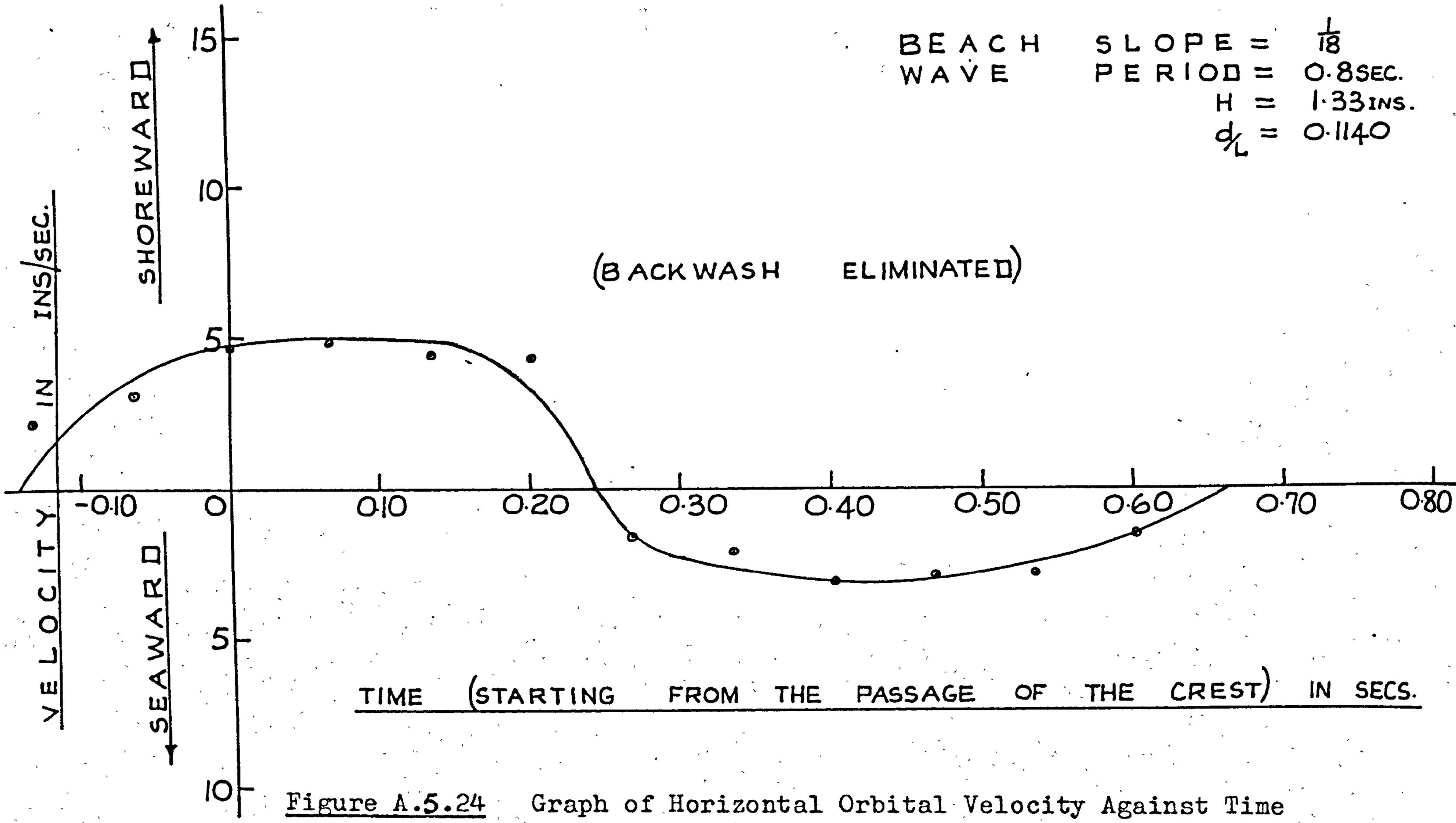

Figure A.5.24 Graph of Horizontal Orbital Velocity Against Time

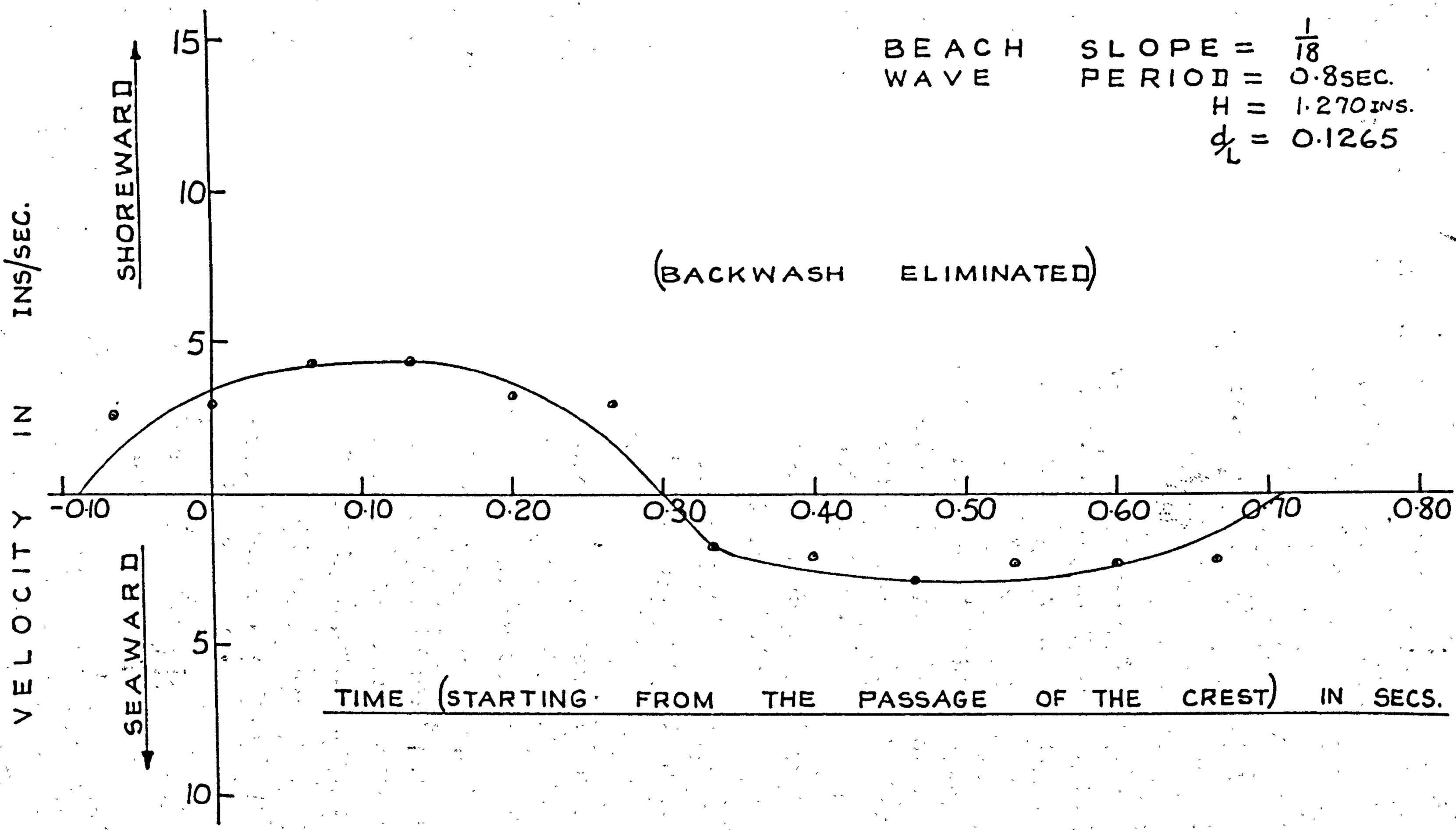

Figure A.5.25 Graph of Horizontal Orbital Velocity Against Time

APPENDIX 6

References

1. Allen, J and Gibson D.H. - Experiments on the displacement of water by waves of various heights and frequencies. Proc. I.C.E. vol. 13, July 1959, pp 363-386.

2. Bagnold, R.A. - Motion of waves in shallow water - Interaction between waves and sand bottoms. Proc. Roy. Soc. London Ser. A. vol. 187, 1946 with appendix by G.I. Taylor.

3. Beach Erosion Board Interim Report. U.S. Army Corps of Engrs. April 15, 1933.

4. Benjamin, T.B. and Lighthill, M.J. - On Cnoidal waves and bores. Proc. Roy. Soc. A. 224, 1954 pp 448 - 60.

5. Biesel, F. - Study of wave propagation in water of gradually varying depth. Gravity waves circular No. 521. Nat. Bureau of Standards Washington D.C. 1951.

6. Bretschneider, C.L. and R.O. Reid - Modification of wave height due to bottom friction, percolation and refraction. Beach Erosion Board. Tech. Memo No. 45, 1954.

7. Burington R.S. and Torrance, C.C. - Higher Mathematics with applications to science and engineering. McGraw Hill Book Company Inc. New York and London, 1939.

8. Eagleson, P.S. Properties of shoaling waves by theory and experiment. Trans. Amer. Geophys. Un. 37 No. 5, 1956 pp 565-72 and 38 (5) 1957 pp 760-763.

9. Eagleson, P.S. and Dean, R.G. - Wave induced motion of bottom sediment particles. Trans. Amer. Soc. of Civil Engrs. vol. 126 1961 Part 1. pp 1162 - 1189.

10. Goddet, J. - Etude du debut d'entrainement des materiaux mobiles sous l'action de la houle. La Houille Blanche 2, Mars - Avril 1960 pp 124 - 133.

11. Grant, U.S. - Waves as a sand-transporting agent Amer. Jour. Sci. vol. 241 1943, pp 117-123

12. Hamada, T. - Breakers and beach erosions. Rept. Transportation Tech. Res. Inst. Tokyo, Report no. 1, Dec. 1951.

13. Huon Li - Stability of oscillatory laminar flow along a wall. B.E.B. Washington, D.C. Tech. Memo No. 47, 1954.

14. Inman, D.L. and Nasu N. - Orbital velocity associated with wave action near the breaker zone. Beach Erosion Board. Washington D.C. Tech. Memo No. 79 1956.

15. Ippen A.T. and Kulin G - The shoaling and breaking of the solitary wave. Proc. Fifth Conf. Coastal Engineering September 1954, Published 1955, pp 27-47.

16, Iversen, H.W. - Waves and breakers in shoaling water. Proc. Third Conf. Coastal Engineering, 1952, Published 1953, pp 1 - 12.

17. Iwasa Y. - Analytical considerations on cnoidal and solitary waves. Memoirs of Faculty of Engineering, Kyoto Univ. Japan, 17, No. 4 1955.

18. Jolliffe, I.P. - An experiment designed to compare the relative rates of movement of different sizes of beach pebble. Proc. of the Geo. Assn. 75, 1964, pp 67-86.

19. Keller, J.B. - The solitary wave and periodic waves in shallow water, Commun. Appl. Math. 1 1948.

20. Kemp, P.H. - Effect of groynes on beach formation and erosion. Ph.D. thesis Univ. of London 1958.

21. Kemp. P.H. - The relationship between wave action and beach profiles. Proc. seventh Conf. on Coastal Engineering 1960, pp 262 - 277.

22. Keulegan, G.H. - Wave Motion. Engineering Hydraulics, Proc. Fourth Hydraulic Conf. Ch.11 (Ed. by H. Rouse) New York: Wiley, 1950.

23. Keulegan, G.H. and Patterson, G.W. - Mathematical theory of irrotational translation waves. J. Res. National Bur. Standards, 24, 1 Jan. 1940. pp 47 - 101.

24. Korteweg, D.J. and de Vries G. - On the change of form of long waves advancing in a rectangular canal, and on a new type of long stationary waves. Phil. Mag. 5th Series 39, 1895 pp 422 - 43.

25. La Fond, Eugene, C. - Sand movement near the beach in relation to tides and waves. Sixth Pacc. Sci. Congr. Proc. vol. 2, 1940. pp 795-99.

26. Laitone, E.V. - The second approximation to cnoidal and solitary waves. Jour. fluid Mech. vol. 9 Part 3, 1960 pp 430-44.

27. Laitone, E.V. - Higher approximations to non-linear water waves and the heights of cnoidal and solitary waves. Univ. of Calif. Inst. of Eng. Res. Tech. Rept. series 89, Issue 6, 130 pp 1961.

28. Larras, J. Effect de la houle et du clapotis sur les fonds de sable - Paris ive Journees de l'Hydraulique, 1956 - Rapport no. 9. question vii - Les energies de la mer.

29. Levi-Civita T. - Determination rigoureuse des ondes d'ampleur finie. Math. Annaleu, 93 1925, pp 264-314.

30. Littman W. - On the existence of periodic waves near critical speed. Commun. Pure Appl. Math. 10, 1957 pp 241 - 69.

31. Longuet-Higgins M.S. - Mass transport in water waves. Philosophical transactions vol. 245 A.903, 1952-53. pp 535-581.

32. Manohar, M. - Mechanics of bottom sediment due to wave action. B.E.B. Tech. Memo No.75 Washington D.C. 1955.

33. Masch, F.D. - Cnoidal waves in shallow water Proc. Ninth Conf. Coastal Engineering 1964. pp 1 - 22.

34. Masch, F.D. and Wiegel, R.L. - Cnoidal waves - Tables of Functions. Council on wave research. The Engineering Foundation, Richmond, Calif. 1961. 129pp.

35. Mason, M.A. - A study of progressive oscillatory waves in water. B.E.B. Tech. Memo no.1 1941.

36. Mason, M.A. - Some observations of breaking waves. Gravity waves circular no. 521, Nat. Bureau of Standards, Washington D.C. 1951. pp 215 - 20.

37. Miche, R. - The reflecting power of maritime works exposed to action of the waves. Bulletin of the Beach Erosion Board. Corps of Engrs. U.S. Army 7, 2 (April 1953)

38. Miller, R.L. and Zeigler, J.M. - The internal velocity field in breaking waves. Proc. Ninth Conf. coastal Engineering 1964. pp 103-122.

39. Morison, J.R. and Crooke, R.C. - The mechanics of deep water, shallow water and breaking waves. Beach Erosion Board. Tech. Memo No.40. 1953.

40. Plinston, D.L. - The effect of waves breaking on beaches. Ph.D. thesis Univ. of London 1966.

41. Reid, R.O. and K. Kajiura - On the damping of gravity waves over a permeable sea bed. Trans Amer. Geophys. Union Vol. 38, no.5 1957 pp 662-66.

42. Russell, R.C.H. and Osorio, J.D.C. - An experimental investigation of drift profiles in a closed channel. Proc. Sixth Conf. Coastal Engineering 1957, Published 1958. pp 171 - 193.

43. Schraub, F.A., Kline, S.J., Henry J., Runstadler, P.W. and Littell, A. - Use of hydrogen bubbles for quantitative determination of the time dependent velocity fields in low speed water flows. Report M.D. 10. Thermosciences division, Dept. of Mechanical Engineering, Stanford Univ. Stanford Calif.

44. Scott, T. - Sand movement by waves. B.E.B. Tech. Memo No. 48. Washington D.C. 1954.

45. Silvester R. - Engineering aspects of coastal sediment movement. Journal of the waterways and Harbors division. Proc. of the Amer. Soc. of Civil Engrs. vol. 85 no. WW3, Sept. 1959. pp 11-39.

46. Skjelbreia, Lars. - Gravity waves, Stokes' third order approximation; tables of functions. Berkeley Calif. The Engineering Foundation Council on wave research 1959.

47. Stokes, G.G. - On the theory of oscillatory waves Mathematical and Physical papers. 1 Cambridge Cambridge University Press 1880.

48. Struick, D.J. - Determination rigoureuse des ondes irratationelles periodiques dans un canal a profundeur finie. Math. Annalen, 95, 1926 pp 595-634.

49. Tucker, M.J. and Charnock, H. A capacitance - wire recorder for small waves. Proc. Fifth Conf. on coastal Engineering 1954. Published 1955.

50. Ursell, F. - The long wave paradox in the theory of gravity waves. Proc. Camb. Phil Soc. V 49(4) 1953.

51. Valembois, J. Quelques considerations sur la similitude dans les essais de houle sur modele ive Journees de l'Hydraulique Paris 1956. Rapport No. 8 Question III - Les energies de la mer.

52. Vincent, G.E. - Contribution to the study of sediment transport on a horizontal bed due to wave action. Proc. Sixth Conf. on Coastal Engineering, Dec. 1957. Published 1958 pp 326-55.

53. Wells, D.R. - On the time varying horizontal water velocity of single, multiple and random gravity wave trains. Thesis Tech. Hogeschule Te. Delft. 1964.

54. Wiegel, R.L. - Experimental study of surface waves in shoaling water. Trans. Amer. Geophys. Union. vol. 31, 1950 pp 377-85.

55. Wiegel, R.L. - A presentation of cnoidal wave theory for practical application. Jour. Fluid Mech. 7, Part 2, 1960 pp 273-86.

56. Wiegel, R.L. - Oceanographical Engineering Publ. Prentice Hall.